April 2010

A Study of Biofuel Production Using Molten Salt Catalysts

Chad Hinden Mondor
Worcester Polytechnic Institute

Kevin R. Bordage
Worcester Polytechnic Institute

Sean Thayer Philbrook
Worcester Polytechnic Institute

Tobin Patrick McGee
Worcester Polytechnic Institute

A Study of Biofuel Production Using Molten Salt Catalysts

Worcester Polytechnic Institute

A Major Qualifying Project
submitted to the Faculty of
WORCESTER POLYTECHNIC INSTITUTE
in partial fulfillment of the requirements for the
Degree of Bachelor of Science

By

Kevin Bordage

Tobin McGee

Chad Mondor

Sean Philbrook

April 29th, 2010

Approved:

Keywords
1. Molten Salts
2. Gasification
3. Biofuel

Ravindra Datta, Advisor

James P. Dittami, Co-Advisor

Abstract

Lignin, cellulose, and hemicelluloses from biomass have been shown to break down into sustainable fuel products when subjected to extreme reaction conditions. However, factors such as energy costs, char generation, and low yields hinder the mainstream use of biofuels. This project investigated the effects of catalytic molten salts on biomass feedstocks in producing gaseous and liquid fuels using the mechanistic chemical pathways of gasification, pyrolysis, thermal depolymerization, hydrolysis, and transesterification. Reaction variables such as flow rates, temperature, pressure, vessel type, reagent type, and time were investigated. Gaseous and liquid products were purified and qualitative observation, NMR and GC data were collected for positive product identification. Optimization techniques such as reducing char buildup by protein digestion, running semi-batch conditions, and the use of microwave reactors were all investigated to increase the efficacy of the system. Specific reaction conditions for gasification, pyrolysis, and predigestion resulting in the desirable production of syngases and biodiesel-like products were identified. Recommendations were made for more specific identification of oily products, improved reactor design, and conditions for depolymerization of plastics.

Acknowledgements

The project group would like to thank the following people for their help and support throughout this project:

- Professors Ravindra Datta and James Dittami for their support as project advisors
- Professor Heilman for his advice pertaining to the biochemistry aspect of this project
- Jack Ferraro and Doug White for their help with setting up, changing, and fixing the flow system and gas chromatograph
- Paula Moravek for help ordering supplies and chemicals necessary for the reactions
- Professor Ilie Fishtik for his help using the NMR machine in Goddard and in Gateway
- Professor Kumar for allowing us to the gas chromatograph in the freshmen chemistry labs
- Victor Kiryak for his help with the microwave reactor
- Jack Ridler – WPI custodian – for always helping to keep our lab clean and just generally being interested in our work
- Maria DeCicco, for letting us into Professor Heilman's lab at all hours of the day and night

Table of Contents

Table of Figures

List of Tables

Executive Summary

Energy has and will always be a main concern for modern life on earth. Fossil fuels will deplete in the long term and alternative sources of energy are needed if we are to meet the energy demand of the technologically developing world. The use of biomass as a fuel has been a rapidly expanding industry because it has the potential to provide renewable, clean energy.

Beyond the issue of dwindling fossil fuels lies the ever-increasing problem of municipal solid wastes accumulating in the environment (The Environmental Protection Agency, 2009). Processing biomass for energy would not only act to reduce human dependence on oil and gas but would also act as a means of recycling nearly all municipal solid wastes.

Biomass can be converted into energy through many different pathways. This project focuses on gasification, pyrolysis, as well as biodiesel transesterification and the hydrolysis of triglycerides. Pyrolysis is the breakdown of a substance due to the addition of heat (Huber 2006). Gasification consists of the pyrolysis of biomass into char and gases such as carbon monoxide, hydrogen, and methane. The concentrations of these gases can be adjusted through reactions such as the water-gas shift reaction and the methanation reaction. Char can also be converted into gas through the Boudard reaction and a steam-reforming step. Transesterification and hydrolysis are typically base or acid catalyzed reactions that cleave ester groups within an organic molecule.

An MQP in 2009 studied the gas compositions from reacted biomass. Molten salts were used because they are highly ionic and can be used as an effective reactive medium. Our project group expanded upon this research in many ways. More research and experimentation in the area of gasification was made, in addition to exploring alternative mechanistic pathways such as hydrolysis/pyrolysis, thermal depolymerization, biodiesel transesterification, and enzymatic digestion of biomass as a pre-treatment step. These methods were investigated to determine their viability to produce usable fuels.

Most notably, the efficacy of these various pathways utilizes an identical semi-batch reactor setup to increase the versatility of production simultaneously in a single system, with similar reactive conditions. Only slight changes in how the reactor was setup or charged were changed between trials. However, the products collected from these trials varied widely. The ability to specifically produce one product over another to tailor the process for a specific need is extremely valuable for a commercial process.

In addition to determining the most effective molecular pathways of biofuels production, ideal reaction conditions were also determined. Running the reactor as a semi-batch process design instead of the previous batch design was necessary to determine the effect on reaction progress. Flow rate of the carrier gas, carrier gas type, reaction temperature, pressure, type of reagent, the biomass feedstock and the amount/type of molten salt used were also variables that were altered and maximized for conversion. These variables were tested to see if they affected the composition of the gaseous/liquid products.

Throughout all experimentation, char would accumulate in the reactor. Char buildup decreased reaction rates and decreased both syngas and liquid fuel production, a negative impact in forward progress. An additional goal was established to reduce the amount of char buildup using predigestive enzymatic digestion before reaction.

Vegetable oil and tributyrin were used as reactant oils. Since the molecular structure of tributyrin is known, specific products could be detected based on the reaction mechanism suspected to be taking place within the reactor. As for our main objective, optimum operating conditions to produce the most useable amount of gas and liquid products were determined.

Gasification trials performed as expected. Hydrogen, carbon monoxide, methane, and carbon dioxide were found in the reactor effluent gas over time. The most important finding was the change in concentration of specific gases over time due to the designed semi-batch reactor system. GC data points yielding flue gas concentrations could be found over time as shown in Figure 1.

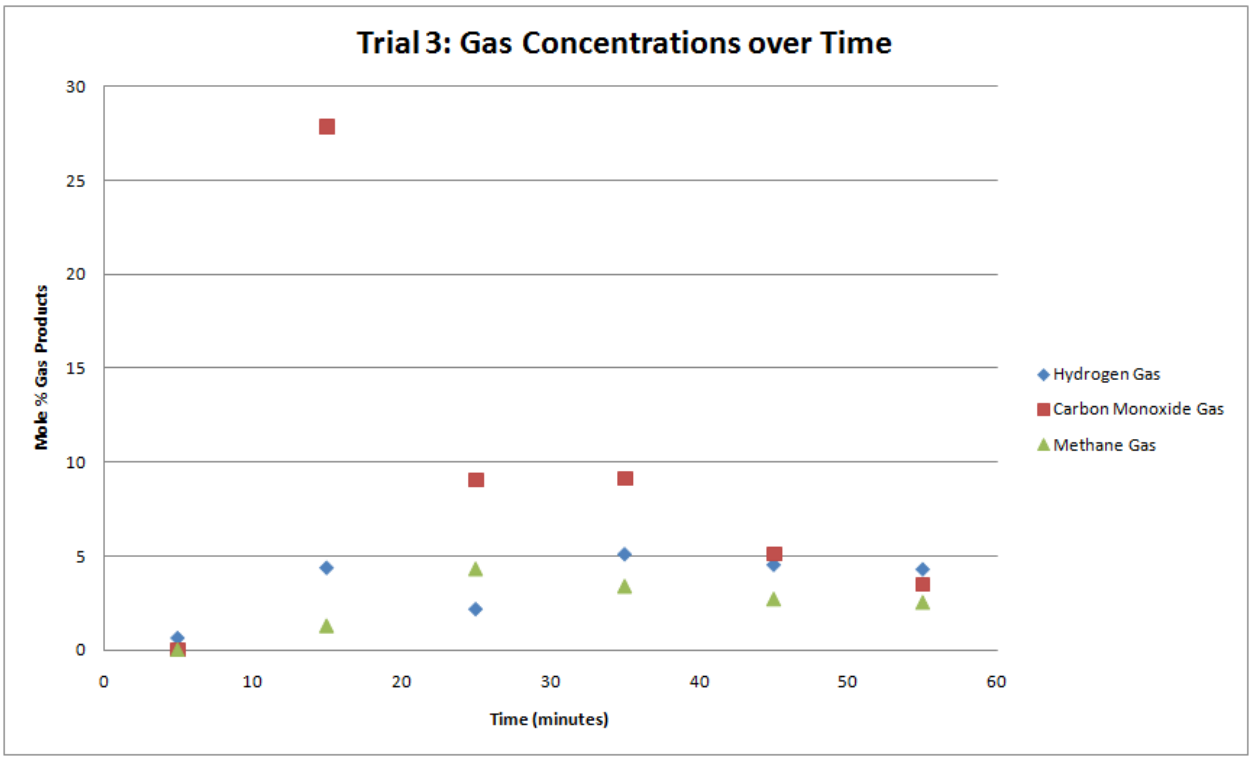

Figure 1: Example of Gasification Effluent Concentrations over Time

As with almost all trials, the concentration of the gases was seen to spike early and decrease sharply afterward. Later trials performed for longer periods of time support these findings. The flow system was upgraded for the later trials to include a cold trap, which collected liquid products early during reaction for every gasification trial. This suggests that the initial pyrolysis of paper occurs early in the reaction to produce the liquid products, the spikes in gas concentrations, and most likely, char. After initial char formation, the char is able to slowly react and form more gases.

With the addition of a sparger to deliver water vapor to the reaction, the gas concentrations changed. No methane was seen in the reactor and carbon monoxide was only seen during the initial phases of the trials. This suggests that water vapor forces the water gas shift reaction to convert carbon monoxide into hydrogen and carbon dioxide, and stops the methanation reaction from occurring. This is supported by the slightly higher hydrogen concentrations observed with a sparger.

These results were compared against gasification trials of tributyrin oil. Similar results were found with high concentrations of hydrogen syngas emitting from the reactor early followed by a steady decline.

Thermal depolymerization of plastics was attempted using molten salts. Initial experiments of submerging plastic in a crucible of molten salt yielded promising results. As the temperature of the salt increased, the plastic began to turn brown and react violently. Evidence of gasification was seen from bubbles forming in the plastic. Trials in the reactor were unsuccessful because the melted plastic always clogged the reactor. Furthermore, the gas could not be analyzed because the gas chromatograph used to identify gases was not in working conditions during these trials.

Our hydrolysis reactions with our model oil, Tributyrin were not able to achieve compounds such as Butyric Acid, which were desired. Trials with vegetable oil yielded mixed results. Lighter, more volatile products were observed when the vegetable oil was at a higher temperature along with water and salt catalysts. This indicates that either hydrolysis or pyrolysis occurred. These products were identifiable with accessible resources and appeared in both GC and NMR spectra.

Our bench top transesterification reactions done on hotplates produced biodiesel from vegetable oil and methyl butyrate from tributyrin. Production of methyl butyrate from tributyrin confirms that the transesterification reaction occurred. However, the transesterification reactions in the reactor produced methyl butyrate in addition to some unknown products. It is possible that these unidentified products can be another useful biofuel because of extreme reaction conditions in the reactor.

The biochemical predigestion step aiming to reduce char buildup within the reactor was accomplished with incubation with Proteinase K enzyme for up to 48 hours prior to gasification. It was determined that the digestion helped to significantly decrease the amount of char accumulation within the reactor as compared to control tests. Additionally, digested samples yielded a significant increase in H_2 syngas produced (up to a 300% increase in some cases). This result would be advantageous to producing H_2 fuel for an application such as a PEM fuel cell. A comparison of H_2 gas output amongst digested samples is plotted in Figure 2.

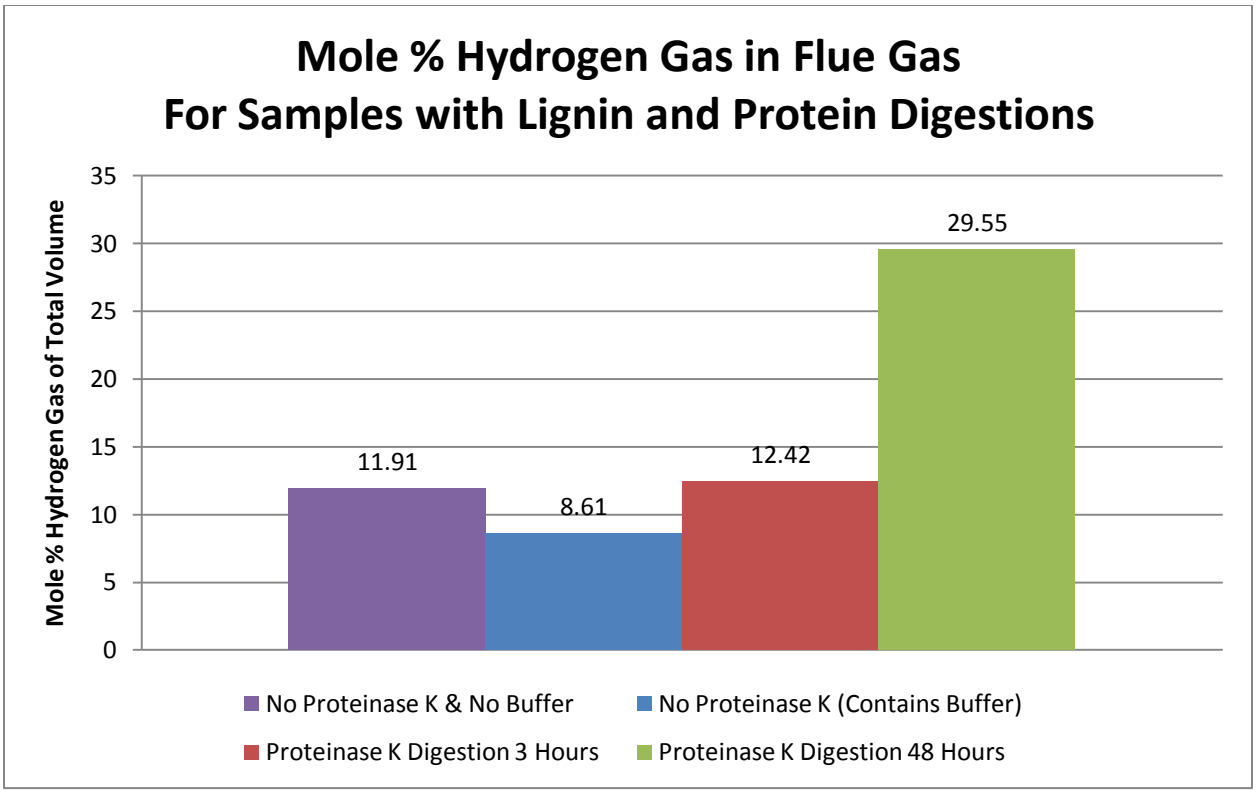

Figure 2: The Effect of Enzymatic Biocatalysis on Gasification

Clearly, predigestion with enzymatic biocatalysis has a positive effect on the yield of desirable products as well as a decrease in amount of char.

Results of using the enzymatic biocatalysis process to pre-treat lima beans used for transesterification reactions were mixed. Oily, volatile components were identified using GC and NMR technologies. However, these products may have been the result of methanol reacting with the buffer solution and not the result of the biocatalysis or transesterification reactions.

Our project group recommends that further steps should be taken in order to investigate further the use of molten salts in biomass reactions. Operating the process in a semi batch state allowed the project group to collect liquid products from almost all of the gasification experiments. More research must be completed to determine how other biomass feedstocks such as wood and algae break down in a semi-batch process. More research into the gasification of plastics will also be useful to finding a broad process capable of processing most municipal solid wastes.

The energy requirement and overall processing times of these products may be decreased with further research into enzymatic biocatalysis. Proteinase K was seen to positively affect the gasification

of lima beans in reducing char and increasing syngas yields. The effect of Proteinase K and similar catalytic enzymes on various biomass feedstocks should be further researched for efficacy. An ideal case may be to feed biomass into a solution consisting of multiple enzymes that work complementary to each other to degrade lignin and celluloses into simple sugars and carbohydrates for energy production.

Many unidentified products were observed in GC and NMR analysis after transesterification and hydrolysis reactions. While present in small amounts, these may be valuable products, and identifying these products and recovering them in greater concentrations may prove useful.

In general, the project group believes that solid, liquid, and gas contact in the reactor is extremely poor. Once char is formed, it most likely will adhere to the sides of the reactor instead of coming into contact with the molten salt bath. This also blocks gas from entering the molten salt. A new reactor capable of alleviating this issue has been suggested for future study. The reactor is slightly larger and bubbles inlet gas through a stirred molten salt and char mixture to ensure all three phases are in contact for optimal reaction kinetics.

Overall, this project suggests that the use of a single reactor is capable of processing many different biomass feedstocks to generate desired products. Molten salts were seen to help catalyze pyrolysis and gasification reactions. Additionally, the hydrolysis and transesterification reactions of oils with molten salts yielded products not seen under normal conditions. After future research and optimization, this reactor may be capable of processing many different feedstocks to generate large quantities of biofuels. Future energy demands may be partially met with the use of a reactor similar to the one used in this project.

1 Introduction

Energy has been a controversial topic in science, politics, and everyday life during the modern age. Concerns of depleting fossil fuel reserves, increasing greenhouse gas production, and increasing pollution have led to renewed interest in investigating alternative sources of fuel. Energy demands in 2005 were approximately 210 million oil-equivalent barrels per day. Over the next few years, this is expected to grow to over 300 oil-equivalent barrels per day, an increase of approximately 35% (ExxonMobil, 2008).

Fossil fuel resources are limited and will eventually extinguish. For years, petroleum fuels have met the majority of all electrical, heating, transportation, and industrial energy needs. In the future, other forms of energy will be used to help alleviate the growing energy demand. These sources include wind, solar, hydroelectric, and biomass. Renewable fuels will begin to flourish as the need for dependable, constant energy increases.

Much of the energy infrastructure related to oil and gas has been greatly optimized. ExxonMobil, the largest energy supplier in the United States, establishes an outlook that states, "From 1980 to 2005, 'energy intensity' – the amount of energy used per unit of economic output – improved by 1 percent per year on average (ExxonMobil, 2008)." Furthermore, this rate of improvement is expected to be 70 percent faster than years past. These energy savings are a result of improving efficiencies in turbines and other devices that convert raw energy into useable power.

1.1 Energy Costs

The cost of petroleum energy has been steadily rising. In 2010, the price per barrel of oil was approximately 84 dollars per barrel (Bloomberg.com, 2010). As the energy demand of the world increases, the price of oil is expected to increase as well. Although it is impossible to determine the future cost of oil, rising demands and depleting supplies will guarantee the price will increase eventually.

Most renewable forms of generating energy are still more expensive to produce as compared to fossil fuel derived oils. These are mostly due to poor conversion efficiencies. For example, current photovoltaic conversion technologies have an efficiency of approximately 20%.

Both renewable and non-renewable energy sources additionally suffer from ample energy loss in transportation from the fuel source to the electronic devices, converters, and battery storage. Compounding all of these losses together increases the amount of source energy that would need to be

captured by sunlight. Critics use this logic to argue that many renewable sources of energy such as wind, solar, and tidal energy are not feasible. However, continued research may improve efficiency until these sources are comparable to the low energy loss associated with fossil fuels.

1.2 Synthetic Fuels

The synthesis of liquid fuels from gaseous or solid materials may help alleviate some of the problems faced by renewable fuels research. The modern transportation fuel infrastructure has been developed to handle large quantities of liquid fuel. Therefore, transforming solids and gases into liquid fuel will be more compatible with the current energy infrastructure.

Many methods exist for converting gaseous products into liquid fuel. Even though energy is lost in the conversion stages, liquid fuel is much more desired than gaseous fuel. Figure 3 demonstrates the basic reaction pathways utilized by modern reactors to form liquid fuel from natural gas.

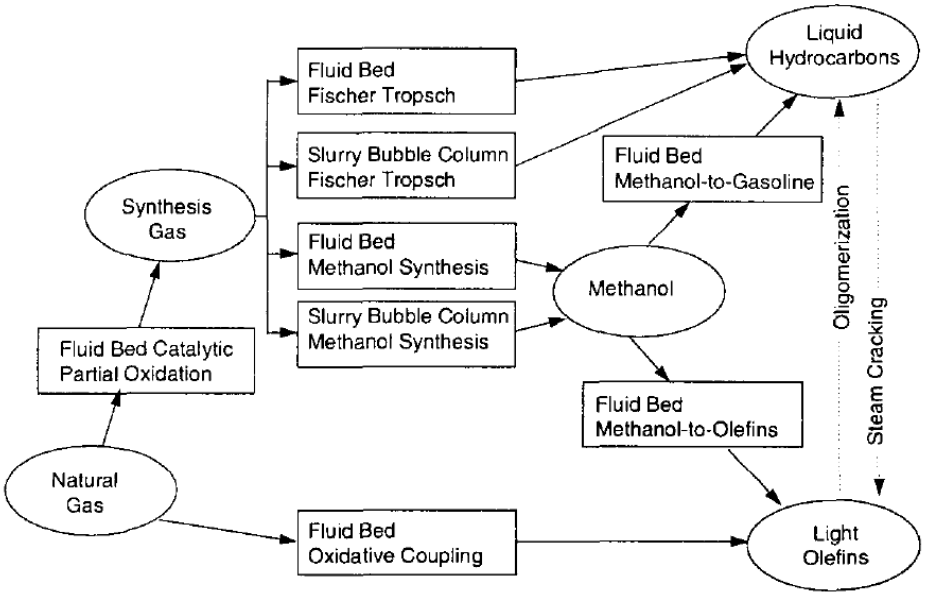

Figure 3: Liquid Fuel Production from Natural Gases (Krishna, 1998)

Synthetic gas, also known as syngas, is another form of synthetic fuel. Syngas is composed of hydrogen and carbon monoxide. The hydrogen can be captured and used immediately as a fuel or can participate in reactions to create other liquid fuels.

1.3 Waste Generation

Solid waste generation is a growing problem for the United States. As the population grows, larger amounts of waste products are generated. This waste is typically incinerated or stored in landfills. Figure 4 depicts the growth of municipal solid waste production over the past few decades.

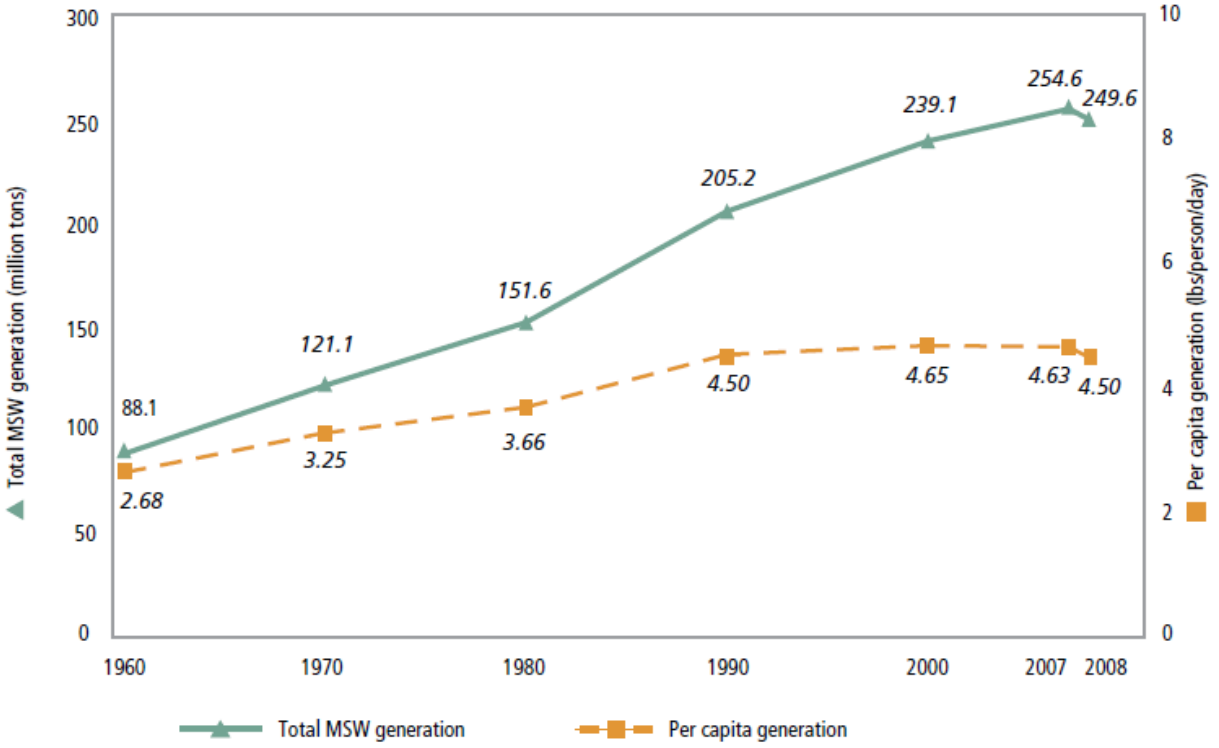

Figure 4: Municipal Solids Waste Generation from 1960 to 2008 (The Environmental Protection Agency, 2009)

In 2008, American families generated 249.6 million tons of solid waste. Of this waste, 82.9 million tons were recycled, 135 million tons were discarded in landfills, and 31.7 million tons were incinerated.

Responsible disposal of waste is critical to maintaining a healthy society. Waste that accumulates in living areas can attract unwanted pests and disease. As population density increases, especially in cities, disposing of waste becomes a more pressing matter. As the volume of waste increases, the prospect of recovering a portion of energy or producing energy from waste becomes more enticing. Currently, processes such as incineration allow for the recovery of a portion of the energy within wastes. However, modern research aims to develop new methods of capturing energy from waste. The process of breaking down biomass and plastics into useable fuels is one of these possible solutions. Processes that produce fuel from biomass and plastics not only add to the repertoire

of methods used to produce clean and renewable fuel, they may also assist in reducing a large portion of the waste generated by the general population.

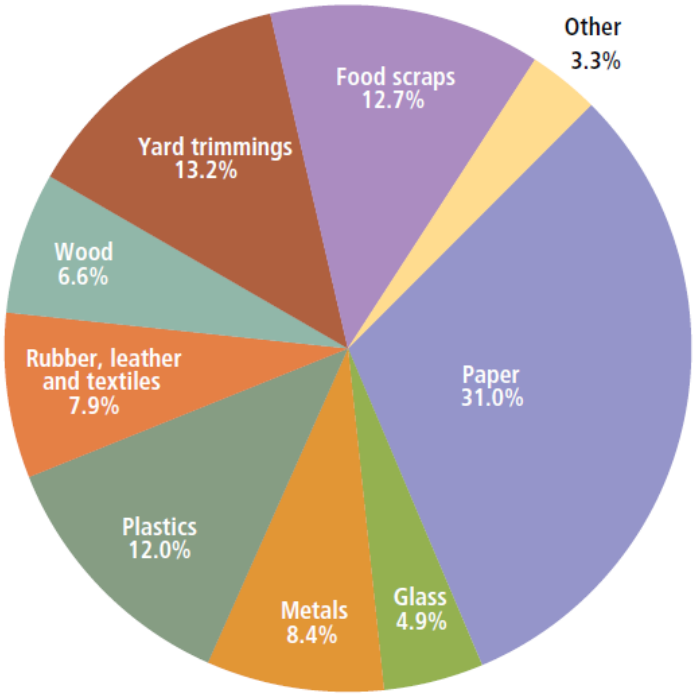

Figure 5: Total Municipal Solids Waste Generation by Material, 2008 (EPA, 2009)

Processes capable of breaking down biomass and plastics can be applied to nearly all municipal solid waste. Most of the categories of waste shown in Figure 5 can potentially be processed in a bioreactor to decompose materials into useable fuel via several different reaction pathways.

1.4 Pollution Reduction

The rise of industry in the past two centuries has contributed to an increase in pollution. The topics of global warming, acid rain, and air quality have been debated for decades.

1.4.1 Greenhouse Gas Emissions

Global warming and greenhouse gas emissions have recently become a topic of interest in recent years. The most common greenhouse gases are carbon dioxide, methane, nitrous oxide, and fluoridated gases (The Environmental Protection Agency, 2010).

Most of these gases are stored underground and released during the refining of natural gases, oil, and coal. Livestock and the decay of waste in landfills also produce greenhouse gases. By releasing greenhouse gases that have been stored underground via refining processes, human pollution may

permanently affect the global climate in some unforeseeable manner. Unfortunately, current theoretical predictions and computing power are simply too limited to accurately predict exactly how these gases will affect the earth's atmosphere.

Technologies such as carbon dioxide sequestration and gas scrubbers have begun to reduce the amount of these gases emitted into the atmosphere. However, there is still a net increase in greenhouse gas emissions every year due to rising energy demands.

The advantage of biomass processing is that the carbon released by burning biofuel was originally fixated in the same ecosystem. Therefore, this process is carbon neutral. Plants capture carbon dioxide from the atmosphere and it is processed by photosynthesis for growth in the forms of lignin and celluloses. The bonds within these structures are broken during the burning of biofuel to produce energy. An increase in the use of biomass for fuel will result in a decrease in greenhouse gas emissions in the atmosphere.

1.4.2 Effects of NO_x and SO_2 in the Atmosphere

The production and burning of coal leads to a buildup of NO_x and SO_2 in the atmosphere (Environmental Protection Agency, 2007). These emissions can be reduced through scrubbing technologies. Figure 6 shows the pathway of acid rain production from greenhouse gas emission in the environment.

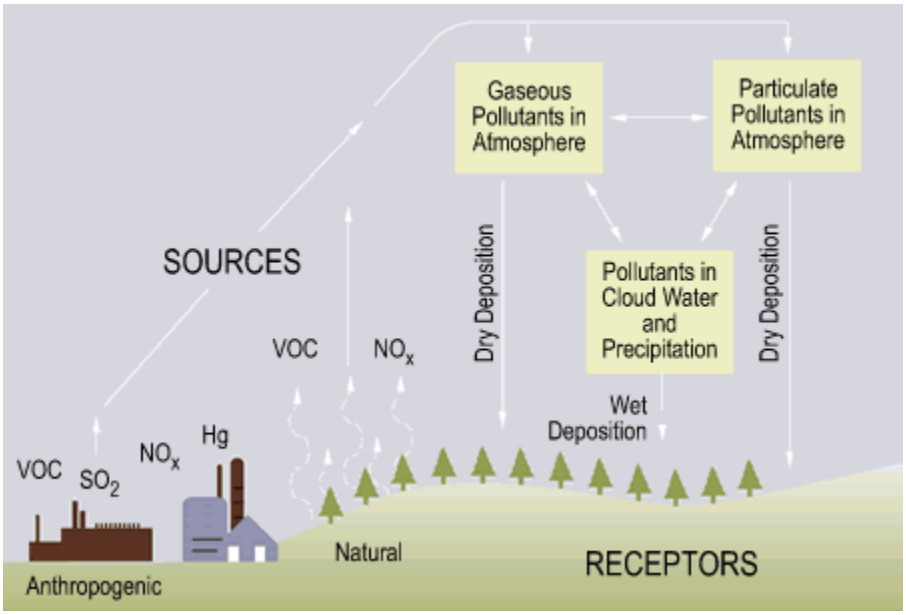

Figure 6: The Production of Acid Rain (EPA, 2007)

If NO_x and SO_2 emissions are released in a humid atmosphere, acids are formed. These acids can precipitate and may seriously harm or kill local plant and animal wildlife. If these emissions are released in a dry atmosphere, particulates may absorb NO_x and SO_2 and fall to the ground. Groundwater streams may absorb these pollutants, harming surrounding plant and animal life.

In short, fossil fuels are an attractive resource to satisfy the increasing demand for energy in the world. These fuels are finite and will eventually be completely exhausted. Additionally, fossil fuels contribute to pollution and may contain harmful chemicals. The increased use of renewable energy sources will help alleviate these problems and begin to foster a more sustainable lifestyle for populations everywhere. Energy derived from biomass is beneficial because it is a carbon neutral source and may also alleviate the growing concern of producing and accumulating solid waste.

2 Literature Review

2.1 Biomass

Mankind has been burning wood, a form of biomass, for thousands of years as a primary means to heat and cook. Until the mid 19th century, wood accounted for 90% of the energy consumed in the United States of America (The Need Project, 2008). Over the past century, this biomass derived fuel has been replaced by fossil fuels, such as coal and petroleum, as the dominant source of energy consumption. However, biomass is reemerging as an energy source to satisfy the demand by industry and individuals. Lignocellulosic biomass sources, such as unused wood and tree bark from forests, the stems and leaves of harvested crops, and leftover urban residues such as wood from construction, are simply burned or discarded. Little effort is made to recover the energy stored in biomass. It is estimated that these biomass sources contain the energy equivalent of 3.8 Billion barrels of oil (The Need Project, 2008).

2.1.1 Forms of Biomass

Biomass is derived from solar energy that has been converted and stored in bonds between sugar monomers. Sugars, such as sucrose, are small carbon backbone rings that contain oxygen and hydrogen. The structure of the sucrose compound is shown in Figure 7. The energy stored in these compounds is contained in breaking the bonds between atoms.

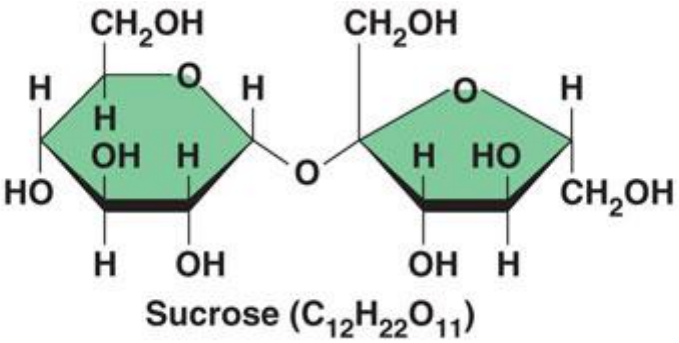

Figure 7: Sucrose Structure (Bio Miami, 2009)

Cellulose also stores energy within bonds between molecules. Cellulose is a polymer consisting of hundreds to thousands of glucose molecules bonded together. This polymer is the primary constituent of the cell wall found in all plant cells. All parts of plants contain cellulose, the bonds of which can be used for energy production. Paper and cardboard also contain cellulose, meaning these

materials can be processed to extract energy. Hemicellulose is closely related to cellulose. Hemicellulose has a more random structure and is less rigid. It is also found in the cell walls of plants. Many types of rapidly growing grasses and trees are being planted in order to harvest the cellulose and hemicellulose content. Figure 8 shows the contents of the cell wall including cellulose and hemicellulose.

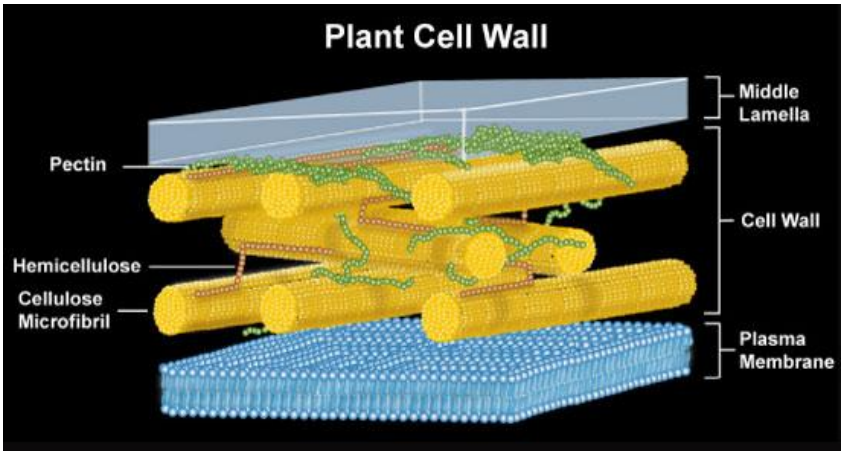

Figure 8: Plant cell wall containing cellulose (Sigma-Aldrich, 2009)

Lignin is also found is the cell walls of plant cells. Lignin is composed of a complex arrangement of carbon rings and has a varied structure. Lignin fills the spaces between cellulose and hemicellulose and acts like an adhesive that helps hold the components of the cell wall in place distributing force onto the cellulose fibers. The structure of lignin can be seen in Figure 9.

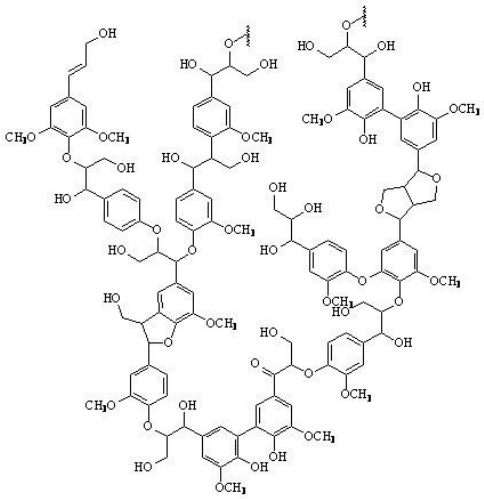

Figure 9: Structure of lignin (Gregory, 2009)

This project will focus on breaking down the cellulose, hemicellulose, and lignin in biomass to form syngas and liquid products. These structures are found in waste products, making the breakdown of these materials economically sustainable and environmentally desirable. For example, rather than just burning or discarding the unused stems of harvested crops, the energy stored in those plant cells can be recovered.

2.1.2 Biomass Cycle

The burning of biofuel is a carbon neutral process. CO_2 is removed from the atmosphere and becomes part of the plant through photosynthesis. Biomass gasification will transform energy derived from organic material into syngas or liquid fuel. These fuels will release carbon once fixated in plants back into the atmosphere. The net result is no CO_2 added or removed from the system. This is in contrast with burning fossil fuels, which releases CO_2 once trapped underground for thousands of years. Because fossil fuels are not renewable, the net result is the addition of CO_2 to the carbon cycle detailed in Figure 10.

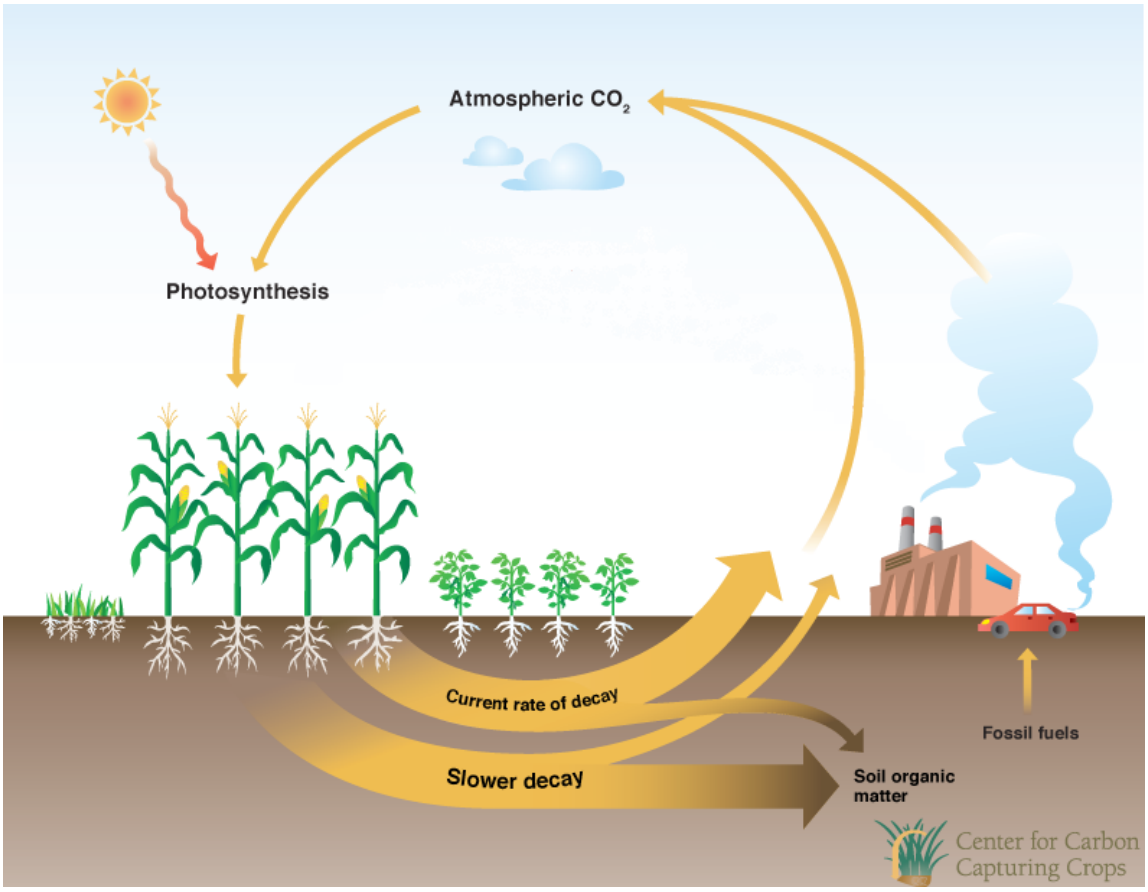

Figure 10: Carbon Cycle (IAState, 2009)

2.1.3 Feasibility of Using Biomass for Fuels

Financial, economical, and technological barriers still exist barring biomass from being utilized as the sole provider of energy.

Growing Biomass

One of the largest problems with using biomass as a main source for fuel is the amount of land needed to grow enough biomass to accommodate fuel consumption. Table 2 lists estimates of the amount of land needed to satisfy the US energy demand for diesel and motor gasoline use.

Table 1: Equivalent Land Required for Meeting US Energy Requirements (Akinci, 2008)

Plant	Land area needed to replace transportation diesel consumption		Land area needed to replace sum of diesel and motor gasoline consumption	
	(km^2)	(% US land)	(km^2)	(% US land)
Corn	12,166,420	133	45,917,664	501
Oat	9,640,060	105	36,382,849	397
Cotton	6,462,018	71	24,388,503	266
Soybean	4,704,349	51	17,754,830	194
Safflower	2,693,330	29	10,164,979	111
Sunflower	2,205,164	24	8,322,577	91
Peanut	1,982,170	22	7,480,968	82
Rapeseed	1,764,131	19	6,658,061	73
Jojoba	1,154,536	13	4,357,370	48
Microalgae	120,831	1	456,032	5

Data from Tickell (2000), USDA. Agricultural Research Service (2002), U.S.DOE, EIA, Annual Energy Review (2006), Central Intelligence Agency, (2001), and NREL (1998a, b).

To satisfy only the diesel needs of the US with corn derived biodiesel, 133% of the total US land would be needed just to grow to crop. In contrast, 501% of US land area would be needed to satisfy both diesel and gasoline demand. Therefore, corn would not be a suitable crop to meet energy demands. However, other types of biomass, such as rapeseed, jojoba, and microalgae, have potential for feasible fuel production should effective gasification, hydrolysis, pyrolysis or biocatalysis processes be developed (Akinci, 2008).

Processing Biomass

Biomass requires both a large amount of land for growth and extensive resources to harvest, fertilize, transport, and process the crop. Figure 11 displays data from a number of sources comparing energy input versus output for ethanol production and use. The net energy gain of using ethanol fuel is shown to be small, if any, using current processing technologies (Akinci, 2008).

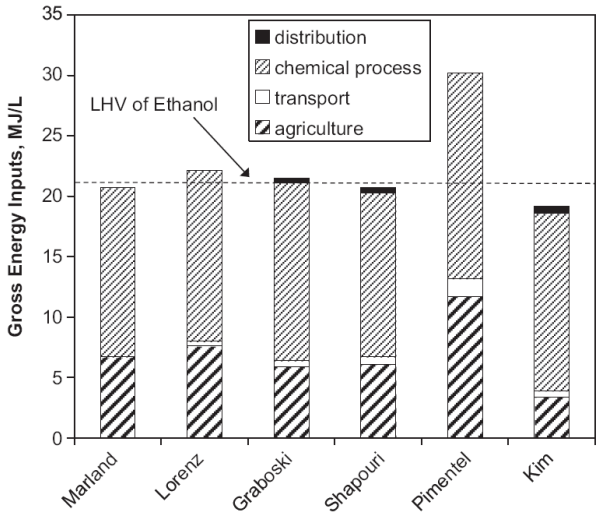

Figure 11: Ethanol Energy Requirements (Akinci, 2008)

2.1.4 Microalgae

The low land area dependence of microalgae has made it one of the top considerations in biodiesel production from biomass. Microalgae have the advantage of being able to be grown in water. Therefore, the large area of unused ocean, pond, and even wastewater could be used to cultivate microalgae.

A major issue in growing a sustainable population of algae is choosing a strain which would survive in large open bodies of water. There are concerns that undesired algal strains could outcompete microalgae in proliferation. For example, microalgae could be fed upon by zooplankton, or other unknown factors could result in the spoil of microalgae crops. An algal strain which survives in an extreme environment could be used to prevent extinction of the species. Therefore, only the desired species would survive in these extreme environments. *Spirulina* is a strain of algae that grows in high alkalinity water, which makes it a possible candidate for selection. Unfortunately, this extremophile has low reproduction rates and other strains are being investigated for faster crop production. An added benefit of microalgae is that it could be used to simultaneously treat wastewaters. Municipal, agricultural, mining, etc. wastewater streams contain nutritional properties, which would allow for algal growth (Schulz, 2006).

2.2 Plastics

The use of plastics is widespread throughout industry. Plastics are polymers, such as polyethylene, that are derived from crude oil. Producing plastic is a relatively cheap process and saves

energy as compared to other shipping and storage containers (Guillet, 2002). Many different types of plastic are discarded as waste. Packing materials are the most common source of plastic wastes. These materials are primarily made from polyolefins such as polyethylene, polypropylene, polystyrene, and polyvinyl chloride (PVC) (Scott, 1990).

Plastics are typically disposed in landfills. This process is becoming more expensive as landfills reach their capacity. Incineration of plastics severely pollutes the environment (Scott, 1990). It is estimated that in the UK alone, the amount of plastic wastes in 2010 may be as high as 35 megatons (Miskolczi, 2004). Approximately 65-70% of plastics are disposed in landfills, 20-25% of plastics are incinerated, and only 10% are recycled. Possible methods of degrading plastics to obtain useable fuels have been studied by many different researchers. Most methods involve the thermal degradation of plastics, applying heat to break the polymers into smaller components (Miskolczi, 2004). The breakdown of plastics into useable fuels may provide an adequate and environmentally friendly method of disposing of plastic waste while capturing energy as a product.

2.3 Versatile Reaction Systems

Biomass and plastic can be converted into useable fuels through many different methods. Fuel can be produced in gaseous and liquid states by many different mechanisms. An efficient reaction system will be able to breakdown biomass and plastic with varying feedstocks to produce a desired fuel. There exist processes capable of processing both plastics and biomass (Lemley, 2003). Systems exist that may process everything from turkey offal to old computer components, converting them into gaseous and liquid products. Researchers have already begun working on “recipes” that they can use to create specific products (Lemley, 2003). This serves as a major advantage in that the reaction system is capable of processing nearly any feedstock.

An ideal system would be capable of processing nearly all municipal wastes. In addition, the system should be easily controlled to yield the desired products. Small changes in starting conditions and feedstocks, as well as reaction conditions, should be able to produce different products. If a versatile system can be constructed, nearly all waste products could be converted into potential fuel systems. This will drastically reduce problems such as landfills, land and ocean pollution from plastics, as well as reduce harm to wildlife that may be affected by pollution.

For these reasons, research into literature suggests that if a universal reactor and flow system could be designed, it could be used to process various feedstocks into desired products.

2.3.1 Microwave Reactors

It is believed that biomass and plastics may be reacted more rapidly by using Continuous Microwave Reactors (CMR's) as opposed to conventional heating methods.

Extensive research on continuous microwave reactors has been completed by Teresa Cablewski, et al (1994). Continuous laboratory-scale microwave reactors have been used for organic synthesis. Most reactors have withstood a maximum of 1400 kPa and 200°C for chemical reactions. Older reactors did not have a means to easily control nor monitor the temperature and pressure of the system. However, this limitation has been overcome and is now standard in all microwave reactors. Even though the reactors are not very popular commercially, microwave reactors used for organic synthesis have become increasingly popular since the 1980's.

The continuous microwave reactor (CMR) functions by passing the reaction mixture through a pressurized microwave-transparent coil that is located in the microwave cavity. A figure of the CMR is shown in Figure 12.

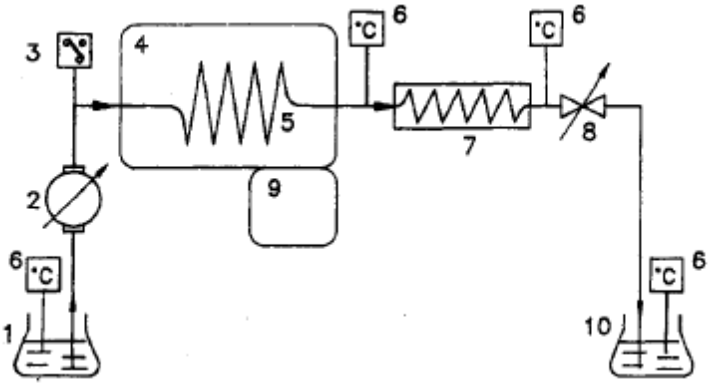

Figure 12: CMR (Cablewski, Faux, Strauss, 1994)

The reaction mixture (1) is pumped through a pressure sensor (6) and into the microwave cavity (4, 5). The microwave reactor has an electrical keypad and display (9). The mixture flows out of the cavity and through a temperature sensor to the heat exchanger (7). The flow comes out of the heat exchanger, through another temperature sensor, and through a pressure control valve (8). The flow finally progresses out of the valve and collects as product (10).

To ensure that a CMR remains safe and operable, many specifications must be met. There must be a means to determine and control the temperature and pressure of the reaction mixtures within the

vessel while the reaction is in progress. In addition, if the reaction were to runaway or malfunction (due to blockages or ruptures in the reaction coil), there must be a fail-safe mechanism for the reactor to shut down quickly. The microwave reactor does have the disadvantage of processing only low volumes of reactants and operating as a batch system. Finally, the CMR must have the potential to scale up or down depending on the chemical process.

The development made in microwave reactor technology allows it to become a possible method for processing biomass due to rapid heating rates.

2.4 Biomass and Plastic Reactions for the Production of Fuels

Biomass can be broken down by various processes, aided by catalysts, to produce a number of different products. These products can be further refined for use as renewable energy. Figure 13 shows the known chemical and biochemical pathways in which biomass can be broken down into basic hydrocarbon molecules. Blue boxes in Figure 13 indicate intermediate products. Red boxes indicate chemical pathways discussed below. Green boxes indicate the final clean energy product.

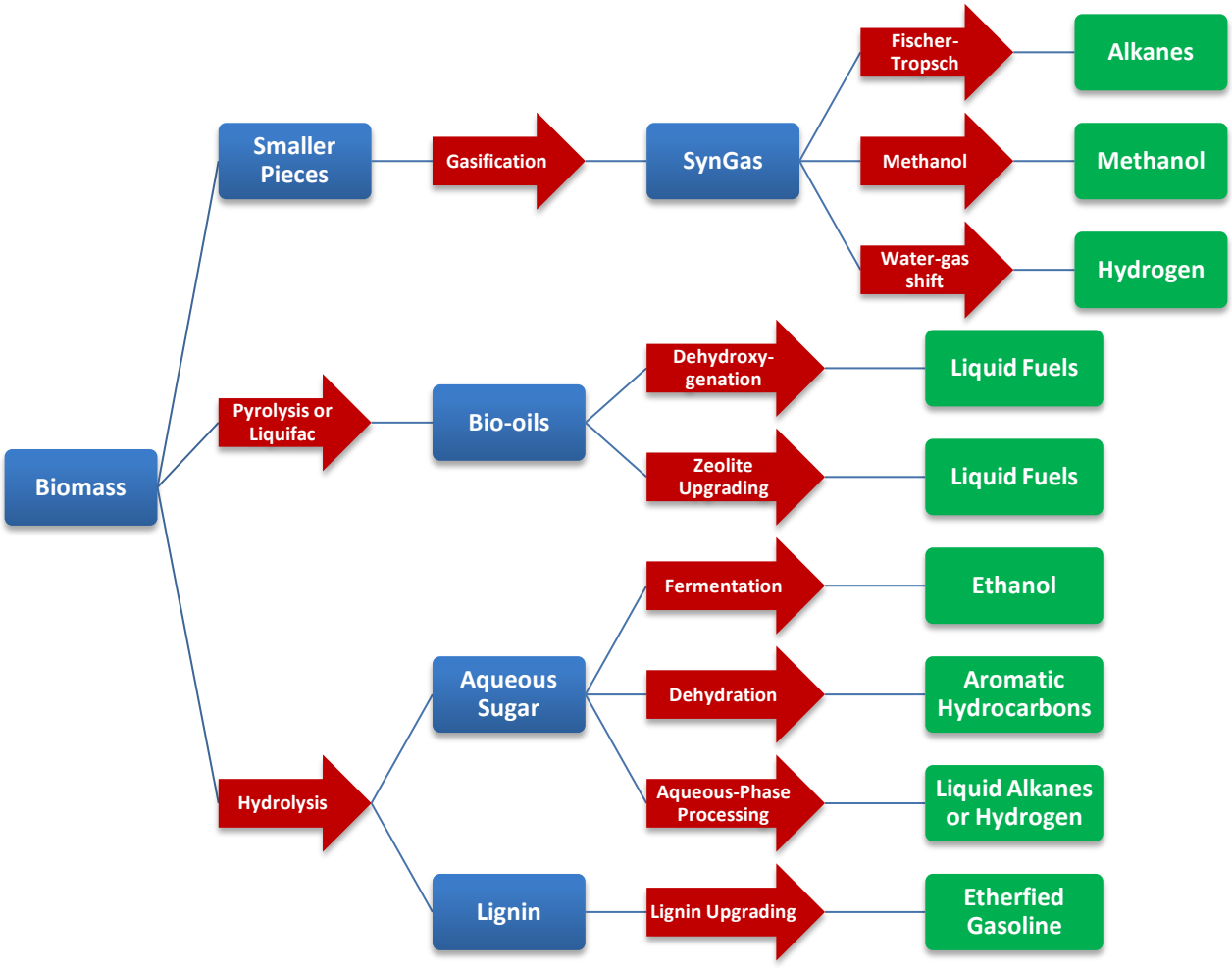

Figure 13: Biomass Breakdown Pathways

2.4.1 Hydrolysis

Hydrolysis is the process of cleaving organic material with water. Specifically, hydrolysis excels at breaking down polymers into smaller components. In liquid biomass, the cellulose and hemicellulose can be broken down into simple sugar monomers. Acids that have stronger effects due to low pH levels which usually catalyze this breakdown of polymers. Once broken down into simple sugars, the mixture is typically used in a yeast fermentation process. Yeast fermentation produces ethanol, which may be used as a fuel. This process is often aided by an organic or inorganic catalyst. Hydrolysis of biomass results in products that can be further processed using other techniques to yield a variety of gaseous and liquid fuels (Talebnia, 2009).

The most common form of hydrolysis is when a compound is split into two parts by a water molecule. One part of the compound receives the hydrogen ion from the water while the other portion obtains the hydroxyl group.

The mechanism of base catalyzed hydrolysis involves the nucleophilic attack of deprotonated water (hydroxide group) on the central carbon atom bound to a carboxyl group. This new bond that is formed, transforms the double bond of the carboxyl group into a single bond, moving the lone pair of electrons to the oxygen atom. This is a resonance-stabilized hybrid. Next, the lone pair of electrons on the oxygen reforms a double bond to the carbon molecule. To maintain four bonds on carbon, a side group, preferably a good leaving group such as an ester, is cleaved. This yields the final product of the hydrolysis reaction. Acid catalyzed hydrolysis occurs similarly with the exception of the hydronium ion attacking the carboxyl group, facilitating cleavage.

2.4.2 Pyrolysis

Liquid fuels can be obtained from bio-oil. Figure 13 shows that processes such as pyrolysis or liquefaction can ultimately lead to the production of biofuel.

Pyrolysis is achieved by feeding biomass to a reactor and heating to between 450°C and 550°C (Huber, 2006). The high temperatures of the reactor break the biomass down into smaller components, which then liquefy. The negative aspect of this reaction is a buildup of char in the system. This poses a problem during production because this char is difficult to remove and can damage equipment. On a large scale, char is an issue because it can damage equipment (such as pumps) and will require frequent costly maintenance to clean (Demirbas, 2000).

The following is an accepted mechanism behind the hydrogeneolysis of cellulose, which takes place at temperatures above 535K (Demirbas, 2000):

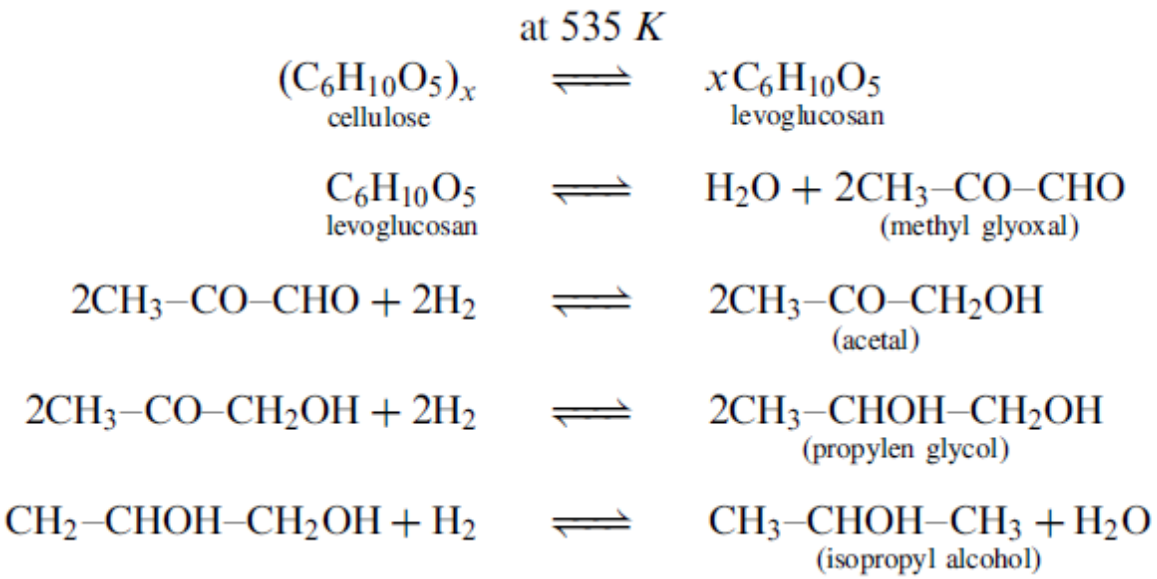

Figure 14: Hydrogeneolysis of Cellulose (Demirbas, 2000)

Here, cellulose undergoes rapid decomposition with a weight loss that increases with rising temperature. Finally, decomposition via pyrolysis occurs.

A.V. Bridgewater has studied the production of high-grade fuels from fast or flash pyrolysis. This research found that fast heating rates and low vapor residence times (less than one second) cause products containing 85% liquids to form. Hydrotreating the biomass and zeolite catalysts were used in the experiments (Bridgewater, 1996).

The following Pyrolysis mechanism behind degrading lignin, as shown in Figure 15, has been proposed by Demirbas et al using free radicals.

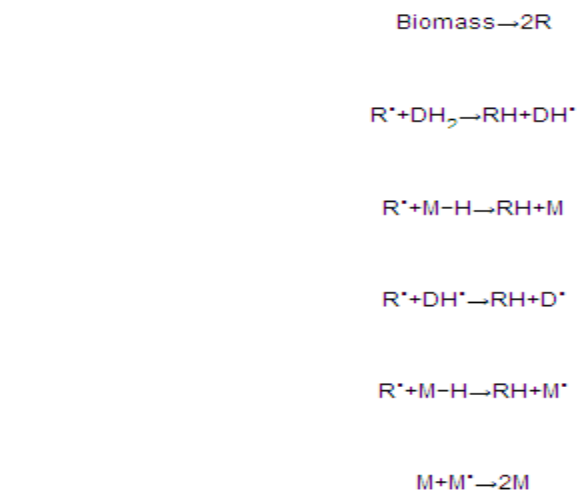

Figure 15: Decomposition of Lignin Via Pyrolysis (Demirbas, 2000)

Pyrolytic reactions are primarily connected with C-O bond cleavage. A specific example of this mechanism can be seen from the methyl radical formed from the methyl C-O bond cleavage which abstracts hydrogen from guaiacol (a component of biomass) to form methane, as shown in Figure 16. This may subsequently combine with another methyl radical to form ethane (Demirbas, 2000).

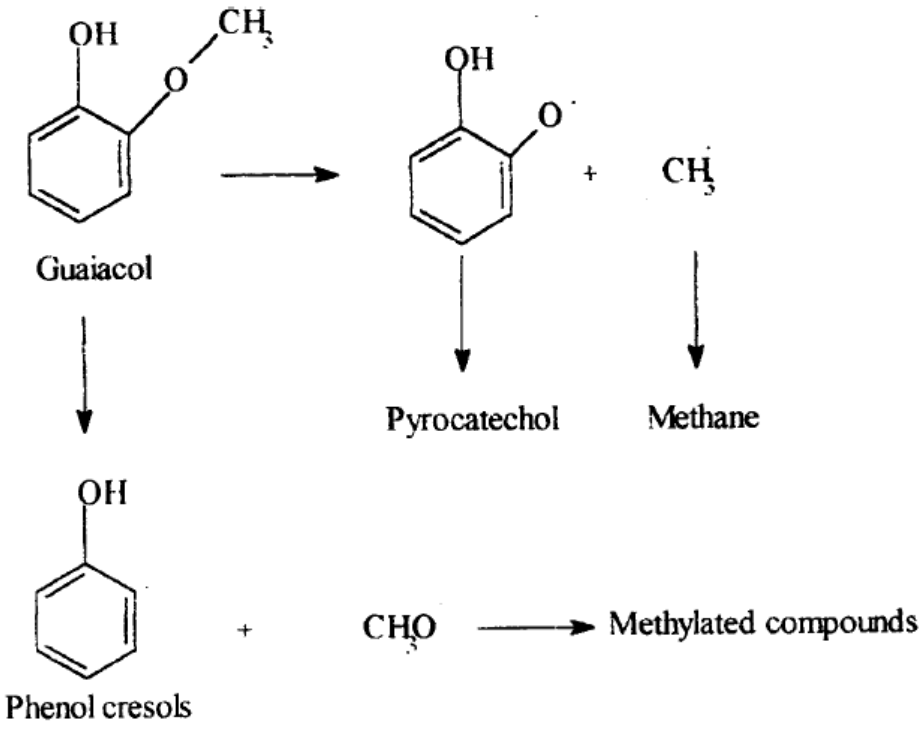

Figure 16: Decomposition of Guaiacol using proposed Pyrolysis Mechanism (Demirbas, 2000)

In short, further research is needed to discover the complicated mechanisms behind the breakdown of lignin, cellulose, and hemicelluloses. The products of this gasification project will further elucidate possible mechanisms and reaction shifts that are taking place within the reaction vessel.

2.4.3 Gasification

Gasification is the process of breaking down biomass into syngas (Alden, et. al, 2009). Syngas contains CO, H_2, CO_2, CH_4, and N_2, which can be used as a fuel in many different applications. Biomass gasification is principally the incomplete combustion of biomass with controlled oxygen to produce CO, H_2, and CH_4.

Pyrolysis and partial oxidation reactions act to degrade biomass into gases (Huber, 2006). Pyrolysis simply breaks down the biomass into char and gas due to the intense heat of the reaction. Due to the low oxygen level in the reactor, oxidation is not complete and carbon monoxide is formed rather than carbon dioxide. Additionally, hydrogen gas is formed instead of water, which is normally observed in combustion reactions (Huber, 2006). Examples of pyrolysis reactions and partial oxidation reactions of biomass can be found in Table 2. Hydrogen and carbon monoxide produced via pyrolysis and partial oxidation of biomass may then react via the water gas shift reaction:

$$CO+H_2O \rightarrow CO_2+H_2 \quad (1)$$

or the methanation reactions:

$$(2n+1)H_2+nCO \rightarrow C_nH_{2n+2}+nH_2O \quad (2)$$

The water gas shift reaction converts carbon monoxide into both carbon dioxide and hydrogen gas using steam. The methanation reaction uses hydrogen gas and carbon monoxide, both created in the reactor, to form methane and steam. The methanation reaction is the simplest form of the Fischer-Tropsch reactions.

One of the disadvantages of gasification reactions includes the formation of char, which is usually treated as a waste product. However, the following reforming reaction with steam is expected to occur within the reactor and will act to reduce the amount of char (Huber, 2006):

$$C+H_2O \rightarrow CO+H_2 \quad (3)$$

The Boudard reaction is a major step in the gasification of biomass:

$$C + CO_2 \rightarrow 2CO \quad (4)$$

In the reaction above, carbon from biomass reacts with a carbon dioxide feed gas to produce carbon monoxide. This carbon monoxide can then be processed in a reforming step with water to produce hydrogen gasses via equation (1) above.

In this reaction, steam is expected to react with the char inside of the reactor to form additional carbon monoxide and hydrogen gases. Carbon in char will react via the Boudard reaction with carbon dioxide. Table 2 is an overview of the various pyrolysis and gasification reactions, which contribute to the production of gases in the reactor system (Huber, 2006).

Table 2: Pyrolysis and Gasification Reactions to Produce Syngas (Huber, 2006)

classification	stoichiometry	enthalpy (kJ/g-mol) ref temp 300 K
pyrolysis	$C_6H_{10}O_5 \rightarrow 5CO + 5H_2 + C$	180
	$C_6H_{10}O_5 \rightarrow 5CO + CH_4 + 3H_2$	300
	$C_6H_{10}O_5 \rightarrow 3CO + CO_2 + 2CH_4 + H_2$	−142
partial oxidation	$C_6H_{10}O_5 + {}^1/_2\, O_2 \rightarrow 6CO + 5H_2$	71
	$C_6H_{10}O_5 + O_2 \rightarrow 5CO + CO_2 + 5H_2$	−213
	$C_6H_{10}O_5 + 2O_2 \rightarrow 3CO + 3CO_2 + 5H_2$	−778
steam gasification	$C_6H_{10}O_5 + H_2O \rightarrow 6CO + 6H_2$	310
	$C_6H_{10}O_5 + 3H_2O \rightarrow 4CO + 2CO_2 + 8H_2$	230
	$C_6H_{10}O_5 + 7H_2O \rightarrow 6CO_2 + 12H_2$	64
water-gas shift	$CO + H_2O \rightarrow CO_2 + H_2$	−41
methanation	$CO + 3H_2 \rightarrow CH_4 + H_2O$	−206

Thus, gaseous products should be produced due to pyrolysis followed by various reforming steps. Table 2 demonstrates that pyrolysis, as well as partial oxidation reactions, is expected to liberate carbon monoxide, hydrogen, and char from the biomass. If present, steam will also contribute to gasification by directly degrading the biomass into carbon monoxide, carbon dioxide, and hydrogen gas. Subsequently, the water gas shift and methanation reactions will convert carbon monoxide into carbon dioxide, hydrogen, steam, and methane gases. The Boudard reaction and a steam reforming process can be expected to convert char into carbon monoxide (Huber, 2006). The project group will investigate running these processes in a continuous flow system to determine if the production of char can be eliminated due to the reforming reactions.

2.4.4 Enzymatic Biocatalysis

An additional method of biomass breakdown not detailed in Figure 13 is enzymatic biocatalysis. Enzymatic biocatalysis is a biochemical process in which enzymes are used as catalysts to perform alterations to organic compounds. Biomass may be subject to enzymatic biocatalysis in a process called hydrolysis in which enzymes isolated from living organisms can be used to break down bonds in cellulose, hemicelluloses, and lignin, the three major components of plants.

To ensure that the biological process of converting biomass to biofuels is effective, several conditions must be met. First, cellulose and hemicellulose must be liberated from their complex with lignin. Second, depolymerization of the carbohydrate polymers must occur to produce free sugars. Finally, fermentation of mixed hexose and pentose sugars must occur to produce ethanol. If lignin-degrading microorganisms, their necessary living environments, and optimal bioreactor design conditions are all met, this process would be possible. Recent research (Lee, 1997) dictates that some thermophilic anaerobes and recombinant bacteria may act as biocatalysis agents in direct microbial conversion of cellulose to ethanol. However, new fermentation technology in converting xylose to ethanol needs to be further developed to make the overall conversion process more cost-effective.

Goals of Pretreatment

The overall goal of pretreatment is to remove lignin and hemicelluloses, increase the porosity of the lignocellulose materials to allow for greater contact between reagents, and to reduce the crystallinity of cellulose to ease in the breaking of bonds.

Essentially, pretreatment must meet the following conditions to remain effective and beneficial as a process (Kumar, 2009):

1. Improve the formation of sugars
2. Avoid degradation of carbohydrates
3. Avoid formation of inhibitory byproducts
4. Be cost effective

Techniques that follow these requirements are varied and include physical pretreatment, pyrolysis, physicochemical pretreatment, ammonia fiber explosion (AFEX), carbon dioxide explosion, chemical pretreatment using ozonlysis, acid hydrolysis, oxidative delignification, biological pretreatment, and pulsed-electric-field pretreatment.

Conversion of Celluloses

The most frequently cited and utilized method for the conversion of cellulose to glucose comprises of endo-1, 4-β-glucanase, exo-1, 4-β-glucanase, and most commonly, β-glucosidase. Cellulolytic enzymes with β-glucosidase act sequentially to degrade cellulose to glucose. B-Glucosidase hydrolyzes cellobiose to glucose. This particular enzyme is responsible for the regulation of the cellulolytic process and is the rate limiting factor during enzymatic hydrolysis of cellulose. For complete hydrolysis of cellulose to glucose, these three enzymes must be in the proper proportions (Saha, 1997).

Total hydrolysis of hemicelluloses requires endo β-1,4-xylanase, β-xylosidase, and other accessory enzymes. Lignin has a high tolerance for microbial attack and only a few organisms can function to degrade it. Removal of lignin from lignin-carbohydrate complex (LCC) has been shown to be catalyzed by the basidiomycete *Phanerochaete chrysosporium*, however findings on organisms functioning as effective lignin degraders are limited. (Saha, 1997). Figure 17 lists lignin-degrading cultures which have been shown to break down lignin to an extensive amount for ethanol production (Lee, 1997).

Recent examples of lignin-degrading cultures

Fungal strain	Comment	References
Basidiomycetes		
Phanerochaete chrysosporium	Production of lignin peroxidase and Mn-dependent peroxidase	Venkatadri and Irvine, 1993 Bonnarme et al., 1993 Schoemaker and Leisola, 1990 Linko, 1988 Zhong et al., 1988 Pellinen et al., 1989
Phanerochaete chrysosporium PSBL-1 (mutant)	Overproduction of lignin peroxidase and Mn-dependent peroxidase under nutrient-rich conditions	Tien and Myer, 1990
*Coriolus hirsutus**	Degradation of wheat straw and pine wood	Arora and Garg, 1992
*Daedalea flavida**	Best decomposer*	
*Polystictus sanguineus***	Best laccase producer**	
Daldinia concentrical		
Postia plancenta		
Phlebia radiata *Phlebia tremellosa*	Production of lignin peroxidase, Mn-dependent peroxidase, and laccase under N-limited condition	Hatakka and Niemenmaa, 1991
Phlebia radiata Fr. 79	Production of lignin peroxidase, Mn-dependent peroxidase, and laccase under N-limited condition	Niku-Paavola et al., 1990
Phlebia tremellosa	Delignification of aspen wood	Reid, 1989
Coriolus versicolor	Delignification of wheat straw	Zafar et al., 1989
Rigidoporus lignosus	Production of laccase and Mn-dependent peroxidase	Galliano et al., 1991
Panus tigrinus 8/18	Production of Mn-dependent and various oxidases	Golovleva et al., 1991
Coriolus versicolor	Review on *Trametes versicolor* peroxidases	Lobarzewski, 1990
Actinomycetes		
Streptomyces viridosporus T7A *Streptomyces lividans* TK 64.1	Production of peroxidases	Korus et al., 1991
Streptomyces viridosporus	Degradation of wheat lignocellulose to release soluble lignin-rich fragments	Seelenfreund et al., 1990

Figure 17: Lignin Degrading Cultures (Lee, 1997)

Biological Pretreatment

Biological treatment using fungi is a safe and environmentally friendly method of digesting biomass (Kumar, 2009). During biological pretreatment, fungi are used to degrade lignin and hemicelluloses in waste material, which do not require high energy for lignin removal from lignocellulosic biomass. Digestion with fungi has shown to reduce lignin to sugars anywhere up to 77% by mass (Kumar, 2009), however the time taken to accomplish this is anywhere between one to two months, which is most likely undesirable on a commercial basis. The overall purpose of biological pretreatment with wood-rot fungi is to reduce the energy input required for the separation of wood

components by a process such as ethanolysis. This process has also been shown to increase yield up to 60%.

In short, biological pretreatment allows for low energy requirements and mild environmental conditions. However, this pretreatment entails a very low rate of hydrolysis, which makes large-scale time-dependent operations difficult, if not completely unfeasible.

Protein Digestion

It has been suggested that Proteinase K may be used to predigest biomass into simpler sugars and carbohydrates for use in pyrolysis and gasification. Proteinase K is a stable serine protease with broad substrate specificity (Sigma-Aldrich, 2010). It degrades proteins in even in the presence of detergents or other usually strong inhibitors. Proteinase K was isolated from a fungus and is able to digest native keratin (hair), hence its name. The predominant site of cleavage is the peptide bond adjacent to the carboxyl group of an aliphatic acid as displayed in Figure 18.

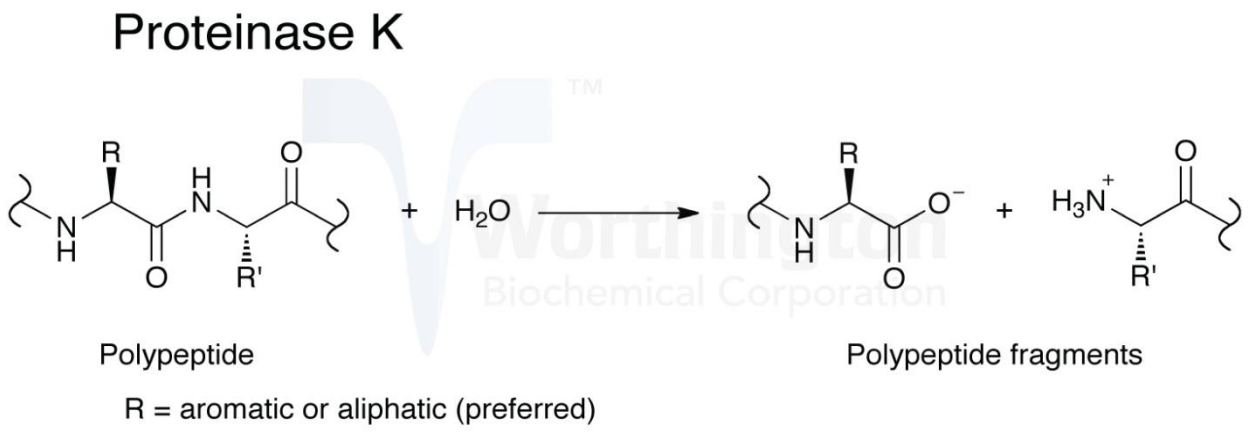

Figure 18: Proteinase K Digestion of Nucleic Acid Residue (Worthington, 2010)

Proteinase K is used to digest unwanted proteins, DNA, and RNA after an incubation time of between 30 minutes to 18 hours which is significantly less time than treatment with fungus.

In the case of digesting biomass, Proteinase K should prove to be useful in degrading most unprocessed forms, such as case examples with lima bean. In contrast, little digestion, if any, is expected with processed materials such as plastics or paper as they contain little protein content.

Proteinase K is active in buffers of 1% TRITON X-100 and 0.5% SDS in a pH range of 7.5-12.0 with a maximum activity at 37°C. Proteinase K is inhibited by DIFP and PMSF and inactivated by EDTA. One unit of Proteinase K will hydrolyze urea-denatured hemoglobin at 1.0µmol of tyrosine per minute.

2.4.5 Biodiesel Transesterification

Essentially biodiesel is some kind of organic (plant or animal) based diesel fuel, containing long chain mono-alkyl esters. The importance of biodiesel has only continued to increase based on the limited supply of fossil fuels. Biodiesel is also much more environmentally friendly in terms of emissions as compared to fossil fuels. Suppliers have begun to blend biodiesel with common petro diesel in order to economically begin the transition to green fuel.

Biodiesel is typically made by reacting fatty oils with alcohol. Vegetable oils consist of common fats such as soybean oil, jatropha oil, rapeseed oil, palm oil, sunflower oil, corn oil, peanut oil, canola oil and cottonseed oil. Animal fats can also be used in the biodiesel process. Some examples are beef tallow, lard, waste cooking oil, greases, and algae. The most common alcohol that is used is methanol.

The reaction that takes place to produce biodiesel is shown in Figure 19 where vegetable oil reacts with methanol over a catalyst to form biodiesel and glycerol.

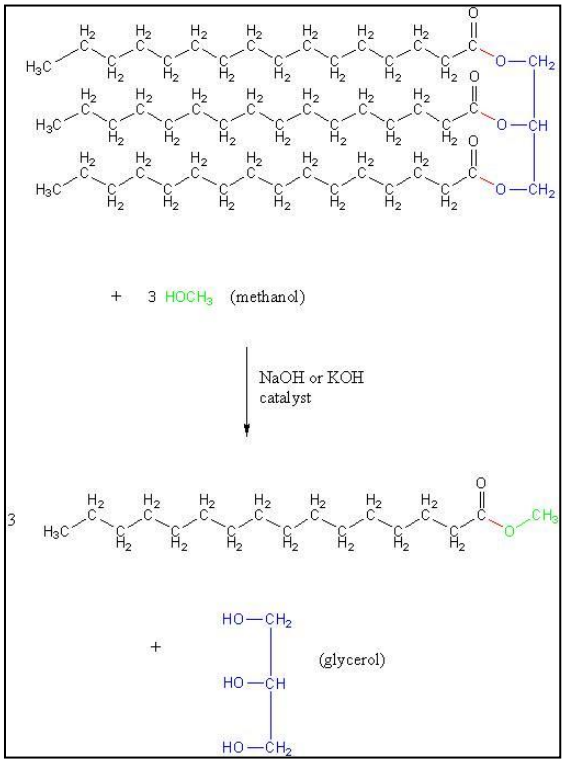

Figure 19: General Biodiesel Transesterification Reaction (Goshen Chemistry, 2010)

The fatty ester oil reacts with the alcohol in the presence of a catalyst, which is either the alkali salt KOH or NaOH. The alkali salts react with the oil and alcohol as the compounds undergo transesterification.

Transesterification may be base or acid catalyzed as a result of the pKa of the molten salt used. In base catalyzed transesterification, an anionic base, such as deprotonated methanol, attacks the carbon atom attached to the carboxyl group in the compound. This causes the double bond on the carboxyl group to move a lone pair of electrons onto the oxygen atom. The molecule is stabilized by resonance. Next, the lone pair of electrons moves back to the carbon atom forming a double bond. To retain only four bonds bound to the central carbon atom, the ester attached to the central carbon is cleaved, completing the transesterification process. Acid catalyzed transesterification undergoes a similar mechanism with the exception that the carboxyl group is protonated, facilitating the cleavage of the ester from the chain.

Transesterification yields glycerol byproduct and the biodiesel. (Ranganathan, S. V et al). In order to carry out this process efficiently, the temperature of the reaction must reach 60^{o}C.

Microalgae have been explored as an option in the use of biodiesel production. The fact that algae can take up many nutrients due to their high surface to volume body ratio is important. In addition, microalgae live in the water, which allows them to obtain many more nutrients, and can convert sunlight much more efficiently than land plants. This enables the algae to grow at a much more rapid rate than any other photosynthetic plant. (Schulz, T. 2006).

The main problem with most biodiesel production is that the cost effectiveness of producing high quantities is currently not competitive with fossil fuel alternatives. Figure 20 details the economic problems associated with algae biodiesel.

Assumption / Revenue (ha/pa)			**Cost (ha/pa)**	
Algae	~30 grams	*Cost Item (ha/pa)*	High Cost	Low Cost
Growth	day/sqm			
Price t/CO2	$ 27	*Land (5% pa)*	A$ 8,000	A$ 0
Oil per ha	220 barrel or ~35,000 per litre	*Pond investment (capital charge from 15% to 25% over 20 years)*	A$ 42,000	A$ 27,000
Oil price	A$ 80	*Operation & M*	A$ 16,000	A$ 8,000
Oil $$	A$ 17,600	*CO2 compression & transport*	A$ 6,400	A$ 0
Carbon $$	A$ 3,000	*Risk premium*	A$ 7,200	A$ 0
Revenue	**A$ 20,600**	**Cost**	**A$ 79,600**	**A$ 35,000**

Figure 20: Economic Estimates for the Production of Biodiesel from Algae (Schulz, 2006)

As can be seen in Figure 20, revenues are significantly less than costs, even with the low cost estimate for the microalgae biodiesel production.

Biodiesel has the potential to be the main fuel source of the future. However, methods must be perfected in order to maximize the production of useable fuel. Currently, the price of biodiesel is $0.15 higher per gallon than regular petro diesel. Additionally, land crop alternatives for biofuel production may compete with land area needed for agriculture. Microalgae could provide an answer to this problem, assuming that the ability to harvest from the sea becomes more efficient and cheaper.

2.4.6 Pyrolysis of Plastics

Previous research has shown that the production of liquid fuels is possible by subjecting plastics to pyrolysis. The work of Scott et al attempted the pyrolysis of various plastic polymers with a fluidized bed, as shown in Figure 21.

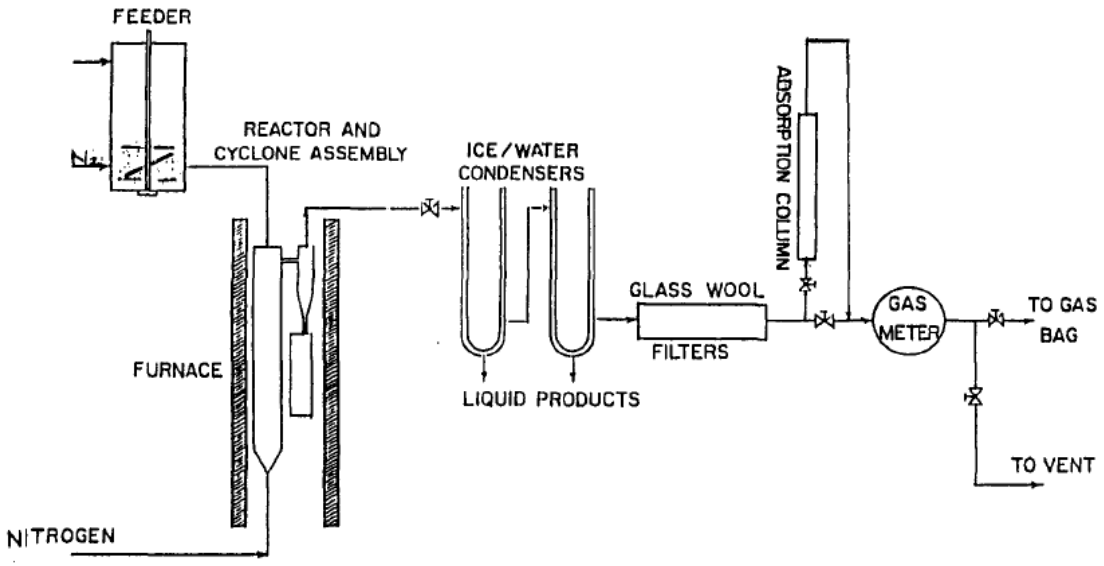

Figure 21: Experimental Pyrolysis Process (Scott, 1990)

Scott conducted experiments by continuously feeding crushed plastics to a fluidized bed reactor which was heated to high temperatures, usually above 600 °C, and atmospheric pressures in a continuous flow system (Scott, 1990). Downstream processes such as condensers and filters separated the gaseous and liquid products preparing the products for analysis.

These experiments formed many different liquid and gaseous products for all of the tested plastic polymers. Scott performed experiments on various types of plastics including poly(vinyl chloride) (PVC), polystyrene, polyethylene, and scrap plastics. Experiments involving PVC yielded primarily gaseous hydrochloric acid and were not continued due to corrosion of the reactor. Experiments involving polystyrene yielded mostly styrene with some other longer chain hydrocarbons. Polyethylene is the largest waste plastic available. It has undergone extensive testing in different reactions situations. The study concluded that nearly 80% of all polyethylene could be converted into liquid and gaseous hydrocarbons through pyrolysis reactions with a high amount of aromatic compounds (Scott, 1990).

2.4.7 Thermal Depolymerization

Thermal depolymerization of plastics is accomplished by heating plastic wastes in the presence of high-pressure steam. The process is simply pyrolysis in the presence of water (hydrous pyrolysis).

One company, Changing World Technologies (CWT), aims to reduce organic materials into a form of crude oil using thermal depolymerization (Lemley, 2003). CWT uses the following method for thermal depolymerization. The feedstock is grounded up and fed into the reactor at 250^{o}C where steam

pressure increases to 600psi. The reaction then sits for 15 minutes, and the pressure is rapidly released to remove the product (Lemley, 2003).

Plastic was not the only material used by CWT, however plastic did produce the highest amount of liquid products. Other materials used include medical waste, tires, turkey offal (intestines), sewage sludge, and paper. Table 3 presents data from CWT's process.

Table 3: CWT Process Data Table (Lemley, 2003)

Average TDP Feedstock Outputs				
Feedstock	Oils	Gases	Solids (mostly carbon based)	Water (Steam)
Plastic bottles	70%	16%	6%	8%
Medical waste	65%	10%	5%	20%
Tires	44%	10%	42%	4%
Turkey offal	39%	6%	5%	50%
Sewage sludge	26%	9%	8%	57%
Paper (cellulose)	8%	48%	24%	20%

The types of material used greatly affected product composition. This project will attempt to recreate the conditions of the Changing World Technologies reactor, using high pressure and temperature steam in a batch reactor system.

2.5 Molten Salts

Molten salts are inorganic salts that melt above 100°C. These salts are normally solid at standard temperature and pressure. Salts that are liquids at STP are called room temperature ionic liquids, which are usually organic (Wilkes, 2007). Even so, molten salts are technically a class of ionic salt. Molten salt eutectics can be used to increase reactivity of reactions as catalysts. Salts such as these may function as strong oxidizing agents, corroding agents, or agents of catalysis in breaking down of organic material (Jin et al, 2005). Molten salts are being studied for a variety of situations such as the removal of soot from biodiesel exhaust due to their high reactivity (Jelles at el, 1999). They have also been used in the steel and non-ferrous industrial heat treatments well as electrolysis (Mishra, 2004).

For the purpose of gasification and pyrolysis, it is believed that the ions in the molten salt are small enough to easily break bonds within biomass. This allows for effective cleavage of the biomass and assists in the pyrolytic gasification of the biomass (Jin et al, 2005).

Due to the large amount of salts available, molten salt eutectics can be used for operation under specific conditions. A molten salt eutectic is a mixture of two or more molten salts at specific concentrations designed to lower the melting point to its minimum possible value. The reactivity of the salts, mixture melting point, and other properties may be adjusted by changing the eutectic for a specific system (Jin et al, 2005). For example, some carbonate salts have a melting of point of over 700°C. By creating a eutectic with potassium carbonate and lithium carbonate, the melting point can be lowered to approximately 500°C (Molten Salt Database –Eutectic Finder-, 2009). This will result in lower operating costs for the system because less heating is required.

Table 4 demonstrates how various compositions produce eutectics with different melting points.

Table 4: Example Eutectics (Molten Salt Database –Eutectic Finder-, 2009)

Composition vs. Melting Point		
Salts	**Composition**	**Melting Point (°C)**
LiOH	100	450-470°C
NaOH	100	318°C
KOH	100	360°C
Li_2CO_3	100	723°C
Na_2CO_3	100	851°C
K_2CO_3	100	891°C
K_2CO_3-Li_2CO_3	41-59	468 C
K_2CO_3-Li_2CO_3	56-44	474 C
K_2CO_3-KOH	9.3-90.7	366 C
K_2CO_3-Li_2CO_3-Na_2CO_3	26.8-42.5-30.6	393 C
K_2CO_3-Li_2CO_3-Na_2CO_3	25-43.5-31.5	397 C
K_2CO_3-Li_2CO_3-LiOH	16.4-26.4-57.1	372 C

Molten salts are desirable as catalysts because of their high reactivity. Jelles notes that, "The activity of these [molten salt] catalysts can be up to five times higher than the activity of chemically related solid oxide catalysts" (1999). The higher activity is most likely due to the ionic nature of the salts.

2.5.1 Non Biomass Applications of Molten Salts

Molten salts have many applications outside of biomass processing. Another exploitable property of molten salts is their ability to store thermal energy. This makes molten salts a viable heat transfer fluid (HTF) for solar power plants. Solar power plants operating today in California produce up

to 354 MW of power. However, these plants use mineral oil HTFs and cannot operate at hotter, more efficient temperatures or easily scale up. These problems may be overcome with the use of molten salts (Herrmann, 2003).

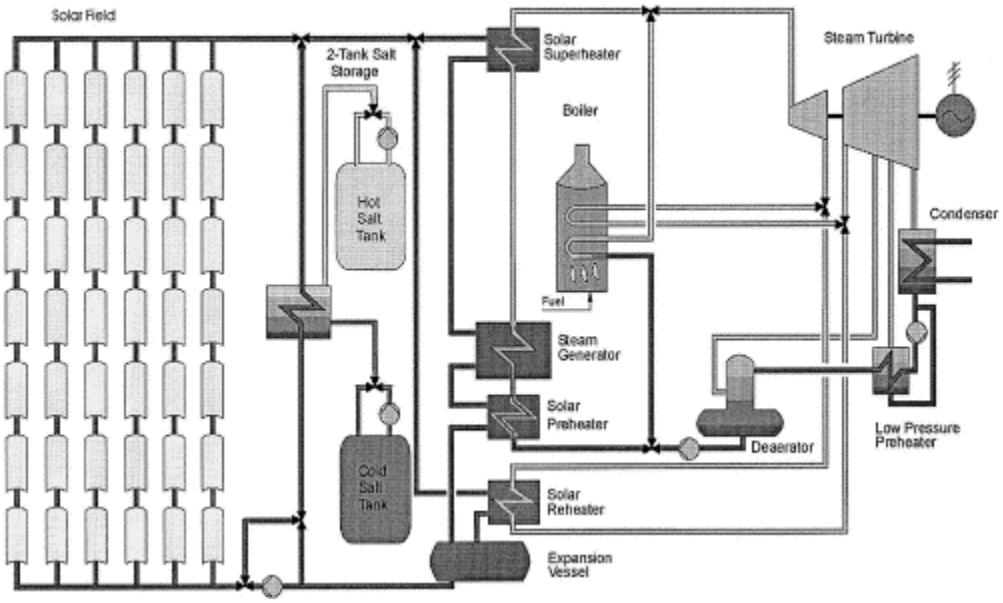

Figure 22: Application of Molten Salts in Solar Power Plants (Herrmann, 2003)

Figure 22 shows a common equipment layout for a power plant utilizing molten salts. In this plant, nitrate salts are stored in two storage tanks. Solar energy is stored in the molten salts, and this energy is used to generate steam to drive turbines that create electricity. The molten salt HTF reaches temperatures of up to 385°C from solar energy alone. During the summer months, these plants can operate at full electric capacity from solar energy for 10-12 hours per day. This technology has been demonstrated to be successful. Molten salts are cheaper than conventional HTFs, making them more economically viable. As a result, they will most likely see use in solar power plants in the near future (Herrmann, 2003).

Molten salts have been used in many pyrochemical processes that produce and purify actinide metals. These pyrochemical processes include Direct Oxide Reduction (DOR), Molten Salt Extraction (MSE), and Salt Scrub (SS) (Mishra, 2004). One specific example of molten salts being able to produce metals is in the production of calcium. Molten calcium chloride electrolyte is capable of dissociating calcium oxide to produce calcium electrolytically (Mishra, 2004).

Molten salts are also being researched for their possible application and use in batteries. Molten salts have long been studied for use in batteries because of their high ionic conductivities and

low vapor pressures. These batteries consist of two parts. One part heats the molten salt above the melting point and the other part is the electrochemical cell system that is capable of generating large amounts of electricity (Fujiwara, 2009).

The energy within these batteries can be stored for over ten years with the molten salt in the solid phase. Once a proper heat source is applied to the battery to melt the salt, the salt activates and begins generating electricity because it acts as a strong electrolyte. Research has shown that iodine salts serve as effective storage mediums for charge in batteries. The iodine salt mixtures have low enough melting points (Below 400 °C), are more electrically conductive, and result in batteries with a better discharge-rate (Fujiwara, 2009).

Molten salts can also be used to gasify other energy sources such as coal. Yaw D. Yeboah has successfully used molten salt eutectic mixtures to increase the kinetic rates of coal gasification. Yeboah found that the use of lithium, sodium, and potassium carbonates resulted in the greatest kinetic performance of the gasification of coal (Yeboah, 2004). Sulfate and nitrate salts were also tested in these experiments. It was found that ternary eutectics were more successful than binary eutectics, which performed better than single salts (Yeboah, 2004).

2.5.2 Application of Molten Salts to the Gasification Processes

Previous research (Jin, 2005) determined that a eutectic of K_2CO_3 – Li_2CO_3 – Na_2CO_3 increased the reactivity of the gasification process as compared to not using salt catalyst. The work of Jin et al concluded that the presence of molten salts enables the decomposition of wastepaper using the gasification reactions described above.

This reaction was not seen at any reachable temperature without the use of molten salts. Also, a mixture of the molten salts produced better results rather than any single molten salt. Temperature was also seen to improve the kinetics of the reaction.

As the biomass enters the molten salt the (b-1.4)-glucosidic bond is cleaved (Jin et al). This cleavage is believed to be a result of the small cations in the molten salt efficiently interacting with the biomass. This process would allow active carbon atoms to more easily undergo the gasification reactions, increasing the yield of syngas.

The reactor used for this study is presented in Figure 23. Biomass and salt were inserted into the reactor. Next, gasses are continuously passed through the reactor at various temperatures to test

the temperature dependence of the reaction. The reactor itself was made of ceramic to withstand the intense conditions necessary to facilitate the reactions. Exiting gasses were cooled to remove any water vapor and fed to a gas chromatograph for sampling.

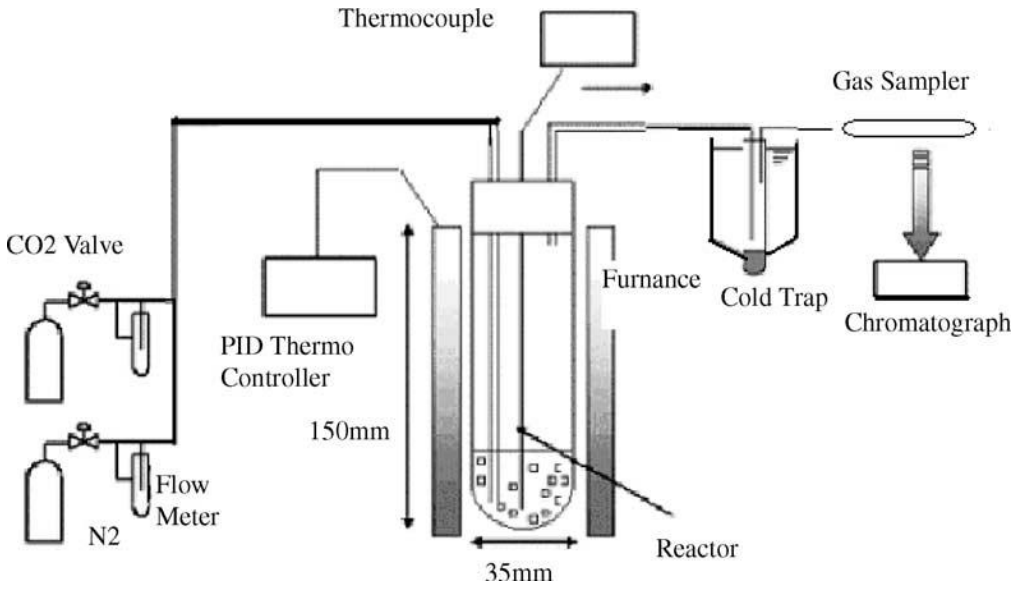

Figure 23: Gasification Reactor (Jin, 2005)

Many different variables were explored to find the effects of salts on the desired reaction. First, the actual salt mixture was varied to explore how the reaction rate changes with the salt composition. Figure 24 shows that a mixture of lithium, sodium and potassium carbonate salts produced significantly more desirable results than no salt at all. In addition, a mixture of simply sodium and potassium was examined and shown to have slightly less desirable reaction kinetics. Most importantly, no reaction was observed with the lack of a catalyst. It was seen that the reaction kinetics improved at temperatures above the melting point of the salt. The three-salt mixture has a lower melting point, and thus produced more desirable reaction kinetics.

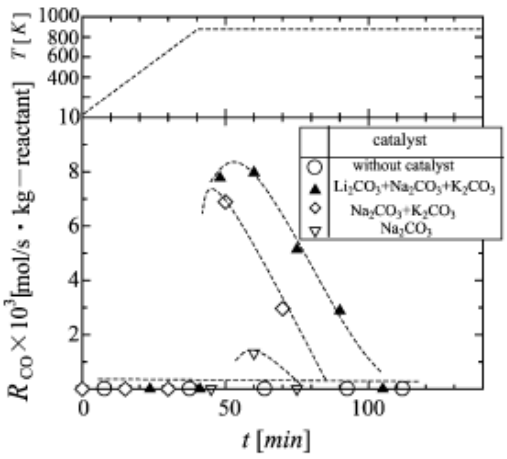

Figure 24: Effect of catalyst on Reaction Rate (Jin, 2005)

Other experiments examined the effect of temperature and heating rate on the reaction kinetics. Results are shown in Figure 25. Due to the endothermic nature of the Boudard reaction, an increase in temperature predictably results in an increase in reaction rate. Interestingly, research (Jin et al.) demonstrated that a fast heating rate also increases the performance of the reaction. Thus, it is important to rapidly heat the reactor rather than gradually increase the temperature to obtain a greater yield of desirable products.

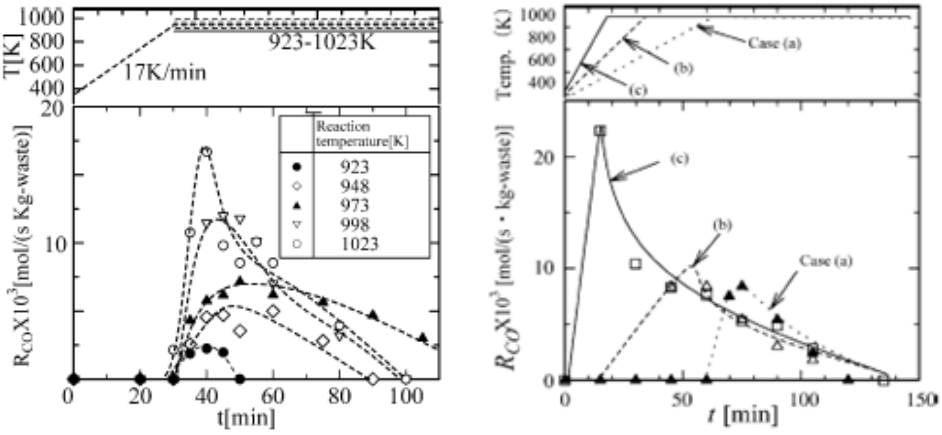

Figure 25: Temperature and Heating Rate Effects on the Rate of the Reaction (Jin, 2005)

Other researchers have found similar results using molten salts to promote the pyrolysis and breakdown of biomass. Roman Adinberg and colleagues successfully built a reactor to collect solar radiation to melt sodium and potassium carbonate salts (Adinberg, 2004). They found that at extremely high temperatures (1188K) over 94% of the initial biomass cellulose feedstock was present in the reactor as char, as opposed to 28% when not using the carbonate salts. Syngases produced in this system

included carbon monoxide, hydrogen, methane, and carbon dioxide (Adinberg, 2004). The advantage to this design was the use of solar energy to power the heating of the salt. This would be incredibly useful as fuels would not have to be consumed for the breakdown of biomass.

Papers published by Adinberg and Jin have both successfully demonstrated the use of carbonate salts at high temperatures to promote the pyrolytic breakdown of biomass into syngas.

2.5.3 Previous Research Completed at Worcester Polytechnic Institute

Previous research at Worcester Polytechnic Institute (Datta, 2009), the basis of this study, used the findings of Jin and colleagues to find an optimal salt eutectic. This resulted in a salt with high reactivity and a low temperature, allowing for safe operation in the laboratory and an economically competitive process. A eutectic composed of 27-wt% sodium carbonate, 40 wt% lithium carbonate, and 33 wt% potassium carbonate was chosen. To this mixture, 25-wt% hydroxide salts, a 50-50 mixture of potassium hydroxide and sodium hydroxide, was added. This resulted in a melting point of 440°C. By adding hydroxide salts, this temperature can be lowered. However, it is believed that the carbonate salts play a major role in the reactions taking place, so eliminating all carbohydrates from the eutectic was avoided.

Molten salts are used in the gasification process to oxidize the bonds within biomass. This reduces the biomass to smaller molecules. Carbonate molten salts have already been used in the gasification of wastepaper in a carbon dioxide rich environment (Jin, 2005). The project found evidence of the gasification reactions, which produced carbon monoxide and hydrogen. The project also found evidence of the methanation reaction due to a large percent of the final product consisting of methane gas. This project will expand upon last year's experiments by modifying the process to operate in semi-batch conditions. Furthermore, this project will not focus solely on gasification but will examine the feasibility of performing multiple different reactions using the same equipment to produce various forms of biofuels.

2.5.4 Applying Molten Salts to all Biomass and Plastics Reactions

Since molten salts have proven so useful to the gasification process, most likely due to their highly reactive nature, this project studies the effect of these salts on other reactions described in this literature review. Specifically, the addition of molten salts to pyrolysis, depolymerization, and transesterification reactions has not been extensively studied. Due to the highly reactive nature of

molten salts, the project group believes they may serve as a suitable reactive medium to facilitate these reactions.

3 Methodology

3.1 Objectives

This project accomplishes the following goals:

- Reactions investigated:
    - Gasification in a semi-batch process
        - Effect of flow rate
        - Effect of salt
        - Effect of temperature
        - Effect of time
    - Depolymerization of plastics
        - Effect of running the process with and without water
    - Esterification of oils (Production of biodiesel)
        - Effect of temperature
        - Effect of reactants (water, methanol)
        - Effect of time
    - Introducing an enzymatic catalysis step before reactor processing
        - Adding the step before gasification of lima beans
        - Adding the step before the esterification of lima beans
- Reactor versatility:
    - All reactions to be carried out in the same constructed semi-batch reactor flow system
    - The microwave reactor will be investigated for potential application

The project group also made recommendations for future projects. Specific recommendations include:

- Optimization of specific reactions
- Improvements to the flow system as a whole
- Analysis of most favorable reaction pathways
- Future reactor design
- Future research

3.2 General Reactor Setup

3.2.1 Reactor Flow System

The project group modified the reactor flow system utilized by the 2008-2009 molten salt MQP for the experiments. The system is capable of processing batch and semi-batch processes. Figure 26 shows how the gases flow through the system.

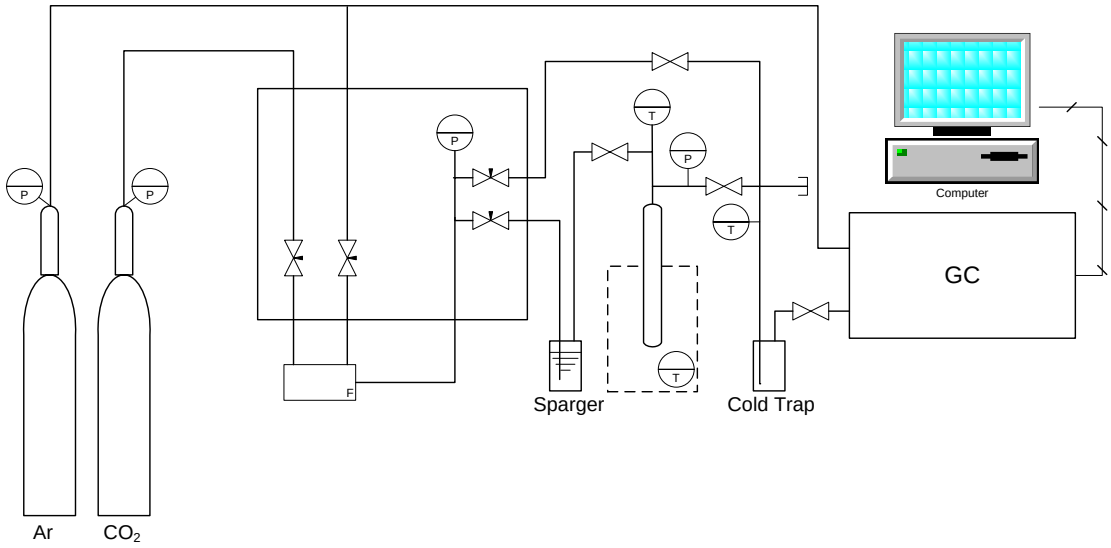

Figure 26: Reactor Flow System

Argon gas was used as the gas chromatograph carrier gas. Gas flows to the reactor were controlled with gas flow meters manufactured by MKS Instruments. Before entering the reactor, the gas was selectively passed through a sparger. By bubbling the gas through water, the project group was able to deliver gas saturated with water vapor to the reactor, if desired. Downstream, a series of valves allowed the water vapor and gas to pass into the reactor, which was heated with a Linberg/Blue tubular heater.

Gas then flows out of the reactor through another series of valves into two cold traps to allow for condensation. The cold trap was used for semi-batch processes. Erlenmeyer flasks submerged in ice were used as cold traps, ensuring that liquid products cooled and condensed out of vapor before reaching the gas chromatograph.

3.2.2 Design Specifications of the Reactor

The reactor used was a ¾" stainless steel cylinder with swagelock fittings on both ends. Water was added to the reactor to obtain the desired pressure for the reactions discussed previously. However, the reactor was carefully monitored to ensure that the pressure did not exceed the reactor limit (Calculations shown in Appendix H). The maximum operating pressure of the reactor was previously reported as 2,000 psi. However, due to wear over time, the maximum pressure allowed by the project group was 1,000 psi. The reactor is leak tight under high-pressure situations.

The reactor is approximately 17" long. A ¾" to ¼" reducer at the top of the reactor is used to attach the reactor to the flow system. A thermocouple approximately halfway down in the heater allows for accurate temperature readings. Reactants generally fill the reactor approximately 7" from the bottom of the reactor when charged. However, this changes depending on the materials charged in the reactor. Figure 27 shows a schematic of the reactor.

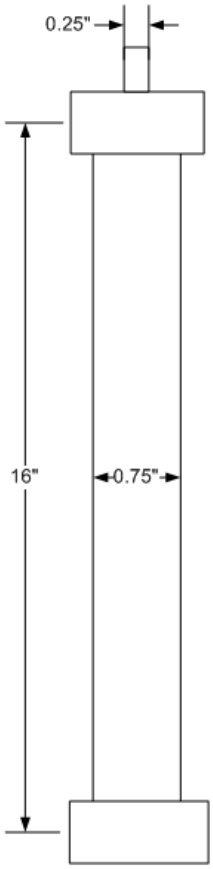

Figure 27: Reactor Schematic

3.2.3 Lindburg/Blue Tubular Heater

As previously mentioned, the furnace used to provide heat to the reactor is a Lindburg/Blue Tubular Heater. The heater is set using PID controls. When the temperature of the system reaches the set temperature, the heater maintains this temperature until it is deactivated. The heater sits on firebricks and insulation, and the tubes immediately upstream and downstream of the reactor are insulated as well. Figure 28 depicts the reactor as it is connected to the flow system and heated by the furnace.

Figure 28: Lindburg/Blue Tubular Heater with Reactor

3.2.4 Gas Controller Calibration

In order to monitor the flow rate through the system, the flow meters needed to be calibrated for each type of gas. A scaling control factor was needed in order to set the scaling control potentiometer dial, as shown in Figure 29, to the appropriate value. The scaling control factor was found using the following equation:

$$Scaling\ Control\ Factor = Gauge\ Factor\ x\ Gas\ Correction\ Factor \quad (5)$$

$$Scaling\ Control\ Factor_{ARGON} = 100\ x\ 1.39 = 139 \quad (6)$$

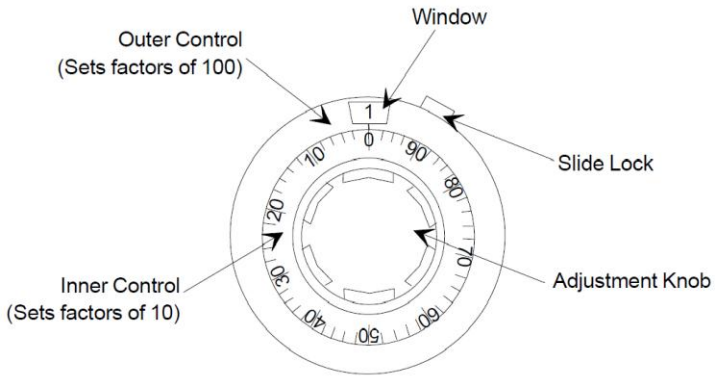

Figure 29: Scaling Control Potentiometer (MKS Instruments User Manual, 2010)

On each of the mass flow controllers, there is a listed flow range. Using the manual provided by MKS Instruments, it was found that a gauge factor value of 100 is used for the flow range of 100 sccm. Next, a table of gas correction factors was used as provided in the MKS Instrument manual. The table gives a value for each individual gas. In the example above, argon had a gas correction factor of 1.39. Next, the gauge factor and gas correction factor values were entered into the equation above, and the scaling control factor was determined. Once this value was obtained, it was set on the flow meter on the scaling control potentiometer. For the example above, the number 1 would appear in the viewing window and the dial would be set so that the tick mark reading "39" was directly below the viewing window.

3.3 Sample Purification

Liquid samples exiting the pipe reactor were prepared for gas chromatography. These samples were placed into test tubes where an equal volume of ethyl acetate was added to the sample. The top of the test tube was then covered with Parafilm and shaken by hand vigorously to ensure that the ethyl acetate dissolved the organic matter within the samples. Next, a separatory funnel was used to separate the organic compounds dissolved in the ethyl acetate from the inorganic layer based on density of the fluids. Once placed into the separatory funnel, an additional two milliliters of ethyl acetate was added to the sample to determine which layer, the top or bottom, was the organic layer for chromatography analysis. The inorganic layer was disposed of appropriately. Excess ethyl acetate was removed using the rotary evaporation method. The condensing unit was filled with acetone and dry ice to achieve an optimal condensing temperature. The sample was transferred to an evaporator flask, ensuring that the volume of the flask was at least twice the sample size. The rotary evaporator setup also included a splash guard to prevent any desired sample from splashing up while trying to remove the

ethyl acetate solvent. Next, a gram of sodium sulfate was added for every four milliliters of sample to remove excess water in the sample. The dried liquid was then removed with a pipette. The sample was finally filtered using Leur Lock syringes and filters with pore sizes of 0.45 micrometers. After this purification process, the samples were ready to be injected into the gas chromatograph.

3.4 GC Column and Operating Specifications

An SRI 8610C gas chromatography machine was used by this project for all gas analysis. The gas sample was automatically injected using a switching valve, and all data collection was controlled with the Peak Simple software.

The column selected for the gas separation is packed with 60/80 carboxen 1000 packing. The column is 1/8" wide and 15 feet long. The column was selected for its ability to separate H_2, CO, CO_2, and CH_4 gases. Since the gas concentrations observed in the experiments were rather large, trace elements were insignificant, and a longer, thinner column was not needed.

Argon was used as the carrier gas for the chromatography. Due to the high temperatures and pressures expected within the system, nitrogen was not used because of the possibility it may participate in a reaction. Other possible carrier gases included helium and hydrogen. Helium was not used because it is typically used for FID detection and not TCD detection, as is used in this project. Hydrogen is highly explosive, and it was generated in gasification reactions. Thus, it was not a suitable carrier gas.

The temperature setting of the column was set to 25°C and averaged around 38°C due to ambient heat from the gas chromatograph. The pressure of the carrier gas was increased to 25 psi. This pressure was selected to increase the gas flow ensuring that the TCD filaments did not overheat or burn out.

All gases were analyzed using a thermal conductivity detector (TCD). A flame indicator detector (FID) was not used because the results from the TCD were adequate. In the future, an FID detector may be used if more accurate results are required.

A separate gas chromatograph was used for liquid analysis. The fused silica capillary column in the liquid analysis GC is 15 meters long with a 0.53 mm internal diameter. To ensure that sufficient separation occurred between products of various volatilities and boiling points, a heating scheme was used. The oven started at 60°C for two minutes. Then, the temperature increased by 10°C per minute

to a temperature of 170°C. This temperature was also held for 2 minutes. Finally, the temperature increased by 15°C per minute to a final temperature of 300°C for 10 minutes. Total run time was slightly over 33 minutes.

The GC was controlled using a software program package on the computers in the lab. The software program was capable equilibrating the GC, loading a specific method, and recording the results of the trial.

3.5 Nuclear Magnetic Resonance (NMR) Analysis

All liquid samples obtained were also analyzed using NMR spectroscopy to complement the results given by the GC. The NMR was programmed to automatically take a sample from a rotating sample tray, inject the sample into the NMR machine, and perform a 16-pass proton scan.

Proton NMR spectroscopy was selected for examining the samples. H-NMR was chosen instead of C-NMR because the hydrogen atoms and locations within the liquid samples were expected to vary enough for positive identification. By examining the generated spectra and comparing the experimental results to control spectra of various known chemicals, both expected products and reactants could be detected.

NMR samples were prepared by mixing 0.75 milliliters of deuterated chloroform with approximately 20 microliters of the sample.

3.6 Safety Precautions

This system may operate under high temperature and pressure conditions. To ensure maximum safety, a pressure gauge was installed to monitor the pressure of the reactor. Additionally, a pressure release valve was located just downstream of the reactor which would discharge the contents of the reactor to a fume hood should pressure reach 1,000 PSI. A maximum reaction temperature of 500°C was selected, as higher temperatures may result in the degradation of the reactor due to its carbon content.

Safety goggles and latex gloves were worn whenever handling materials. All hazardous reactants and products were handled with care and disposed of properly.

All gas lines were properly secured and tightened to prevent leaks. All gases were vented into an adjustable ceiling fume hood that was operating at all times. Pressures on the gas tanks, within the gas controllers, as well as within the reactor were monitored at all times.

3.7 Gasification Reactions

Reactions were performed to study syngas production with the use of molten salts in a semi-batch flow system. The effect of temperature, gas flow rate, salt, time, and the presence of water were all investigated.

The reactor was charged with all reagents. The desired amount of salt and biomass was added to the reactor and packed to the bottom with a rod. To ensure consistency, paper was used as biomass. The salt catalyst used varied from a single component, such as sodium or potassium hydroxide, to a multi-component eutectic. The eutectic used was comprised of 20.2 wt % sodium carbonate, 30 wt % lithium carbonate, 24.8 wt % potassium carbonate, and 12.5 wt % of both potassium and sodium hydroxide.

The reactor was then secured to the flow system and checked for leaks. At this point, argon gas was passed through the system to purge out all of the air to avoid combustion at high temperatures. The removal of air from the system was complete when a GC sample had shown no peaks during the purging process. Once the system was purged of all air, argon flow was shut off and carbon dioxide was passed through the system at the desired rate. The tubular heater was turned on and set to the desired temperature. Once this temperature was reached, the gas flowing through the sample was analyzed every seven minutes using the gas chromatograph to detect syngas production.

Some experiments required the system to run continuously overnight. A macro program was used to automatically take samples. This program was able to control the computer software to sample gas from the semi-batch reactor every 7 minutes throughout the night, saving data as appropriate.

All reactions, with the exception of the overnight trials, were allowed to proceed for 90 minutes. Once this time limit was reached, all gas flows were shut off, the heater was shut off, and the reactor was allowed to cool. The piping was cleaned using hot water and air purging. The reactor was cleaned using a sturdy pipe cleaner and soap.

Table 5 lists the conditions of each gasification trial.

Table 5: Reaction Conditions for Gasification Trials

Reactants for Gasification Trials								
Trial No.	Paper (grams)	Salt Used	Salt (grams)	Water (mL)	Temperature (C)	Time (Hours)	Type of gas	Gas Flow (mL/min)
G1	5	KOH	5	0	200	1.0	CO_2	75.00
G2	5	KOH	10.5	0	500	1.0	CO_2	12.50
G3	5	Eutectic	10	0	500	1.0	CO_2	10.00
G4	5	Eutectic	10	0	500	2.0	CO_2	10.00
G5	5	Eutectic	10	0	500	8.9	CO_2	10.00
G6	5	KOH	10	0	500	9.0	CO_2	10.00
G7	5	Eutectic	10	Sparger	500	8.9	CO_2	10.00
G8	5	KOH	10	Sparger	500	10.2	CO_2	10.00
G9	Tributyrin 5 mL	Eutectic	10	0	500	6.4	CO_2	10.00

3.7.1 Gas Constant Determination for Control Gases:

In order to determine the concentration of target gases coming out of the pipe reactor, it was necessary to run pure samples of these gases through the gas chromatograph. The pipe reactor was first attached to the continuous flow system and checked for leaks. Carbon dioxide, carbon monoxide, hydrogen, and methane gases were run through the Gas Chromatograph separately at flow rates of 10, 20, and 30 standard cubic centimeters per minute (sccm). Retention A constant was established for each gas by taking the inverse of area under the curve produced by the Gas Chromatograph. The calculated gas constant was then averaged between the 10, 20, and 30 sccm control trials. The average retention times were taken in order to distinguish what time the control gases were expected to appear on the GC graph.

3.8 Depolymerization of Plastic Reactions

The depolymerization of plastic into useable fuels was attempted using this reactor in batch conditions. The presence of water and its affect on the reactor was studied.

The reactor was first charged with all desired materials. Five grams of the eutectic described in the gasification section was used as the salt in these experiments. The amount of plastic varied between five and ten grams and was packed down into the salt. If water was desired for the trial, four milliliters was added to the reactor in liquid form.

The reactor was then attached to the flow system and argon was used to purge the air from the reactor. Once no air was present, the valves immediately downstream and upstream of the reactor

were closed to allow the reactor to proceed under batch conditions. The heater was set to 500°C and the system was allowed to run for an hour.

Table 6 lists the conditions of each trial with plastic.

Table 6: Reaction Conditions for Depolymerization of Plastics

Reaction Conditions for Depolymerization of Plastics								
Trial No.	Plastic (grams)	Salt Used	Salt (grams)	Water (mL)	Temperature (C)	Time (Hours)	Gas Flooded	Gas Pressure (psi)
P1	5	Eutectic	10	0.00	500.00	1.00	Ar	60.00
P2	5	Eutectic	5	4.00	500.00	1.00	Ar	60.00

3.9 Transesterification and Hydrolysis

3.9.1 Bench Top Trials

The biodiesel transesterification reaction was first performed under common conditions previously found in literature. First, 0.14 grams of sodium hydroxide was dissolved in ten milliliters of methanol in a flask with a magnetic stirrer. Simultaneously, 10 milliliters of tributyrin was heated to 40°C using a hot plate. Once the sodium hydroxide was entirely dissolved into the methanol and the tributyrin heated to the appropriate temperature, the tributyrin was slowly added to the continuously stirring sodium methoxide solution. The solution was then allowed to proceed for 30 minutes while stirring.

These exact same reaction conditions were repeated using water instead of methanol. This was done to act as a comparison to the reactor trials performed later.

Table 7 lists the reaction conditions for all bench top trials to create biodiesel.

Table 7: Reaction Conditions for bench Top Biodiesel Trials

Reaction Conditions for Bench Top Biodiesel Trials							
Trial No.	Oil Used	Oil (mL)	Salt Used	Salt (grams)	Water / Methanol	Amount (mL)	Time (Hours)
BT1	Vegtable Oil	100	NaOH	0.35	Water	20.00	0.50
BT2	Vegtable Oil	100	NaOH	0.35	Methanol	20.00	0.50
BT3	Tributyrin	100	NaOH	0.35	Water	20.00	0.50
BT4	Tributyrin	10	NaOH	0.14	Methanol	10.00	0.50

3.9.2 Reactor Trials

Various forms of biodiesel transesterification reactions and their viability in this reactor with molten salts were studied. The effect that temperature and time had on the reaction was studied.

Similar to the gasification reactions, the reactor must first be charged. The desired amounts of tributyrin, sodium hydroxide, and water or methanol were added to the reactor. When using methanol in the reactor, sodium hydroxide was first added to the methanol in a beaker and stirred to ensure that sodium methoxide was formed.

The reactor was then attached to the flow system and flooded with argon to eliminate reactions with gases in air. After the reactor had been purged of all air, the valves immediately upstream and downstream of the reactor were closed to allow the system to run under batch conditions.

The heater was then turned on and set to the desired temperature. After this temperature was reached, the reaction was allowed to proceed between 30 minutes and 2 hours. A pressure gauge monitored the system pressure to ensure that the system never approached dangerous levels.

Table 8 lists the conditions for all transesterification reactions performed in the reactor.

Table 8: Reaction Conditions for Hydrolysis/Transesterification Reactions in the Reactor

Reaction Conditions for Hydrolysis/Transesterification Reactions in the Reactor									
Trial No.	Expected Reaction	Oil/Biomass Used	Oil (mL)	Salt Used	Salt (grams)	Water / Methanol	Amount (mL)	Temperature (C)	Time (Hours)
HT1	Hydrolysis	Vegetable Oil	2	KOH	2.00	Water	2.00	200.00	0.25
HT2	Hydrolysis	Vegetable Oil	4	K_2CO_3	4.00	Water	4.00	260.00	0.25
HT3	Hydrolysis	Vegetable Oil	4	K_2CO_3	4.00	Water	8.00	400.00	0.50
HT4	Hydrolysis	Vegetable Oil	4	KOH	4.00	Water	4.00	260.00	0.50
HT5	Hydrolysis	Tributyrin	4	NaOH	0.50	Water	4.00	200.00	0.50
HT6	Hydrolysis	Tributyrin	4	NaOH	0.50	Water	4.00	250.00	0.50
HT7	Hydrolysis	Tributyrin	4	NaOH	0.50	Water	4.00	300.00	0.50
HT8	Hydrolysis	Tributyrin	4	NaOH	0.50	Water	4.00	200.00	0.50
HT9	Hydrolysis	Tributyrin	4	NaOH	0.50	Water	4.00	350.00	0.50
HT10	Hydrolysis	Tributyrin	4	NaOH	0.50	Water	4.00	400.00	0.50
HT11	Hydrolysis	Tributyrin	4	NaOH	0.50	Water	4.00	500.00	0.50
HT12	Hydrolysis	Tributyrin	4	NaOH + K_2CO_3	0.50	Water	4.00	250.00	1.00
HT13	Hydrolysis	Tributyrin	4	NaOH	0.50	Water	4.00	250.00	2.00
HT14	Transesterification	Tributyrin	4	NaOH	0.50	Methanol	4.00	200.00	0.50
HT15	Transesterification	Tributyrin	4	NaOH	0.50	Methanol	4.00	300.00	0.50
HT16	Transesterification	Tributyrin	10	NaOH	0.14	Methanol	10.00	300.00	0.50

3.10 Pretreatment via Enzymatic Biocatalysis

3.10.1 Enzyme Selection

Ligninase and Fungi predigestion were determined to be unfeasible for both the time dependency of fuel production (digestion takes up to 2 months) as well as the financial feasibility of using this method of biocatalysis. Cellulose predigestion was also rejected on the basis that gasification and pyrolysis already occur in our reactor, and these processes had already been shown to easily break down with molten salt catalysts and high temperatures.

Therefore, protein digestion with Proteinase K was determined to be the most feasible predigestion step for our processes due to the low digestion time, high reactivity, low specificity, and ability to form carbohydrates and smaller carbon based derivative chains. Proteinase K was selected to break down biomass to determine if a higher yield of gasification products could be detected. Gasification results remain the most quantifiable data that were collected throughout experimentation. Therefore, gasification was the most desirable method to determine the efficiency of the Proteinase K predigestion step.

3.10.2 Proteinase K Digestion Preparation

Char accumulation within the reactor has been shown to be a common issue in all of the trials performed by the project team. Char is expected to decrease the reaction rate of materials in the reactor as seen by the decrease in fuel production after the beginning stages of each trial. In order to combat the formation of char within the reactor, thereby increasing the reaction kinetics of the system, a protocol for predigestion of biomass was formulated and carried out.

Proteinase K was selected as the enzyme to break down lignin and protein within biomass prior to subjecting feedstocks to pyrolysis and gasification. Dehydrogenated lima beans were selected as the biomass of choice in these reactions due to their consistency as feedstocks throughout trials and their 7% protein by mass composition.

Proteinase K in lyophilized powder form at an activity of over 30 units/mg protein was ordered from Sigma Aldrich. Calculations were made to determine the amount of digestion time needed to digest 4 g of blended lima beans using 1 mg of Proteinase K reconstituted in a 50mM Tris-HCl (pH 8.0), 10mM $CaCl_2$ solution. From these calculations, it was determined that 1 mg of Proteinase K will fully digest 4 g of lima beans (7% protein content) in approximately 2.65 hours assuming full mixing.

3.10.3 Samples Prepared for Digestion

The following samples were prepared for digestion with Proteinase K as shown in Table 9.

Table 9: Proteinase K Predigestion Trial Database

Sample Number	Proteinase K?	Digestion Time	Buffers Used?	Gasification or Transesterification
B1	Yes	48 Hours	Yes	Gasification
B2	Yes	48 Hours	Yes	Transesterification
B3	Yes	3 Hours	Yes	Gasification
B4	Yes	3 Hours	Yes	Transesterification
B5	No (control)	N/A	Yes	Gasification
B6	No (control)	N/A	Yes	Transesterification
B7	No (control)	N/A	Methanol	Transesterification
B8	No (control)	N/A	Water only	Gasification
B9	No (control)	N/A	Sparger only	Gasification

3.10.4 Digestion Protocol

To digest lima bean samples with Proteinase K, the following protocol was followed for sample numbers 1 through 6:

- Proteinase K was reconstituted in the appropriate Tris-HCl/$CaCl_2$ solution
    - 0.2 µL Tris-HCl of 50 mmol/L in final volume
    - 160 µL of 10mM $CaCl_2$ in final volume
- 4 g of blended lima beans were added to containers
- 8 mL of the following solution was added to containers:
    - 1% Triton X-100
    - 0.5% SDS
- For sample numbers 1 through 4, an equivalent of 1 mg Proteinase K in solution was added. For sample numbers 5 and 6, no Proteinase K was added
- Samples were placed in a shaking incubator set to 37°C for the amount of time specified in Table 9. Samples were removed after digestion and inhibited by the addition of EGTA (pH = 8) at a final concentration of 2mM by total volume

Samples 7, 8 and 9 serve as controls for predigestion without Proteinase K. These samples also did not contain the buffers used in the digestion process differentiating them from control samples 5 and 6.

3.10.5 Post Digestion Protocol

Samples were then subjected to either gasification or transesterification pathways using the following protocols:

- Gasification
    - Add 5 mL of H_2O to tube
    - Add 5 g of Eutectic salt to tube
    - Mix and transfer all contents to the reactor
    - Run for 1.5 hours flooded with CO_2 at a temperature of 500°C
    - Take GC reading 30 minutes into reaction for analysis
- Transesterification
    - Add 5 mL of MeOH to tube
    - Add 5 g of NaOH to tube
    - Mix and transfer all contents to the reactor
    - Run for 30 minutes flooded with Argon gas at a temperature of 300°C

After reaction, samples were removed, any liquid products that formed were collected and separated from solid products. Pictures were taken of solid products to qualitatively determine char production. Liquid purification steps according to Section 3.3, were carried out for GC and NMR analysis.

4 Results and Discussion

4.1 Gasification

4.1.1 Preliminary Salt Analysis

Before trials in the reactor were performed, molten salts and their interactions with paper were analyzed using furnaces. Only salts that were used during reactor trials were tested. This included potassium hydroxide, sodium hydroxide, and the eutectic mixture composed of sodium, potassium, and lithium carbonate as well as sodium and potassium hydroxide.

Paper was added to molten potassium hydroxide at approximately 400°C. A small rolled up ball of paper and a flat piece were both added to the salt. Immediately upon placing the paper in the salt mixture, it began to bubble. The flat piece of paper immediately began to turn brown and proceeded to blacken. The small ball of paper took longer to change color. Eventually, the entire mixture consisted of small pieces of char and salt, with a dark brown color.

Figure 30: Paper Submerged in Molten Sodium Hydroxide

Next, paper was added to molten sodium hydroxide at a temperature of 400°C, as seen in Figure 30. The paper reacted very similarly in this trial to the last. The salt underneath the paper began to brown as the paper turned to char. The salt seemed to flow underneath the paper, possibly due to some sort of convection current as a result of rapid temperature changes within the salt. This flow can be seen in Figure 30 by the streaks of color in the salt. Eventually, the paper began to smoke, and part

of the paper began to glow red as it turned into an ember. Submerging paper in potassium or sodium hydroxide had very similar results.

The paper was also added to the eutectic salt mixture at 400°C. Ideally, the paper could be added to the carbonate salts individually. However, the furnace was unable to melt the carbonate salts. The results of this trial are presented in Figure 31.

Figure 31: Paper Submerged in Molten Eutectic Salt

The addition of paper to eutectic salt resulted in a reaction that seemed to progress more rapidly. As seen in Figure 31, bits of char fall off the paper (located in the upper right of the crucible) and spread throughout the mixture. Bubbles emerge from all over the mixture, mostly from areas with larger concentrations of char. The reaction mixture, and the molten salt itself, appeared thicker with a white tint.

All of these trials were allowed to cool off and were inspected closer. Upon inspection, the small bubbles visible during the reaction had hardened into the salt. This was clear in all three trials. Figure 32 is a picture of these bubbles after the reaction of paper submerged in sodium hydroxide.

Figure 32: Hardened Bubbles from the Reaction of Paper Submerged in Sodium Hydroxide

4.1.2 Gasification Reactor Trials

Gasification trials performed in the reactor were designed to study the effect of operation in a semi-batch system. Gas concentrations were recorded over time. Figure 33 presents the results of the first gasification trial.

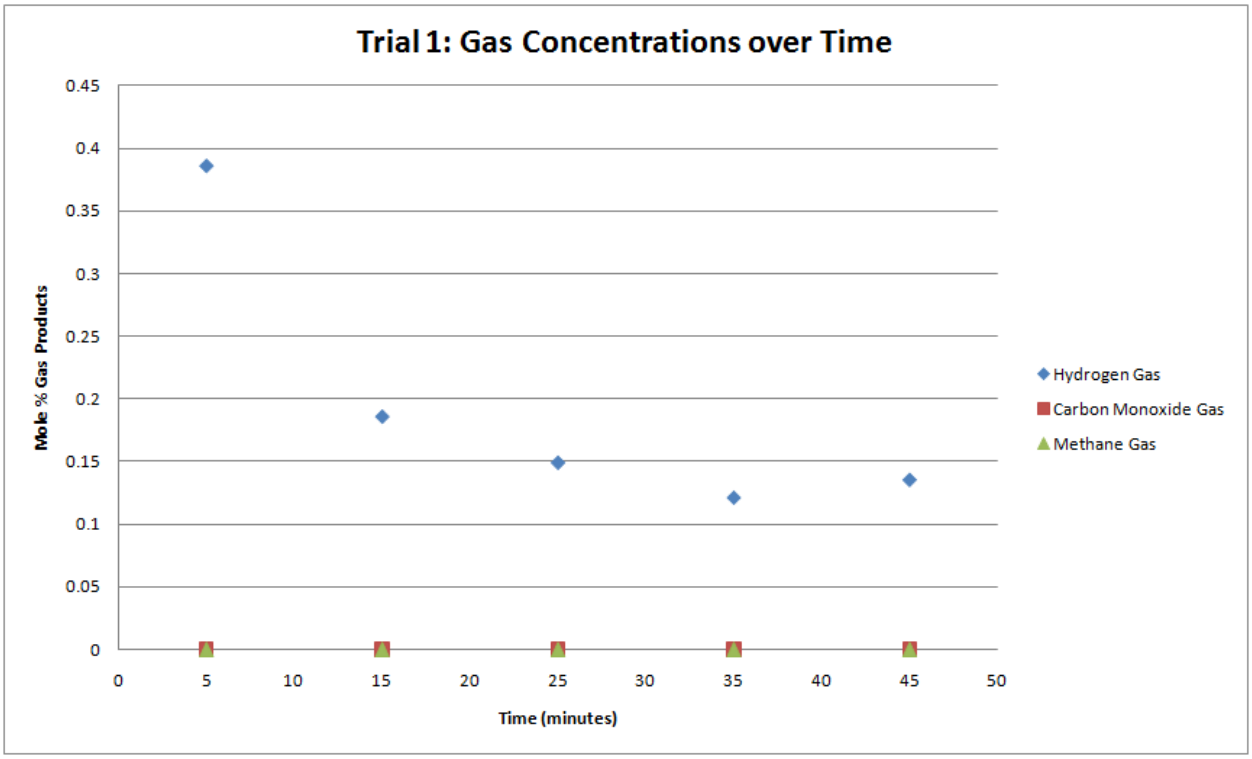

Figure 33: Product Gas Concentrations Over Time - Trial 1

The graph shown in Figure 33 does not include carbon dioxide concentrations. Table 10 numerically presents this information, including carbon dioxide concentrations.

Table 10: Tabulated Product Concentrations for Gasification - Trial 1

Biomass	Gas	H_2	CO	CH_4	CO_2	Time stamp (min)	Salt	T Reactor
Paper	CO_2	0	0	0	0	0	KOH	22
Paper	CO_2	0.39	0	0	99.61	5	KOH	210
Paper	CO_2	0.19	0	0	99.81	15	KOH	218
Paper	CO_2	0.15	0	0	99.85	25	KOH	228
Paper	CO_2	0.12	0	0	99.88	35	KOH	238
Paper	CO_2	0.14	0	0	99.86	45	KOH	250
Paper	CO_2	0	0	0	0	55	KOH	261

This trial did not produce any carbon monoxide or methane, which is unusual. A possible cause is the low reactor temperature of 200°C.

Figure 34 presents the results of the second gasification trial.

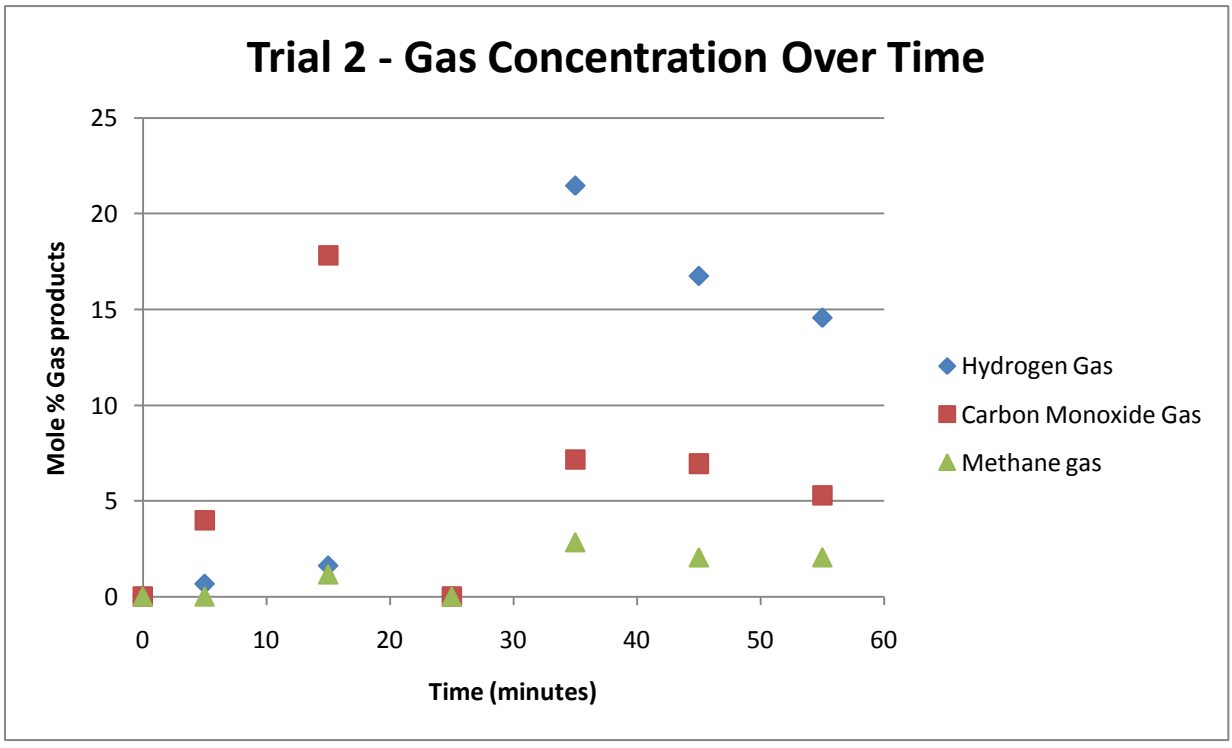

Figure 34: Product Gas Concentrations Over Time - Trial 2

Table 11 presents the results of this trial in tabular form.

Table 11: Tabulated Product Concentrations for Gasification - Trial 2

Biomass	Gas	H_2	CO	CH_4	CO_2	Time stamp (min)	Salt	T Reactor
Paper	CO_2	0	0	0	0	0	KOH	43
Paper	CO_2	0.66	3.98	0	95.36	5	KOH	402
Paper	CO_2	1.61	17.83	1.16	79.41	15	KOH	477
Paper	CO_2	0	0	0	0	25	KOH	499
Paper	CO_2	21.45	7.15	2.83	68.56	35	KOH	499
Paper	CO_2	16.73	6.94	2.04	74.28	45	KOH	503
Paper	CO_2	14.55	5.29	2.05	78.11	55	KOH	507

The increase in temperature improved the concentration of syngas produced. Higher temperature resulted in an increase in pyrolysis to generate carbon monoxide. The presence of methane suggests that methanation also occurred within the reactor. An error taking a sample at 25 minutes resulted in no data being collected for that time.

Figure 35 presents the results of the third gasification trial.

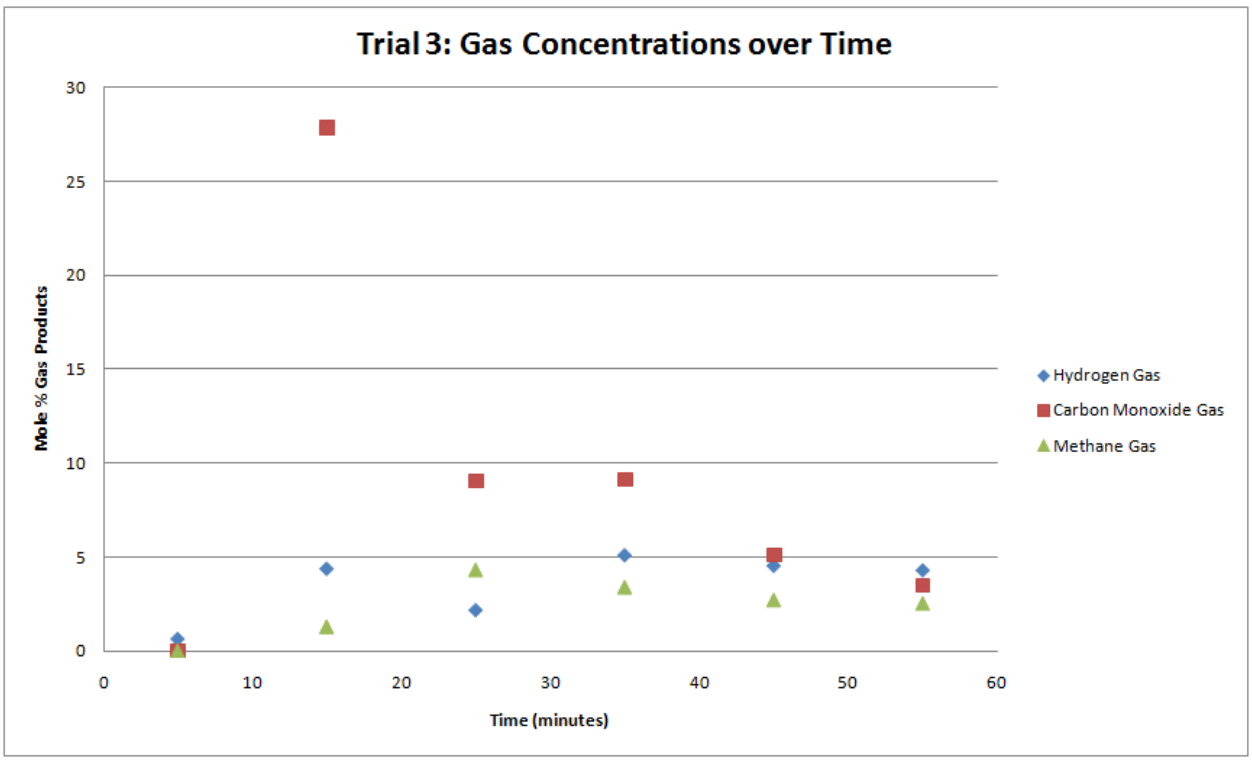

Figure 35: Product Gas Concentrations Over Time - Trial 3

Table 12 presents these results in tabular form.

Table 12: Tabulated Product Concentrations for Gasification Trial 3

Biomass	Gas	H_2	CO	CH_4	CO_2	Time stamp	Salt	T Reactor
Paper	CO_2	0	0	0	0	0	Eutectic	24
Paper	CO_2	0.62	0	0	99.38	5	Eutectic	395
Paper	CO_2	4.38	27.84	1.28	66.50	15	Eutectic	473
Paper	CO_2	2.17	9.03	4.32	84.49	25	Eutectic	498
Paper	CO_2	5.11	9.13	3.39	82.38	35	Eutectic	507
Paper	CO_2	4.54	5.10	2.70	87.66	45	Eutectic	510
Paper	CO_2	4.30	3.49	2.52	89.68	55	Eutectic	514

The difference between the first two trials and trial 3 was the change in salt catalyst to the eutectic salt. This resulted in decreased syngas production. This was not predicted in the literature. Similar to past gasification trials, the concentration of carbon monoxide is largest early in the process. It is worth noting that as the concentration of carbon monoxide decreases, the concentration of methane increases, as would be expected from the methanation reaction.

Figure 36 presents the results of the fourth gasification trial.

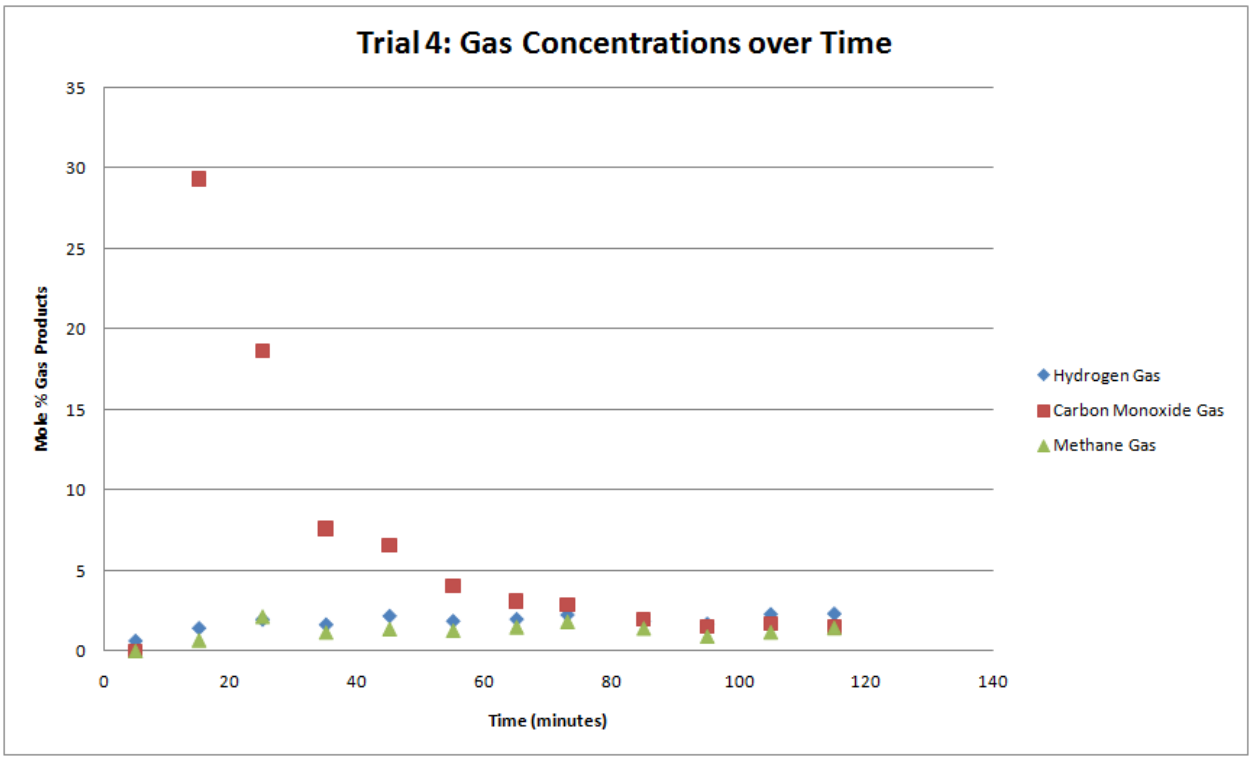

Figure 36: Product Gas Concentrations Over Time - Trial 4

Table 13 presents these results in tabular form.

Table 13: Tabulated Product Concentrations for Gasification - Trial 4

Biomass	Gas	H_2	CO	CH_4	CO_2	Time stamp	Salt	T Reactor
Paper	CO_2	0	0	0	0	0	Eutectic	23
Paper	CO_2	0.60	0	0	99.40	5	Eutectic	397
Paper	CO_2	1.39	29.30	0.68	68.63	15	Eutectic	476
Paper	CO_2	1.94	18.63	2.14	77.29	25	Eutectic	499
Paper	CO_2	1.62	7.59	1.15	89.64	35	Eutectic	507
Paper	CO_2	2.16	6.59	1.37	89.88	45	Eutectic	513
Paper	CO_2	1.84	4.03	1.27	92.86	55	Eutectic	515
Paper	CO_2	1.96	3.09	1.49	93.46	65	Eutectic	518
Paper	CO_2	2.23	2.89	1.83	93.05	73	Eutectic	520
Paper	CO_2	1.83	1.95	1.42	94.80	85	Eutectic	524
Paper	CO_2	1.66	1.51	0.91	95.91	95	Eutectic	528
Paper	CO_2	2.27	1.71	1.17	94.85	105	Eutectic	529
Paper	CO_2	2.30	1.49	1.44	94.77	115	Eutectic	532

The fourth gasification trial was twice as long as any other gasification trial. These results are similar to the third trial in that syngas production tapers off after reaching a maximum early within the trial.

Figure 37 shows the contents of the reactor after the reaction was completed and allowed to cool.

Figure 37: Reactor Contents Post Gasification Reaction

Char accumulates over time and was found as a product in the reactor after every reaction. Small holes were visible in the char as if a surface reaction was occurring, forming gas. This suggests that the Boudard reaction was proceeding, breaking down char to produce carbon monoxide. Data collected suggests that pyrolysis of biomass occurs early after heat is added to the system. The reduction of this char may be accelerated with the addition of water. This allows for reforming reactions and the Boudard reaction to interact with the char simultaneously.

The first overnight reactor trial was charged with 10 grams of eutectic salt and 5 grams of shredded paper. CO_2 was allowed to flow through the system at 10 mL per minute. Figure 38 shows the reactor contents the next morning after being allowed to cool.

Figure 38: Reactor Contents After the First Overnight Trial

The first noticeable difference comparing the hourly trials to the overnight trials is the color of the salt. The salt recovered after overnight reaction appears very white. It looks the same as it did prior to reaction. This is a positive result indicating that the salt may be able to be recycled because it returns to its original state. The goal of the overnight trial was to try to reduce the amount of char in the reactor. Unfortunately, there was still a large amount of char present in the products. This may be the result of the char plugging the reactor and limiting contact with the salt as time progressed.

In addition to the char and salt found in the reactor, liquid products were found to have condensed in the cold traps downstream of the reactor. Figure 39 shows the contents of the cold trap after the reaction.

Figure 39: Liquid Products after the First Overnight Trial

Liquid in the cold trap is of note because no liquids were charged as reactants, meaning that liquids were produced within this process. The reactor contained only salt, paper and carbon dioxide which was passed through the system continuously. The liquid products were formed in the cold trap within the first hour of the reaction, and were not formed again throughout the remainder of the overnight trial. This indicates that the majority of the desirable chemistry occurs early in the reaction. The project team believes this is due to pyrolysis reactions expected to progress when the paper is first exposed to heat in the presence of salt. Following liquid production, only gasification reactions involving char occurred until the char was no longer in contact with the salt.

Table 14 presents the quantitative results of the first gasification trial.

Table 14: Quantitative Gas Results of the First Overnight Trial

	Mole %			
Time Stamp	H_2	CO	CH_4	CO_2
10	5.051507	4.229057	1.769825	88.94961
85	2.207556	0.912087	2.06637	94.81399
160	1.090209	0.661116	0.665809	97.58287
235	0.760663	0.414158	0	98.82518
310	1.707633	1.33039	0	96.96198
385	0.372745	0.394311	0	99.23294
460	0.315363	0.724712	0	98.95993
535	0.364048	1.060695	0	98.57526

These results are similar to the original gasification trials. Allowing the reaction to run longer reveals that the methanation reaction eventually stops occurring. This was seen in all overnight trials. A possible reason could be the lower concentration of hydrogen produced later in the reactions. Due to the lower concentrations of CO and H_2 gases, the methanation may not proceed at a significant rate. Overall, it is apparent that some sort of breakdown of biomass and char occurred throughout the entire night. As stated previously, char was not completely processed due to poor contact between the solid biomass, char, molten salt, and gaseous carbon dioxide.

Both overnight gasification trials without the sparger produced similar results. The only major difference was the addition of a sparger to deliver water vapor to the reaction. This addition of water resulted in a larger amount of liquid collected in the cold trap. With the addition of ethyl acetate, a distinct organic and inorganic layer were observed. This is expected because water vapor should collect in the cold trap with the use of a sparger will not dissolve in ethyl acetate. Table 15 presents the results of the third overnight gasification trial, using the eutectic salt mixture, paper, and a sparger.

Table 15: Quantitative Gas Results of the Third Overnight Trial

	Mole %			
Time Stamp	H_2	CO	CH_4	CO_2
10	0.11825	24.59866	0	75.28309
85	2.234506	0	0	97.76549
160	1.124014	0	0	98.87599
235	0.920882	0	0	99.07912
310	0.943059	0	0	99.05694
385	0.826384	0	0	99.17362
460	0.596382	0	0	99.40362
535	0.469339	0	0	99.53066

Filling the sparger with water significantly reduced the production of carbon monoxide and methane. Large amounts of carbon monoxide produced early in the reaction are most likely the result of the pyrolysis of paper. Any carbon monoxide produced after this initial release of carbon monoxide was quickly reacted. Steam may have reacted with the carbon in char to produce carbon monoxide and hydrogen gas. This carbon monoxide may have reacted with the water vapor to produce additional hydrogen and carbon dioxide, the only two products seen here. This reaction mechanism is supported by the results because the hydrogen content was generally higher with the sparger than without the

sparger. Without the sparger, the hydrogen content fell to roughly 0.3 % as opposed to 0.8% with the sparger. These results were similar for the fourth overnight trial.

The liquid products obtained from the cold trap flask were examined using GC and NMR spectroscopy. Figure 40 below shows the GC results of the third overnight trial.

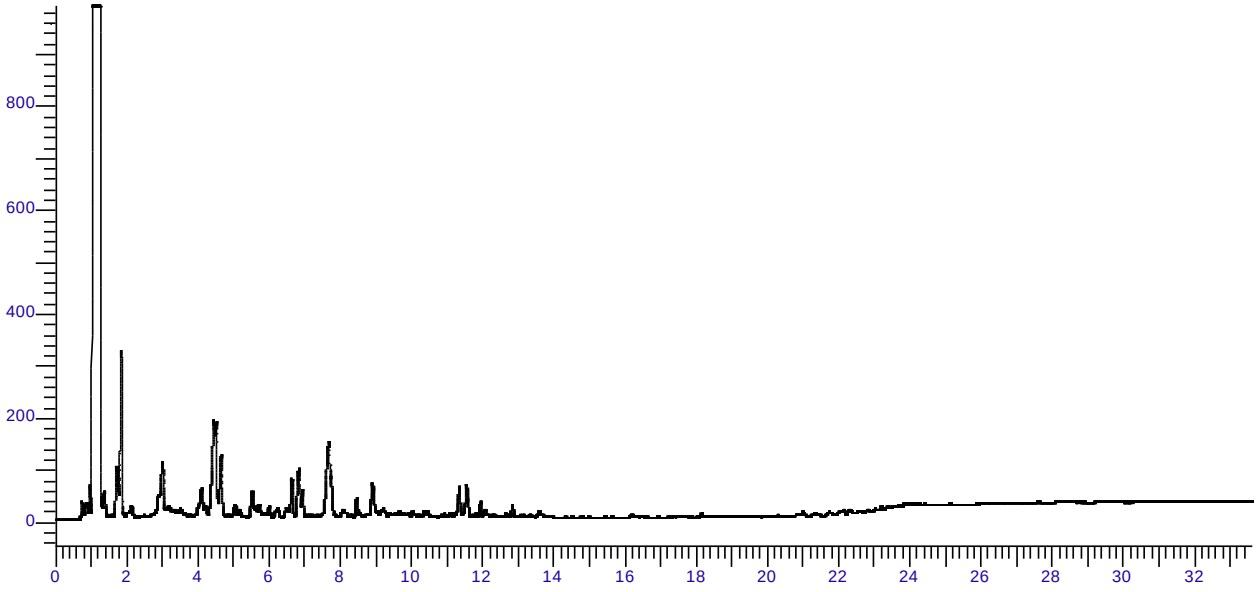

Figure 40: GC Analysis of Liquid Products for Third Overnight Gasification Trial

Many unknown peaks appear between 1 and 12 minutes. These are most likely volatile chemicals, as they appear in the general range of control chemicals such as methyl butyrate and methanol. The pyrolysis of paper into liquid products makes many different products, as evidenced by the many different peaks. Identification of these products is impossible without further analysis using various instrumentation.

The greatest number of unidentified peaks was obtained from trials using molten eutectic. Trials with KOH as the molten salt yielded a lower number of unknown peaks. This supports literature research that claims molten carbonate eutectics provide multiple pathways for the breakdown of biomass in contrast to hydroxide salts alone.

The last gasification experiment was the gasification of tributyrin (G9). The last GC sample was collected 6.4 hours into the reaction. After 4 hours into the trial, little syngas exited the reactor besides CO_2 (and therefore this data is omitted). All GC gas samples showed hydrogen and carbon dioxide

peaks, and the hydrogen peak decreased as time progressed. This data is shown in both Table 16 and Figure 41.

Table 16: Quantitative Gas Results of Tributyrin Gasification

	Mole %			
Time Stamp	H_2	CO	CH_4	CO_2
10	0.62	0	0	99.38
85	5.26	0	0	94.74
160	3.44	0	0	96.57
235	1.42	0	0	98.58

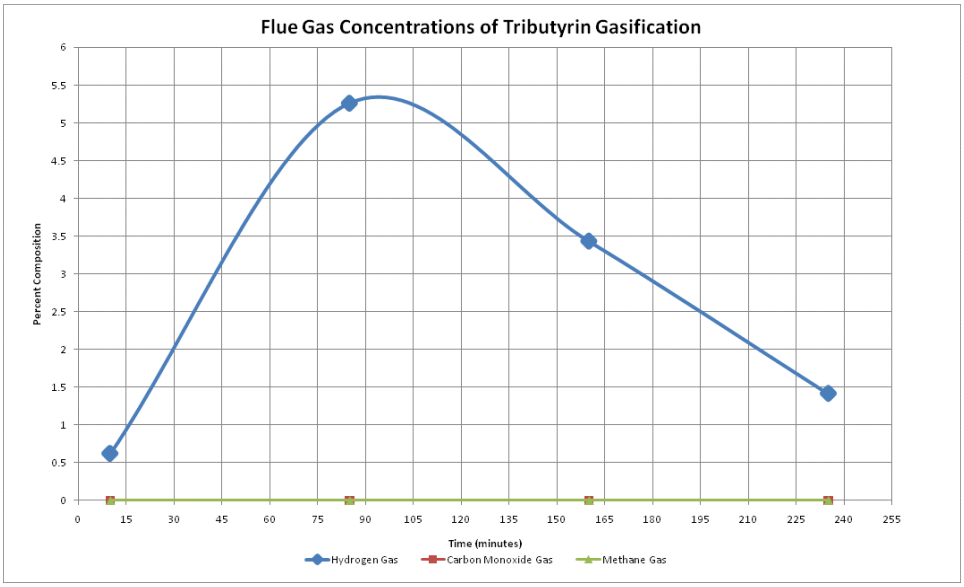

Figure 41: Flue Gas Concentrations of Tributyrin Gasification

This data shows that gasification of oils such as tributyrin yields similar results to other biomass such as paper or lima beans. A peak of syngas occurs early on during reaction followed by a decrease in production according to char accumulation.

Liquid products were also collected in the cold trap and analyzed using a GC. These liquids look similar to the liquids collected from overnight trials. There is a large peak for ethyl acetate and smaller peaks indicating volatile components were present. Interestingly, no tributyrin was found in the liquid according to the GC analysis. This is surprising because hydrogen was produced in some amount for the entire duration of the experiment yet no tributyrin remained leftover. The hydrogen gas production may have been the result of further breakdown of the tributyrin oil.

4.2 Depolymerization of Plastics

4.2.1 Initial Salt Furnace Tests

Before attempting to breakdown plastics in the reactor, they were first introduced to various molten salt compositions that had been melted in a furnace to observe visual effects. Figure 42 is a picture of the result of adding a small amount of plastic to potassium hydroxide at approximately 250°C. The plastic curled into itself and shriveled up as soon as it was introduced to the heat of the salt. No browning or smoking of the plastic occurred whatsoever.

Figure 42: Plastic in Molten Potassium Hydroxide

After the salt and plastic cooled, the plastic was recovered and is shown in Figure 43. There was a noticeable change to the plastic. First, the plastic changed from a clear consistency to a milky white. Also, the salt was noticeably rougher on the surface. These changed may indicate a reaction occurring within the plastic, however no liquids were found once the salt solidified.

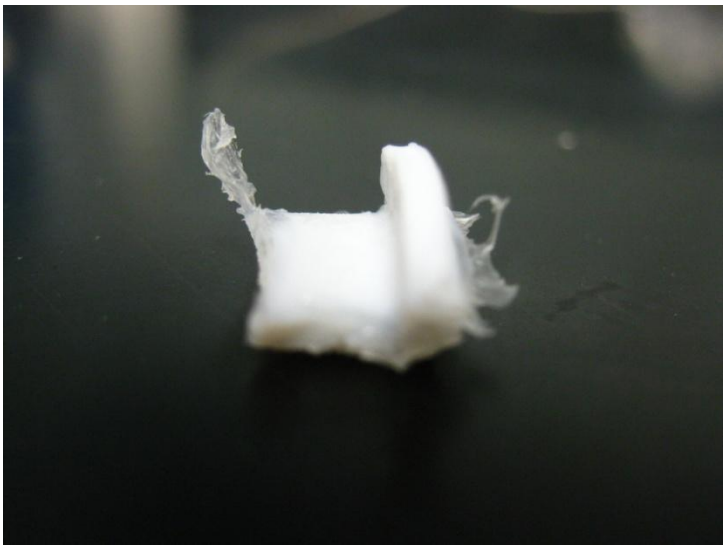

Figure 43: Plastic After Submerged in Molten Potassium Hydroxide

Next, plastic was introduced to molten sodium hydroxide at approximately 400°C. Figure 44 is a picture of the salt bubbling. As soon as plastic was introduced to the molten salt, it became frothy and bubbles were clearly visible. The salt and frothy bubbles solidified.

Figure 44: Plastic in Molten Sodium Hydroxide

The appearance of the plastic was also different after being placed in sodium hydroxide as compared to potassium hydroxide. This plastic did still have the milky white appearance on the top portion of the plastic that did not submerge into the liquid salt. However, the submerged portions of the plastic turned brown, as shown in Figure 45. The plastic seems to have 'inflated', and now appears hollow and full of holes. This indicates the creation, followed by the escape, of gas.

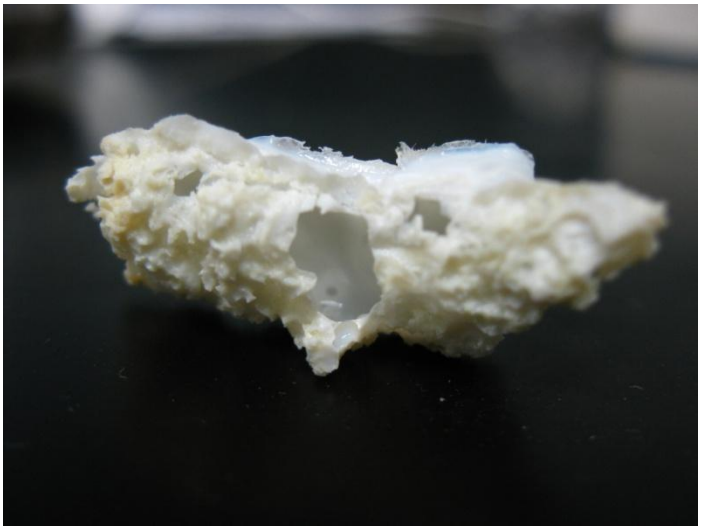

Figure 45: Plastic After Submerged in Molten Sodium Hydroxide

This is significant evidence for gasification. Unfortunately, at the time these experiments were being performed the gas chromatograph was still non-functional. Thus, in the reactor trials no gas samples can be taken to determine the components of the liberated gas.

Figure 46 shows the results of adding the plastic to the eutectic mixture at approximately 430°C. This reacted very similarly to the sodium hydroxide with a few important exceptions. First, the rate of bubble production was a bit slower. In the sodium hydroxide trial, bubbles were formed very rapidly. With the eutectic, bubbles appear from the bottom of the plastic and then flow up and out of the salt. When the plastic was originally placed into the salt mixture, it seemed like some of the salt forced itself up the side of the crucible. This can also be seen in Figure 46. Lastly, small bits of burned plastic broke off the main piece and floated around the molten salt.

Figure 46: Plastic in Molten Eutectic Salt

Figure 47 shows the plastic after it has been cooled and removed from the molten salt. The plastic is browner than the other trials and has larger bubbles. The plastic was extremely brittle and fell apart from the slightest touches.

Figure 47: Plastic After Submerged in Molten Eutectic Salt

The plastic underwent some sort of reaction with all of the molten salts. The weakest reaction, with potassium hydroxide, may have been due to the lower temperature of the salt as compared to the other trials. These reactions may be caused from the heat and not the salt itself. However, the highly ionic nature of the salts may very well be aiding in the breakdown of these plastics. This is suggested because the plastic is reduced to a very brittle state rapidly, whereas if heat was applied to the plastic alone, it simply melted.

4.2.2 Reactor Trials

As can be seen in the methodology, two trials involving plastic were performed in the reactor, one with water and one without. At the conclusion of each trial, unclean water was the only liquid product recovered. In addition, the reactor was clogged with melted plastic at the end of each trial. This required the project group to remove the plastic by submerging the reactor in an acid bath to dissolve the plastic. The results of both of these trials are largely inconclusive. Liquid products were not formed and any gas products could not be analyzed due to problems with the GC. Even so, the pressure at the end of the trial was never greater than 5-10 psi. Therefore, no gas chromatography data is available.

The lack of liquid products was most likely due to the pressure of the system. The trial without water reached 380 psi and the trial with water reached 750 psi. The literature states that the Depolymerization with water reaction should occur with a steam pressure of 600 psi. A possible reason why no liquid products were found is that the reactor was so thin the steam may not have been able to encounter enough plastic to create a measurable amount of liquid. If the plastic melted and formed a seal, only a very small area of this plastic would interact with the high pressure steam.

4.3 Esterification and Hydrolysis

Liquid products were identified using gas chromatography and NMR spectroscopy. Ethyl acetate, tributyrin, vegetable oil, methyl butyrate, butyric acid, and methanol peaks were all identified by running pure components through the machines.

4.3.1 Hydrolysis with Vegetable Oil

No strong evidence of hydrolysis was seen in any trial on the bench top or in the reactor. GC and NMR analysis do not show any peaks that match with butyric acid control peaks. Thus, hydrolysis of fatty acids into smaller acids is not feasible using the reactor at these conditions.

However, other interesting results were observed during experiments in the reactor. In Figure 48 unknown peaks appear in the GC results around 1-2 minutes. This means that small volatile components (similar to methyl butyrate) were created in small amounts.

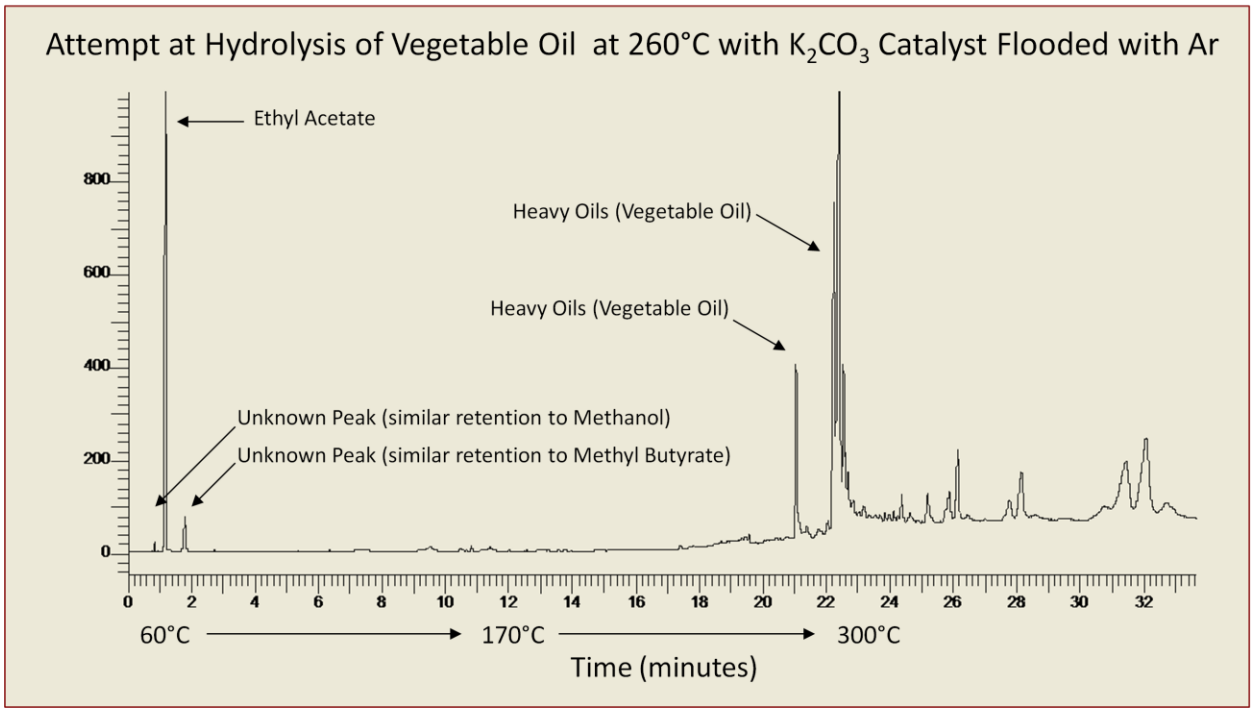

Figure 48: GC Results of the Attempted Hydrolysis of Vegetable Oil

The unknown peaks are most likely not the result of hydrolysis. Instead, the project group believes these peaks to be due to the pyrolysis of vegetable oil at high temperatures. Small, unknown peaks also appear in the NMR results and can be found in the Appendix E.

4.3.2 Hydrolysis with Tributyrin

Due to the may varying components in vegetable oil, tributyrin, a triglyceride, was also used for hydrolysis experiments to establish standards and controls. Tributyrin should produce butyric acid upon hydrolysis which can be detected in the GC and NMR.

Similarly, no hydrolysis products (butyric acid) were found with tributyrin indicating that this mechanistic pathway does not proceed given these conditions. Unknown peaks were not found in any result. All resulting liquids contained only ethyl acetate and tributyrin oil.

4.3.3 Transesterification of Oils with Methanol

All transesterification reactions provided evidence that the reaction is taking place both on the bench top and in the reactor. When reactions were performed with tributyrin, the expected product, methyl butyrate, was clearly identified.

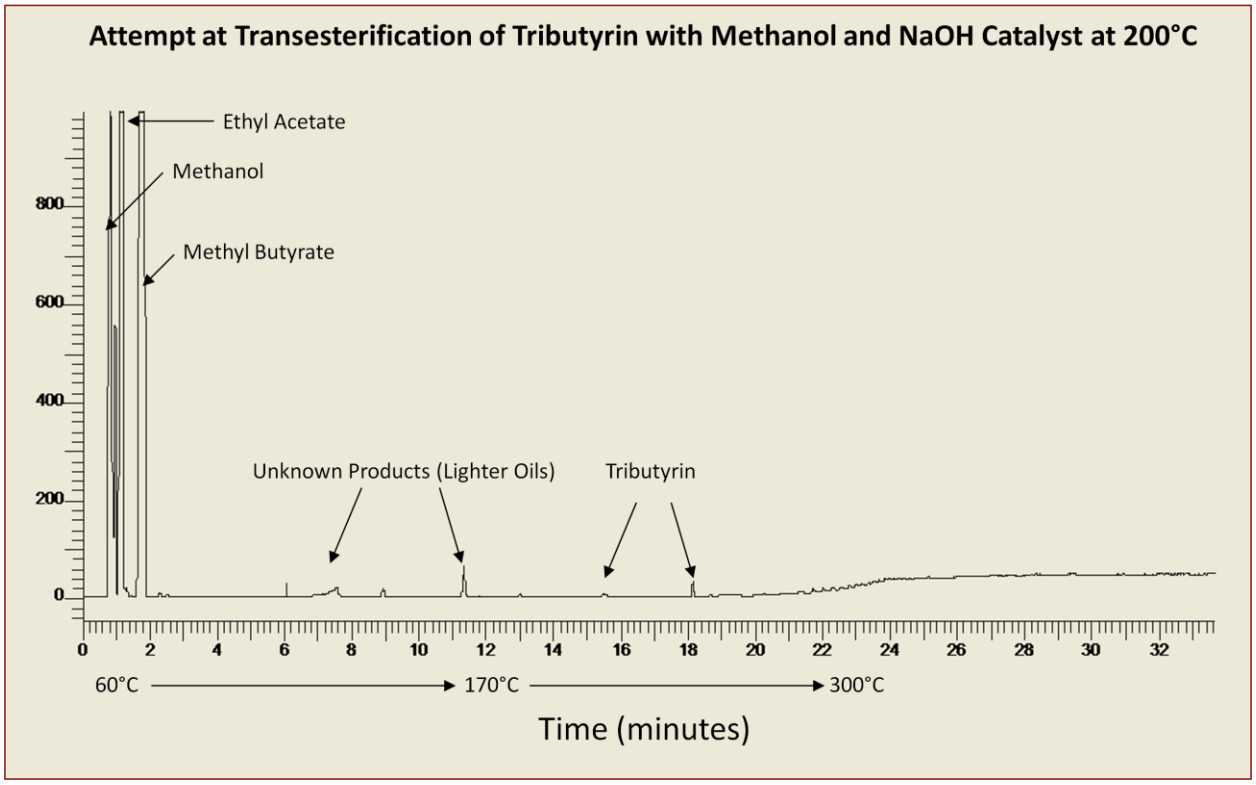

Figure 49: GC Results of the Transesterification of Tributyrin

Figure 49 shows the presence of methyl butyrate, confirming the transesterification process occurs in the reactor. This is also confirmed in the NMR results shown in various appendices attached to this report. There are also small, unknown peaks eluting from 6 to 12 minutes. The project group believes these are the results of pyrolysis and not transesterification. These unknown products are seen in small quantities and cannot be identified. These peaks may be similar chemicals as those found in the gasification of tributyrin discussed above.

4.4 Enzymatic Digestion

Proteinase K was used to pre-treat biomass to determine if a digestion step aids in the gasification and transesterification processes. Lima beans were selected for study due to their high triglyceride and protein content.

4.4.1 Digestion Applied to Gasification Reactions

Three trials and two controls (Table 9) were aimed to determine the effects of predigestion with Proteinase K on gasification yield. Samples were incubated for both 48 hours and 3 hours in addition to a 3 hour control incubation without Proteinase K (but with buffer). One control consisted of lima beans

and 5 mL of water with no digestion buffers and a final control consisted of lima beans and no water charged in the reaction vessel (but a sparger was activated though with CO_2 was pumped).

Trials B1, B3 and B5 (Table 9) produced both gas and liquid products.

One goal of Proteinase K digestion was to reduce the amount of char in the system which could be qualitatively evaluated by observing the amount of char coming out of the reactor after a 90 minute reaction with trials B1, B3, B5 and B8. Hypothetically, B1 and B3 should show the least amount of visible char and B5 along with B8 should show the greatest amount of visible char having not been predigested. The following pictures serve as qualitative evidence of char reduction throughout these trials.

Figure 50: Trial B1 Reactor Products with 48 Hour Digestion

Figure 51: Trial B3 Reactor Products with 3 Hour Digestion

Figure 52: Trial B5 Reactor Products with 3 Hour Incubation (No Proteinase K)

Figure 53: Trial B8 Reactor Products with No Proteinase K, Buffer or Incubation

It is clear that Figure 50 and Figure 51 have less char buildup than the controls without Proteinase K shown in Figure 52 and Figure 53. This suggests that the hypothesis of char reduction via protein and lignin degradation is not only true, but that Proteinase K was effective as an enzyme in actually degrading these structures in lima beans to reduce char in gasification which will allow catalysis reactions to occur more readily.

To quantify the effects of the visible char reduction with digestion with Proteinase K, the concentration of hydrogen gas liberated from each sample was measured 1 hour into each 90-minute trial. The results of this measurement for B1, B3, B5, and B8 are presented in Figure 54 below.

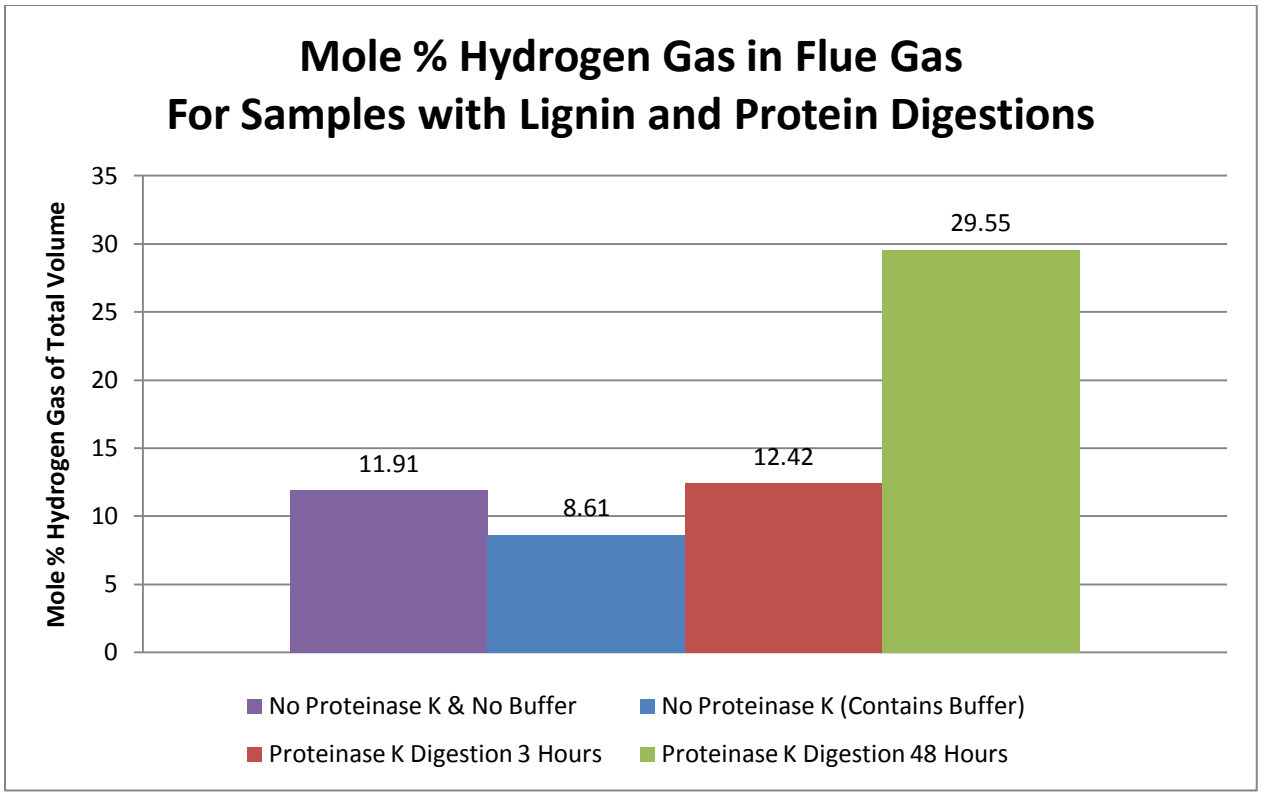

Figure 54: Mole Percentage Hydrogen Gas in Flue Gas for Samples with Proteinase K Digestion

Although digestion for 3 hours with 1 mg of Proteinase K at 30 units/mg activity showed little increase in hydrogen gas production, it is notable that digestion with Proteinase K for 48 hours showed almost a 300% increase in hydrogen gas liberation (Figure 54) due to the lack of char formation in the reactor vessel. This quantitative data shows that char is a major hindrance to allowing gasification reactions to take place as shown by the severe increase in hydrogen gas production. This data strongly supports the efficacy of Proteinase K digestion in yielding desirable products.

4.4.2 Digestion Applied to Transesterification Reactions

Two Proteinase K digestions of 3 hours and 48 hours as well as two control samples were used in the transesterification biodiesel trials. One control consisted of charging the reactor with lima beans, methanol, and salt. The other control consisted of charging the reactor with the same methanol and salt, except the lima beans were soaked in the buffer solution with no Proteinase K used for the digestions.

The lima bean trial with no enzyme or buffer (B7) did not yield any liquid products. Figure 55 is a picture of the lima beans after being removed from the reactor.

Figure 55: Lima Bean Control Products - No Enzyme or Buffer Solution

The lima beans have absorbed all of the methanol. Because no liquids are present, the project group was unable to compare GC and NMR results with other trials. However, the orange color in the lima beans suggests that a reaction has taken place. Many biodiesels are orange, which suggests the methanol and sodium hydroxide were able to react with triglycerides in the lima beans to make methyl esters.

The control of lima beans soaked in the buffer solution yielded very similar results. The only noticeable difference occurred before the mixture was even added to the reactor. As can be seen in Figure 56, the lima beans and buffer began reacting with the sodium hydroxide and methanol as soon as they were mixed to form a red solution.

Figure 56: Reaction from Adding Sodium Hydroxide and Methanol to Lima Beans in a Buffered Solution

The exact nature of this reaction is unknown. It is very likely that the methanol and salt are reacting with one or several components of the buffer.

After the reaction, solid products appear slightly different from the lima bean controls, as seen in Figure 57, the solid products from trial B2.

Figure 57: Trial B2 Solid Products from Reactor

Chunks of lima beans are clearly visible similar to the control. In contrast to the control, there seems to be less lima beans overall, some seem to have decomposed and congealed. This is most likely glycerin and soaps, which may form in the presence of excess sodium hydroxide. Figure 58 shows the liquid products obtained from the reactor from trial B2.

Figure 58: Trial B2 Liquid Products

These liquids are believed to contain methyl esters from the transesterification reaction. The transesterification liquid and solid products for all enzymatic biocatalysis reactions looked similar to the results of trial B2. The project group attempted to extract the organic material from these liquids using ethyl acetate, as described in the methodology. However, the addition of ethyl acetate to these liquids created an irreversible precipitate due to buffer components, which yielded the products unsuitable for analysis, as seen in Figure 59.

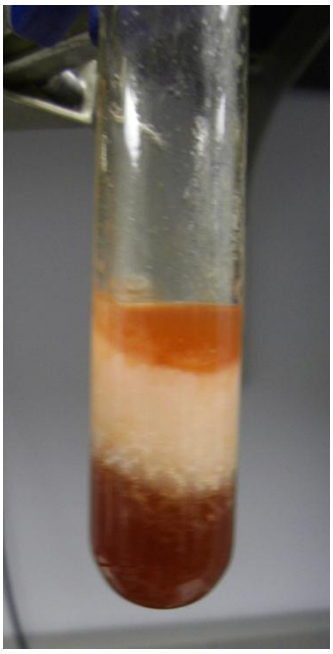

Figure 59: Solid Formed From the Addition of Ethyl Acetate to Trial B2 Liquid Products

Unfortunately, this sample was lost and could not be processed further. The project group believes that the reaction taking place was possibly ethyl acetate and sodium hydroxide reacting to form the solid sodium acetate. Excess sodium hydroxide was most likely in the product liquids because a larger amount of salt and methanol was used in these trials as reactants. The excess sodium hydroxide and methanol were used because it was unknown exactly how many triglycerides are within the beans and if an excess of reactants would be needed to force more products. Because of this reaction, ethyl acetate was not used as a solvent on any of the other biochemical digestion transesterification reactions.

NMR and GC results for transesterification yields both with predigestion and controls show that methyl butyrate products were produced. Peaks are present in the GC analysis at a retention time of between 1 and 2 minutes consistently across all trials as expected (liquid products did not contain ethyl acetate solvent) showing that usable fuels can be produced using this process. No liquid products were isolated from the B7 control showing that the contents of the buffer or the 37°C incubation for 3 hours, even without Proteinase K, was a valuable step, which is an unexpected result. The exact influential step in this preparation cannot be determined without further analysis. Additionally, since GC data was not found to be quantifiable with the equipment at our disposal, we could not determine the efficacy or usefulness of prolonged Proteinase K digestion in the transesterification pathway. Although usable fuel-like products were formed in this process, additional quantitative analysis is needed to determine if

Proteinase K was as effective in advancing the yields in transesterification similar to its effects on gasification. The GC and NMR data for these trials is shown in Appendix F.

4.5 Equipment Performance

4.5.1 Conventional Reactor

In general, the equipment associated with the flow system performed as expected. The reactor was able to withstand temperatures up to 500°C and pressures that reached 750 psi. However, wear and tear of materials and equipment was quite visible as the research progressed.

The most notable problems associated with the equipment were clogs. After most batch trials, the small tube that delivers gases inside of the reactor was clogged with biomass. This tube had to be changed out multiple times, and was often removed to clear the clog. Larger diameter tubing is recommended for easy cleaning.

Over time, the materials subjected to high heat visibly degraded, as shown in Figure 60.

Figure 60: Example of Materials Degrading Over Time

This picture shows how the steel began to flake off the connector that secures the reactor in place. This is the result of the steel oxidizing under high temperatures. This degradation of the system

was most notable after the overnight trials, which subjected the reactor to temperatures of 500°C for extended periods of time. Clearly, these materials cannot be used in commercial application for safety reasons. As the reactor degrades, it becomes more likely to fail under high pressure. Such an event could be catastrophic, causing serious injury or death to anyone standing too close to the system.

4.5.2 Microwave Reactor

The project group attempted to perform preliminary batch gasification trials using a microwave reactor. Due to pressure and temperature constraints, the reactions could not be carried out at the desired conditions. Most trials showed some level of paper degradation. However, it was evident that using the microwave reactor was unfeasible due to the brittleness of the glass vials used by the reactor.

Microwave reactors may be feasible if custom vials can be ordered. The vials must withstand high temperatures and pressures but not be made out of metal, which will not work in the microwave reactor.

5 Conclusions

This research allows the project group to provide many different conclusions relevant to the breakdown of biomass into useful fuel products. Liquid and gaseous products were obtained that may be used as possible fuels. Furthermore, the project group discovered much about the nature of these reactions and possible methods for increasing the yield of desired products.

5.1 Gasification

The extremely high carbon dioxide content of the gases eluting from the column was not a favorable result. The process must be modified in such a way that carbon dioxide has a greater opportunity to react with the biomass. However, successful gasification of paper, lima beans, and tributyrin oil was identified. Paper and tributyrin oil also produced unknown liquid products. These unknown products may be volatile and useful as fuels.

The use of a sparger in the overnight trials provided new insight into which reactions may be occurring. The sparger significantly decreased carbon monoxide and methane production. Thus, water vapor may be reacting with carbon monoxide to form hydrogen and carbon dioxide and acting to stop the methanation reactions. This is favorable for producing hydrogen rich gas that may be used for fuel cells or other technologies.

The overnight trials also suggest that the salt may be well suited as a catalyst. The salt recovered from these trials looked just as clean as the salt that was charged into the reactor. Unfortunately, the char formed during reaction was not able to mix in with all of the salt and gases sufficiently to be broken down easily. Improving the breakdown and catalytic removal of char is critical to the success of this process.

The most notable gasification results were the collection of liquids when using a semi-batch process. All overnight trials and the tributyrin gasification collected liquids approximately one to two hours after the reaction had started. This implies that allowing gas to flow out of the reactor allows the liquids to escape the intense heat before being broken down and reacted further. Analysis of these liquids shows they are a mixture of many different volatile components that may be used as fuels. This supports the hypothesis that these fuels are the result of a nonspecific pyrolytic breakdown of biomass.

5.2 Depolymerization of Plastics

Adding plastic to a crucible of molten salt shows that plastic does breakdown under these conditions. Bubbles formed in the plastic suggest that some gas is produced from the reaction. Attempting to perform these trials in the reactor was unsuccessful due to consistent clogging problems and having a broken GC at the time. Therefore, the components of these gases are unknown.

5.3 Transesterification and Hydrolysis

Transesterification was seen on the bench top and in the reactor. Hydrolysis was not observed in either case. This confirms that traditional biodiesel reactions are possible in the reactor. However, there remains little incentive to heat the reactor above the minimum temperature required by the reaction. At higher temperatures in the reactor, unknown products were found, but in small quantities. These products are most likely the result of pyrolysis of the oils. Increased reaction kinetics remains the only desirable reason to increase the temperature of the system above the minimum feasible temperature needed to allow these transesterification reactions to proceed.

Hydrolysis did not occur whatsoever in our experiments. Similar unknown products were observed (similar to the transesterification reactions) that the project group suspects is the result of pyrolysis. The hydrolysis of oils catalyzed by molten salts does not seem to be a plausible path of breaking down oils into smaller components.

Overall, the addition of molten salts did not seem to affect either reaction in the reactor significantly. Molten salts did not allow hydrolysis in the reactor and did not yield additional transesterification products in any way.

5.4 Pretreatment by Enzymatic Biocatalysis

Proteinase K was selected as a feasible enzyme to predigest the protein and lignin and biomass to positively affect fuel yields as it forms simpler sugars, preserves carbohydrates for energy processing, has short digestion time, and was highly unspecific and robust, meeting all of the necessary criteria for effective theoretical preparation of biomass for conversion.

Digestion with Proteinase K for a period of 48 hours before exposure to gasification and pyrolysis pathways proved to be beneficial in greatly increasing fuel yield and reducing char. Char was visibly reduced exiting the system, demonstrating that predigestion would allow biomass feedstocks to react for a longer period of time at extreme temperatures to increase reaction rate and yield of

liberating usable fuel products. Hydrogen gas concentration increased approximately 300% after digestion, which would prove useful for applications such as hydrogen PEM fuel cells. The extremity of this improvement in syngas yield was greater than expected. These results demonstrate the inverse relationship between char reduction and fuel conversion.

Transesterification reactions were found to take place after digestion, but the increase in yield was unquantifiable.

5 Recommendations

5.1 Flow System Upgrades

This project has determined that the current reactor has outstanding issues that limit the desired reactions from proceeding efficiently. Most likely, the small diameter of the reactor allows char to easily clog the system, limiting contact with the molten salt. Gases are injected through the top of the reactor instead of bubbling up into the molten salts. Therefore, less gas comes into contact with the char or molten salts, simply flowing up and out of the reactor.

The project group proposes a new reactor design to attempt to alleviate some of these problems, as shown in Figure 61.

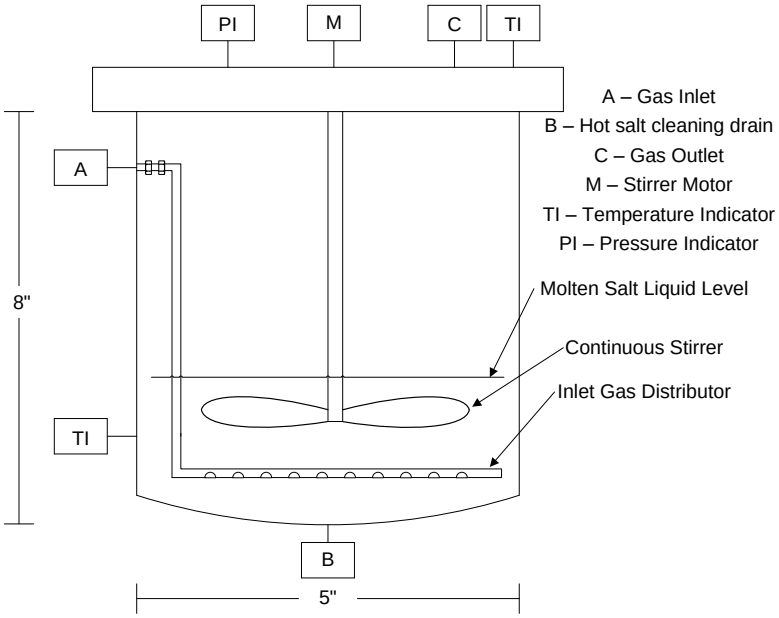

Figure 61: Proposed Reactor Design

This new reactor design allows for better contact between the biomass, molten salt, and gas phases. There are many important facets to this design, formulated from the results of the trials performed during this project:

1. The inlet gas flow is inside of the reactor and enters above the liquid level of the molten salt. This allows the gas to heat up to temperature before contacting the salt and biomass, and stops any molten salt from exiting the reactor via the inlet gas tube.

2. The inlet gas distributor allows the gas to exit via the bottom of the distributor. This allows the salt to be heated to a liquid state and easily drained out of the system (reactor and distributor) for maintenance.
3. The inlet gas distributor is removable for easy maintenance.
4. A concave bottom, and the distributor with holes in the bottom, will allow the salt to easily drain out of the reactor into a suitable container for easy maintenance.
5. A continuous stirrer will ensure that solid, liquid, and gas phases stay in constant contact.

The reactor and associated equipment must be constructed out of low carbon content steel capable of withstanding high temperatures. All inlet and outlet tubing should be at least quarter inch tubing to reduce the number of clogs and make cleaning easier. Larger tube sizes will allow pipe cleaners and other cleaning methods to be effective. The reactor also has a larger diameter. The larger diameter will stop biomass (including plastics) from clogging in the reactor. The biomass and plastics will fall into the molten salt rather than sticking to the wall.

The top of the reactor and stirrer should be removable. This will allow easy access to the reactor internals for cleaning and maintenance. The reactor must also be properly insulated. Heat loss is an issue with the current reactor and reducing that loss will allow for accurate heat and energy balance calculations. Table 2 shows that most of the pyrolysis and gasification reactions are exothermic. Using better insulation, further experiments can be performed to investigate the possibility of heating the molten salt up to start the reaction, but then allowing the heat of the pyrolysis reactions to partially power the reactor.

This reactor design still contains problems outside of the scope of this project. First, there is no heating method available in the laboratory capable of powering the reactor. The tubular furnace is not capable of handling a reactor of this size. Therefore, a larger furnace or other heating method must be designed around the reactor. The larger reactor will require an increase in materials for experimentation. This will be more costly. However, if future project groups recycle the molten salt catalyst, the added expense may decrease. Using larger amounts of molten salt catalyst may also make it easier to study the quality of the catalyst, and how long it can be used without being recharged or changed.

Design problems are also associated with this reactor. Building a reactor with a continuous stirrer that is gas tight under high pressure is more complicated than the traditional setup. Building and

testing this reactor may be possible with a joint MQP between the chemical engineering and mechanical engineering departments. Mechanical engineers will study the design of the materials of construction, stresses, and capabilities of the reactor while chemical engineers can continuously make improvements to the layout of the reactor to increase efficiency.

The cold traps performed well in removing liquids and collecting particulates. However, it is still likely that some particulates are being injected in the GC. This will continue to decrease the performance of the GC as it fills with solid particulates that clog tubing or the packing of the column. A filter should be added before the inlet of the GC that allows gas to flow uninhibited but stops fine particulates. Ideally, this filter should be easily cleaned and re-used.

5.2 Gasification

The liquids generated in the gasification reactions should be identified to determine their use as fuels. The liquid products created in the reactor are significant because producing liquid from solid biomass can have important implications. The production of usable fuel gases from biomass may very well be possible. Therefore, these products need to be identified for possible use as fuels.

Research into how to increase the yield of liquid products over gaseous products may also be performed. Liquid products are more useful as transportation fuels and easier to fit in the modern infrastructure than gaseous products.

The reactions should also be carried out in the proposed reactor above. This may allow for better concentrations of the syngas and shorter reactions times.

5.3 Depolymerization of Plastics

The gases produced when adding plastic to molten salt should be identified using GC instrumentation. Should these gases be syngases, plastics may be processed in conjunction with paper or other cellulose biomasses in the reactor. The reactor will be capable of handling most municipal solid wastes if it can produce fuels from biomass and plastics in tandem.

5.4 Pretreatment by Enzymatic Biocatalysis

In short, experiments with Proteinase K treatment were definitive in displaying that char reduction and increase in fuel yield are results of proper predigestion using the constructed system. A cost-benefit analysis between the increase in efficacy of the overall system and yield vs. the cost of

Proteinase K predigestion would need to be completed to determine if the overall process could be financially feasible on a large commercial scale.

Future studies may expand beyond Proteinase K and examine other enzymes. A mixture of enzymes may prove to be more beneficial in processing various kinds of biomass and creating a more versatile system.

For the process to be viable on a large scale, the enzymes must be separated from the biomass before they are processed in a reactor. This will allow the enzymes to be recycled, drastically reducing operating costs. Possible solutions may include washing the enzyme off the biomass sludge. This is a process that needs to be further researched, developed, and implemented.

5.5 Transesterification and Hydrolysis

The project group recommends identifying the unknown peaks obtained from vegetable oil and tributyrin at high temperatures in the reactor. These may be the result of pyrolysis and have the potential to be useful fuels. If the unknown peaks are the result of pyrolysis, the oils can be processed in tandem with solid biomass, increasing the reactor versatility. As the number of starting materials and wastes the reactor is capable of processing increases, the reactor becomes more valuable.

The project group does not recommend further study in the transesterification and hydrolysis mechanisms for use in this reactor. These processes can be carried out in other reactors without the large amount of heat required by this system.

5.6 Molten Salts

Molten salts allowed for the formation of gas and liquid products from solid feedstocks. Further research into expanding the type of salts used should be performed. The eutectic may be improved with the addition of additional carbonate or hydroxide salts. Also, the addition of metal salts such as nickel may increase the reactivity of the molten media.

6 References

Adinberg, R., Epstein, M., & Karni, J. (2004). Solar gasification of biomass: A molten salt pyrolysis study. *Journal of Solar Energy Engineering (Transactions of the ASME), 126*(3), 850-857.

Akinci, B., Kassebaum, P. G., Fitch, J. V., & Thompson, R. W. (2008). The role of biofuels in satisfying US transportation fuel demands. *Energy Policy, 36*(9), 3485.

Alden, N., Humerick, Z., Teixeira, A., Datta, R., & Dittami, J. (2009). *Molten salt gasification of biomass*. Worcester, MA: WPI.

Basu, P., & Mettanant, V. (2009). Biomass gasification in supercritical water - A review. *International Journal of Chemical Reactor Engineering, 7*

Bio Miami. (2009). *Proteins.* Retrieved 11/2, 2009, from http://www.bio.miami.edu/~cmallery/150/protein/c8.8x13.hydrolysis.sucrose.jpg

Bridgwater, A. V. (1995). The technical and economic feasibility of biomass gasification for power generation. *Fuel, 74*(5), 631.

Cablewski, T., Faux, A. F., & Strauss, C. R. (1994). Development and applicatino of a continuous microwave reactor for organic synthesis. *J. Org. Chem, 59*, 3408.

Calzavara, Y., Joussot-Dubien, C., Boissonnet, G., & Sarrade, S. (2005). Evaluation of biomass gasification in supercritical water process for hydrogen production. *Energy Conversion and Management, 46*, 615.

Courson, C., Udron, L., Swierczynski, D., Petit, C., & Kiennemann, A. (2002). Hydrogen production from biomass gasification on nickel catalysts - tests for dry reforming of methane. *Catalysts Today, 76*, 75.

Dale, B. E. (2008). Grassoline in your tank: Myths and realities about biofuels. *Microsc Microanal, 14*

Delgado, J., Anzar, M., & Corella, J. (1997). Biomass gasification with steam in fluidized bed: Effectiveness of CaO, MgO, and CaO-MgO for hot raw gas cleaning. *Industrial Engineering Chemical Res., 36*, 1535.

Demirbas, A. (2000). Mechanisms of liquefaction and pyrolysis reactions of biomass. *Energy Conversion and Management, 41*, 633.

El-Rub, Z. A., Bramer, E. A., & Brem, G. (2004). Review of catalysts for tar elimination in biomass gasification processes. *Industrial Engineering Chemical Res., 43*, 6911.

Energy prices. (2010). Retrieved April, 12, 2010, from http://www.bloomberg.com/markets/commodities/energyprices.html

ExxonMobil. (2008). *2008 summary annual report*

Feng, L., & Chen, Z. (2008). Research progress on dissolution and functional modification of cellulose in ionic liquids. *Journal of Molecular Liquids, 142*, 1.

Fujiwara, S., Kato, F., Watanabe, S., Inaba, M., & Tasaka, A. (2009). New iodide-based molten salt systems for high temperature molten salt batteries. *Journal of Power Sources, 194*(2), 1180-1183. doi:DOI: 10.1016/j.jpowsour.2009.06.063

Gil, J., Aznar, M., Caballero, M., Frances, E., & Corella, J. (1997). Biomass gasification in fluidized bed at pilot scale with steam - oxygen mixtures. product distribution for very different operating conditions. *Energy and Fuels - an American Chemical Society Journal, 11*(6), 1109.

Gil, J., Corella, J., Aznar, M., & Caballero, M. (1999). Biomass gasification in atmospheric and bubbling fluidized bed: Effect of the type of gasifying agent on the product distribution. *Biomass and Bioenergy, 17*, 389.

Gregory, A. P. (2009). *Green energy.* Retrieved 11/2, 2009, from http://www.rgs.uky.edu/odyssey/winter07/green_energy.html

Gusta, E., Dalai, A., Uddin, A., & Sasaoka, E. (2009). Catalytic decomposition of biomass tars with dolomites. *Energy and Fuels, 23*, 2264.

Herrmann, U., Kelly, B., & Price, H. (2004). Two-tank molten salt storage for parabolic trough solar power plants. *Energy, 29*(5-6), 883-893. doi:DOI: 10.1016/S0360-5442(03)00193-2

Huber, G. W., Iborra, S., & Corma, A. (2006). *Synthesis of transportation fuels from biomass: Chemistry, catalysts, and engineering*. Quimicia: Valencia, Spain: Instituto de Tecnologia.

Iowa State. (2009). *Center for carbon capturing crops.* Retrieved 11/2, 2009, from http://c2c2.iastate.edu/images/carbon_cycle.png

Jelles, S. J., van Setten, B. A. A. L., Makkee, M., & Moulijn, J. A. (1999). Molten salts as promising catalysts for oxidation of diesel soot: Importance of experimental conditions in testing procedures. *Applied Catalysis B: Environmental, 21*(1), 35-49. doi:DOI: 10.1016/S0926-3373(99)00011-9

Jin, G., Iwaki, H., Arai, N., & Kitagawa, K. (2005). Study on the gasification of wastepaper/carbon dioxide catalyzed by molten carbonate salts. *Energy, 30*, 1192.

Krishna, R., Ellenberger, J., & Sie, S. T. (1996). Reactor development for conversion of natural gas to liquid fuels: A scale-up strategy relying on hydrodynamic analogies. *Chemical Engineering Science, 51*(10), 2041-2050. doi:DOI: 10.1016/0009-2509(96)00061-9

Kruse, A., & Faquir, M. (2007). Hydrothermal biomass gasification - effects of salts, backmixing, and their interaction. *Chemical Engineering Technology, 30*(6), 749.

Laureano-Perez, L., Teymouri, F., Alizadeh, H., & Dale, B. E. (2005). Understanding factors that limit enzymatic hydrolysis of biomass. *Appliied Biochemistry and Biotechnology, 121-124*

Lee, J. (1997). Biological conversion of lignocellulosic biomass to ethanol. *Journal of Biotechnology, 56*, 1.

Lemley, B. (2003, May 1). Anything into oil. *Discover Magazine,*

Mishra, B., & Olson, D. L. (2005). Molten salt applications in materials processing. *Journal of Physics and Chemistry of Solids, 66*(2-4), 396-401. doi:DOI: 10.1016/j.jpcs.2004.06.049

Miskolczi, N., Bartha, L., Deák, G., & Jóver, B. (2004). Thermal degradation of municipal plastic waste for production of fuel-like hydrocarbons. *Polymer Degradation and Stability, 86*(2), 357-366. doi:DOI: 10.1016/j.polymdegradstab.2004.04.025

NSF. (2008). *Breaking the chemical and engineering barriers to lignocellulosic biofuels: Next generation hydrocarbon biorefineries*. Washington D.C.: University of Massachusetts Amherst. National Science Foundation. Environmental, and Transport Systems Division.

Parveen Kumar, Diane M. Barrett, Michael J. Delwiche, Pieter Stroeve. (2009). Methods for pretreatment of lignocellulosic biomass for efficient hydrolysis and biofuel production. *Ind. Eng. Chem. Res., 48*, 3713-3729.

Peng, Q., Ding, J., Wei, X., Yang, J., & Yang, X. The preparation and properties of multi-component molten salts. *Applied Energy, In Press, Corrected Proof* doi:DOI: 10.1016/j.apenergy.2009.06.022

Qiagen. (2010). *Qiagen proteinase K protocol.* Retrieved 4/1, 2010, from http://www1.qiagen.com/products/accessories/accessoryenzymes/qiagenproteinasek.aspx

Rajvanshi, A. K. (1986). Biomass gasification. *Alternative energy in agriculture* (Volume II, Ed. D ed., pp. 83). Maharashtra, India: CRC Press.

Raner, K. D., Strauss, C. R., & Trainor, R. W. (1995). A new microwave reactor for batchwise organic synthesis. *J. Org. Chem., 60*, 2456.

Ranganathan, S. V., Narasimhan, S. L., & Muthukumar, K. (2008). An overview of enzymatic production of biodiesel. *ScienceDirect, 99*, 3975.

Rapagna, S., Jand, N., & Foscolo, P. U. (1998). Catalytic gasification of biomass to produce hydrogen rich gas. *Int. J. Hydrogen Energy, 23*(7), 551.

Roche. (2010). *Roche applied science - proteinase K, recombinant, PCR grade.* Retrieved 4/1, 2010, from http://www.roche-applied-science.com/pack-insert/3115887a.pdf

Saha, B. C., & Woodward, J. (1997). *Fuels and chemicals from biomass* (Symposium sponsored by the Division of Biochemical Technology. Washington, D.C.: American Chemical Society.

Schulz, T. (2006). *The economics of micro-algae production and processing into biofuel*. Western Australia: Department of Agriculture and Food.

Scott, D. S., Czernik, S. R., Piskorz, J., & Radlein, D. S. A. G. (1990; 1990). Fast pyrolysis of plastic wastes. *Energy & Fuels, 4*(4), 407-411.

Sigma-Aldrich. (2009). *Lysing enzymes.* Retrieved 11/1, 2009, from http://www.sigmaaldrich.com/life-science/metabolomics/enzyme-explorer/learning-center/lysing-enzymes.html

Sigma-Aldrich. (2010). *Sigma-aldrich - proteinase K.* Retrieved 4/1, 2010, from http://www.sigmaaldrich.com/life-science/metabolomics/enzyme-explorer/analytical-enzymes/proteinase-k.html

Stevens, D. J. (2001). *Hot gas conditioning: REcent progress with larger-scale biomass gasification systems* (Subcontractor Report No. NREL/SR-510-29952). Richland, Washington: National Renewable Energy Laboratory.

Talebnia, F., Karakashev, D., & Angelidaki, I. (2010). Production of bioethanol from wheat straw: An overview on pretreatment, hydrolysis and fermentation. *Bioresource Technology, 101*(13), 4744-4753. doi:DOI: 10.1016/j.biortech.2009.11.080

Terwiesch, P., Ravemark, D., Schenker, B., & Rippin, D. W. T. (1998). Semi-batch process optimization under uncertainty: Theory and experiments. *Computers Chemical Engineering, 22*(1-2), 201.

The Environmental Protection Agency. (2007). *What is acid rain?* Retrieved April, 12, 2010, from http://www.epa.gov/acidrain/what/

The Environmental Protection Agency. (2009). *Municipal solid waste generation, recycling, and disposal in the united states: Facts and figures for 2008*

The Environmental Protection Agency. (2010). *Greenhouse gas emissions.* Retrieved April, 12, 2010, from http://www.epa.gov/climatechange/emissions/

The Need Project. (2008). *Biomass*. Manassas, VA: Secondary Energy Infobook.

Tijmensen, M. J. A., Faaij, A. P. C., Hamelinck, C. N., & van Hardeveld, Martijn R. M. (2002). Exploration of the possibilities for production of fischer tropsch liquids and power via biomass gasification. *Biomass and Bioenergy, 23*, 129.

Unknown. (2009). *Molten salts database -eutectic finder-.* Retrieved 11/2, 2009, from http://ras.material.tohoku.ac.jp/~molten/molten_eut_query1.php

Wilkes, J. S. (2007). *Molten salts and ionic liquids - are they not the same thing?* (ECS Transactions Trans.). Electrochemical Society:

Worthington Biochemical Corporation. (2010). *Worthington - proteinase K.* Retrieved 4/1, 2010, from http://www.worthington-biochem.com/PROK/default.html

Yaman, S. (2003). Pyrolysis of biomass to produce fuels and chemical feedstocks. *Energy Conversion and Management, 45*, 651.

Yaw D. Yeboah, Atul Sheth, & Pradeep Agrawal. (2004). *Catalytic gasification of coal using eutectic salt mixtures* No. DE-FG26-97FT97263--01). United States: USDOE Office of Fossil Energy (FE).

Yeboah, Y., Xu, Y., Sheth, A., Godavarty, A., & Agrawal, P. Catalytic gasification of coal using eutectic salt mixtures.

Appendices

Appendix A Gas Chromatograph Operation

The SRI 8610C gas chromatograph is controlled by a program released by SRI called "peakSimple." This program is capable of reading data from multiple detectors, set to different channels. For the purpose of studying the gases in this project, the GC used a thermal conductivity detector set to channel 2.

To begin, the program had to be set to read information from the correct COM port on the back of the computer. After the program was loaded, it will fail to recognize the GC and return the error message, "Acquisition System Not Functioning." At this point, the dialog box is closed and the correct COM port is selected by clicking on "edit" in the menu bar and then "Overall", the dialog box that appears is presented in Figure 62.

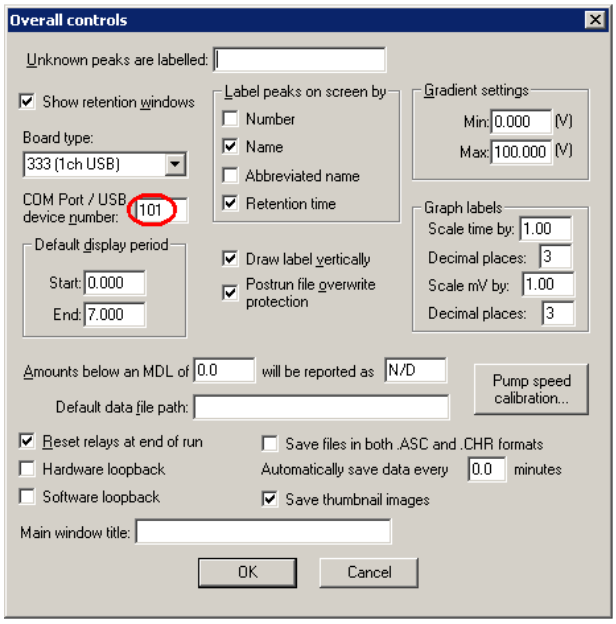

Figure 62: PeakSimple Overall Controls

The value circled in red is set to "2" and the program can then connect to the gas chromatograph. After this, the gas chromatograph must be configured to read data from the correct channel and to perform every trial correctly. The user must again select "edit" from the menu bar and then select "channels", Figure 63 is the dialog box that appears.

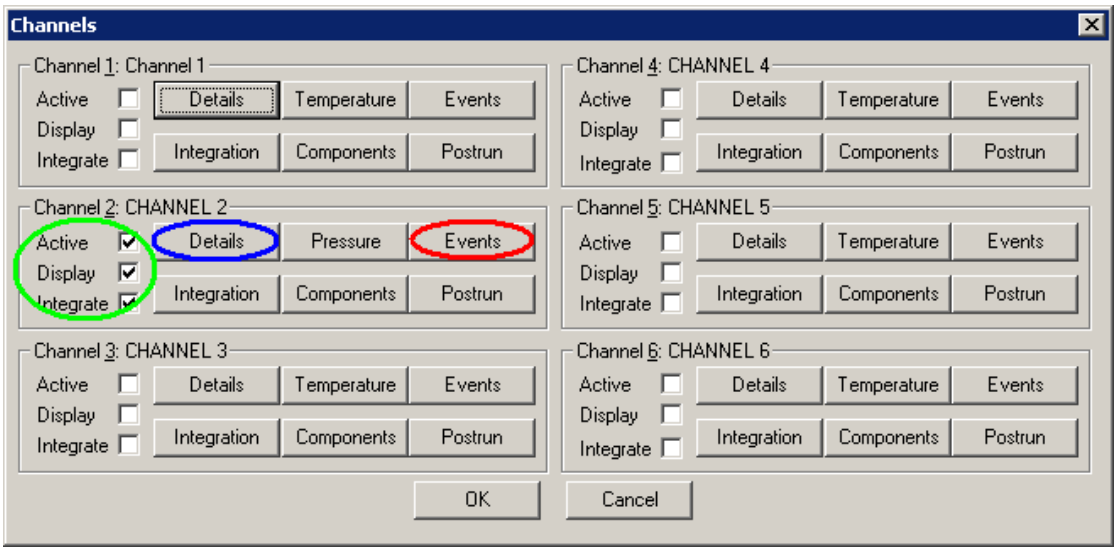

Figure 63: PeakSimple Channels Controls

Originally the three check boxes for channel "1" will be marked. These must be unmarked and the channel "2" boxes must be checked. The "details" button is then selected which will bring up the dialog box presented in Figure 64.

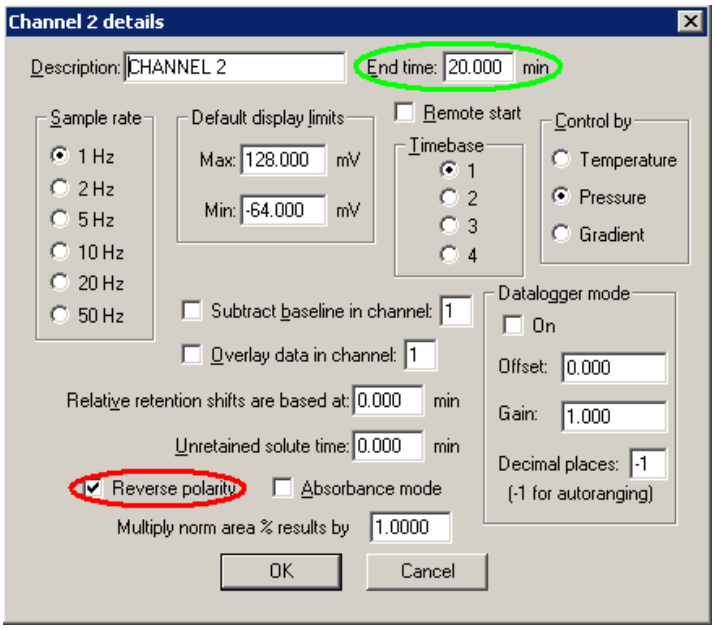

Figure 64: PeakSimple Channel Details Box

Two important functions were changed for these experiments. First, the polarity was reversed to ensure that all peaks spiked upwards. Then, the end time of the experiment was adjusted. Before the column was changed and the GC broke, the end time was usually set to 10 minutes to allow all gases

to exit the detector. After the column stopped functioning correctly and a new column was installed the end time was adjusted to 75 minutes, to allow time for the carbon dioxide to exit the column. Then, the "events" box must be opened, as shown in Figure 65.

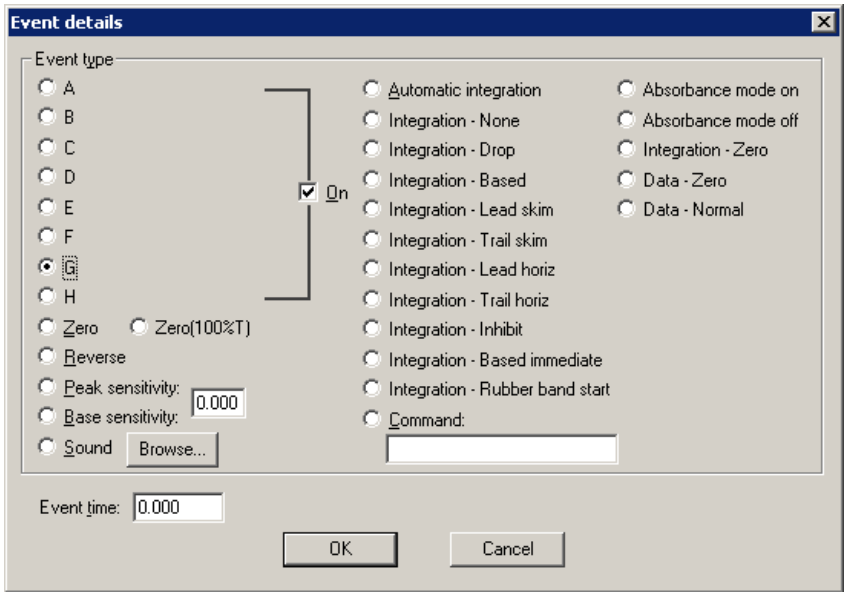

Figure 65: PeakSimple Channel Events Box

For every run three events were programmed into the machine. First, the machine was set to zero the baseline at an event time of 0.000 minutes. Then, the "G" button was selected with the checked "On" to activate the switching valve at an event time of 0.000 minutes. This switching valve is what allows sample gases to flow into the system and through the detector. Finally, the "G" button was selected again with the "On" box unchecked at an event time of 0.100 minutes. This last command switched the valve back to its original position after 6 seconds, more than enough time to collect and adequate gas sample.

After this, the gases collected in the switching valve flowed through the system. The TCD would record any peaks and the data was saved to the hard drive on the computer for later interpretation.

Appendix B Raw Data for Gas Analysis – Gasification

G1

5 Minutes:

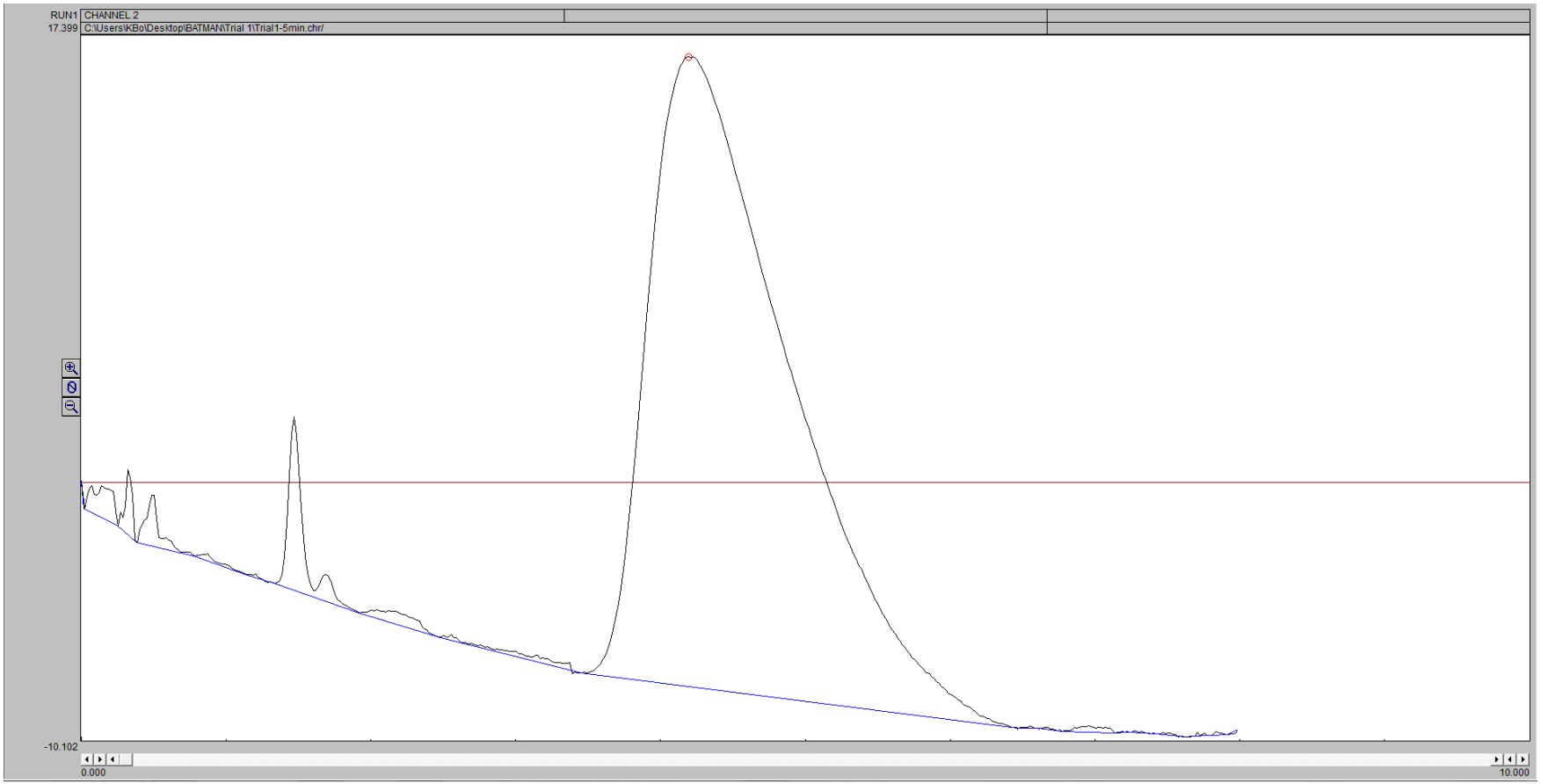

15 Minutes:

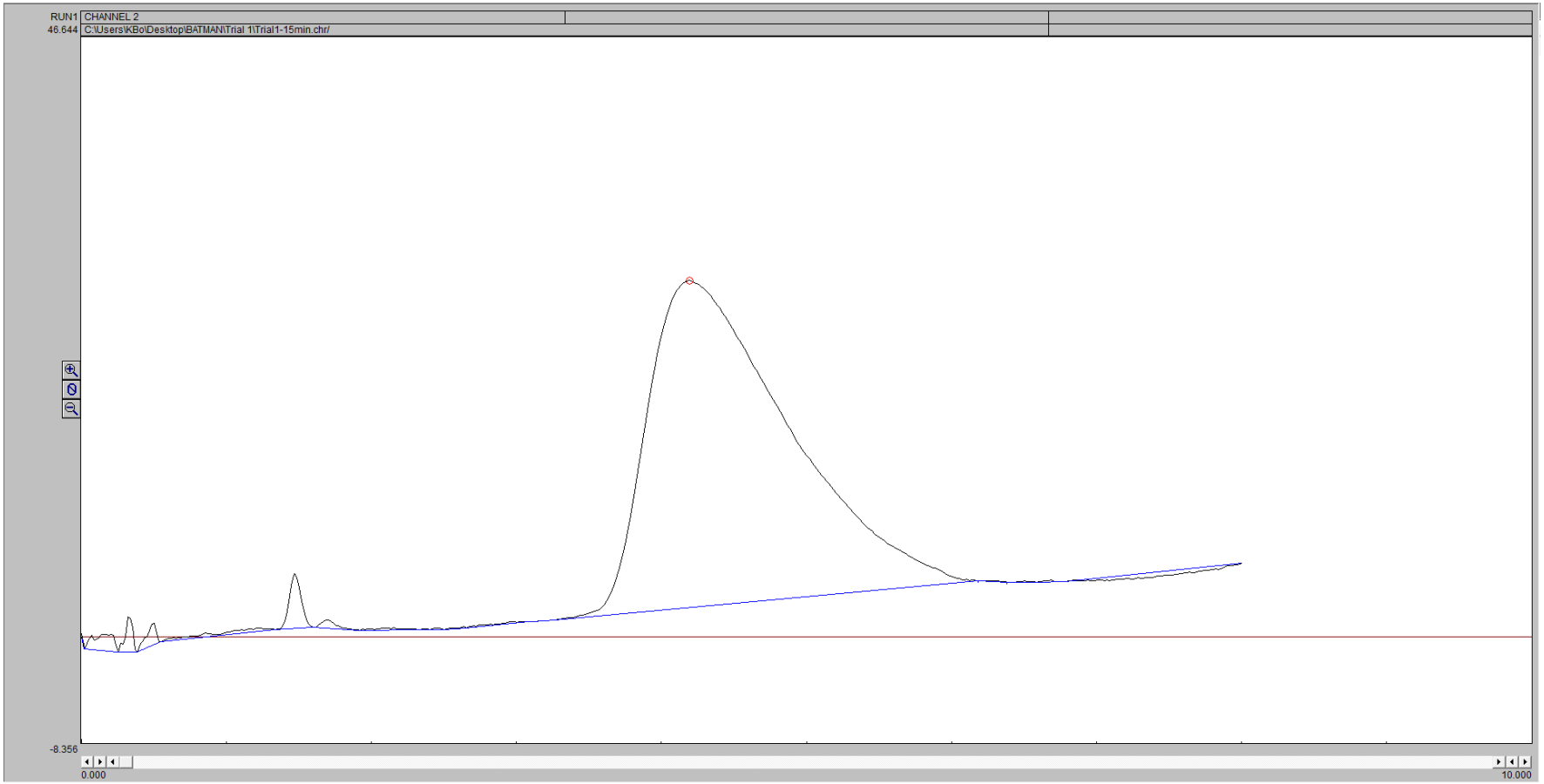
RUN1
CHANNEL 2
46.644
C:\Users\KBo\Desktop\BATMAN\Trial 1\Trial1-15min.chr/
-8.356
0.000
10.000

25 Minutes

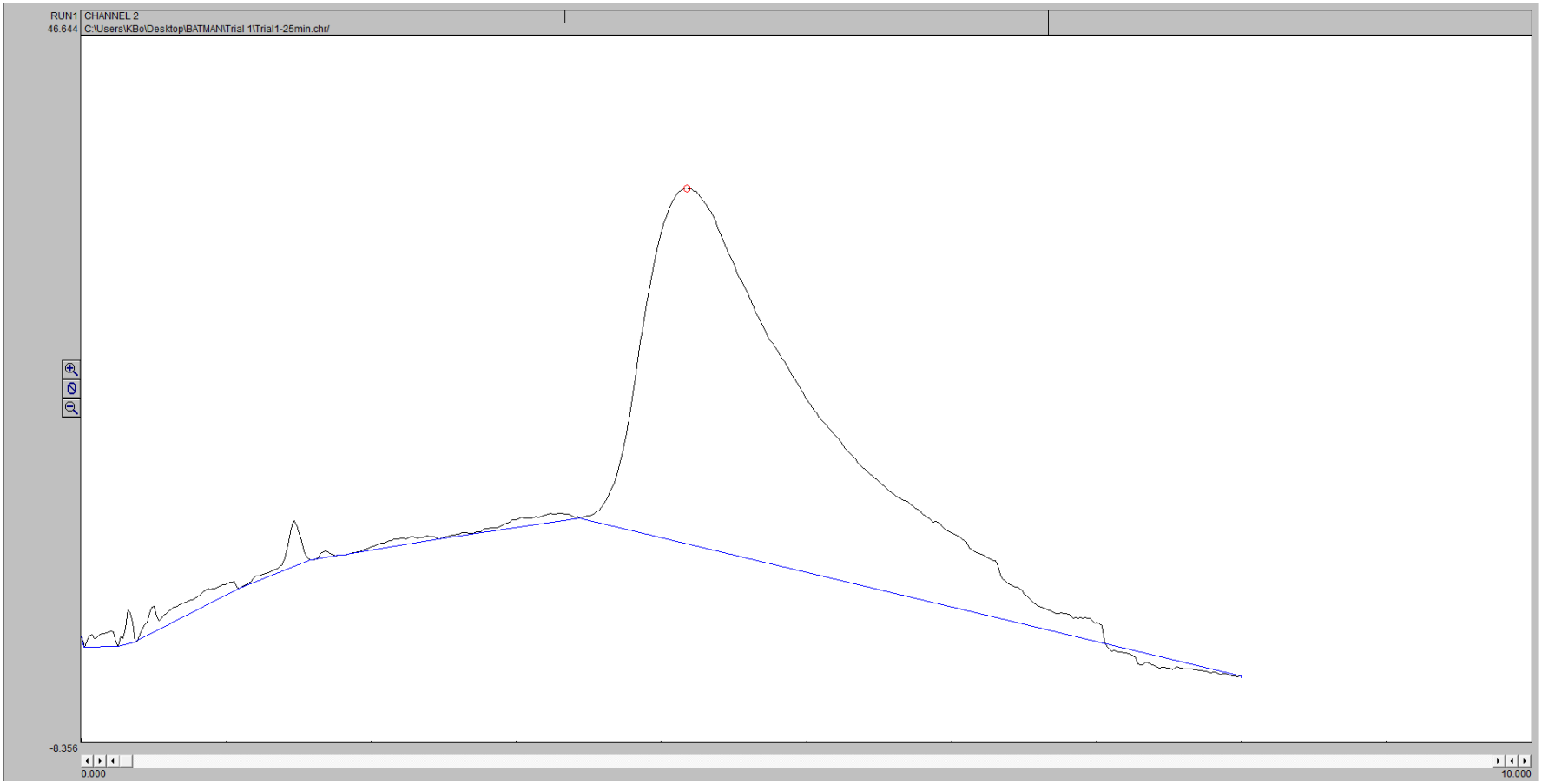
RUN1
CHANNEL 2
46.644
C:\Users\KBo\Desktop\BATMAN\Trial 1\Trial1-25min.chr/
-8.356
0.000
10.000

35 Minutes

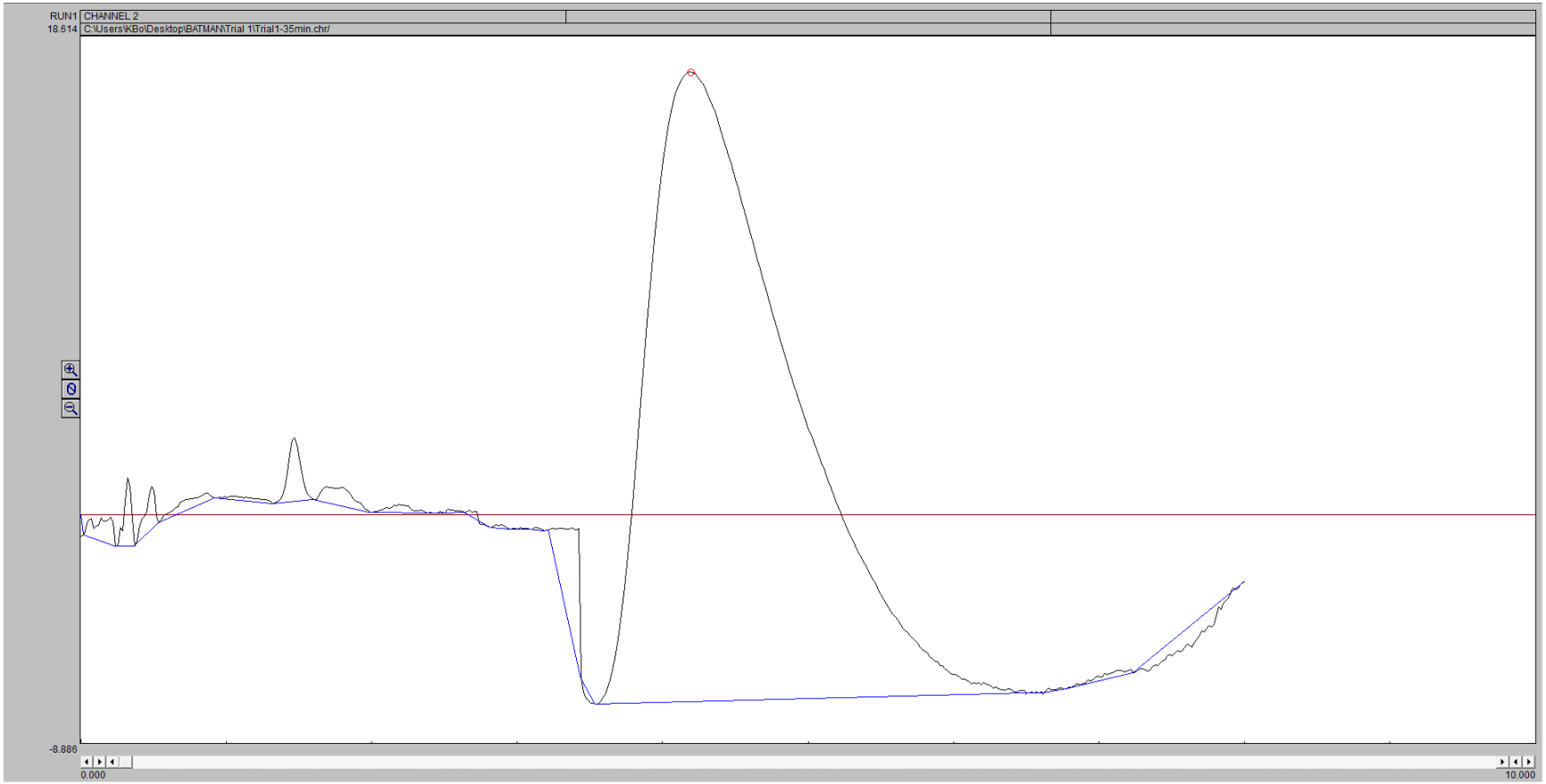
RUN1 CHANNEL 2
18.614
C:\Users\KBo\Desktop\BATMAN\Trial 1\Trial1-35min.chr/
-8.886
0.000
10.000

45 Minutes

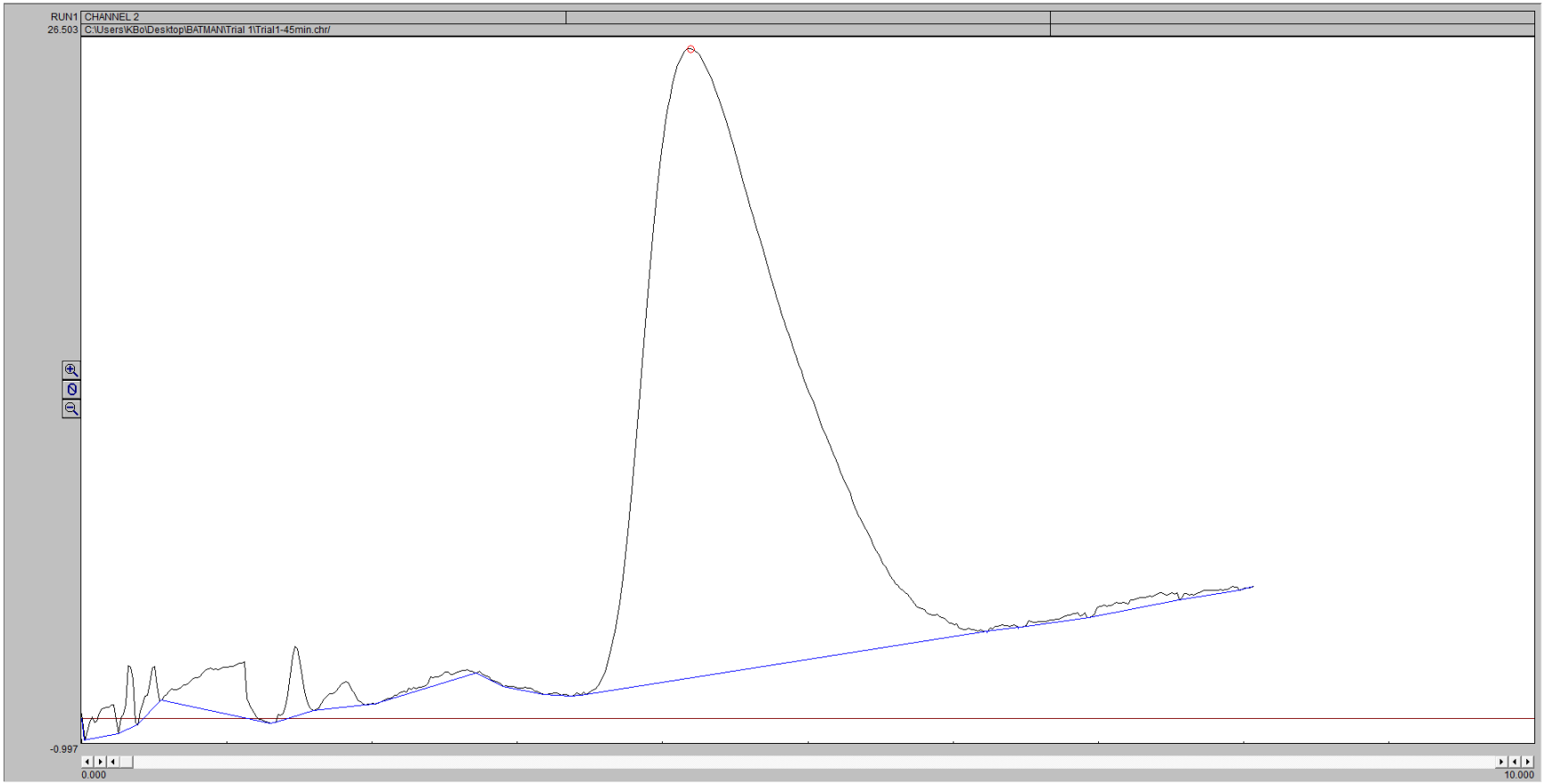
RUN1
CHANNEL 2
26.503
C:\Users\KBo\Desktop\BATMAN\Trial 1\Trial1-45min.chr/
-0.997
0.000
10.000

G2

5 Minutes:

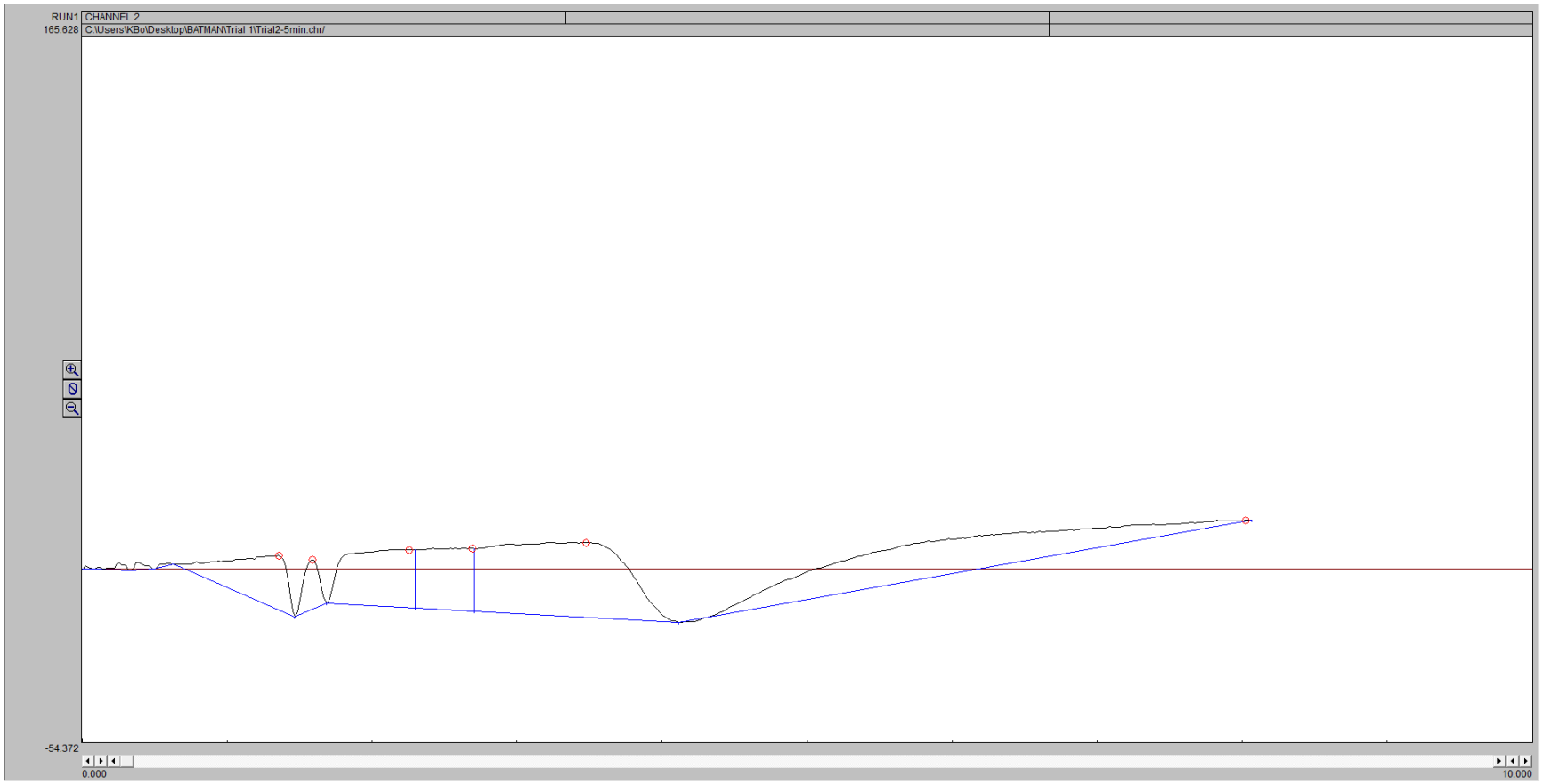
RUN1
CHANNEL 2
165.628
C:\Users\KBo\Desktop\BATMAN\Trial 1\Trial2-5min.chr/
-54.372
0.000
10.000

15 Minutes:

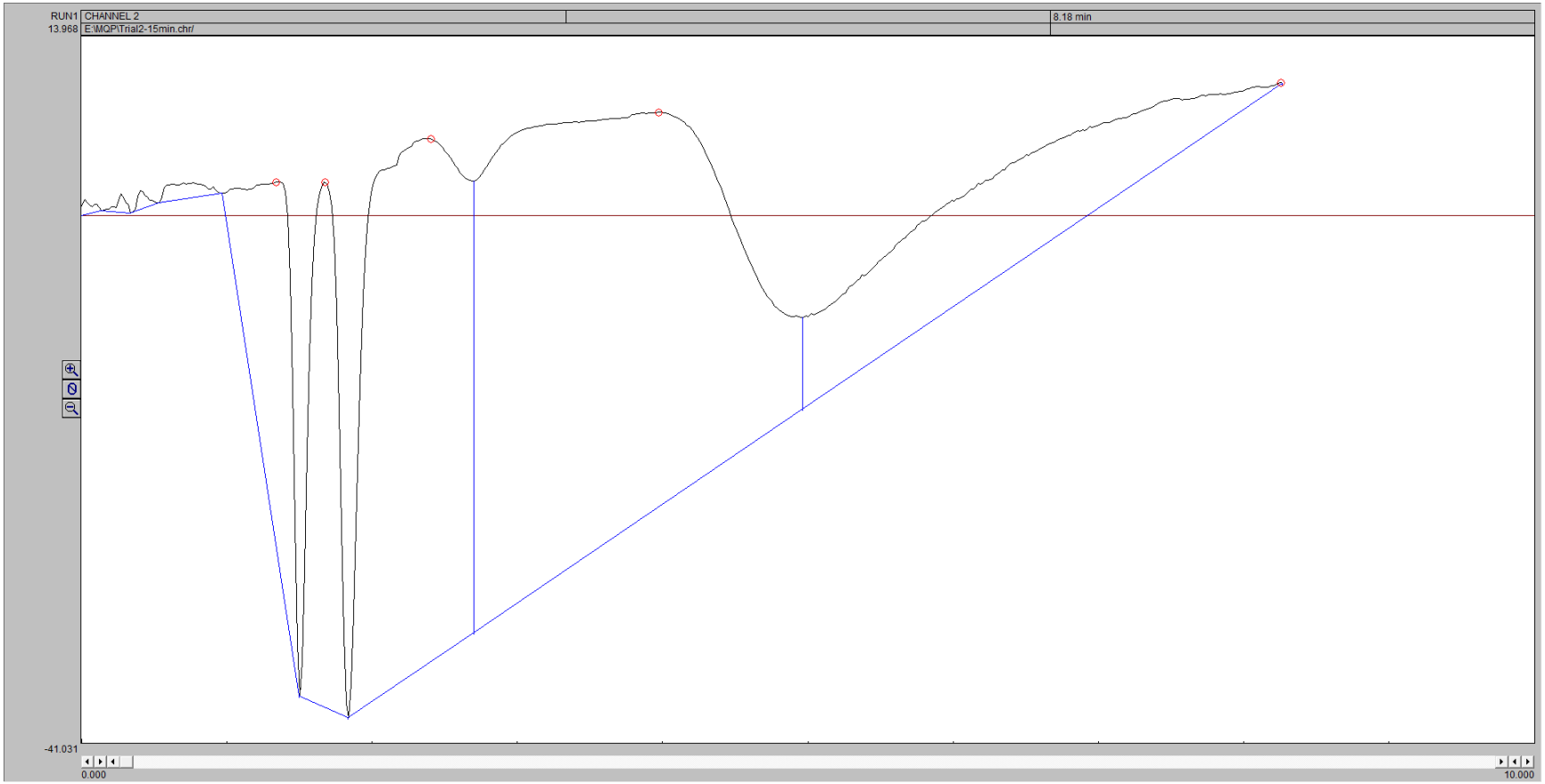
RUN1
CHANNEL 2
8.18 min
13.968
E:\MQP\Trial2-15min.chr/
-41.031
0.000
10.000

35 Minutes

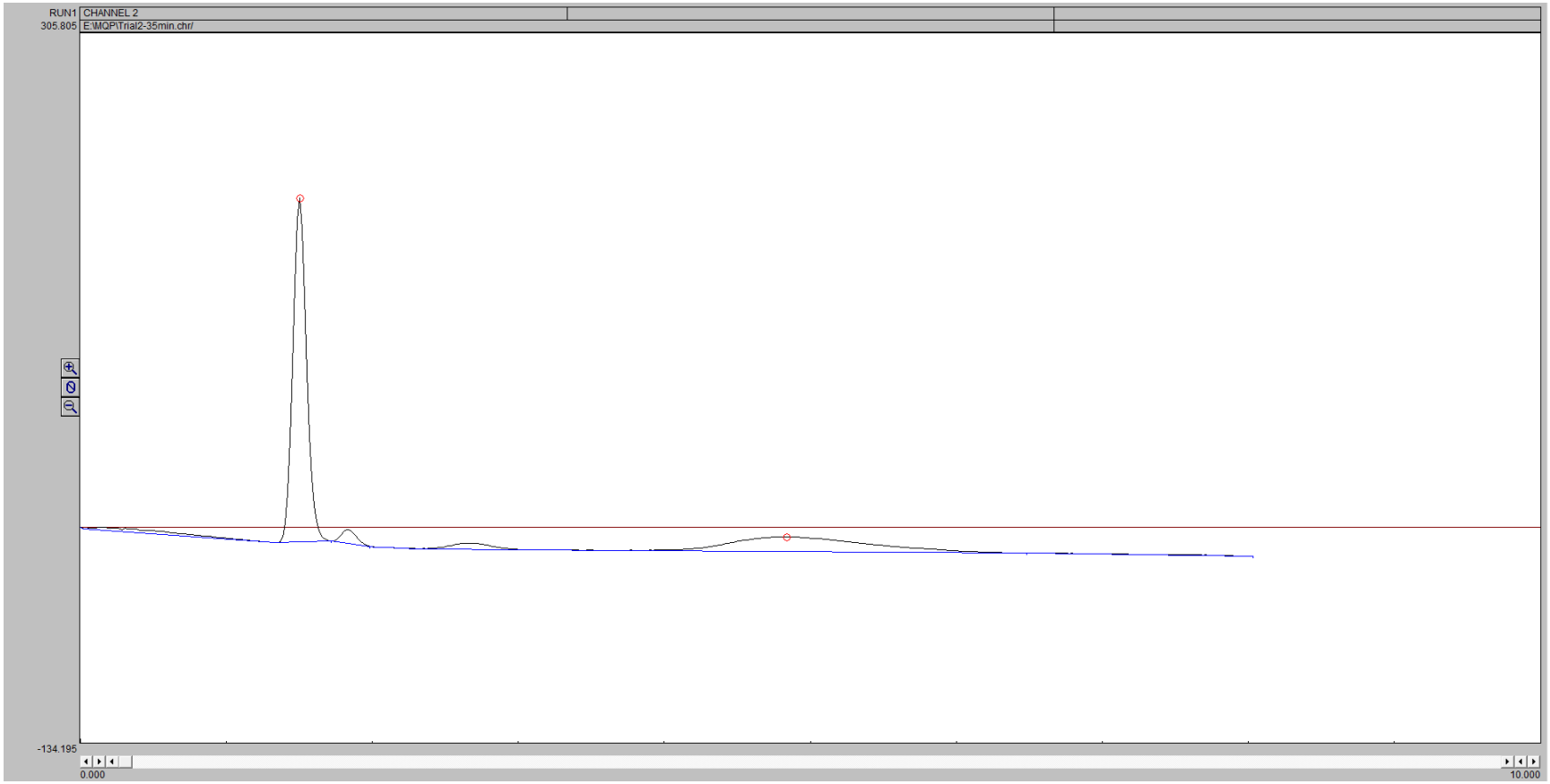
RUN1
CHANNEL 2
305.805
E:\MQP\Trial2-35min.chr/
-134.195
0.000
10.000

45 Minutes

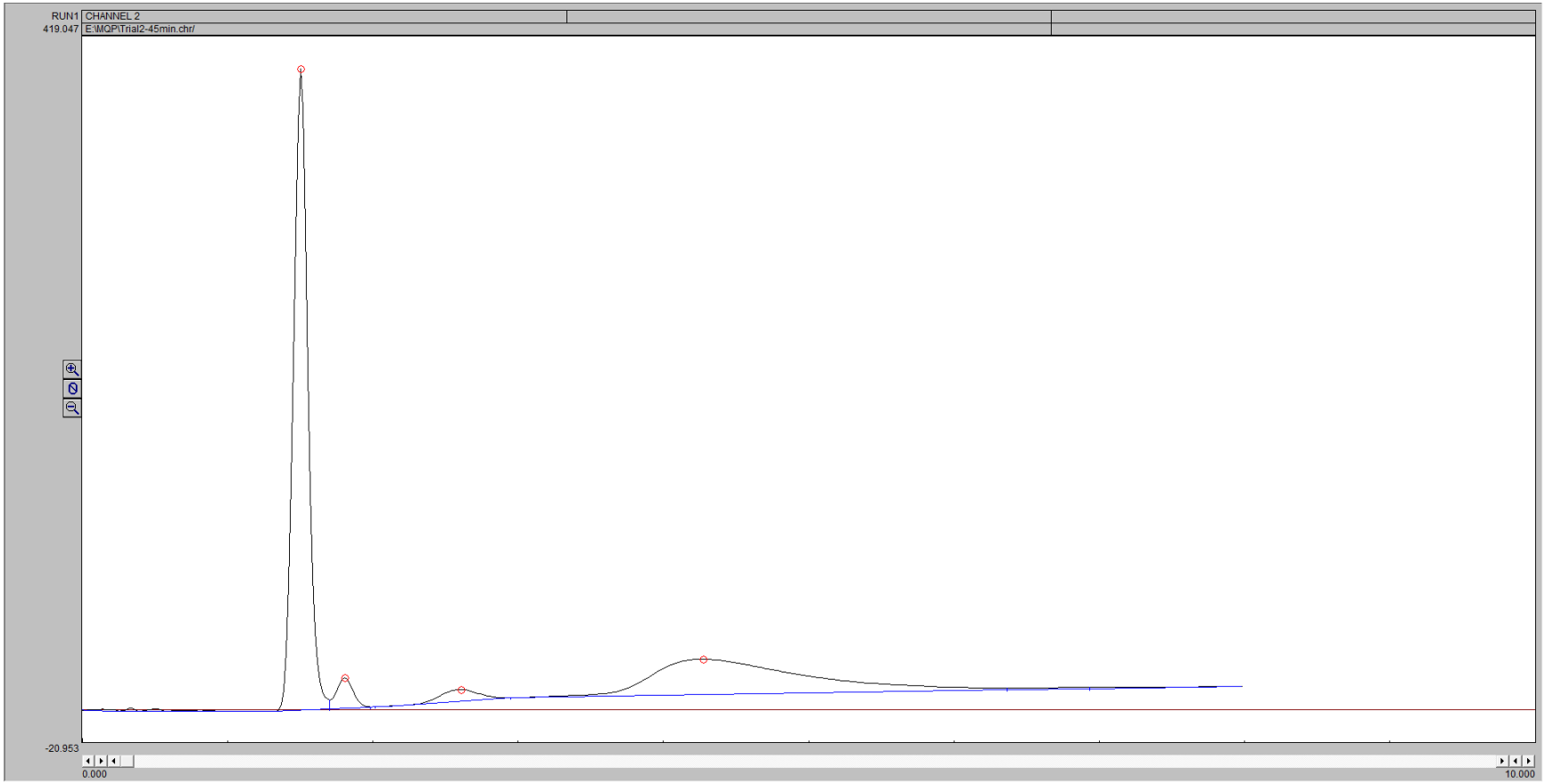
RUN1
CHANNEL 2
419.047
E:\MQP\Trial2-45min.chr/
-20.953
0.000
10.000

55 Minutes

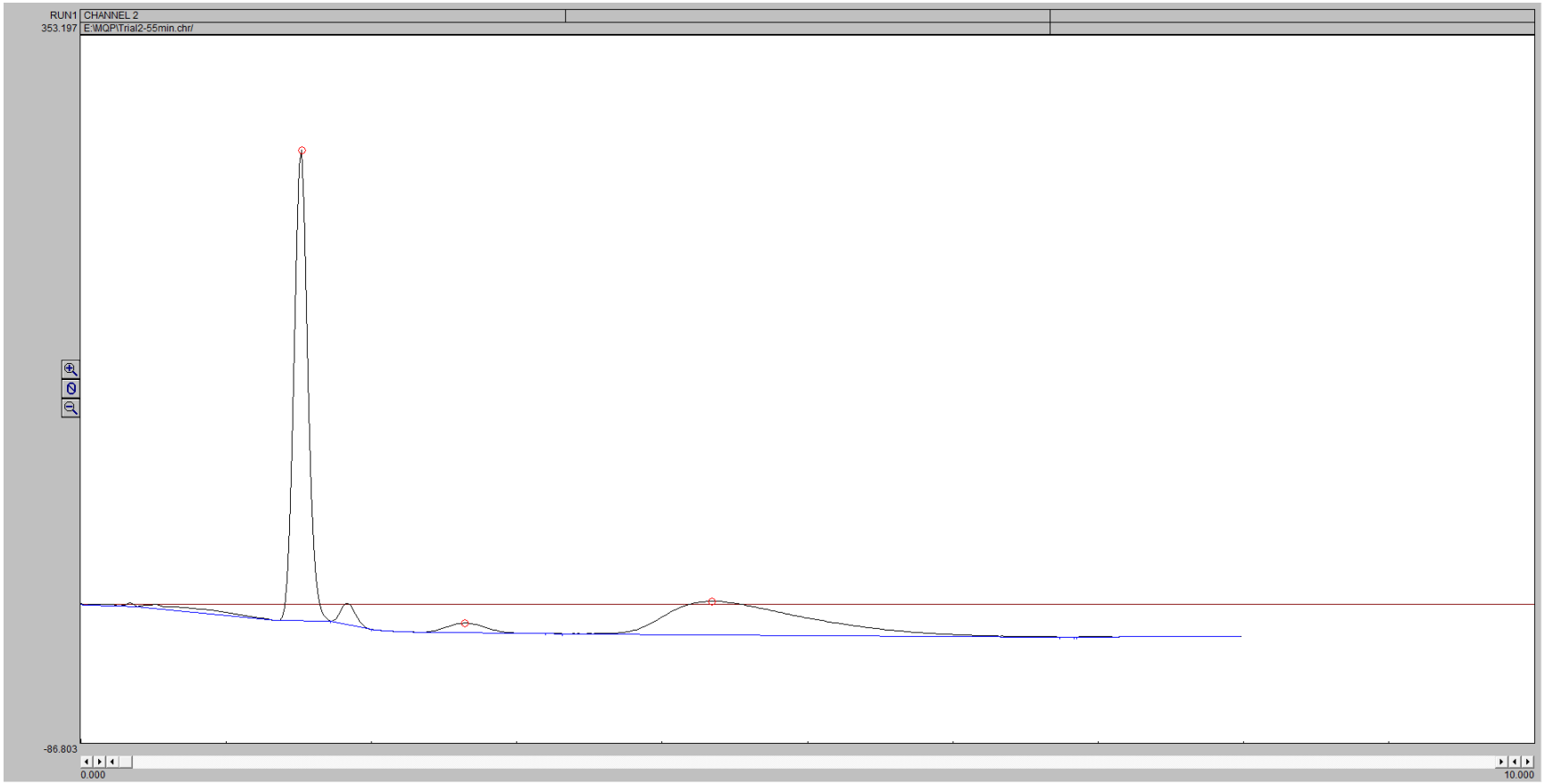
RUN1
CHANNEL 2
353.197
E:\MQP\Trial2-55min.chr/
-86.803
0.000
10.000

G3

5 Minutes:

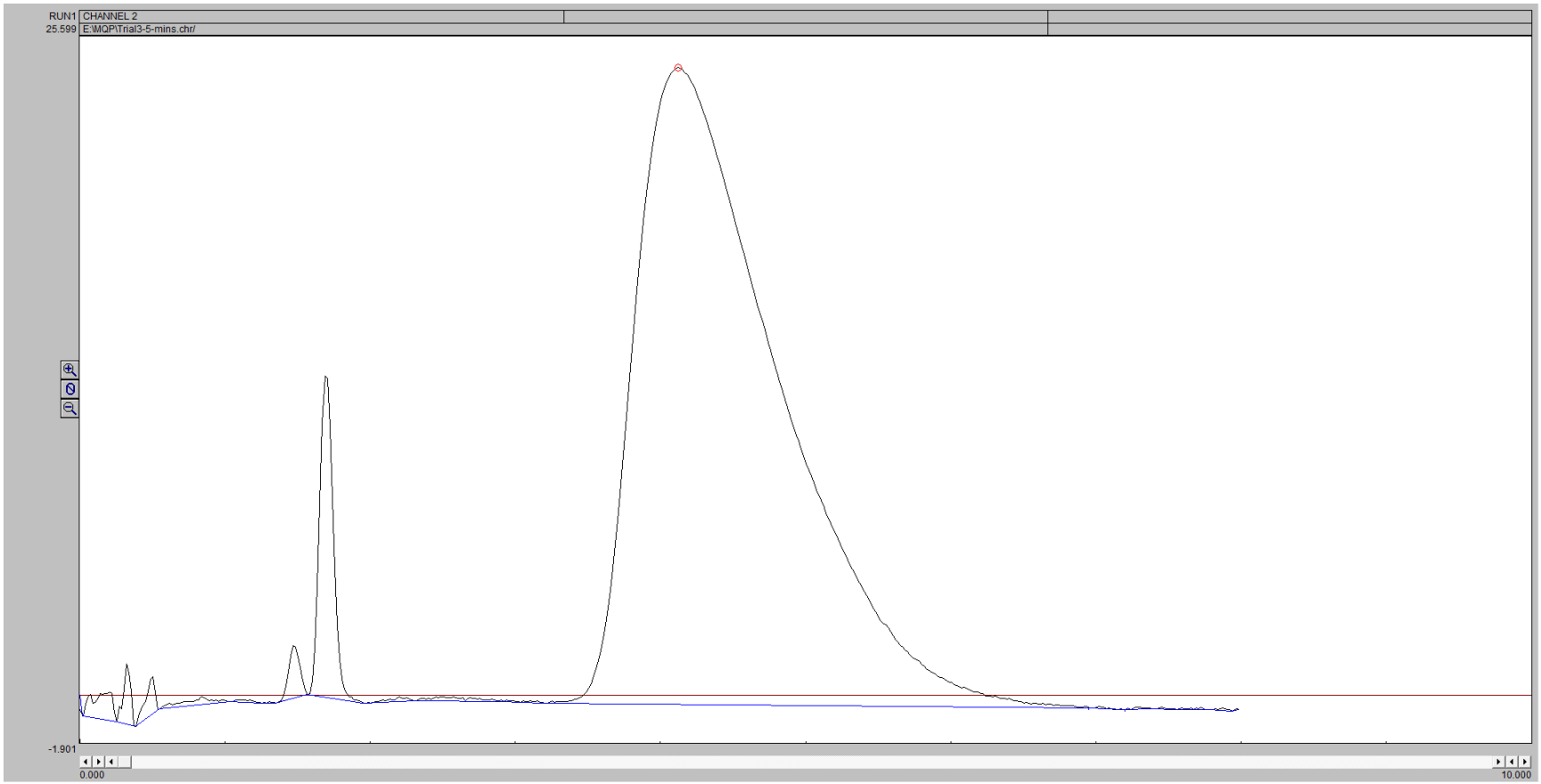

15 Minutes:

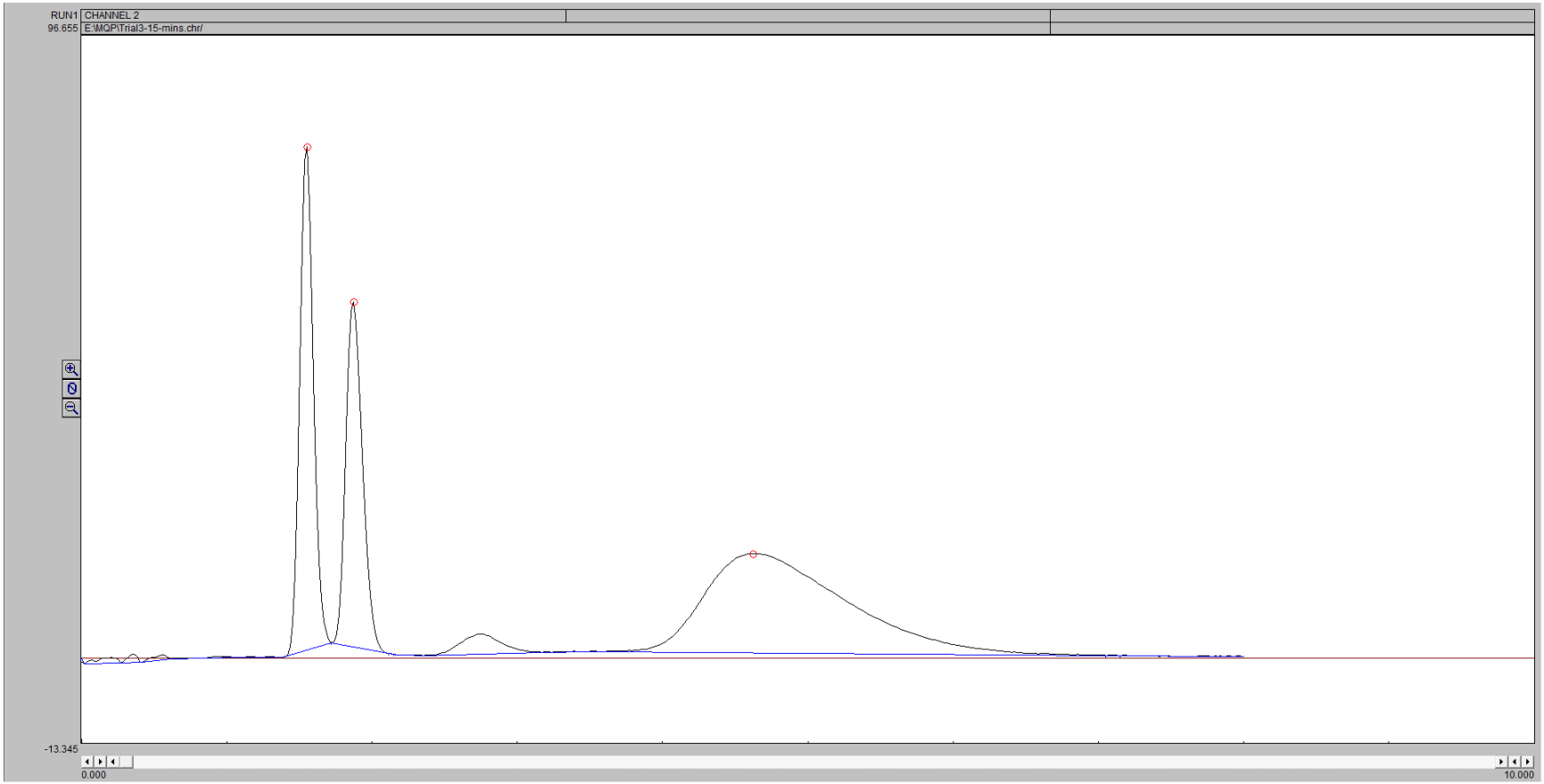
RUN1
CHANNEL 2
96.655
E:\MQP\Trial3-15-mins.chr/
-13.345
0.000
10.000

25 Minutes

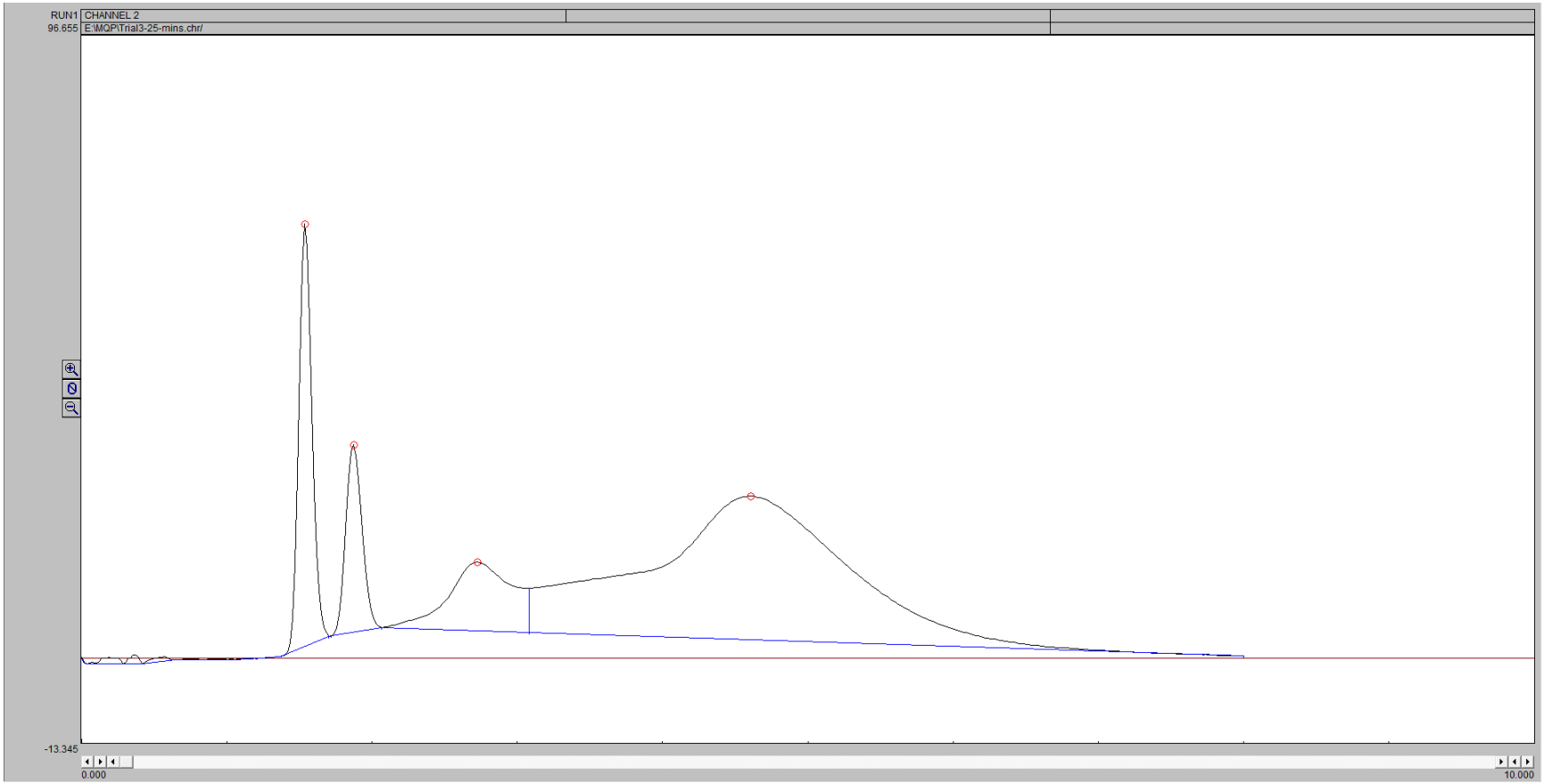
RUN1
CHANNEL 2
96.655
E:\MQP\Trial3-25-mins.chr/
-13.345
0.000
10.000

35 Minutes

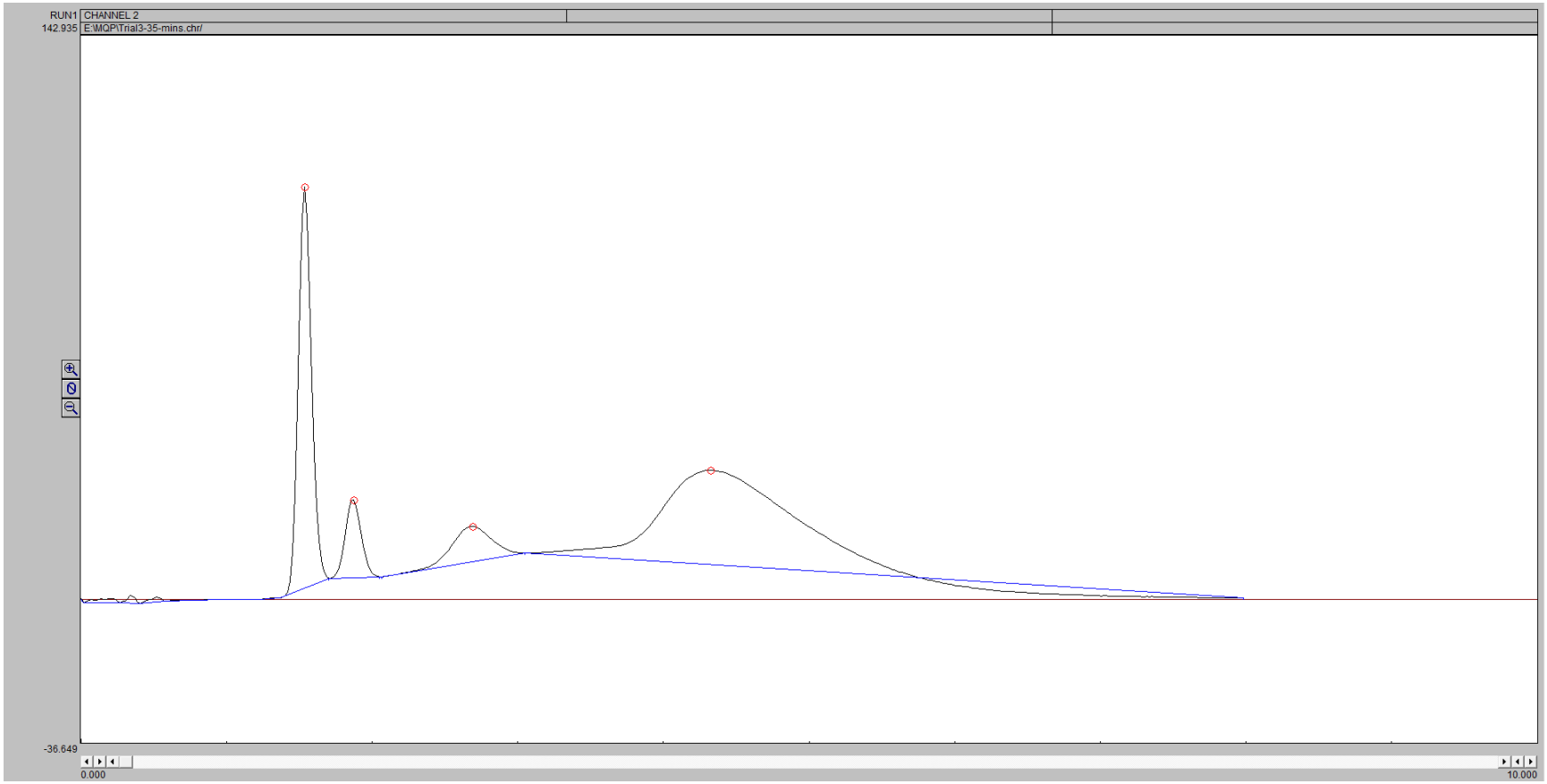
RUN1
CHANNEL 2
142.935
E:\MQP\Trial3-35-mins.chr/
-36.649
0.000
10.000

45 Minutes

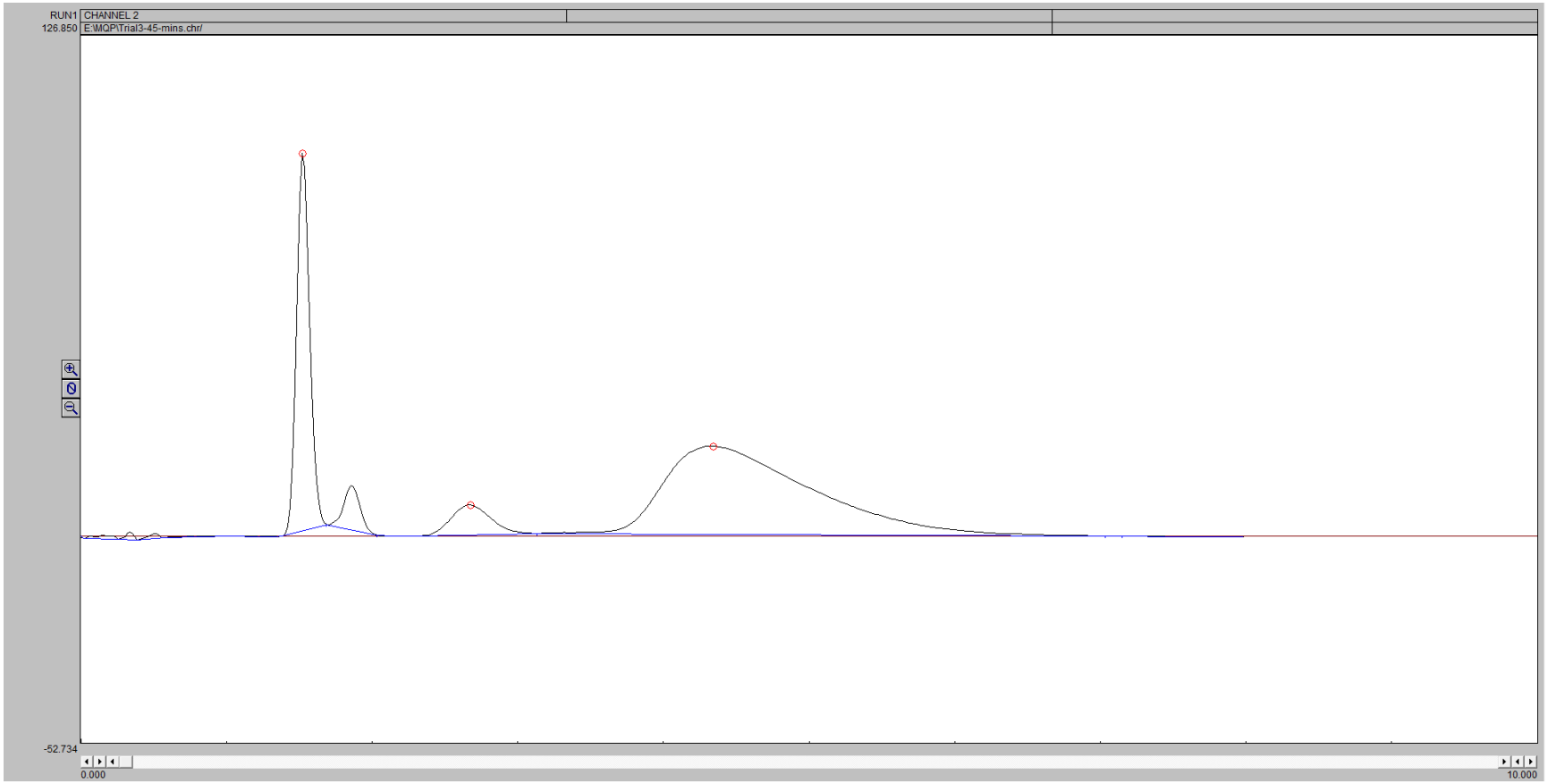
RUN1
CHANNEL 2
126.850
E:\MQP\Trial3-45-mins.chr/
-52.734
0.000
10.000

55 Minutes

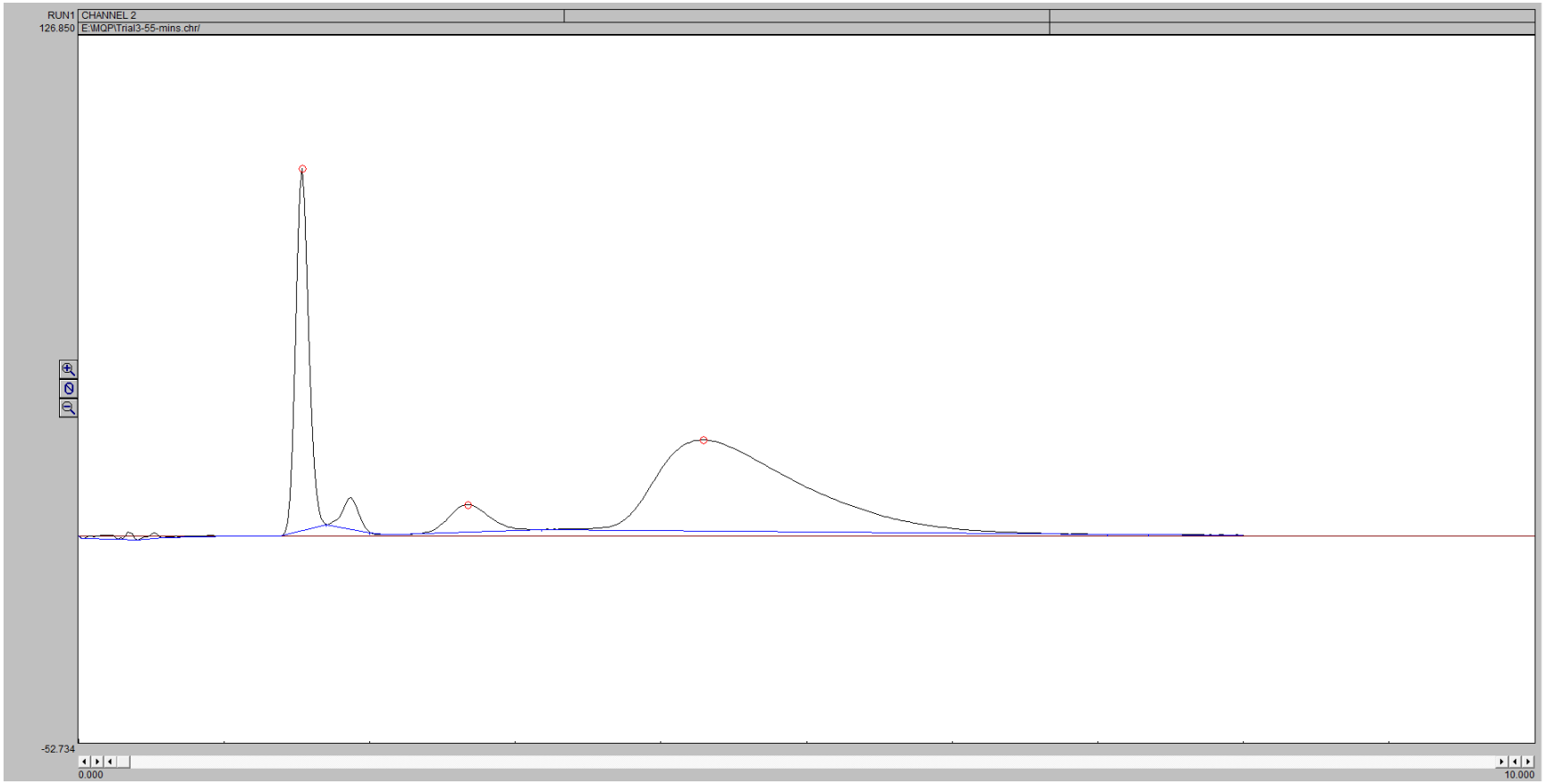
RUN1 CHANNEL 2
126.850 E:\MQP\Trial3-55-mins.chr/
-52.734
0.000
10.000

G4

5 Minutes:

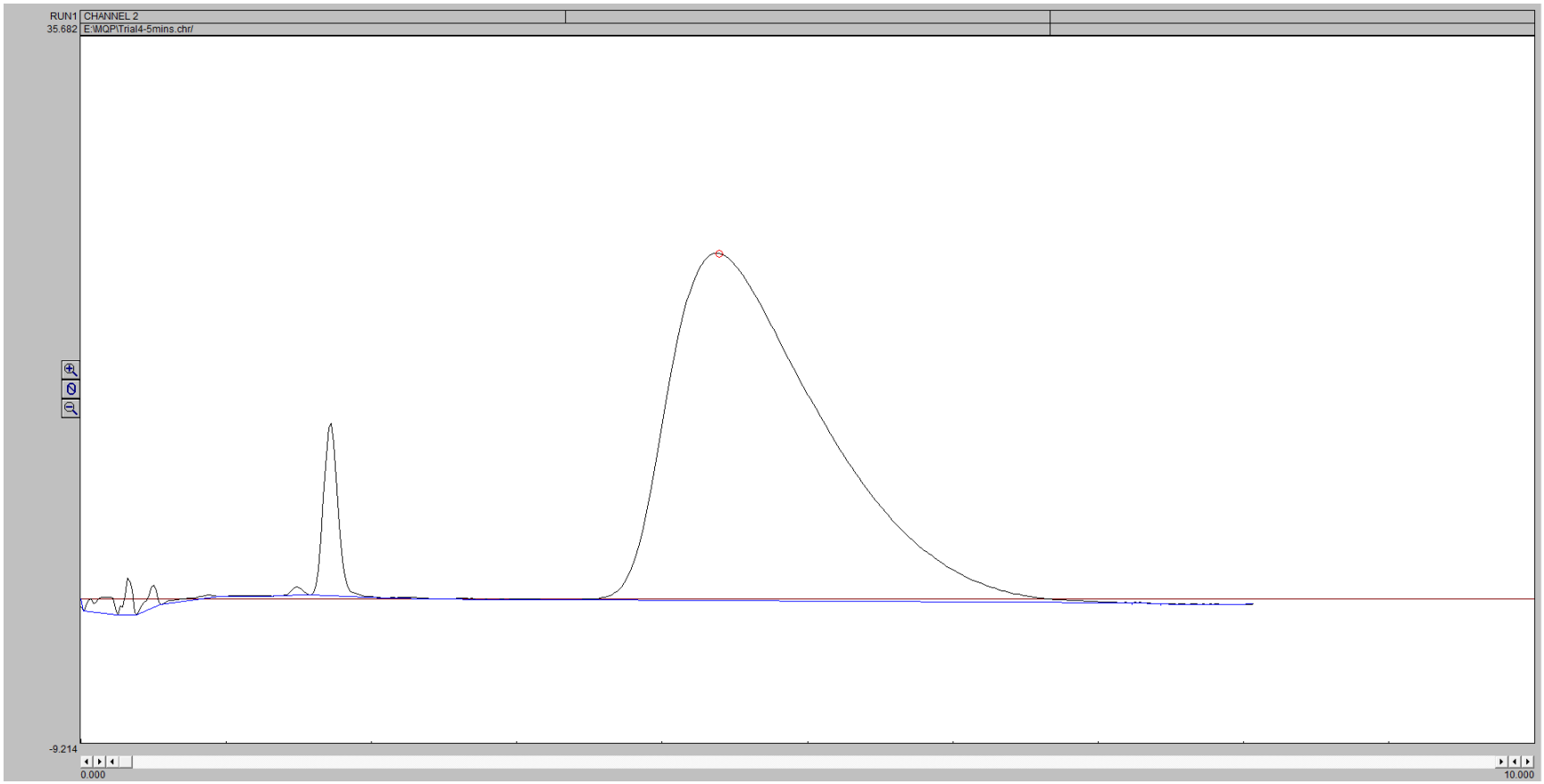

15 Minutes:

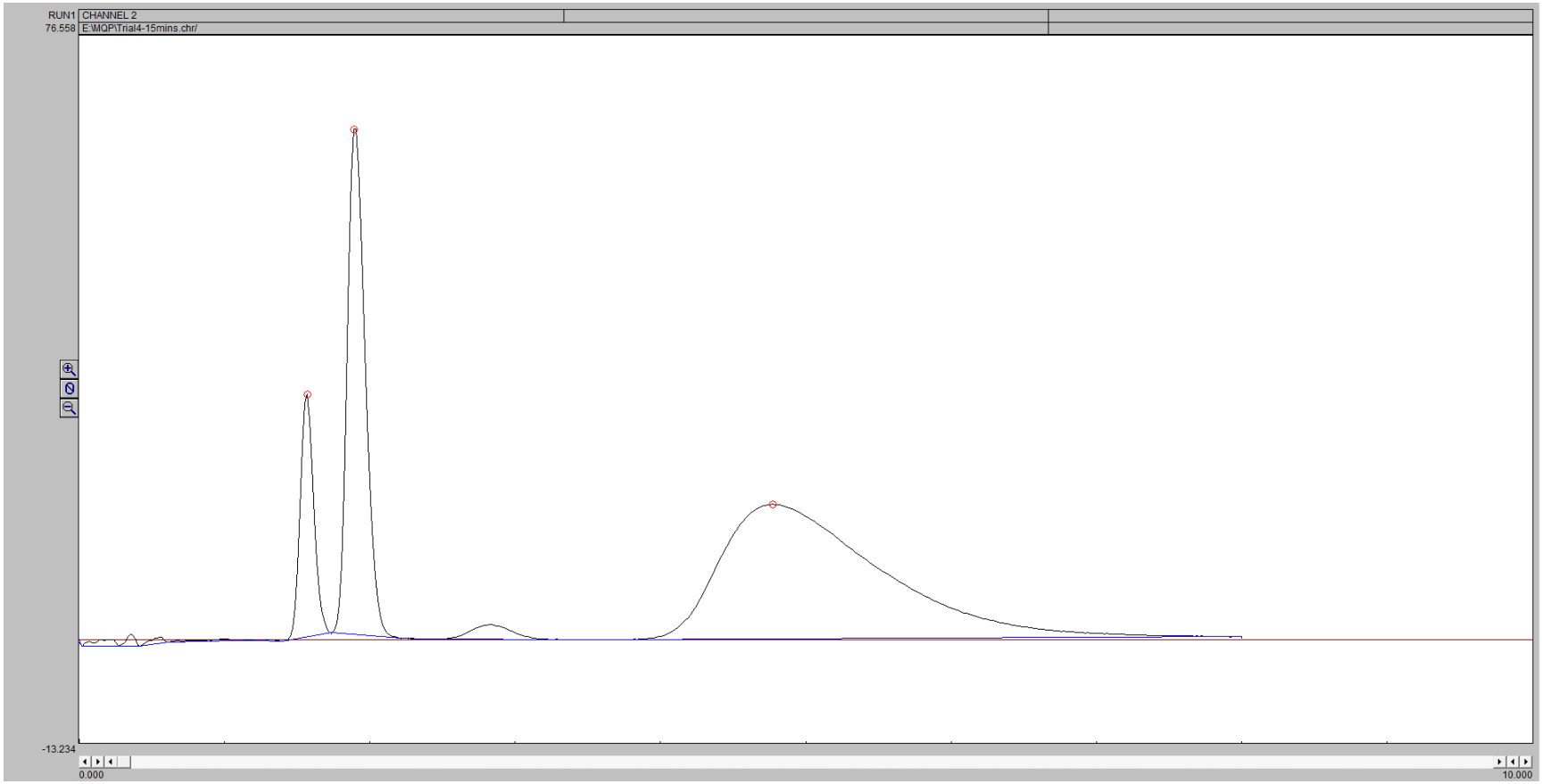
RUN1 CHANNEL 2
76.558 E:\MQP\Trial4-15mins.chr/
-13.234
0.000
10.000

25 Minutes

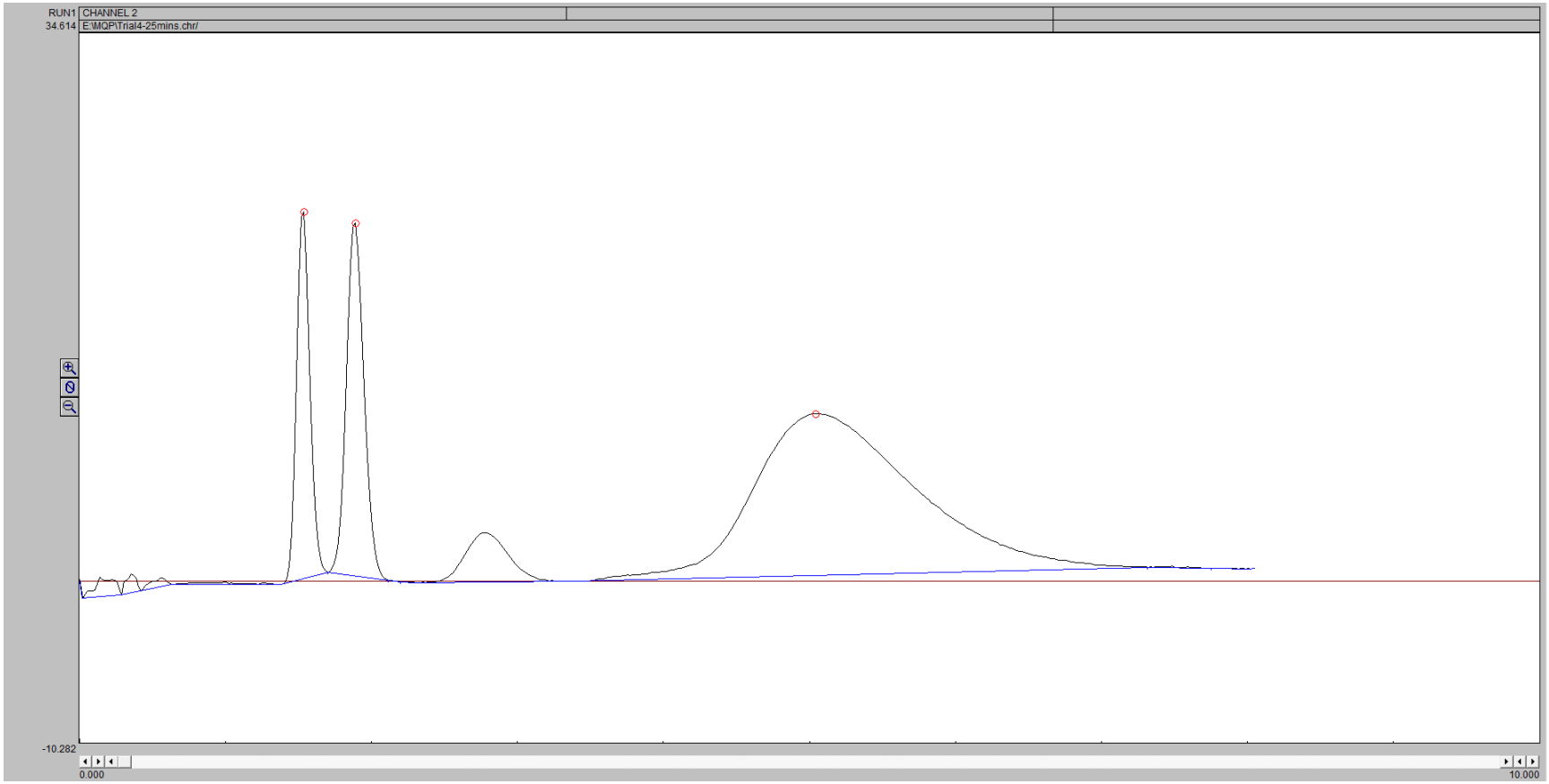
RUN1 CHANNEL 2
34.614 E:\MQP\Trial4-25mins.chr/
-10.282
0.000
10.000

35 Minutes

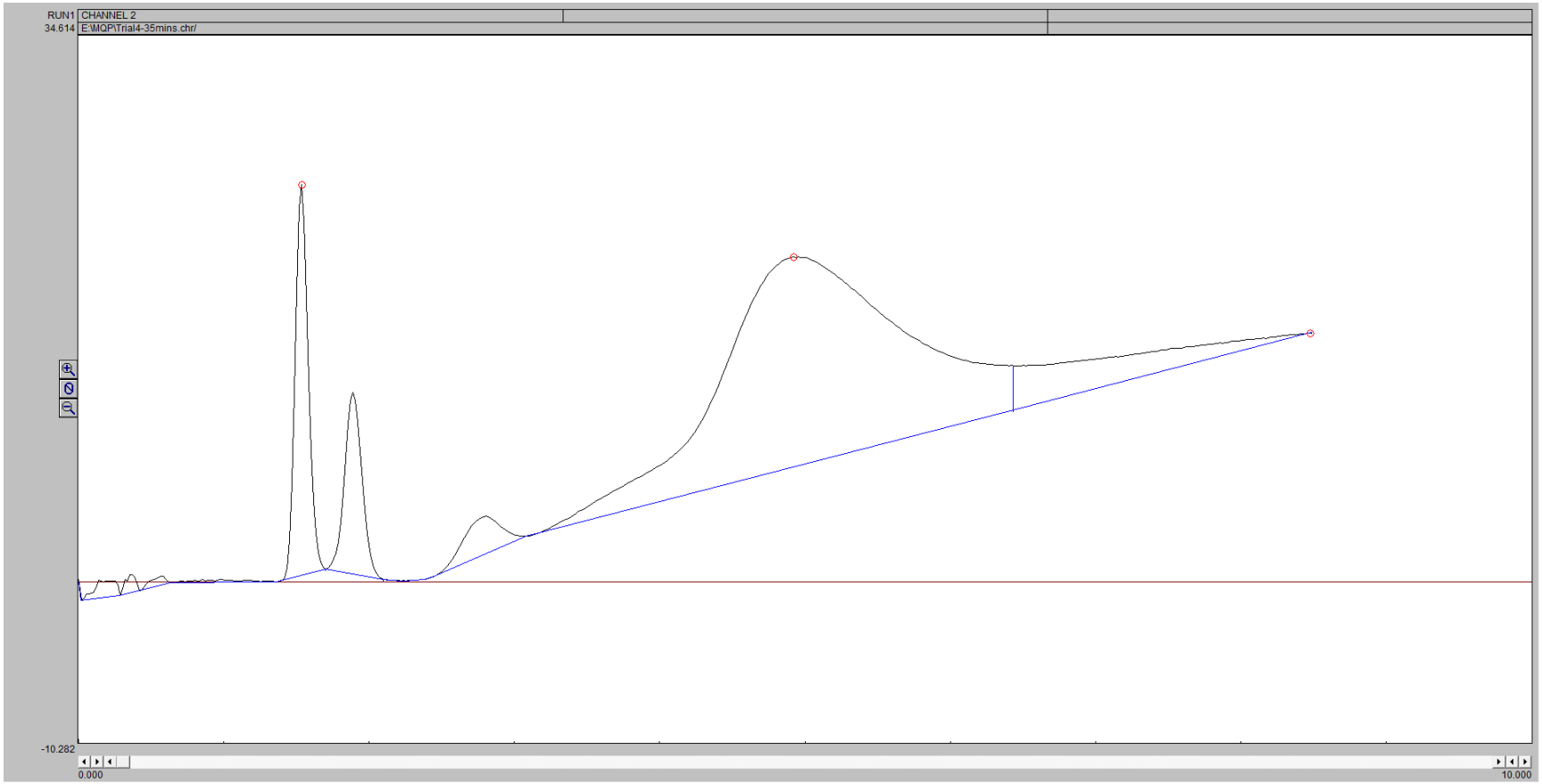
RUN1 CHANNEL 2
34.614 E:\MQP\Trial4-35mins.chr/
-10.282
0.000
10.000

45 Minutes

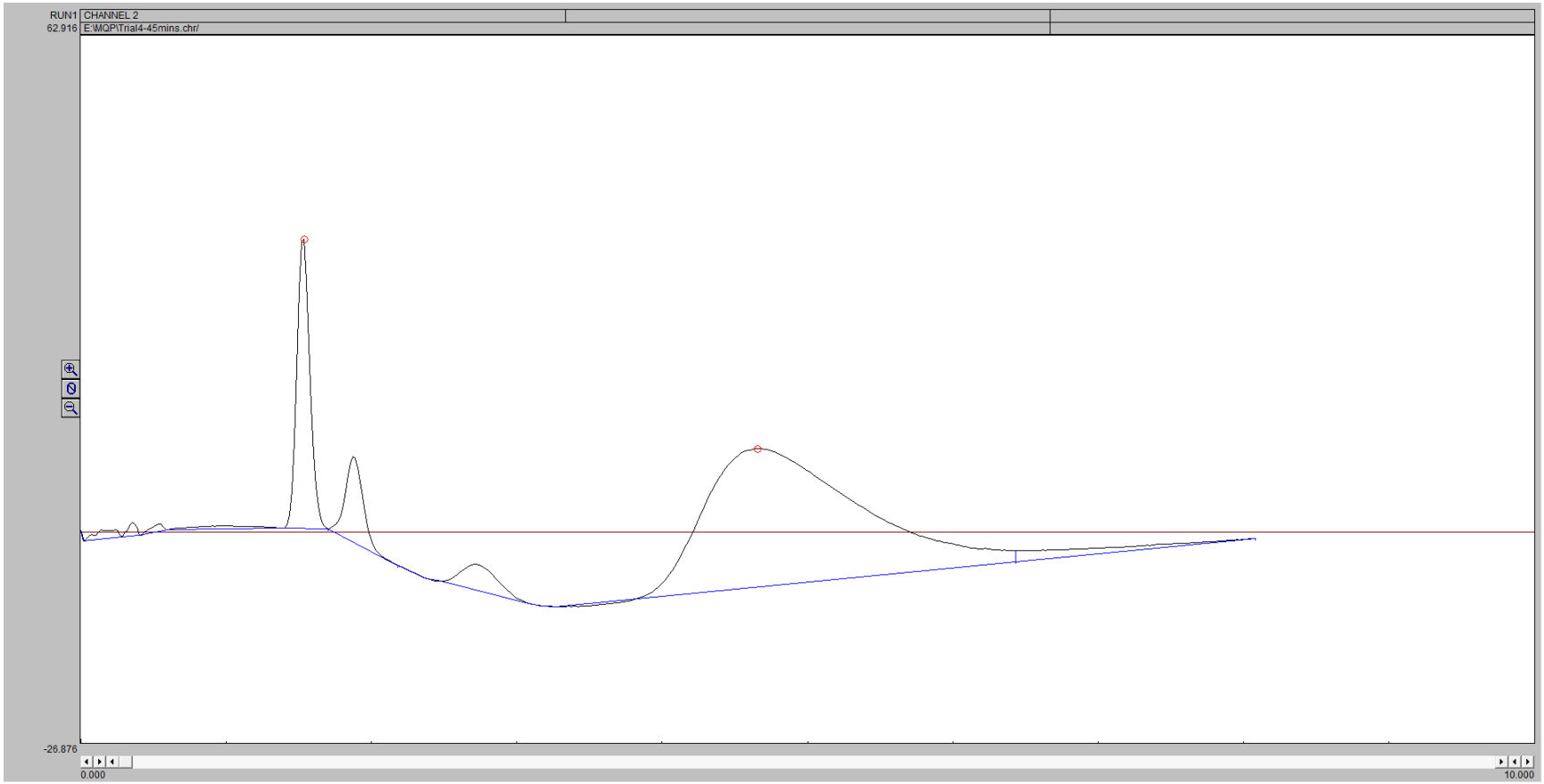
RUN1
CHANNEL 2
62.916
E:\MQP\Trial4-45mins.chr/
-26.876
0.000
10.000

55 Minutes

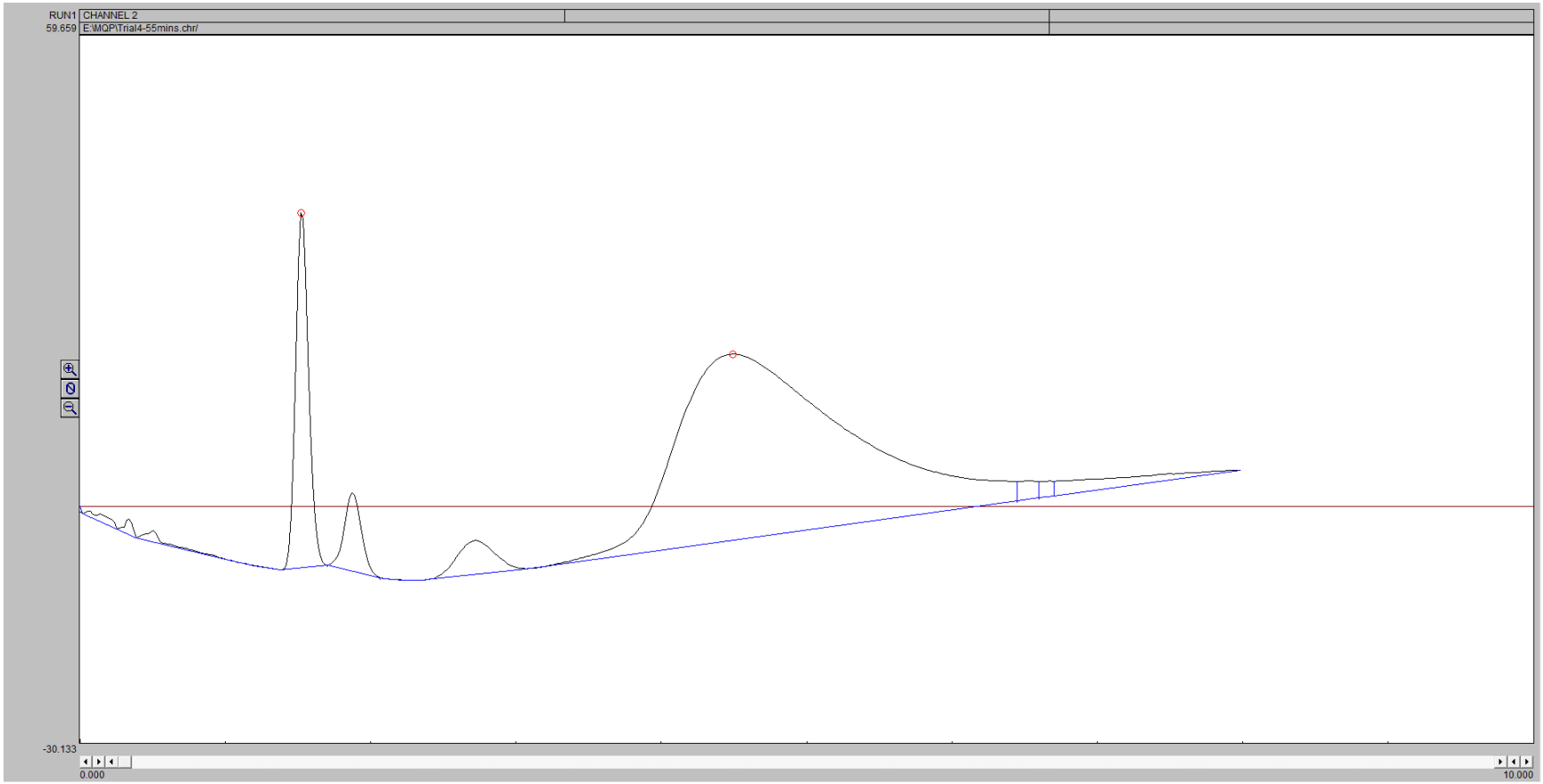
RUN1
CHANNEL 2
59.659
E:\MQP\Trial4-55mins.chr/
-30.133
0.000
10.000

65 Minutes

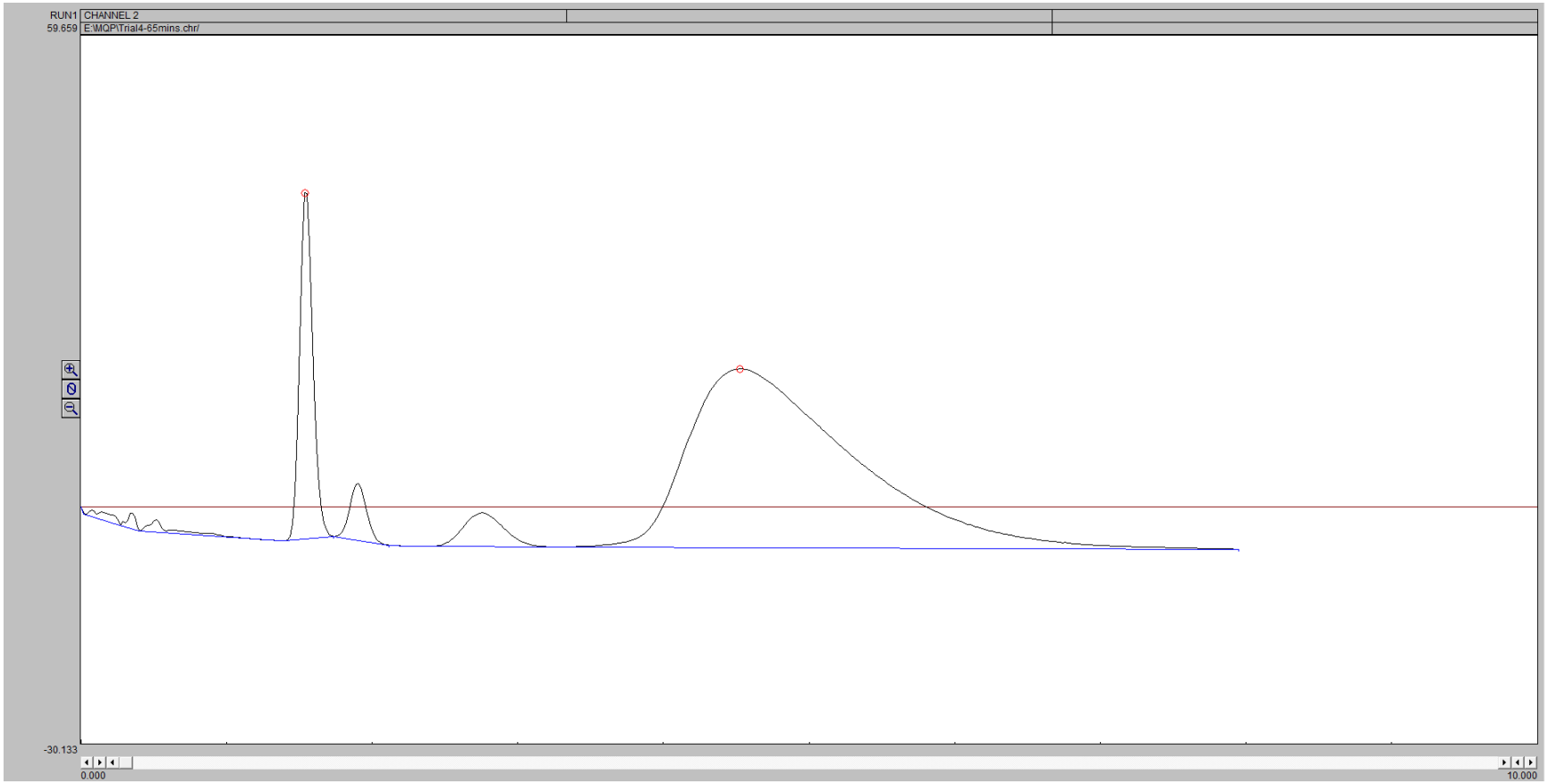
RUN1
CHANNEL 2
59.659
E:\MQP\Trial4-65mins.chr/
-30.133
0.000
10.000

75 Minutes

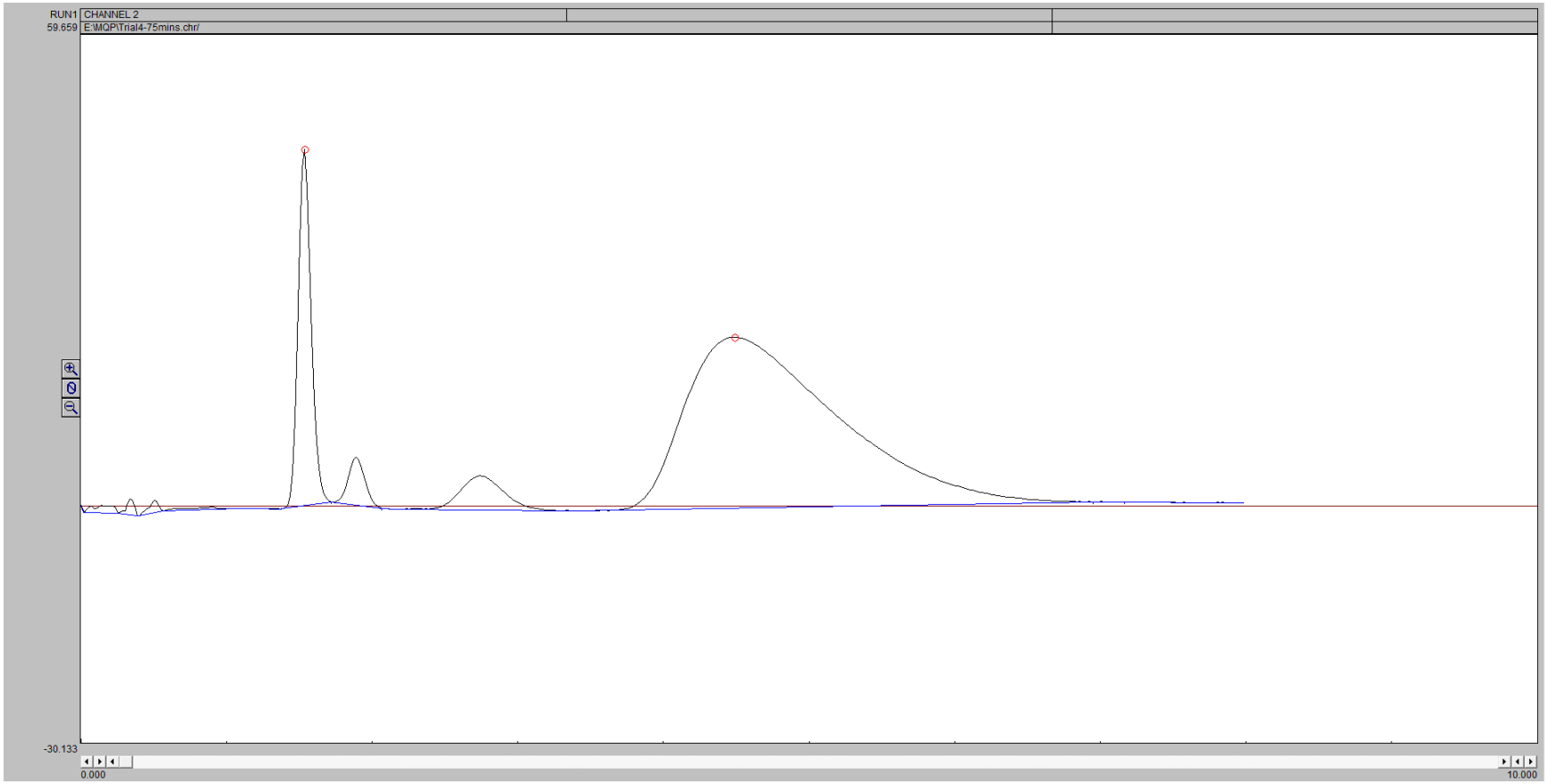
RUN1
CHANNEL 2
59.659
E:\MQP\Trial4-75mins.chr/
-30.133
0.000
10.000

85 Minutes

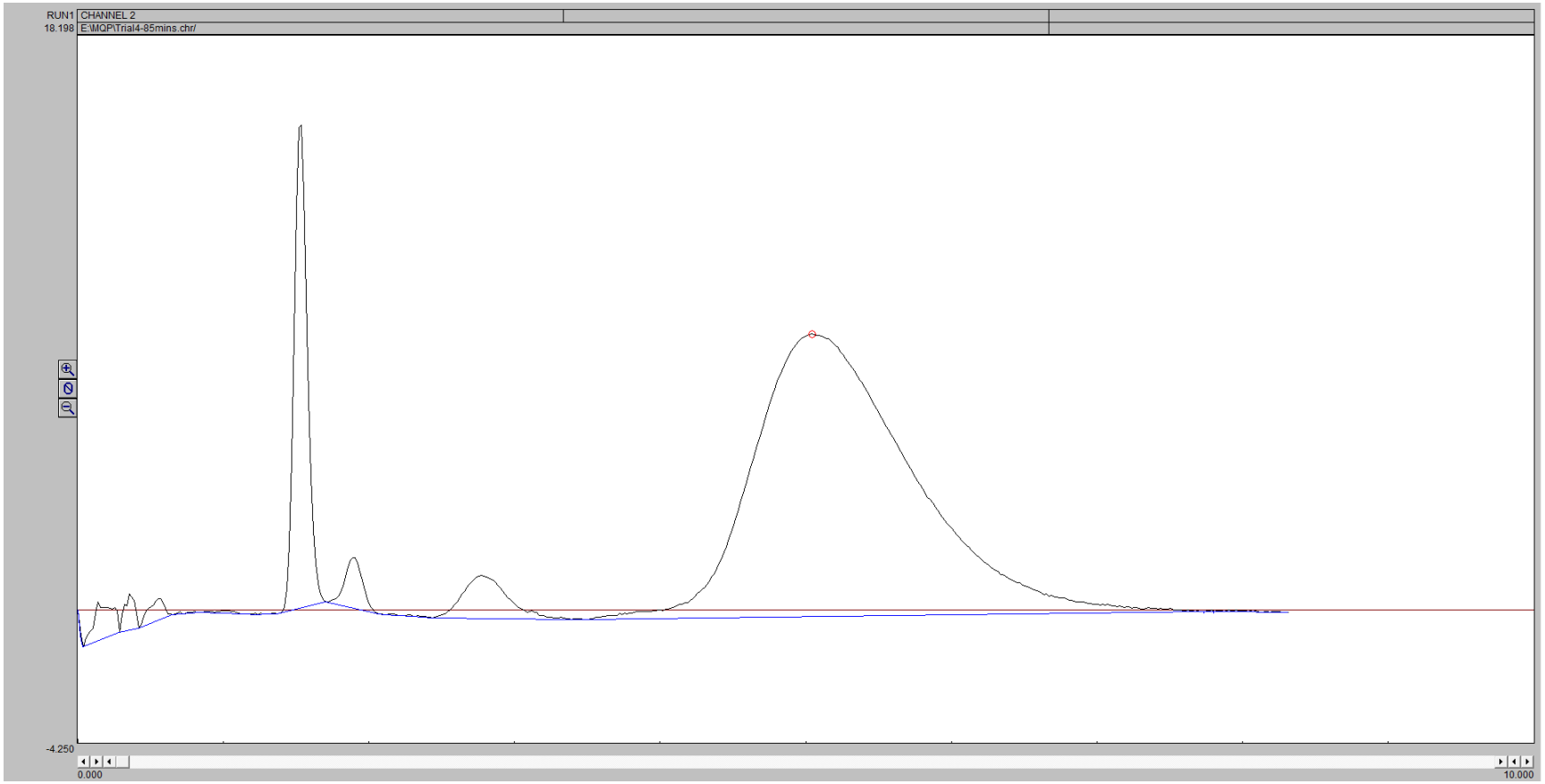

95 Minutes

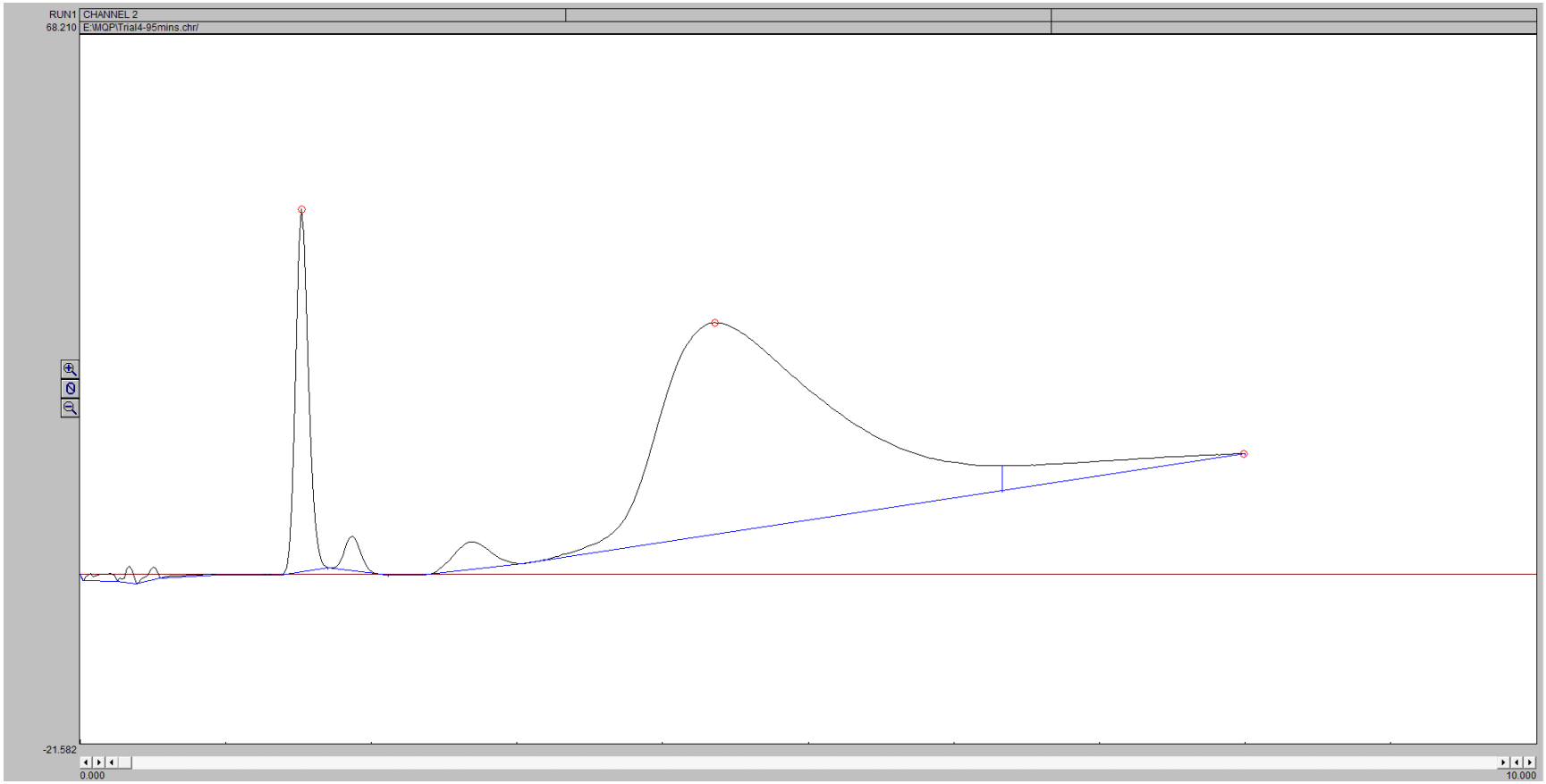
RUN1 CHANNEL 2
68.210 E:\MQP\Trial4-95mins.chr/
-21.582
0.000
10.000

105 Minutes

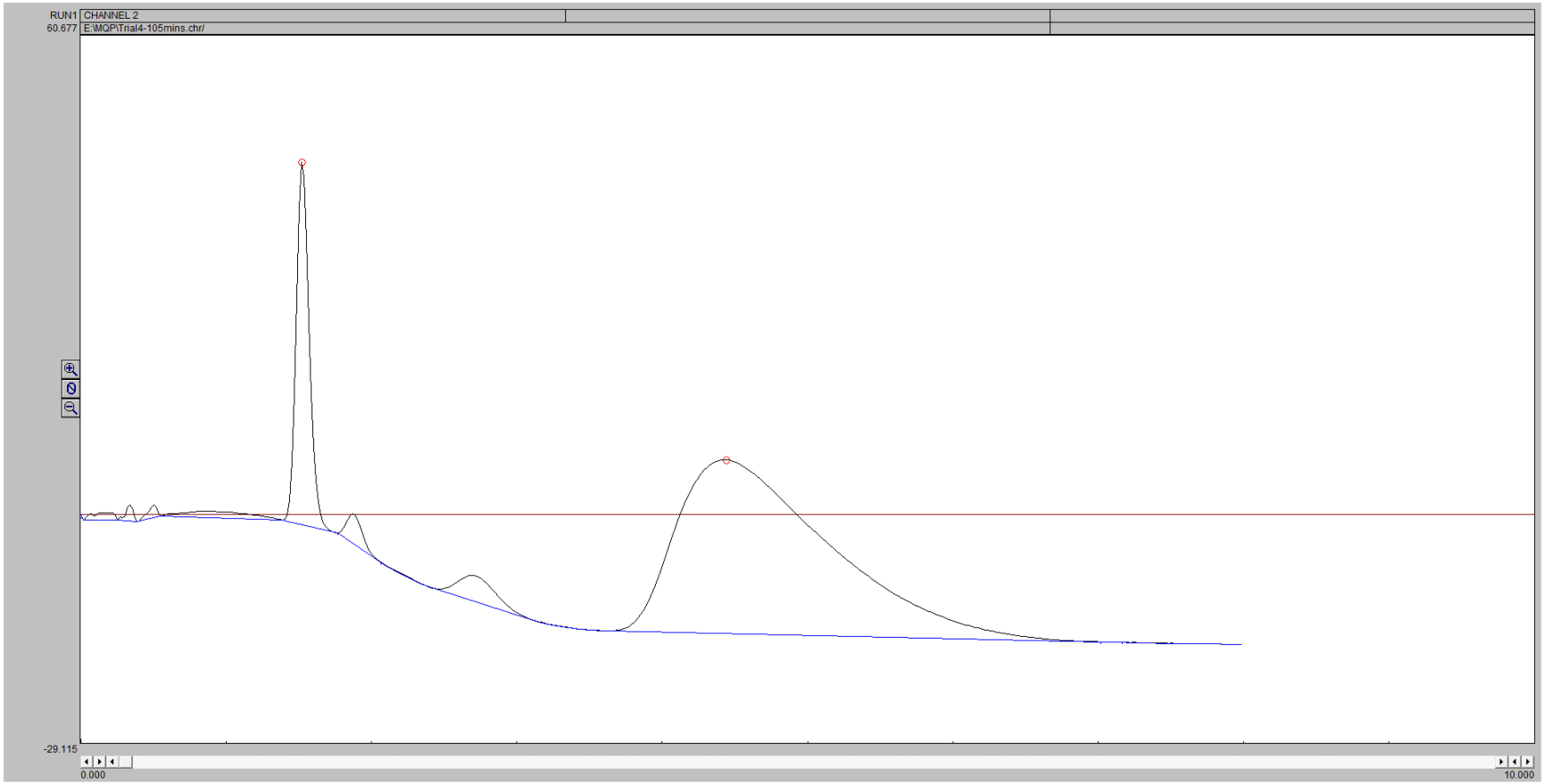
RUN1
CHANNEL 2
60.677
E:\MQP\Trial4-105mins.chr/
-29.115
0.000
10.000

115 Minutes

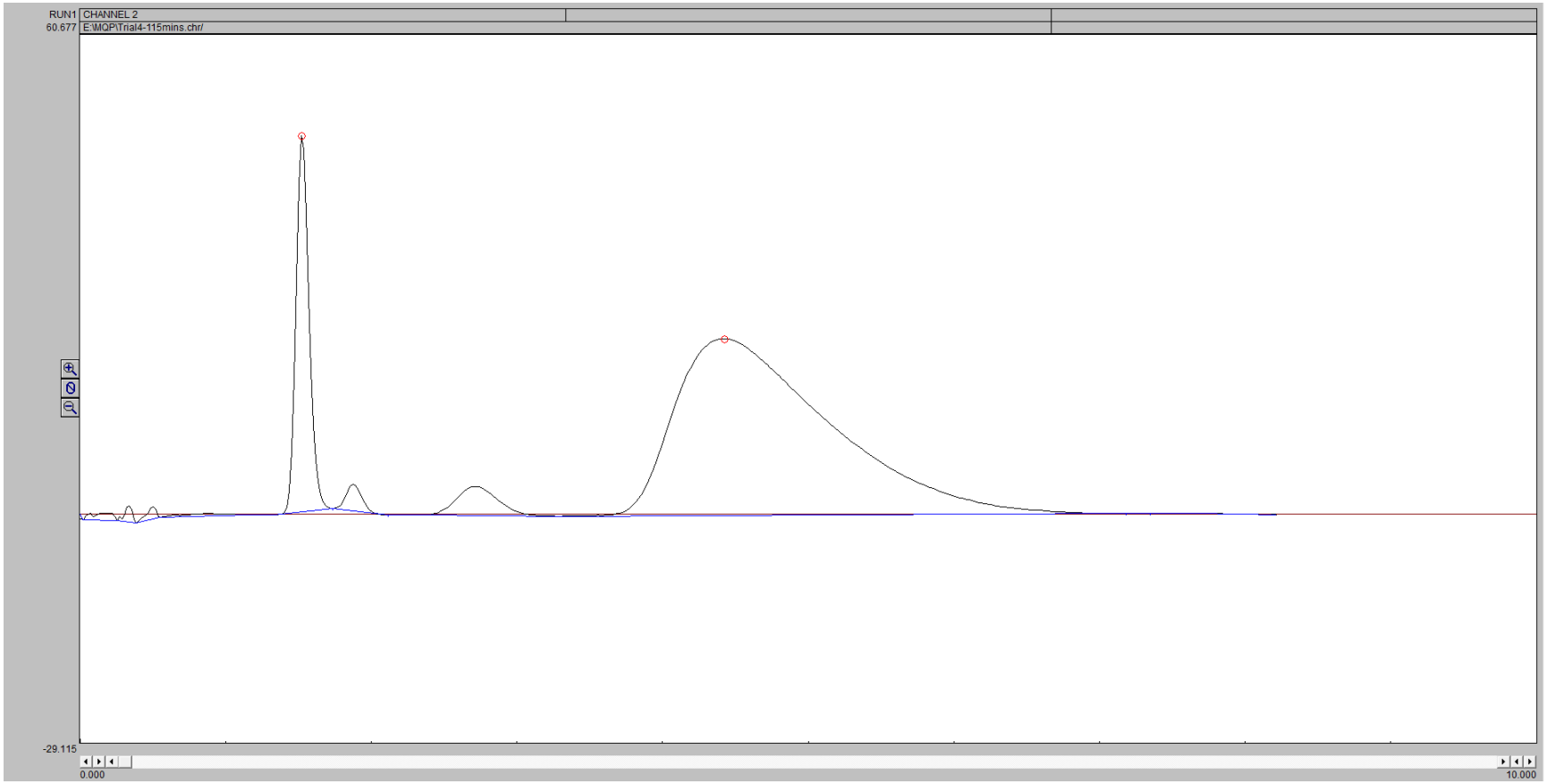
RUN1
CHANNEL 2
60.677
E:\MQP\Trial4-115mins.chr/
-29.115
0.000
10.000

Appendix C Raw Data for Liquid and Gas Analysis – Overnight Gasification

G5

Gas Concentrations over Time

	Mole %			
Time Stamp	H_2	CO	CH_4	CO_2
10	5.051507	4.229057	1.769825	88.94961
85	2.207556	0.912087	2.06637	94.81399
160	1.090209	0.661116	0.665809	97.58287
235	0.760663	0.414158	0	98.82518
310	1.707633	1.33039	0	96.96198
385	0.372745	0.394311	0	99.23294
460	0.315363	0.724712	0	98.95993
535	0.364048	1.060695	0	98.57526

Gas Sample 10 Minutes

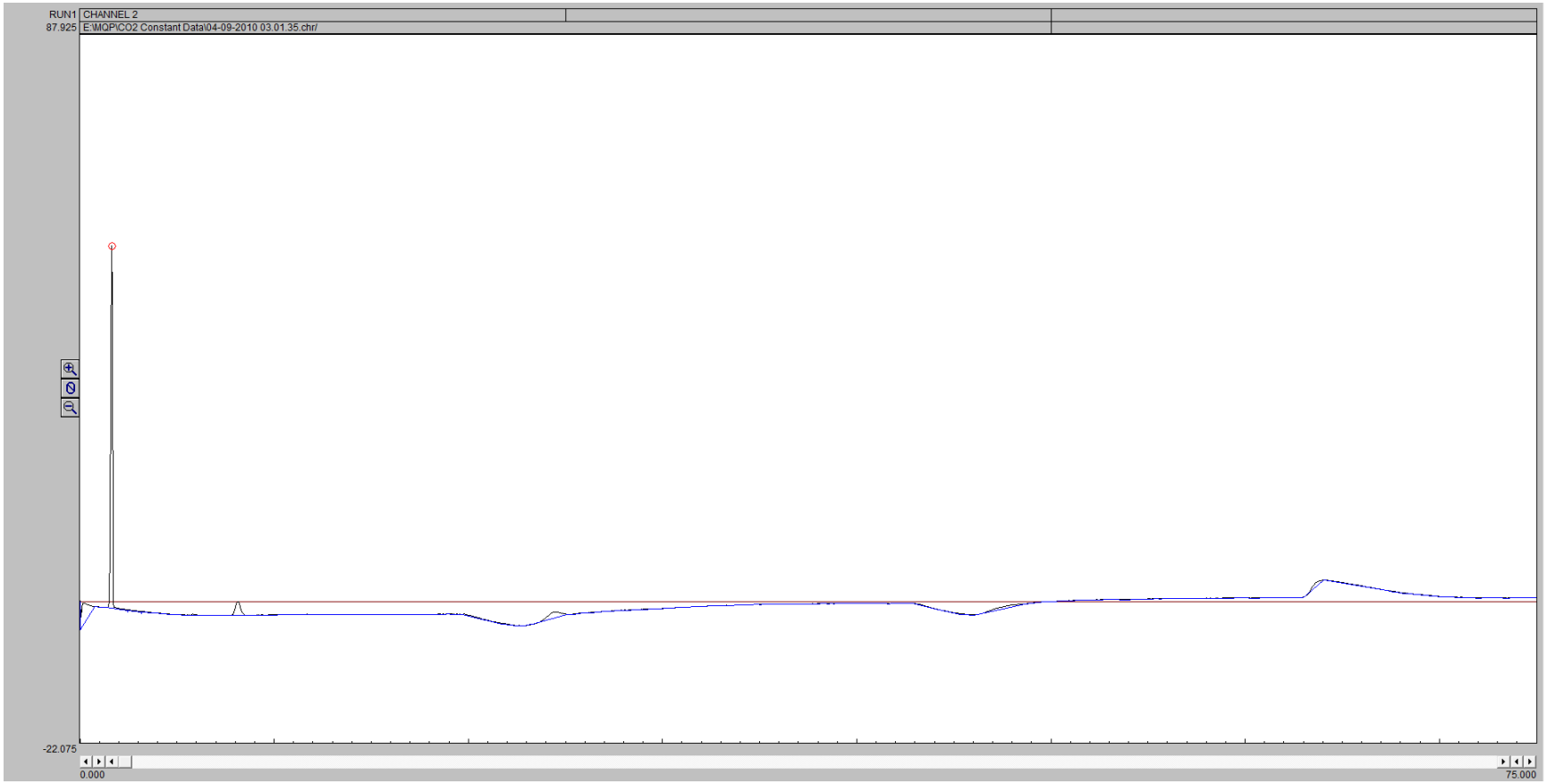

Gas Sample 85 Minutes

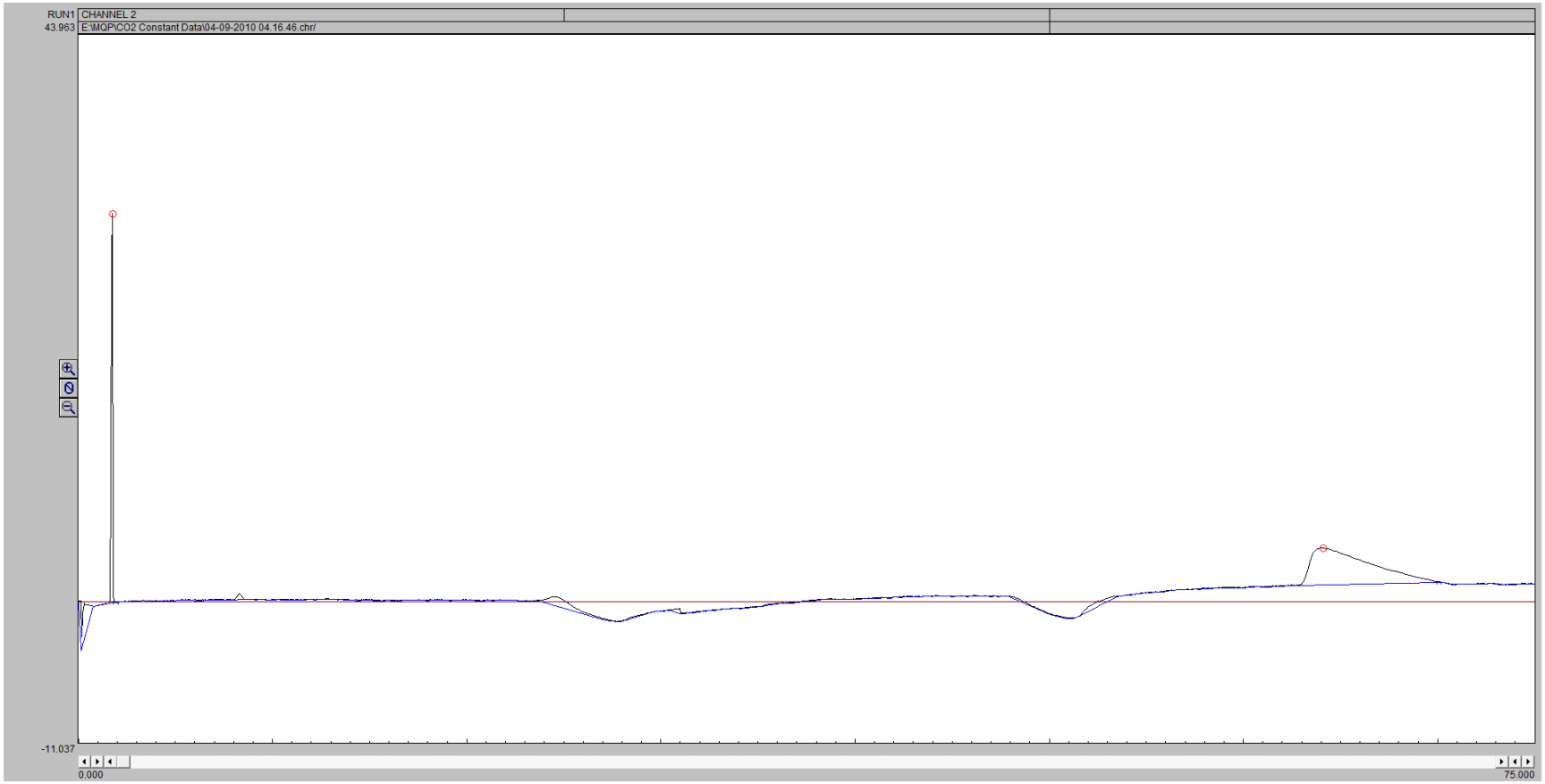

Gas Sample 160 Minutes

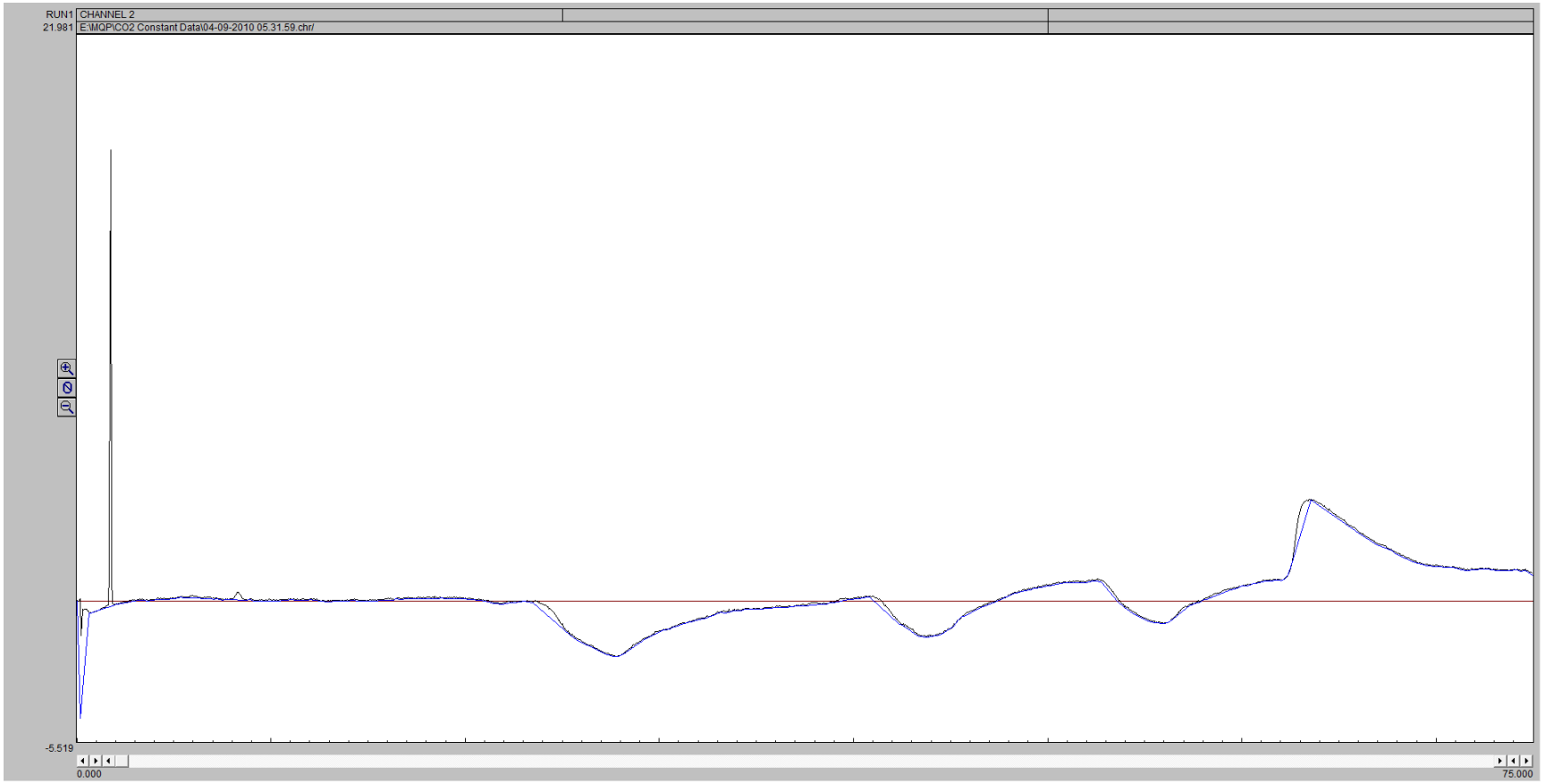

Gas Sample 235 Minutes

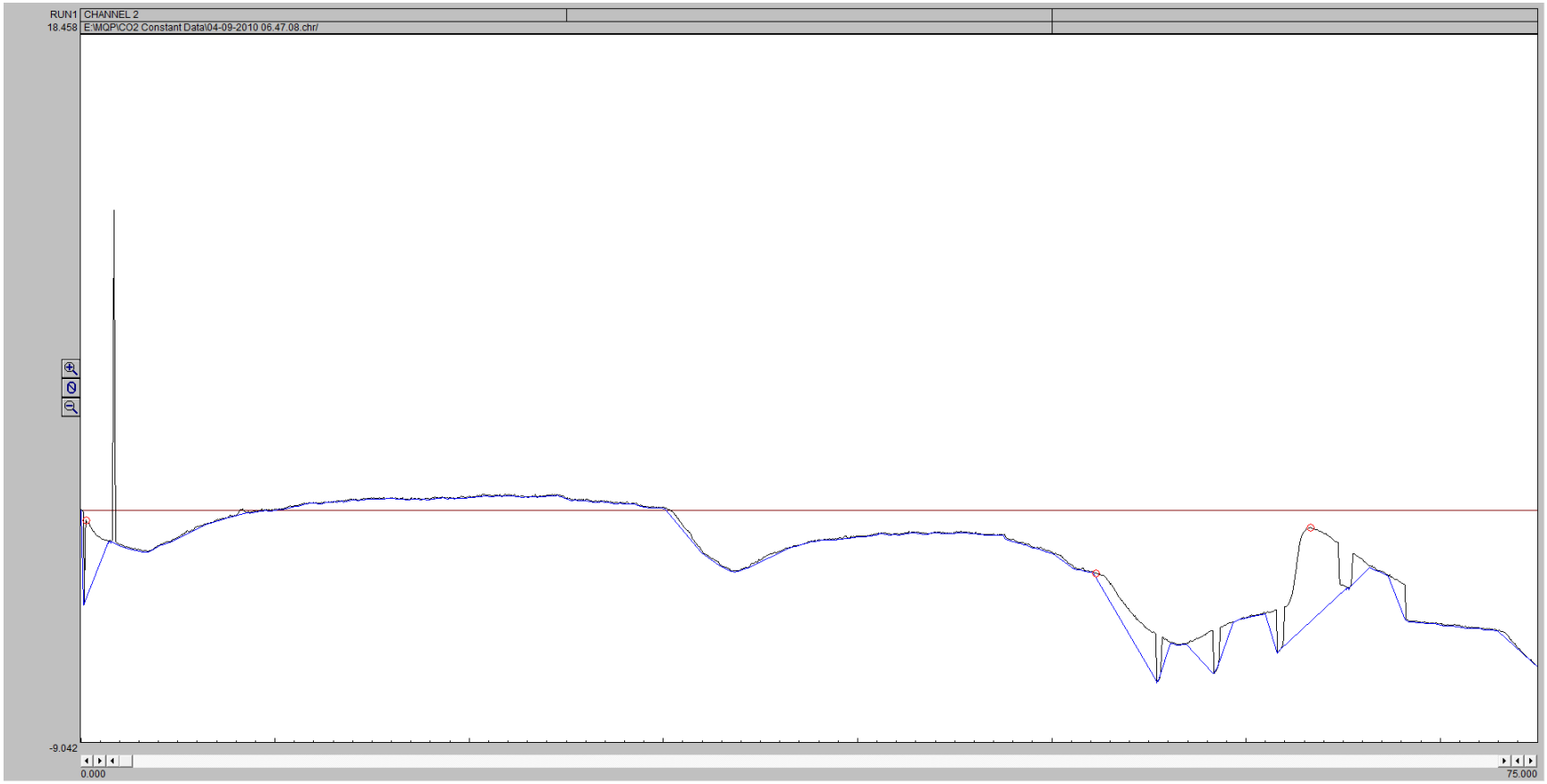

Gas Sample 310 Minutes

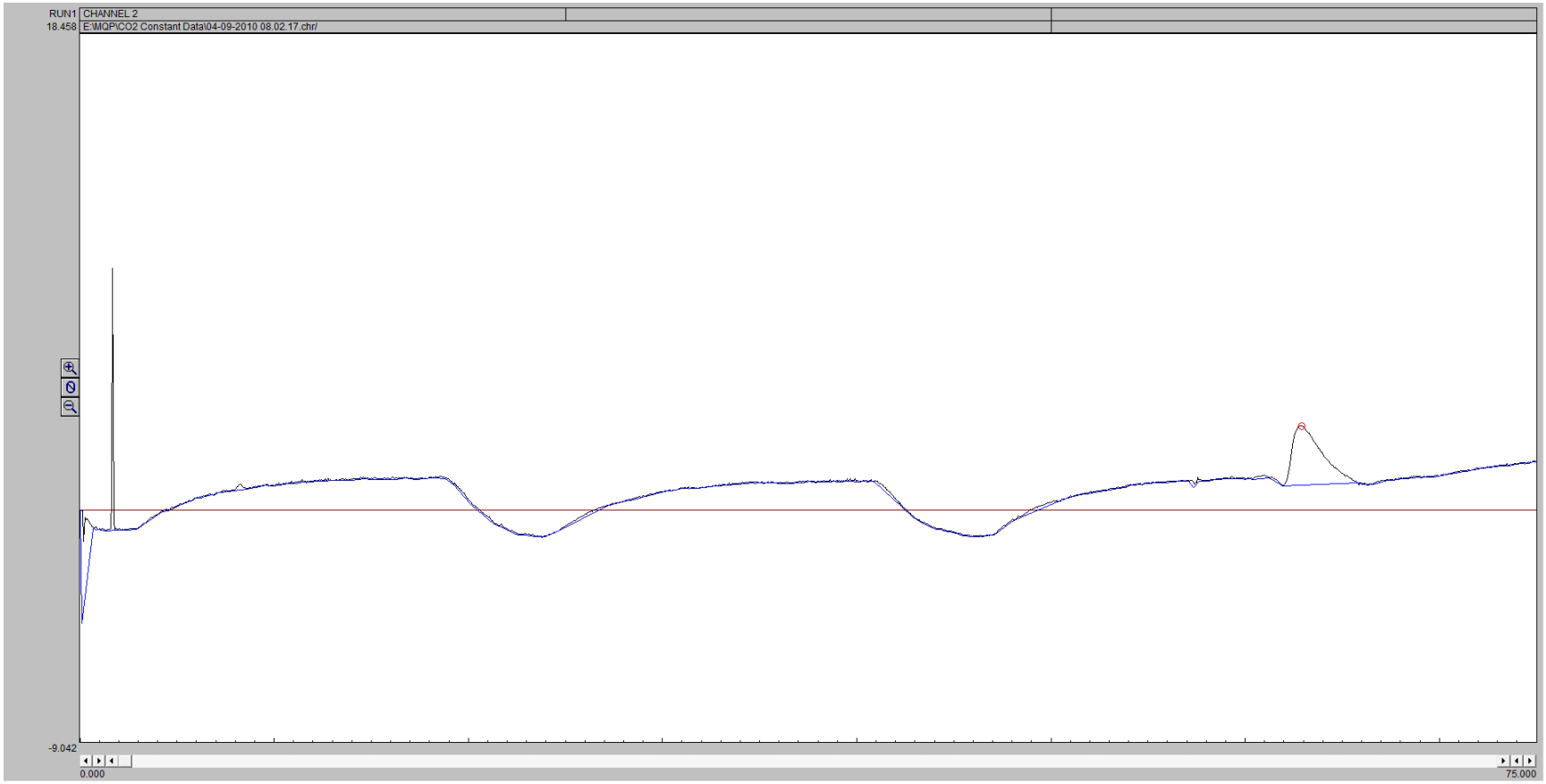

Gas Sample 385 Minutes

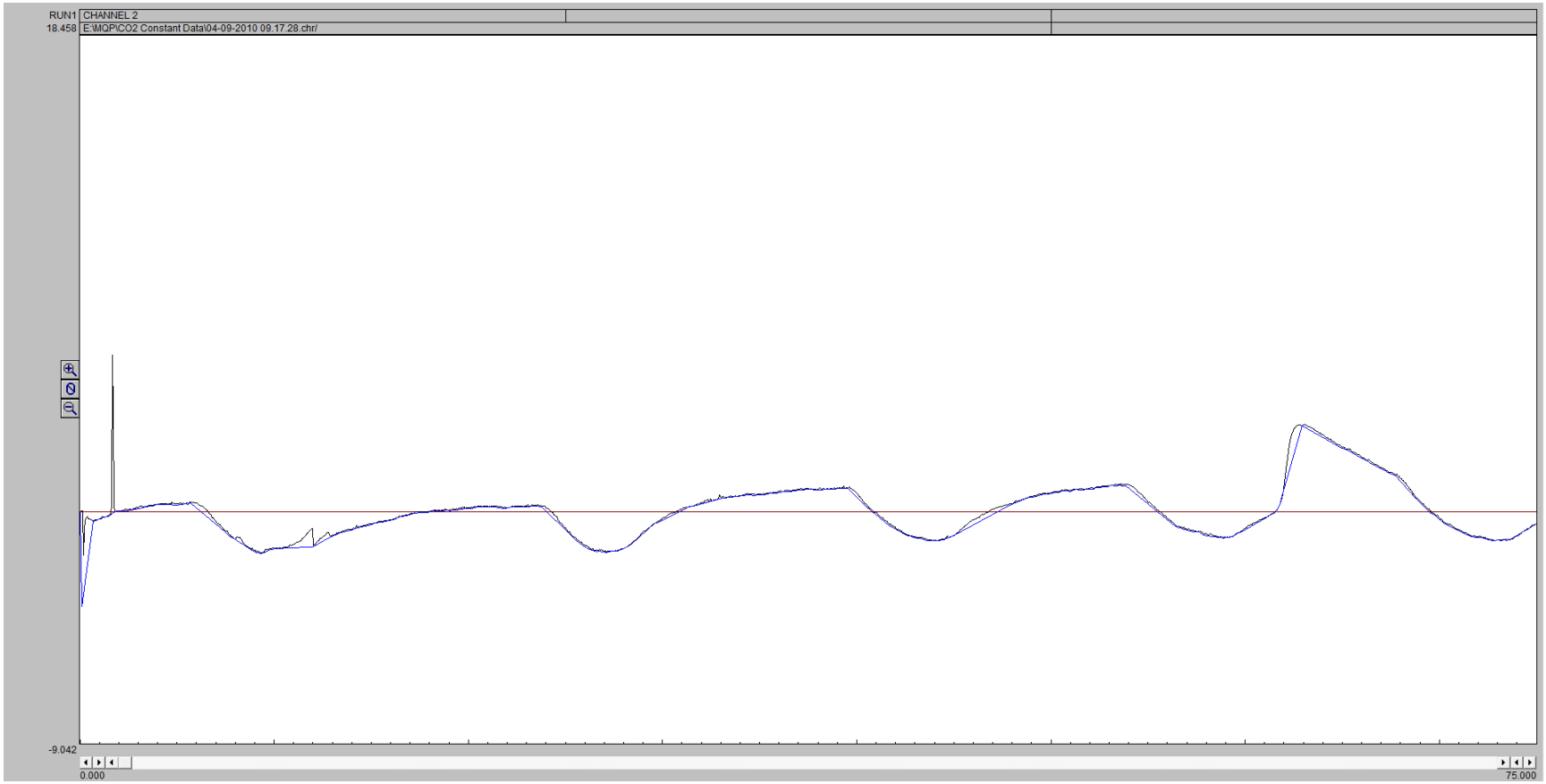

Gas Sample 460 Minutes

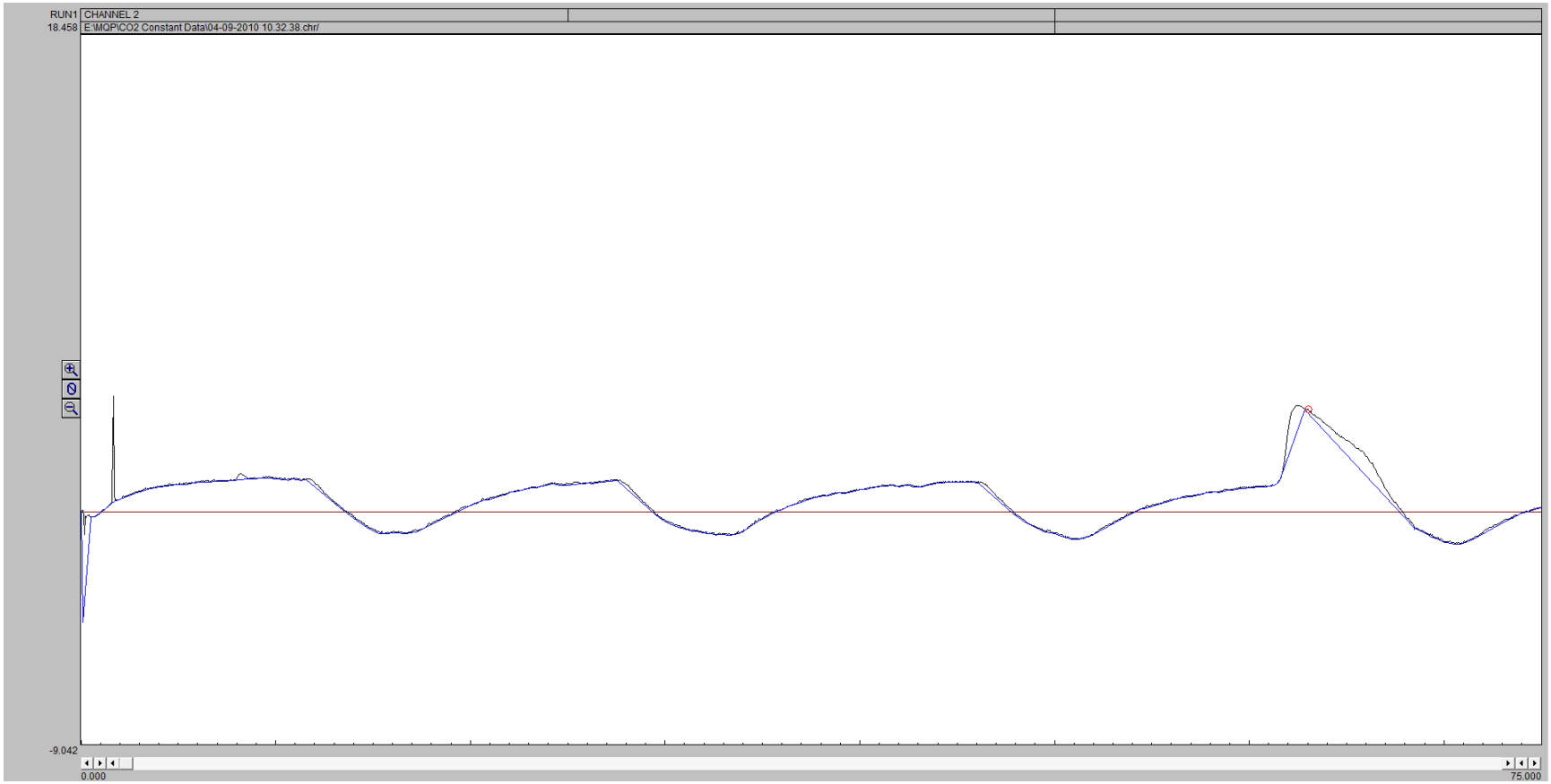

Gas Sample 535 Minutes

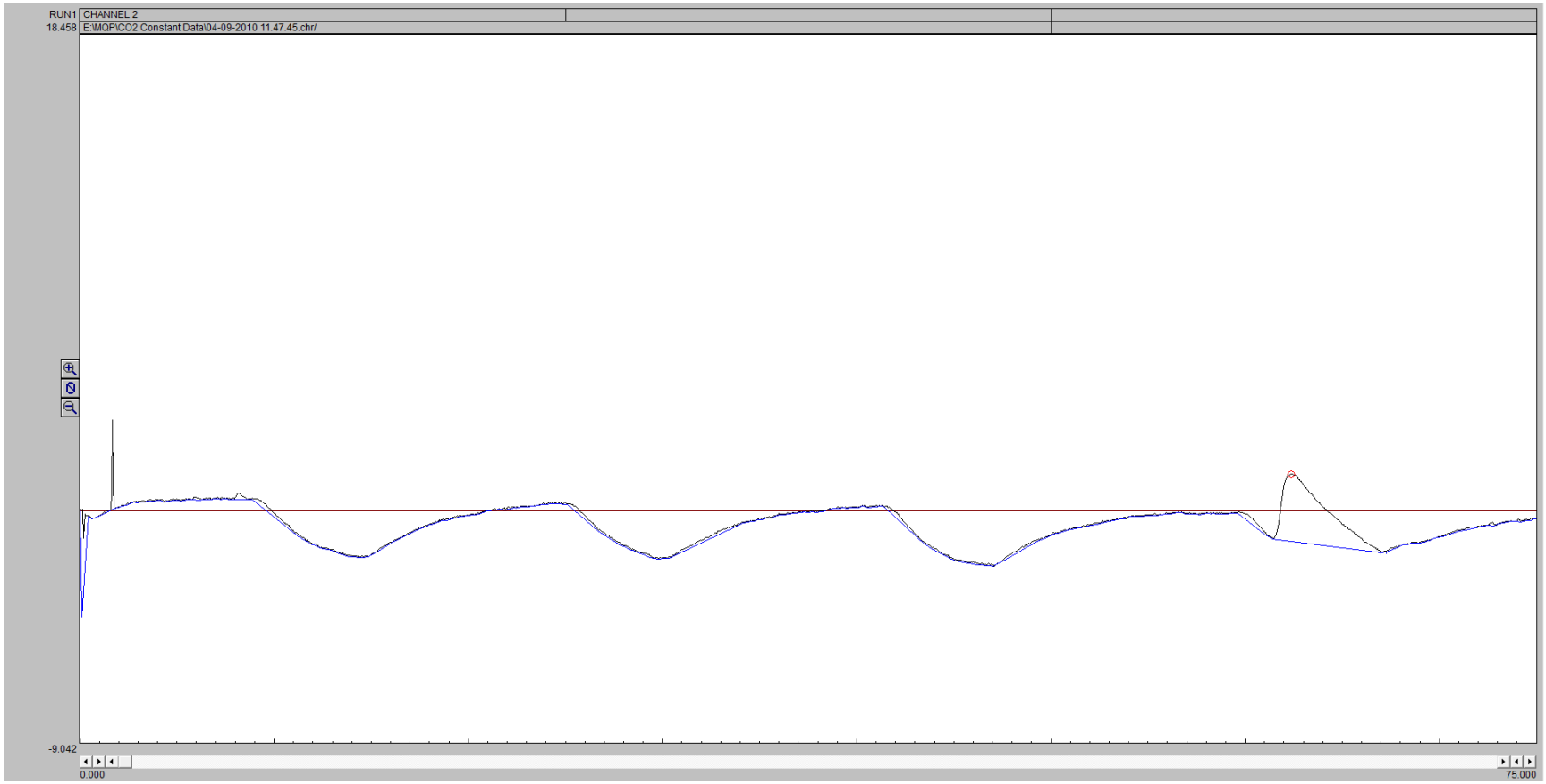

GC Liquids Data

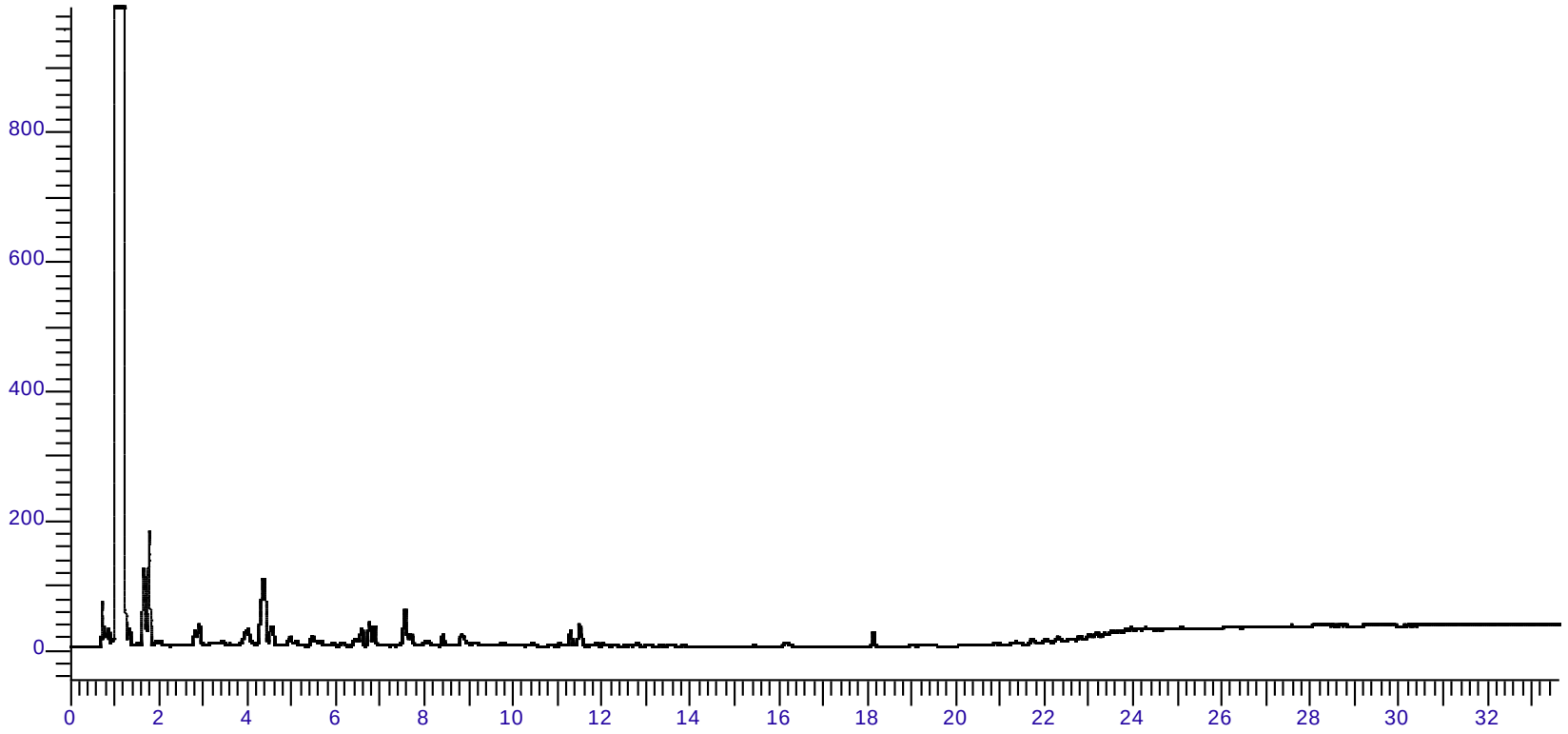

NMR Liquids Data

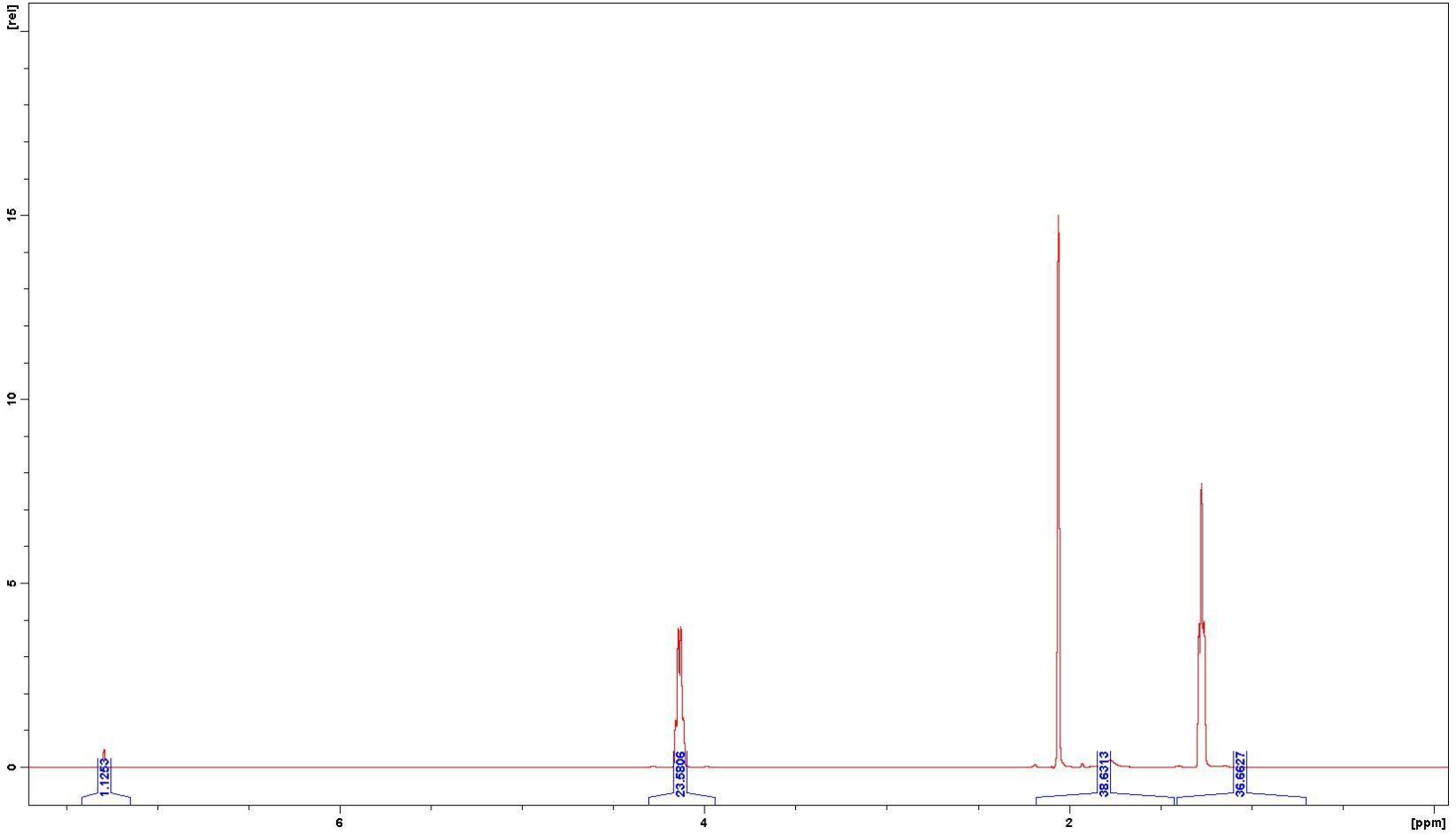

G6

Gas Concentrations over Time

	Mole %			
Time Stamp	H_2	CO	CH_4	CO_2
15	5.051507	4.229057	1.769825	88.94961
90	2.207556	0.912087	2.06637	94.81399
165	1.213989	0.736178	0.741404	97.30843
315	1.687098	1.314391	1.202554	95.79596
390	10.03732	0	0	89.96268
465	0.300072	0.689572	0	99.01036
540	0.364048	1.060695	0	98.57526

Gas Sample 15 Minutes

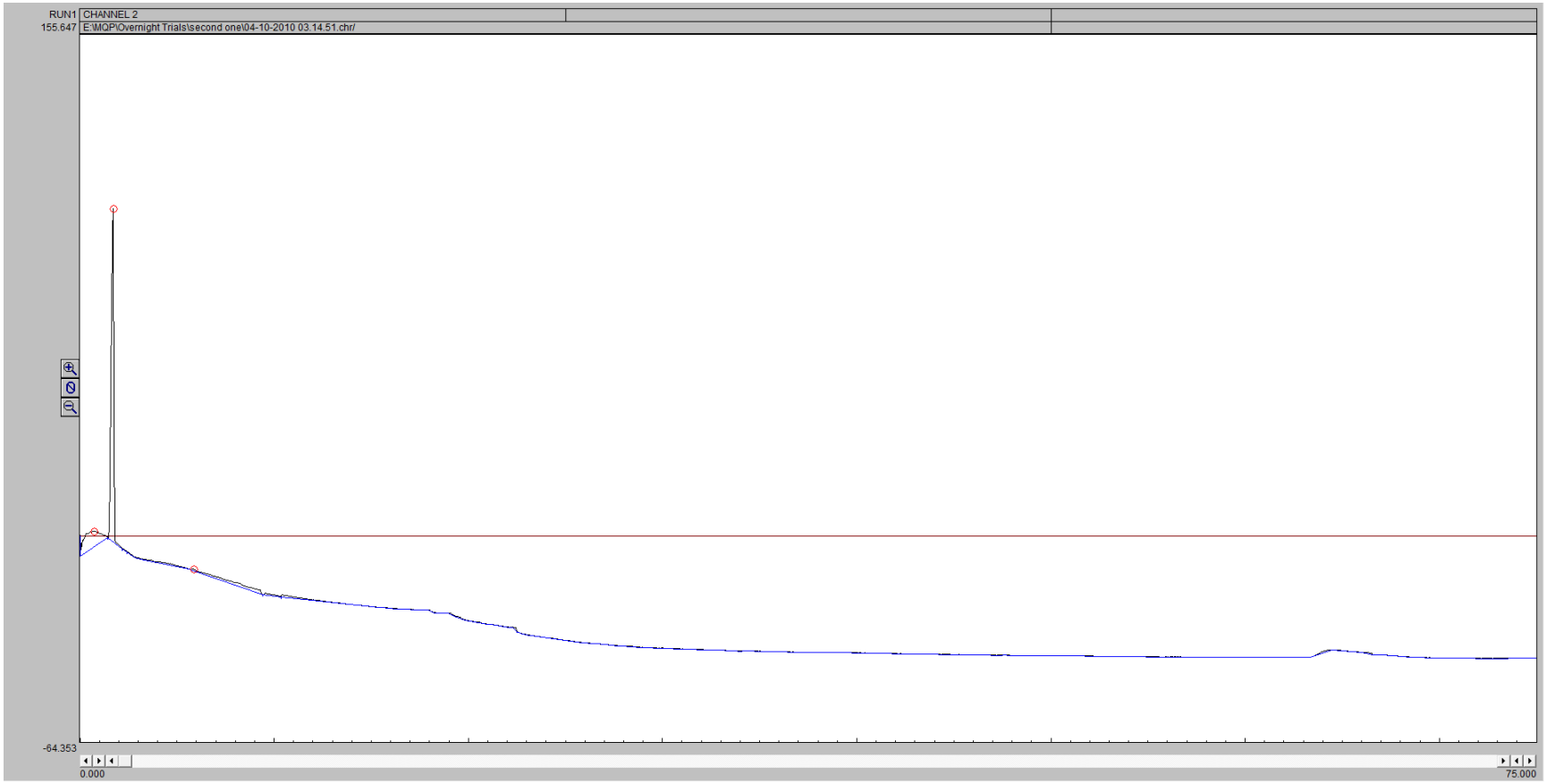

Gas Sample 90 Minutes

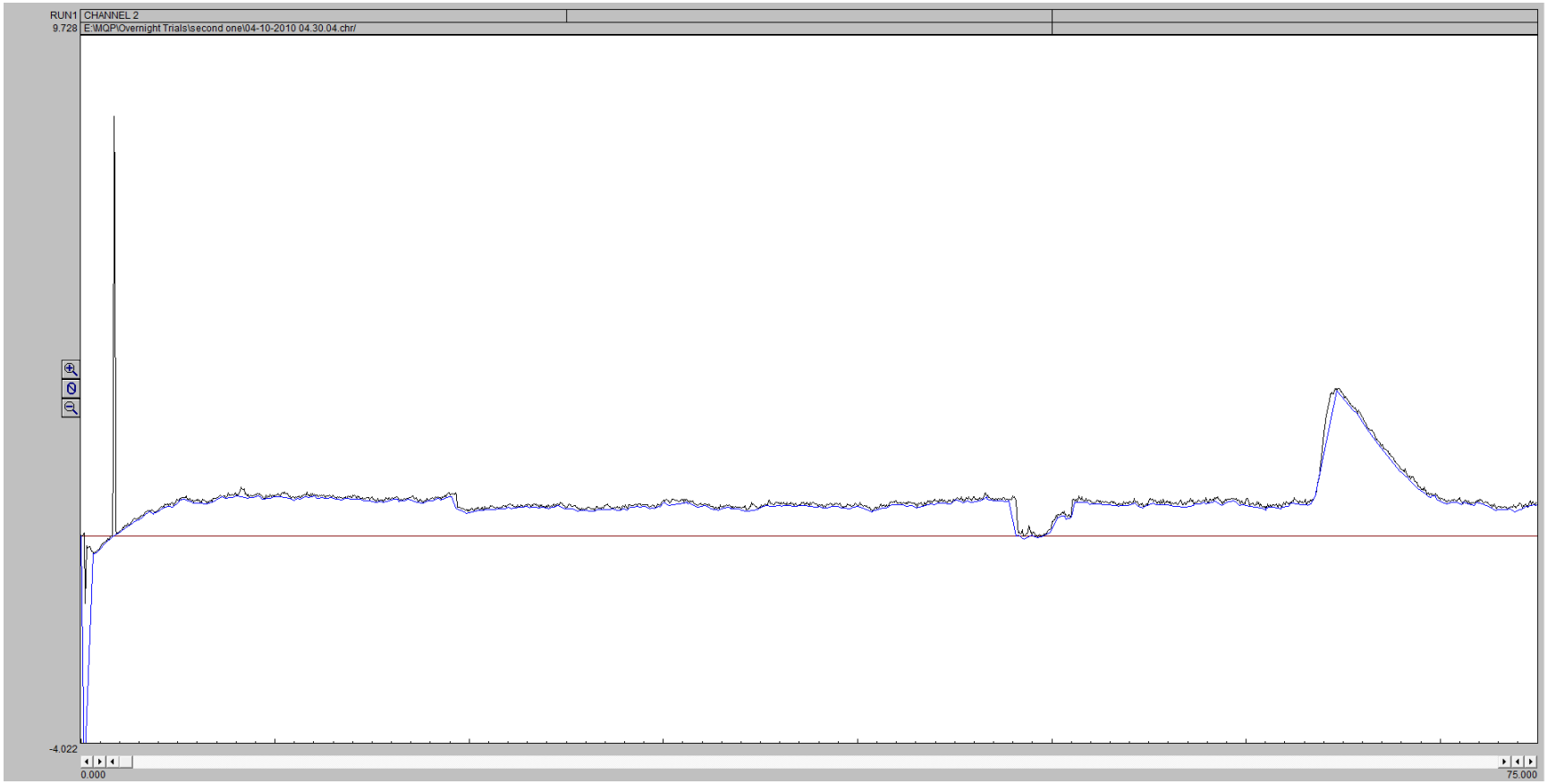

Gas Sample 165 Minutes

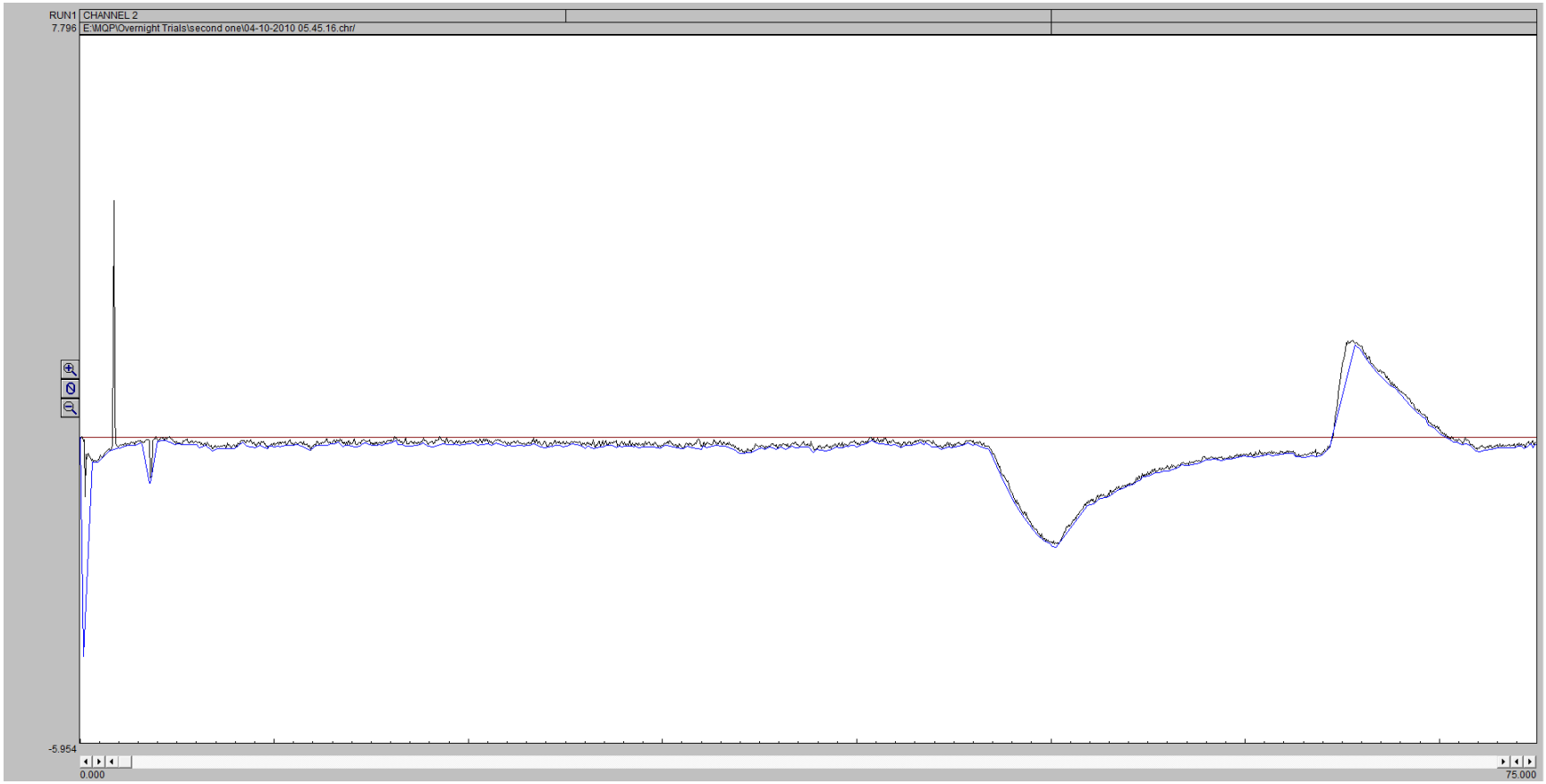

Gas Sample 315 Minutes

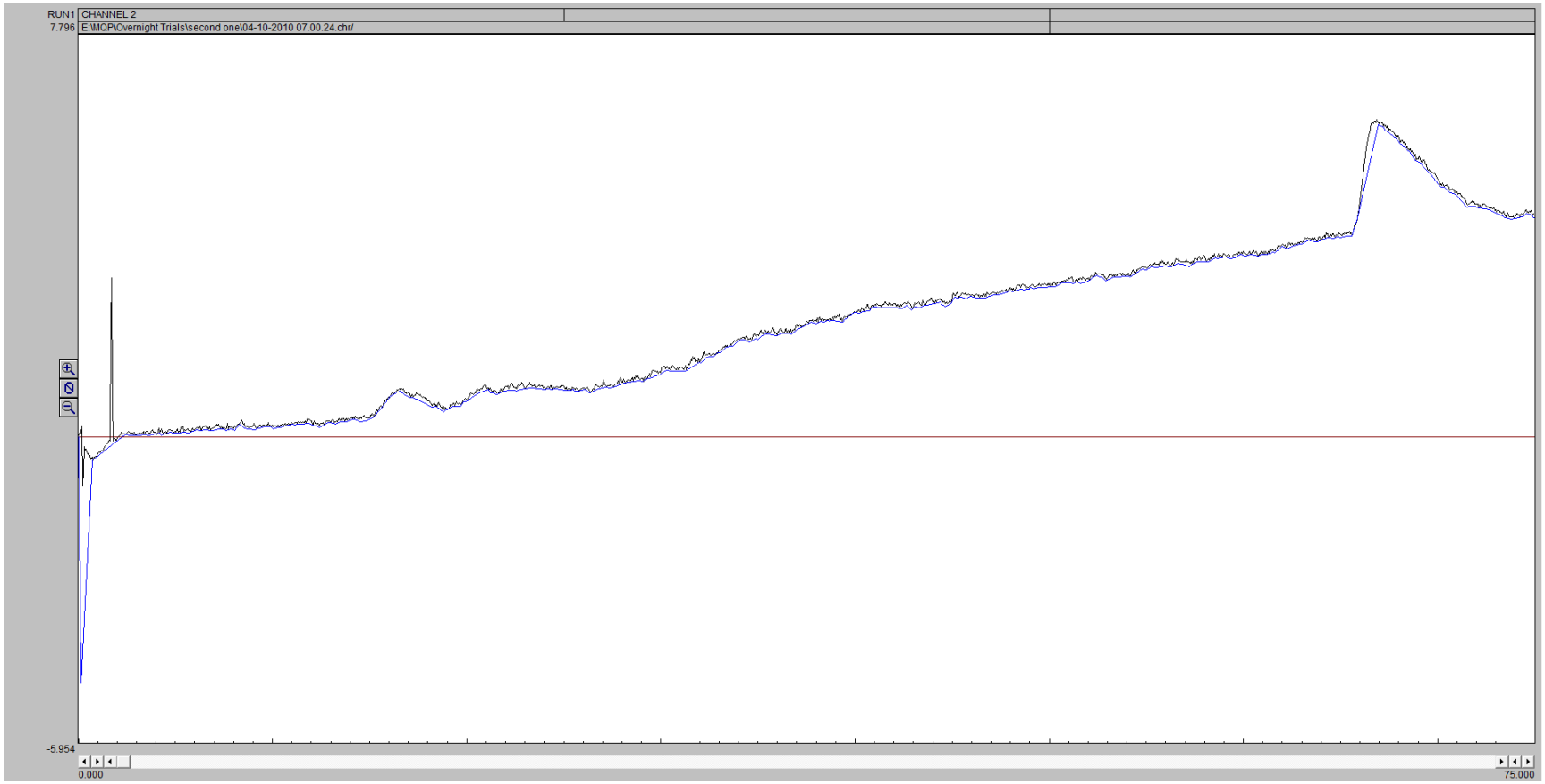

Gas Sample 390 Minutes

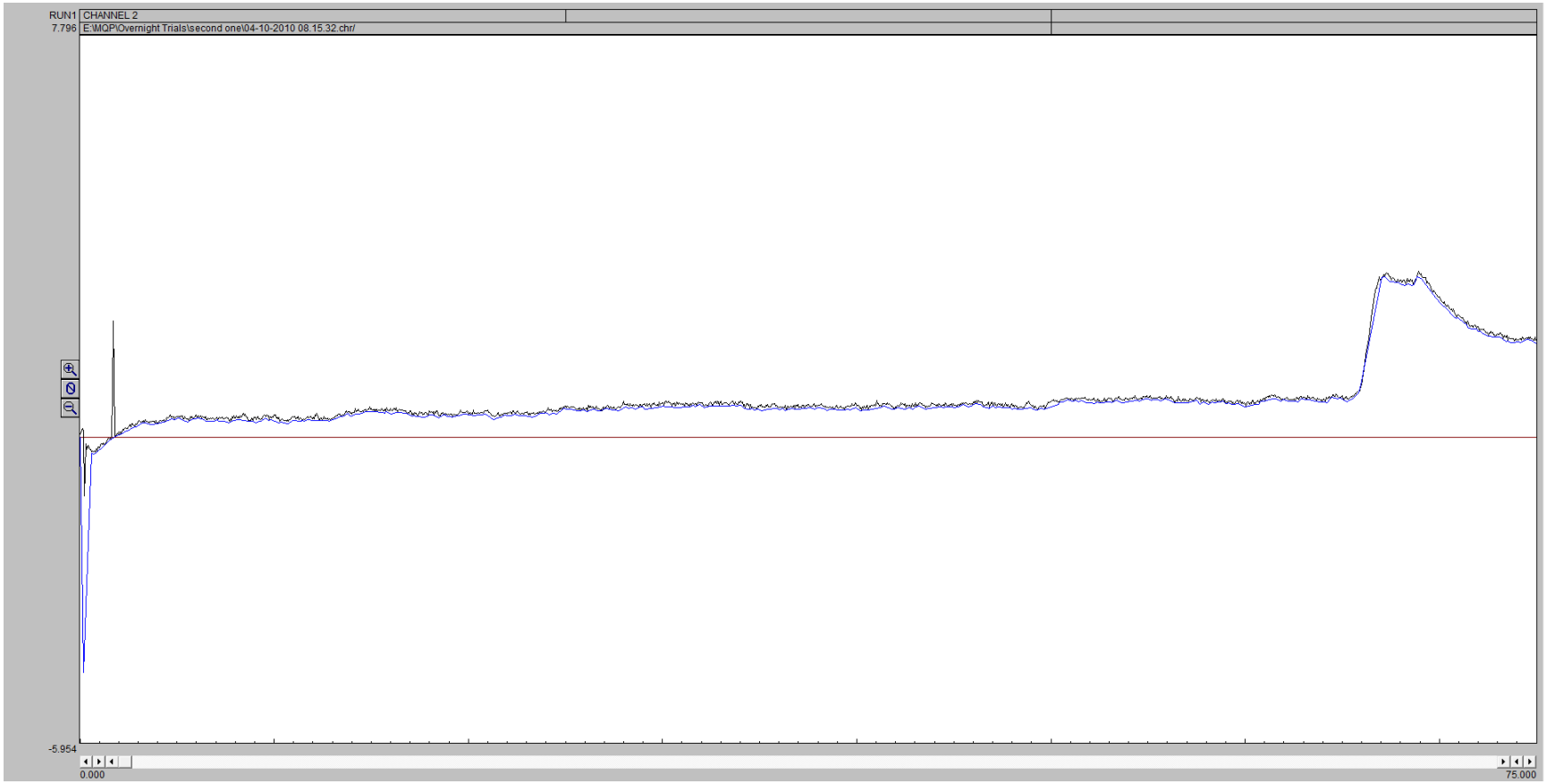

Gas Sample 465 Minutes

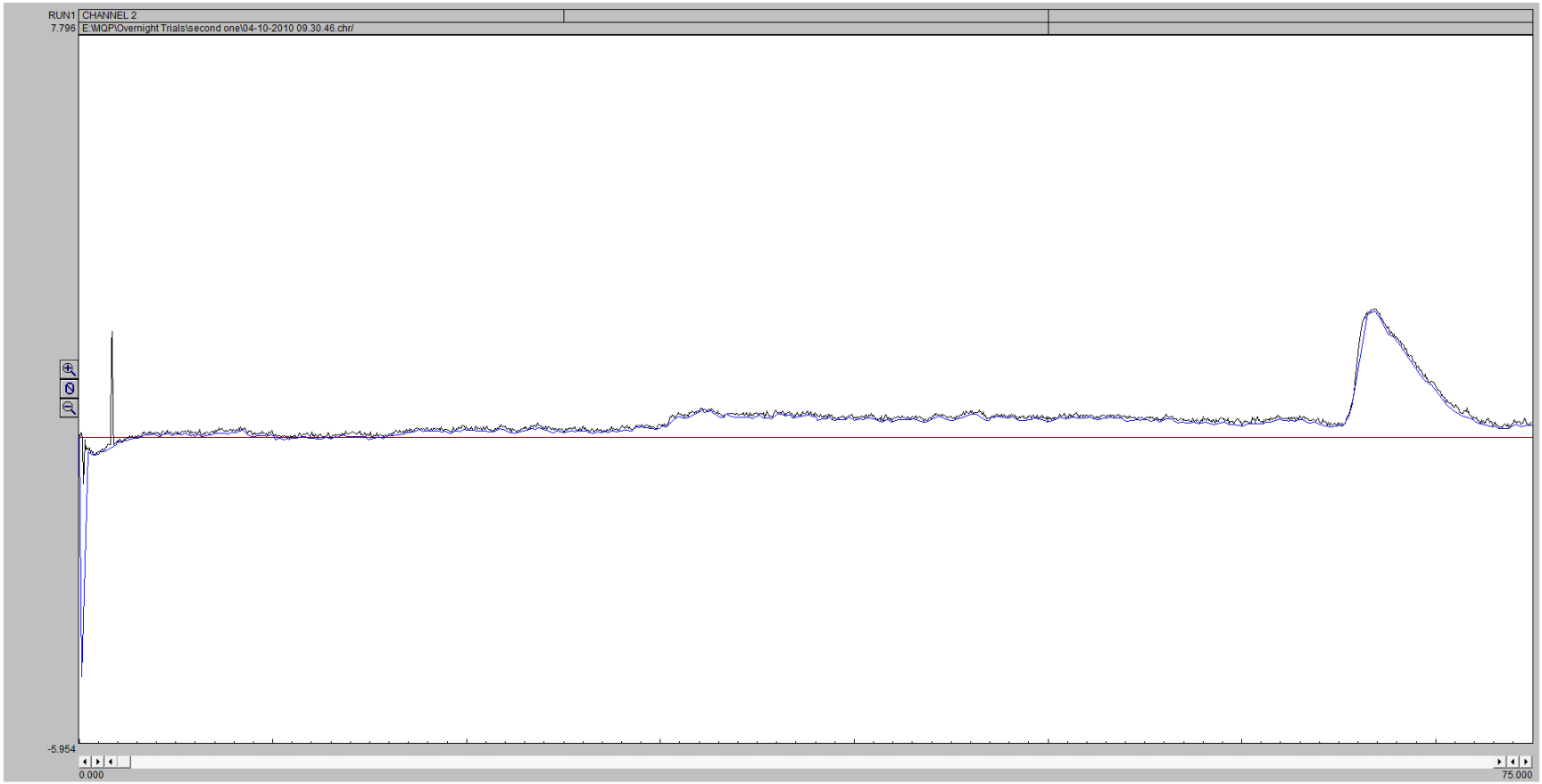

Gas Sample 540 Minutes

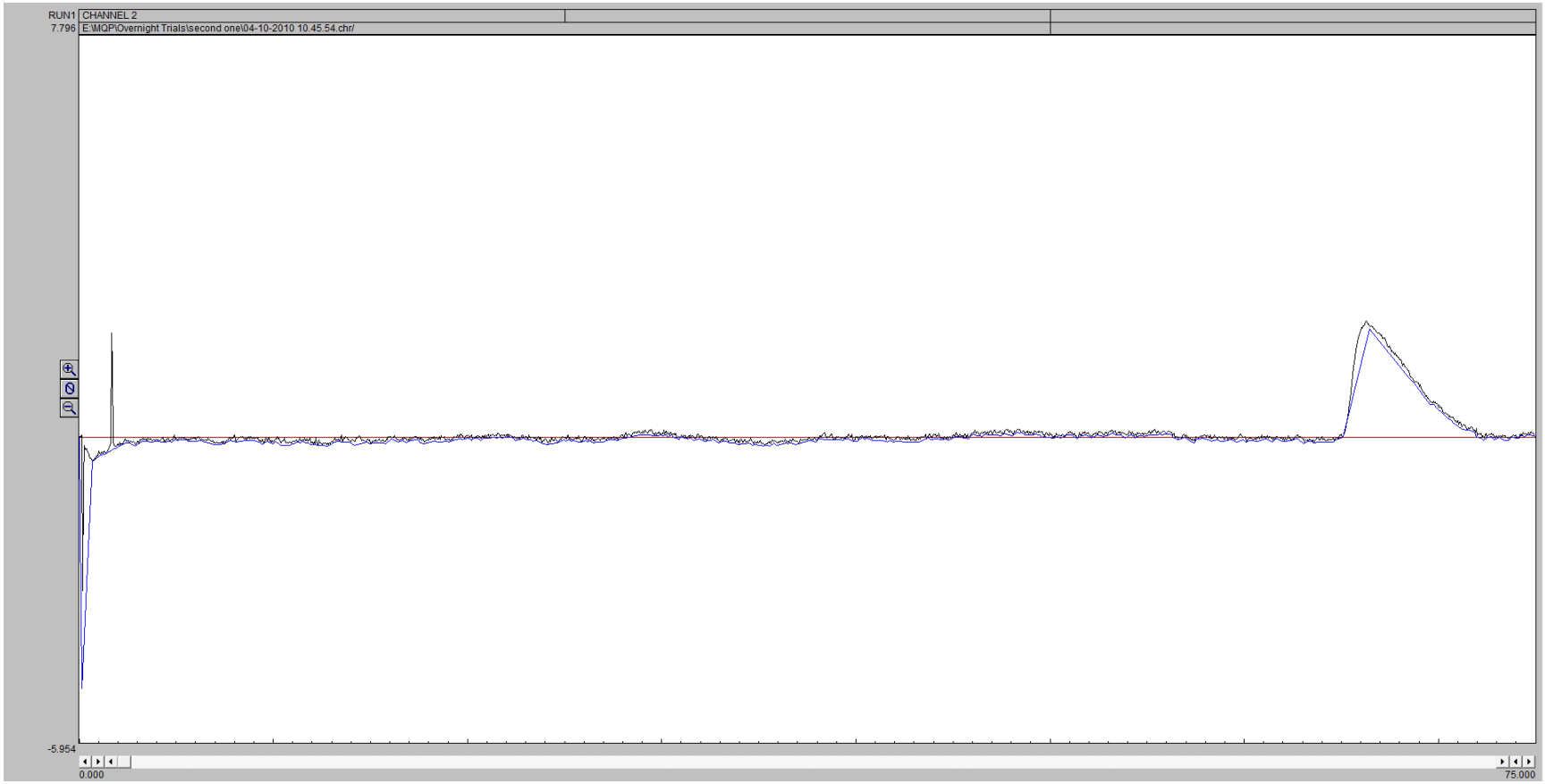

GC Liquids Data

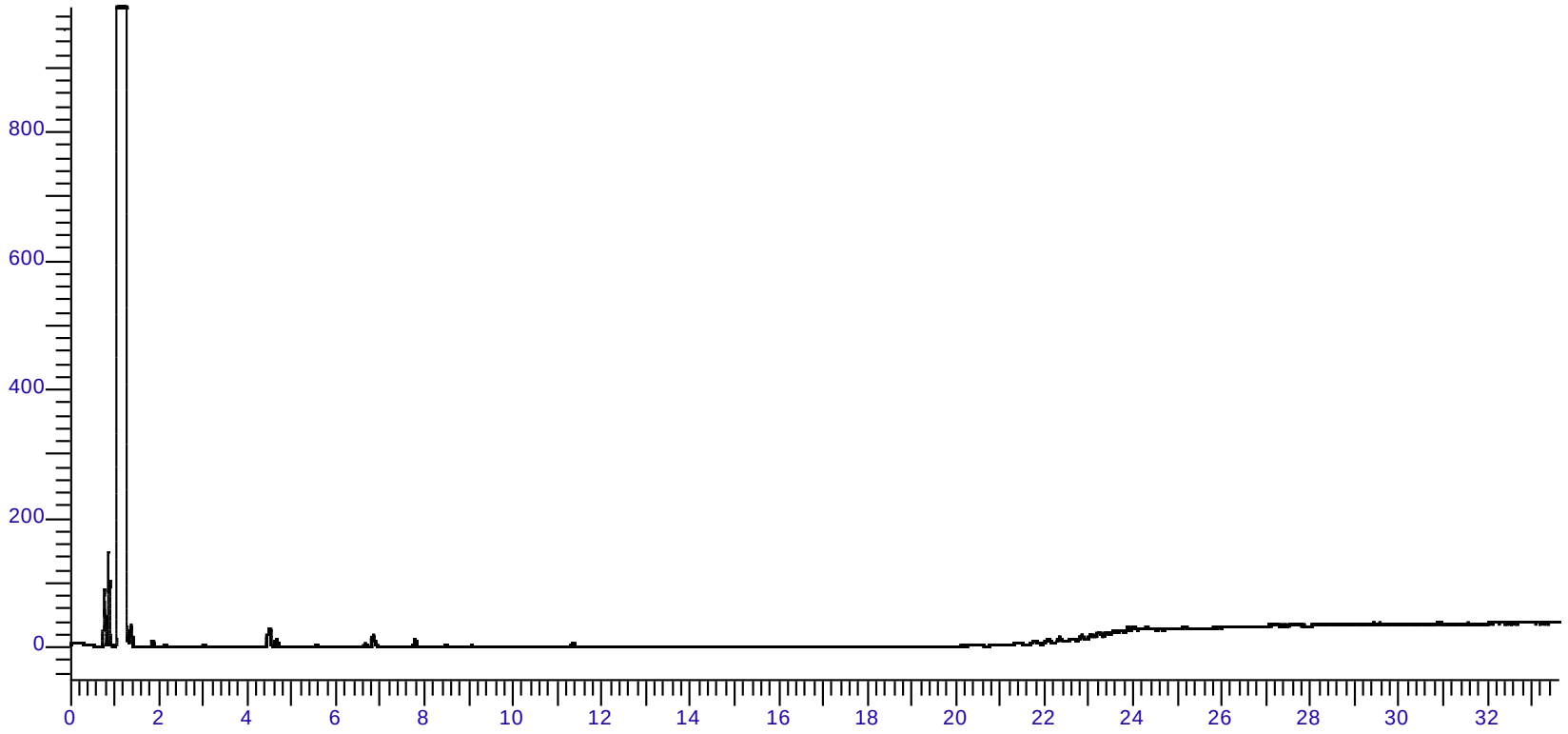

NMR Liquids Data

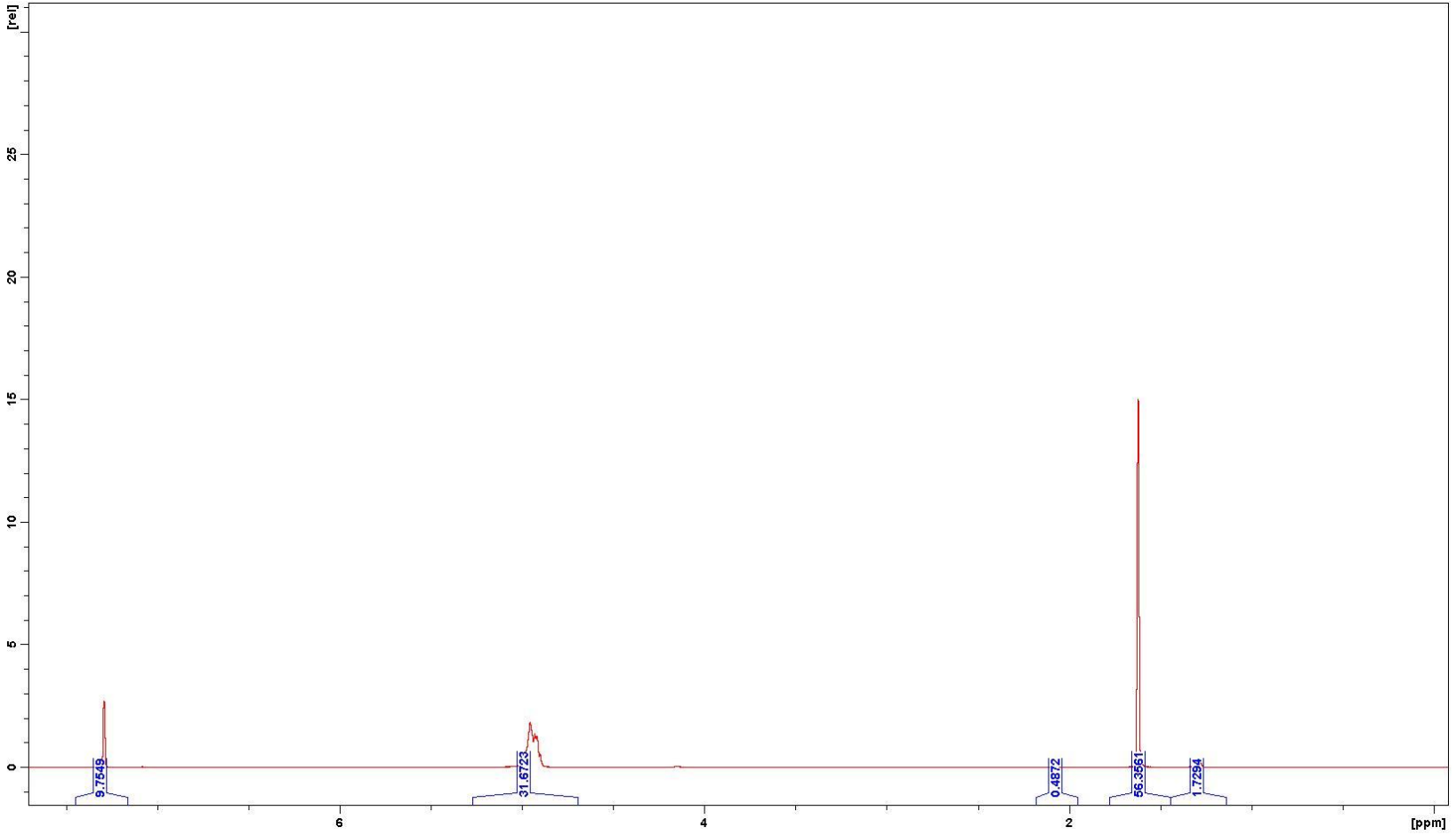

G7

Gas Concentrations over Time

	Mole %			
Time Stamp	H_2	CO	CH_4	CO_2
10	0.11825	24.59866	0	75.28309
85	2.234506	0	0	97.76549
160	1.124014	0	0	98.87599
235	0.920882	0	0	99.07912
310	0.943059	0	0	99.05694
385	0.826384	0	0	99.17362
460	0.596382	0	0	99.40362
535	0.469339	0	0	99.53066

Gas Sample 10 Minutes

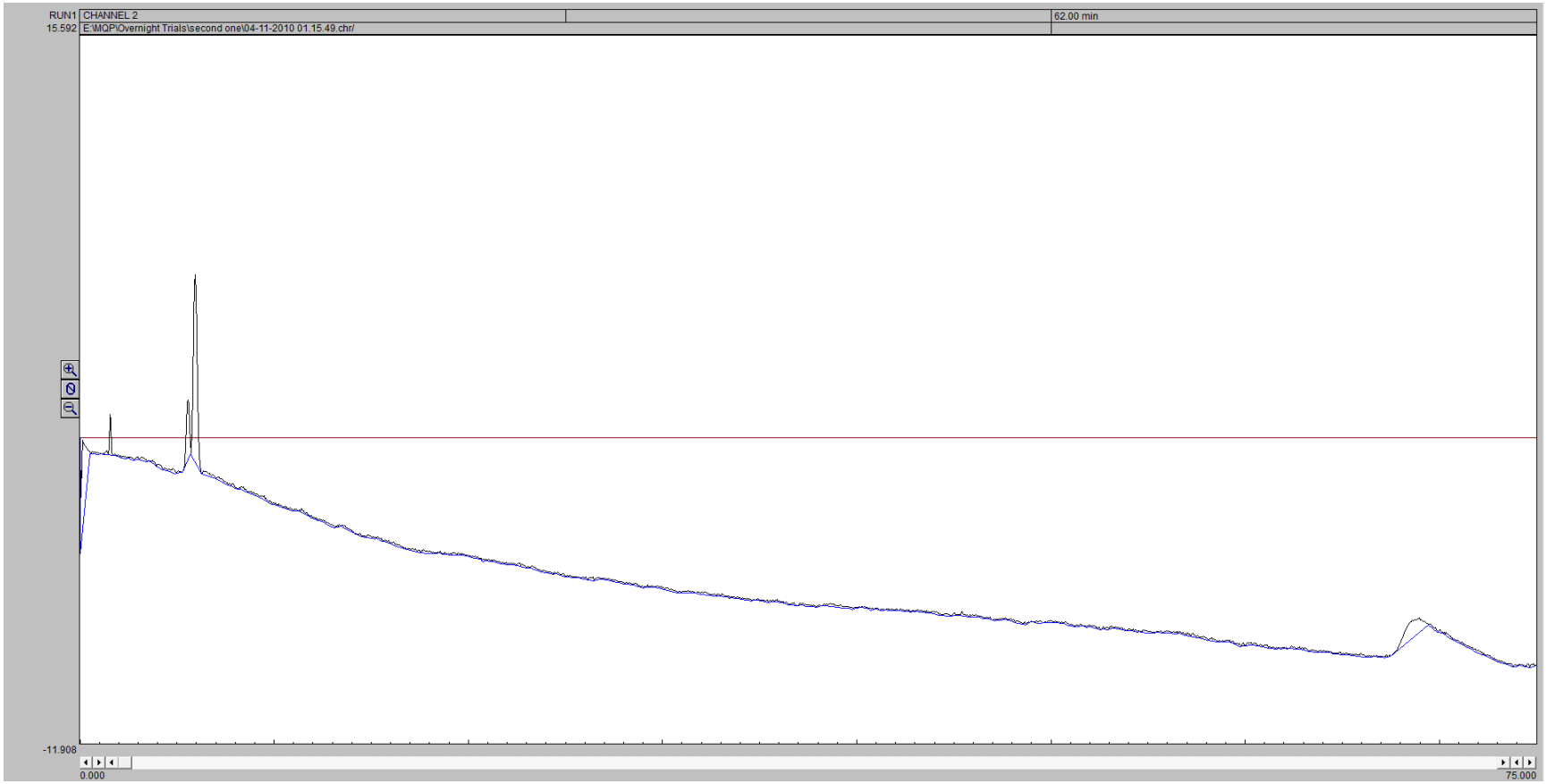

Gas Sample 85 Minutes

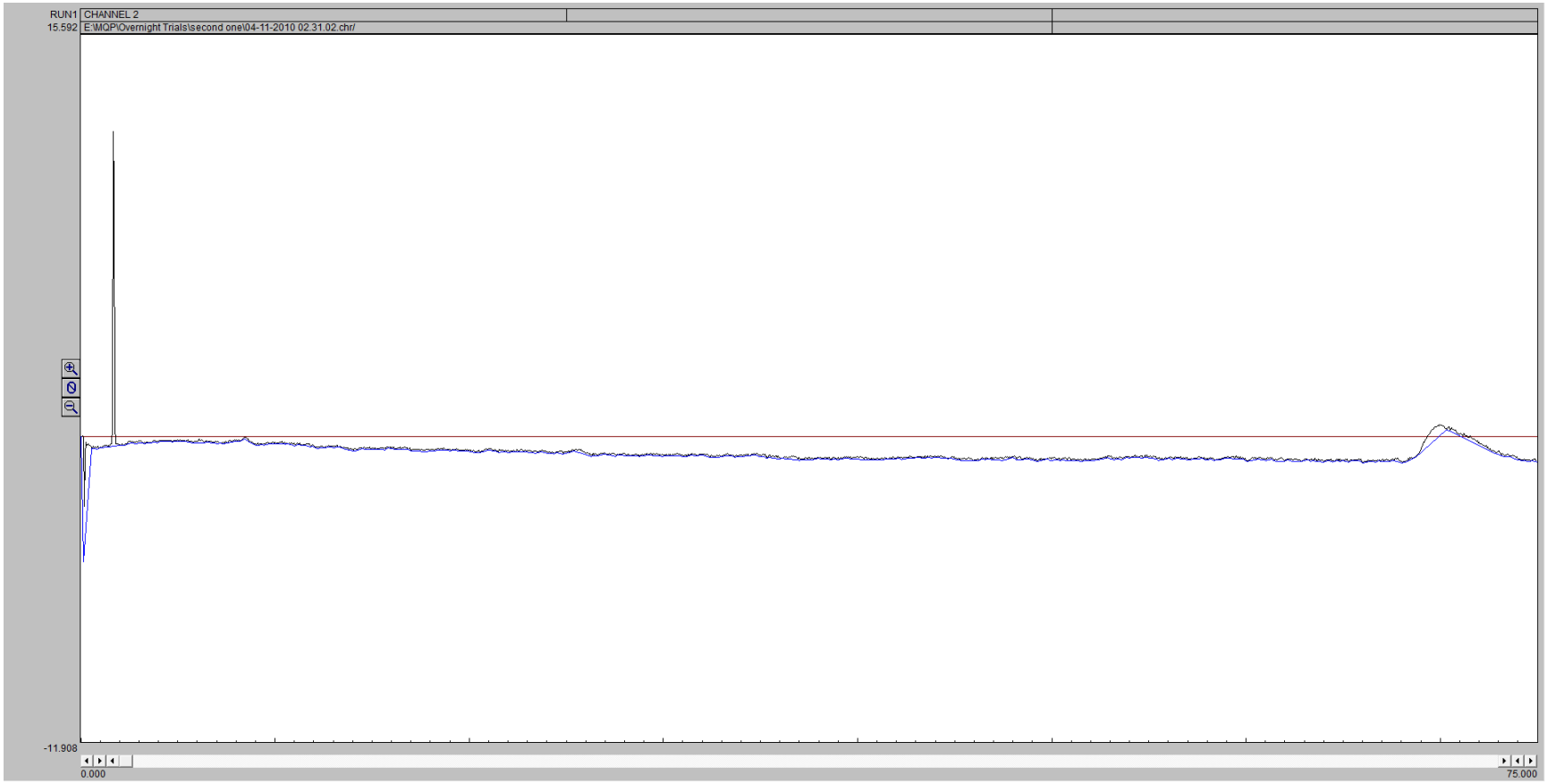

Gas Sample 160 Minutes

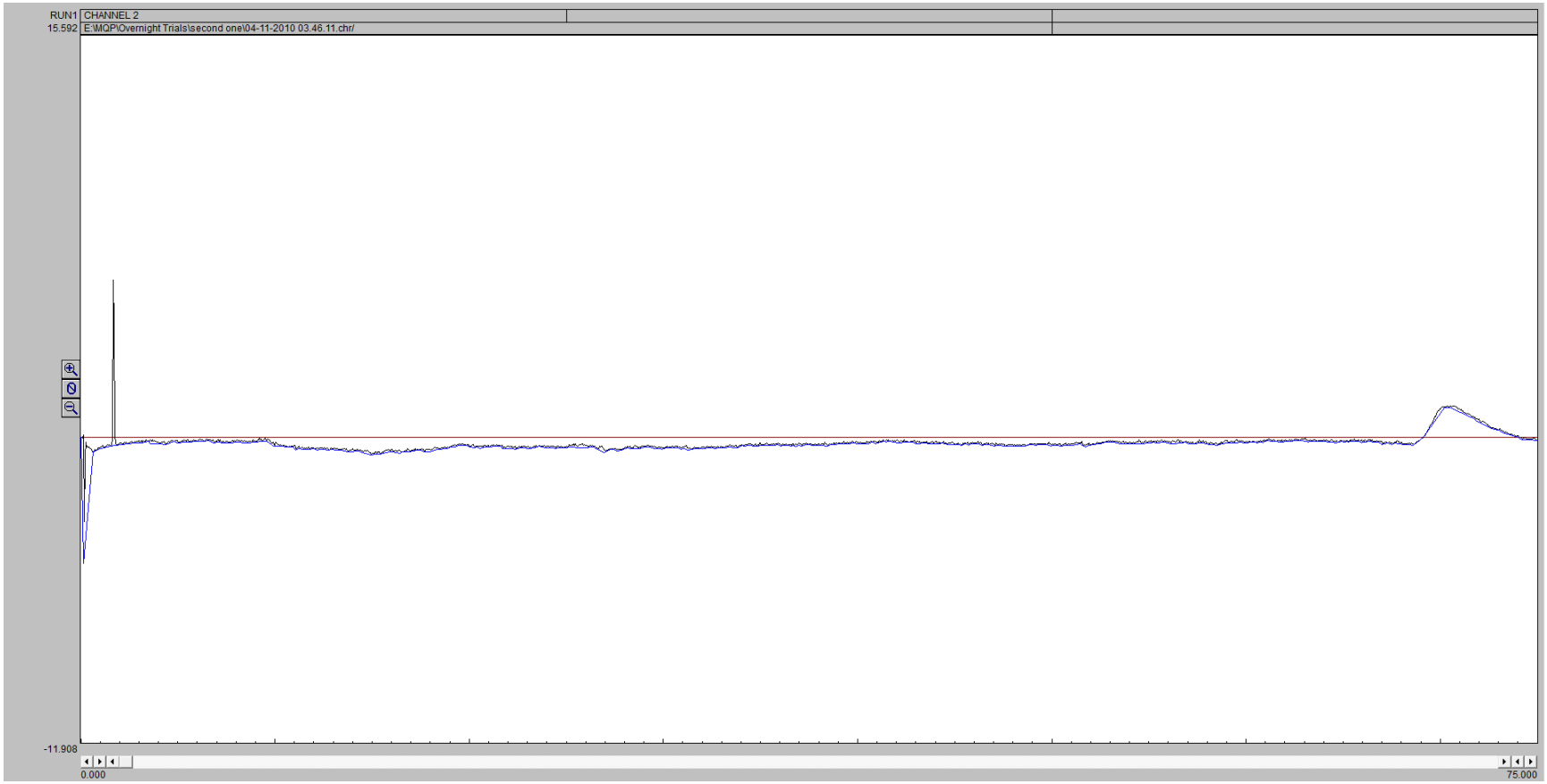

Gas Sample 235 Minutes

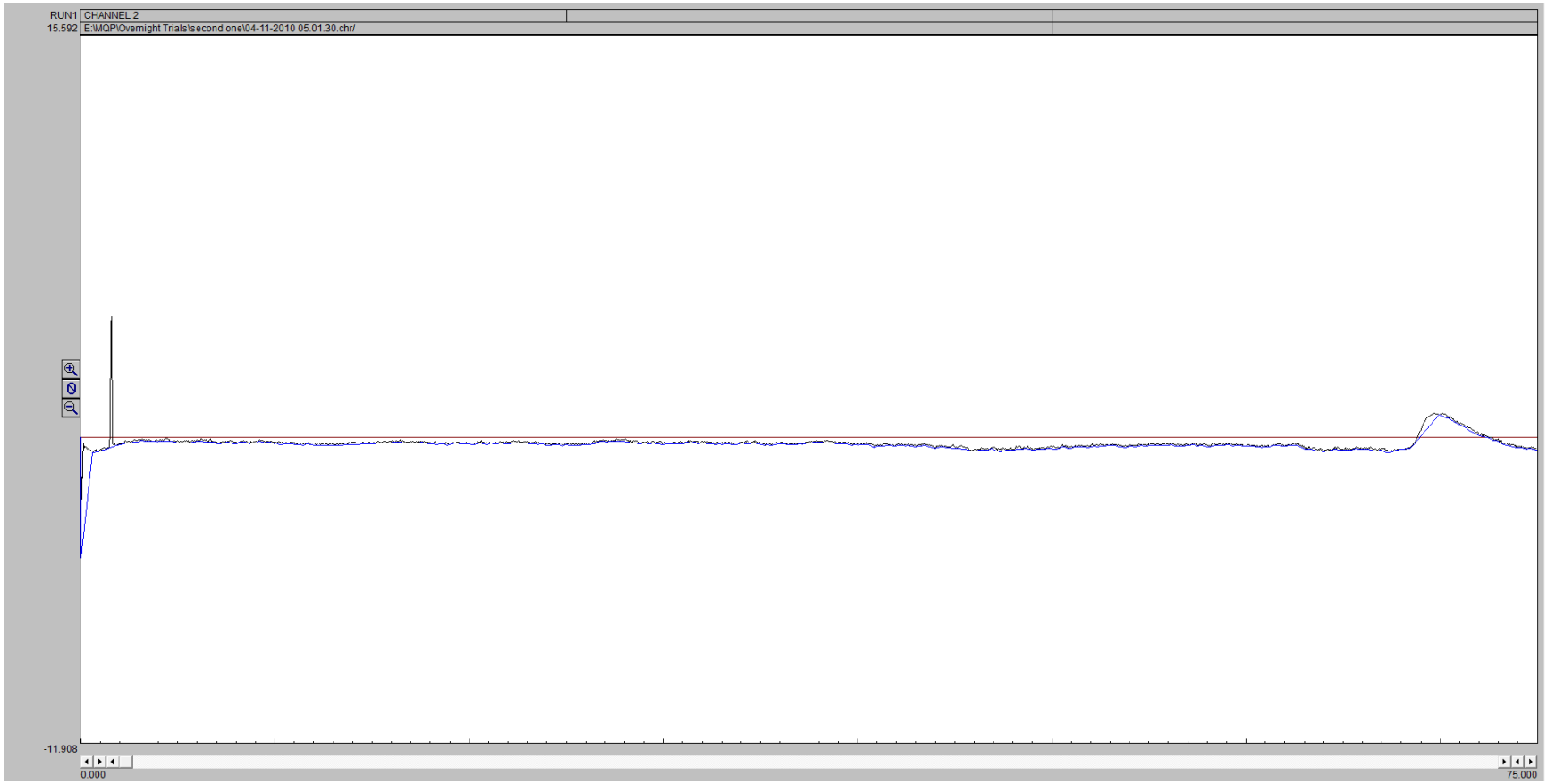

Gas Sample 310 Minutes

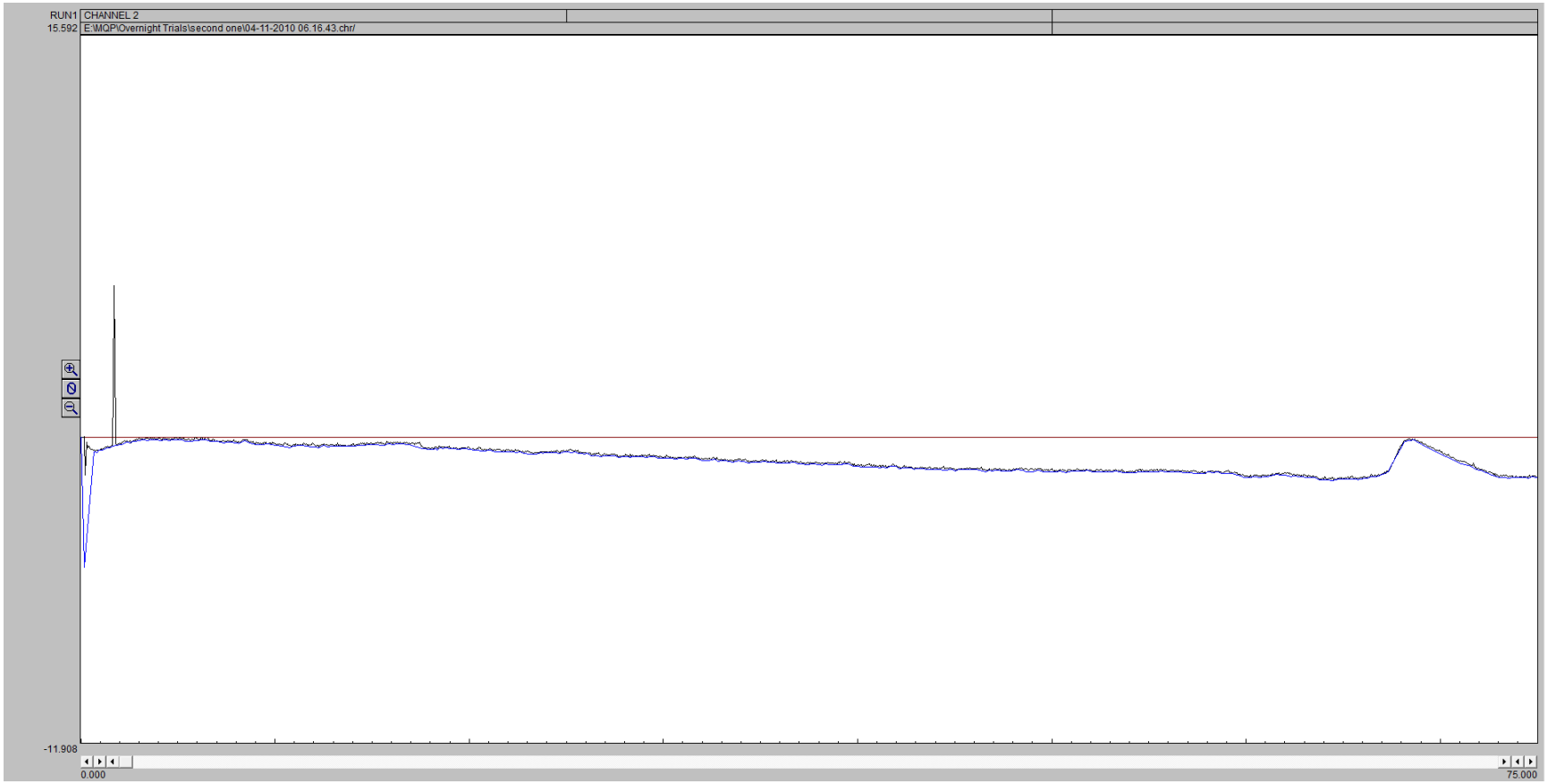

Gas Sample 385 Minutes

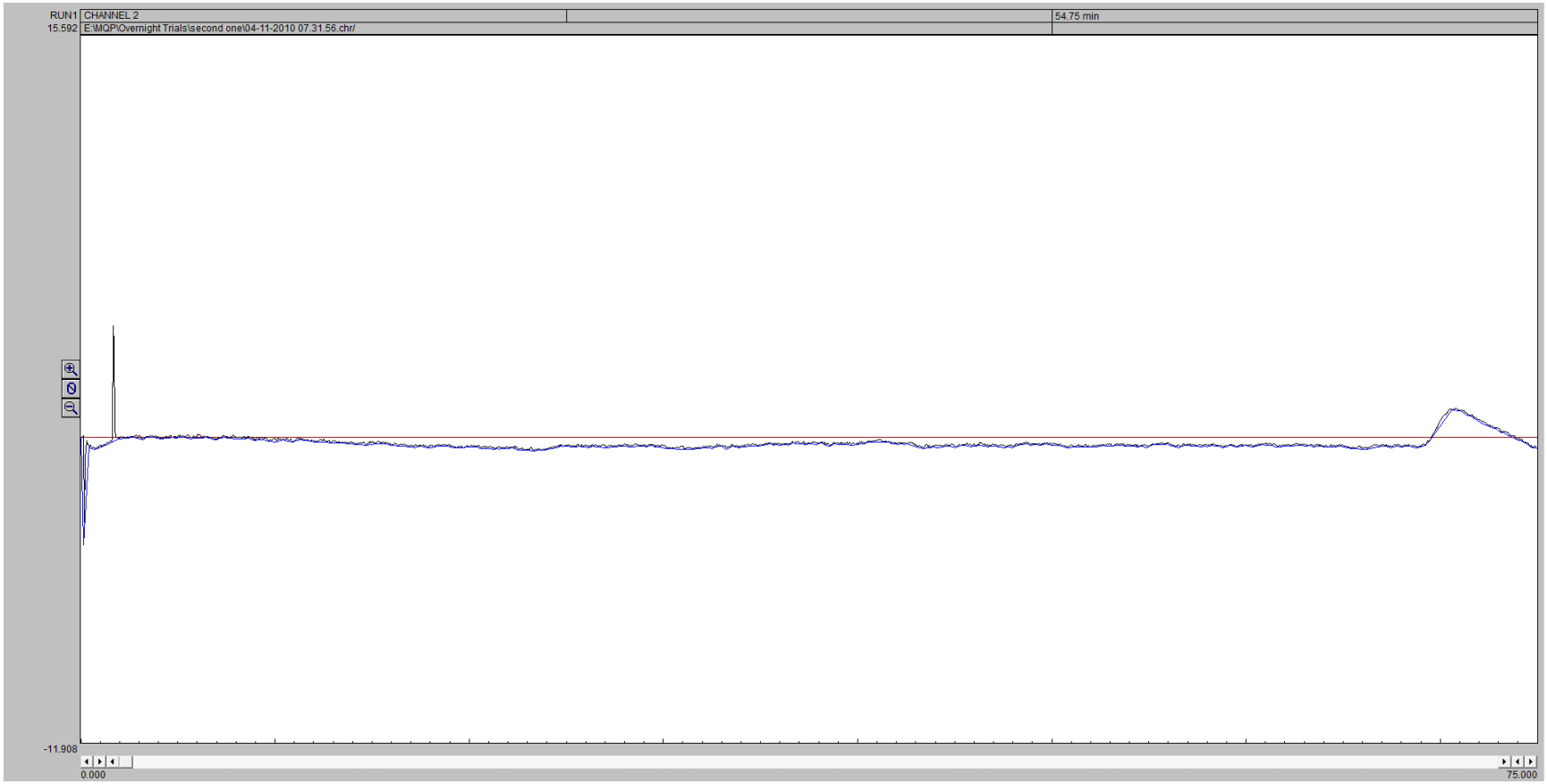

Gas Sample 460 Minutes

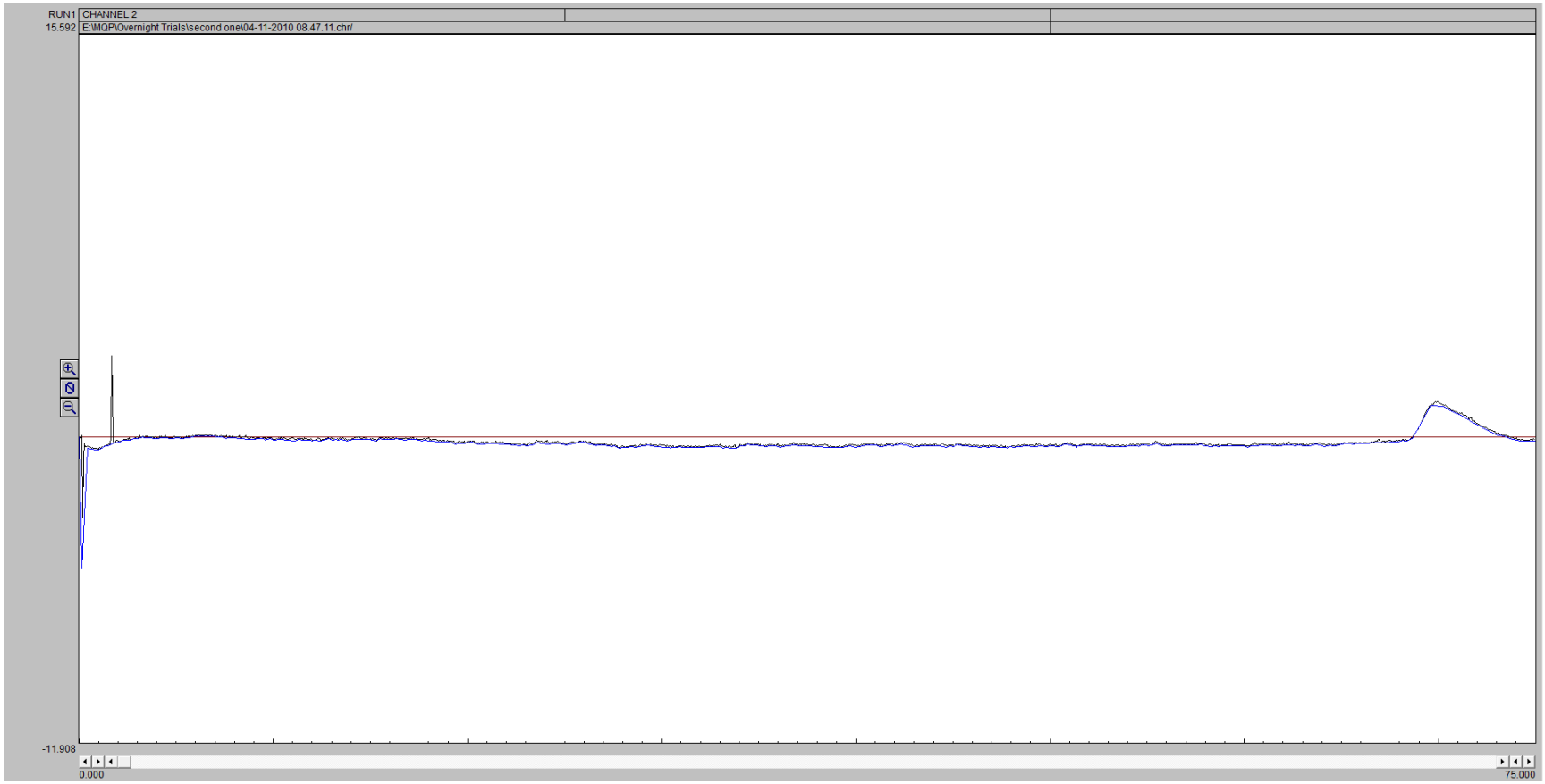

Gas Sample 535 Minutes

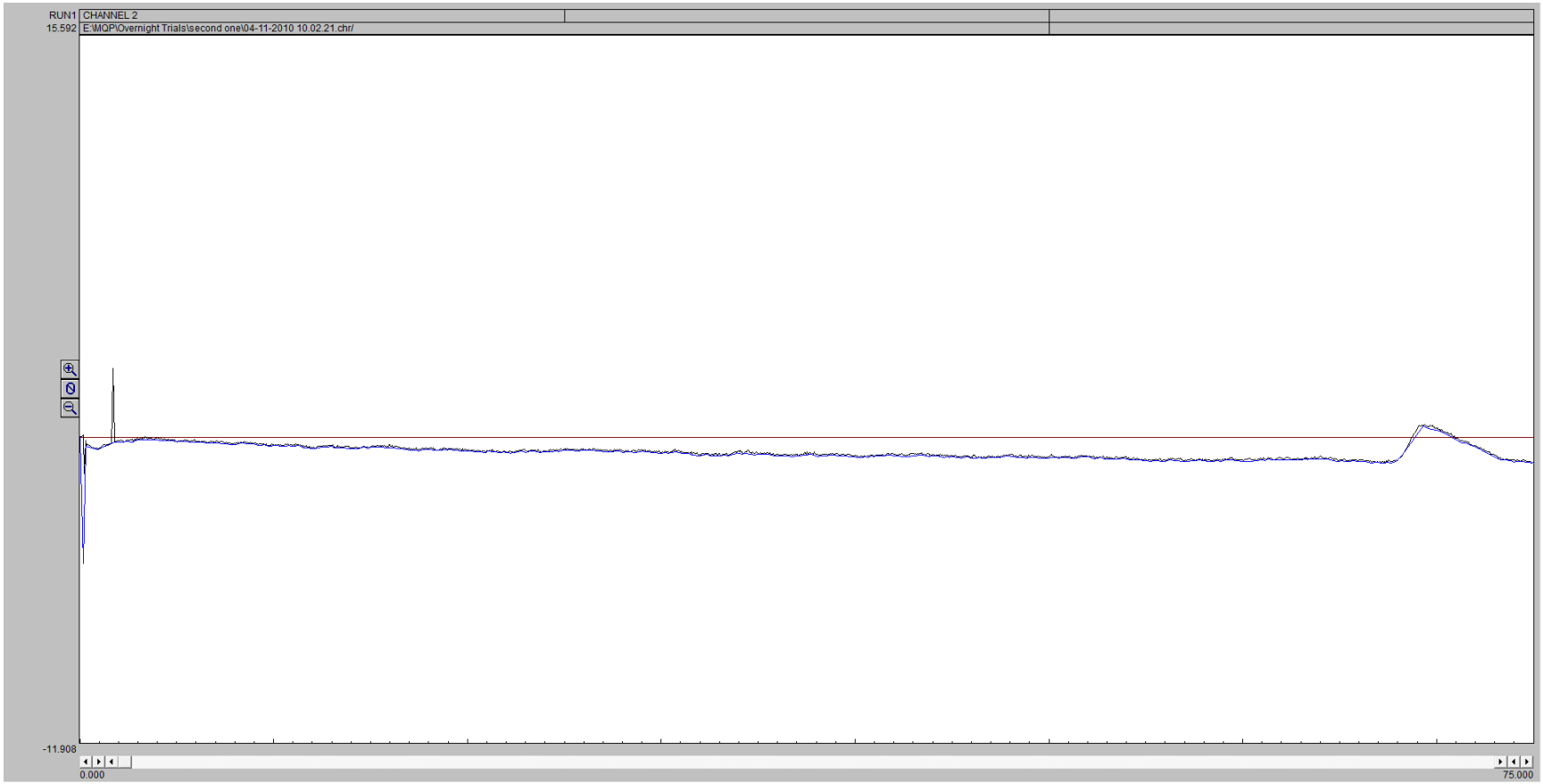

GC Liquids Data

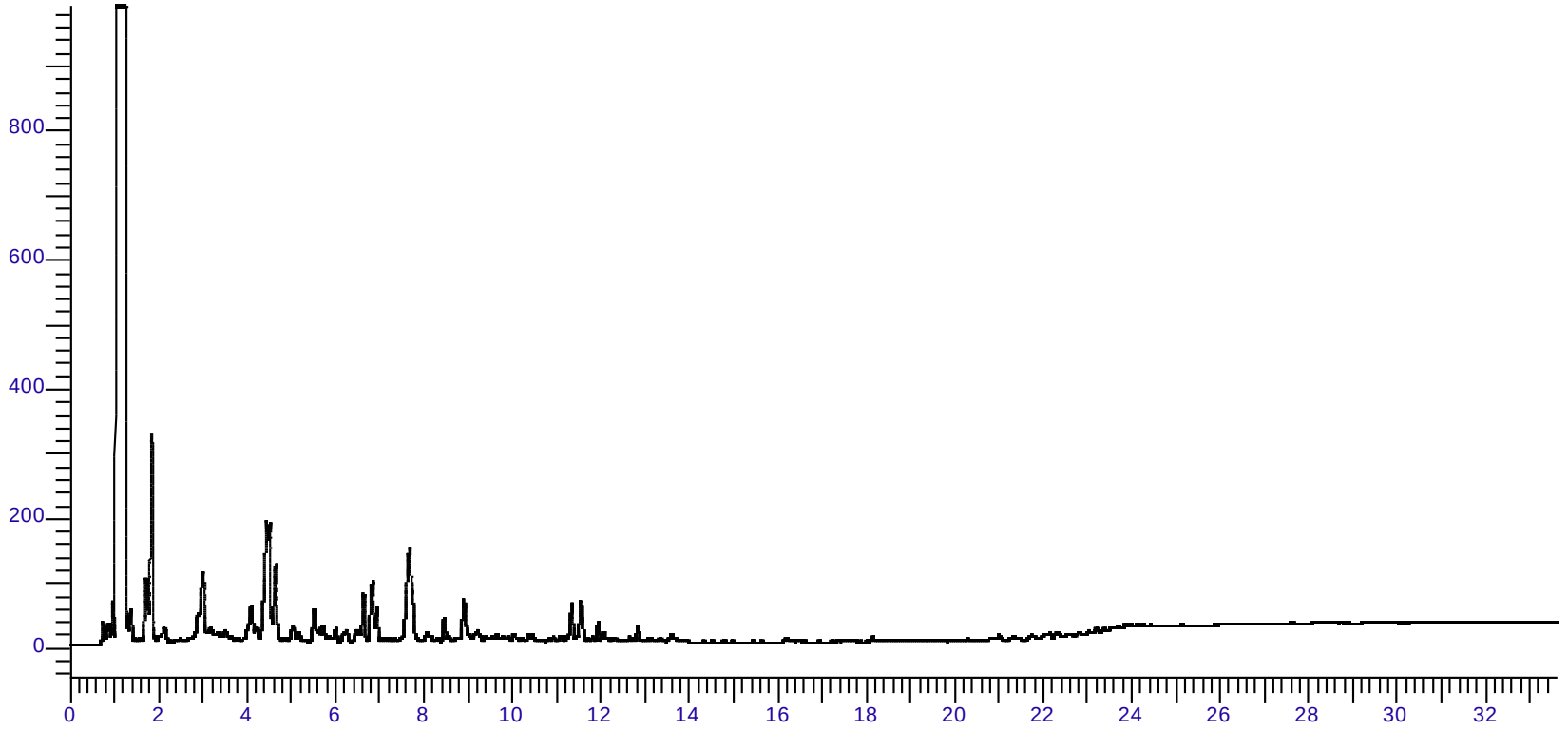

NMR Liquids Data

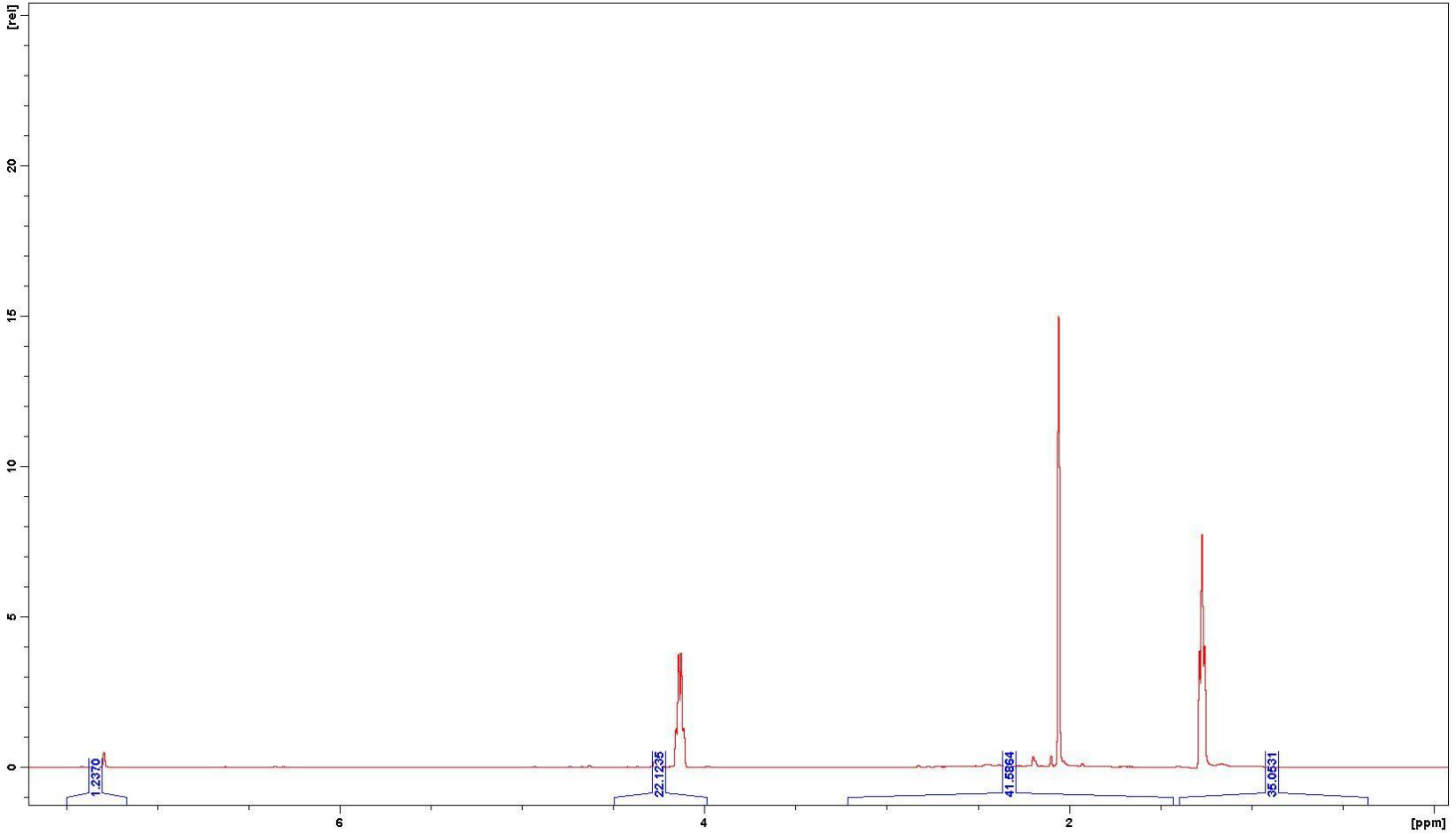

G8

Gas Concentrations over Time

	Mole %			
Time Stamp	H_2	CO	CH_4	CO_2
85	0	0	0	0
160	0	0	0	100
235	2.602096	1.254956	0	96.14295
310	1.791192	0	0	98.20881
385	1.996609	0	0	98.00339
460	1.725796	0	0	98.2742
535	1.346172	0	0	98.65383
610	0	0	0	0

Gas Sample 235 Minutes

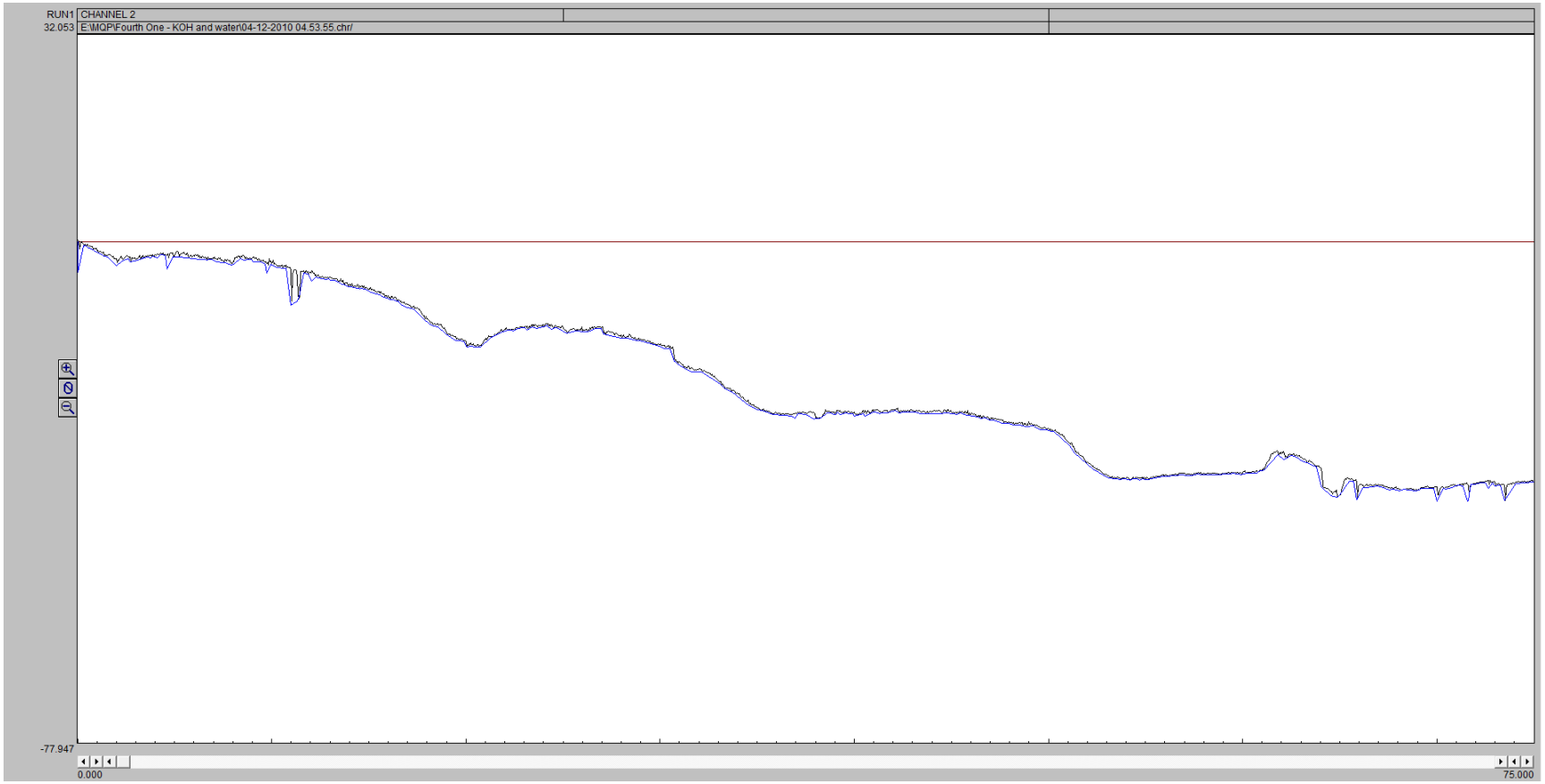

Gas Sample 310 Minutes

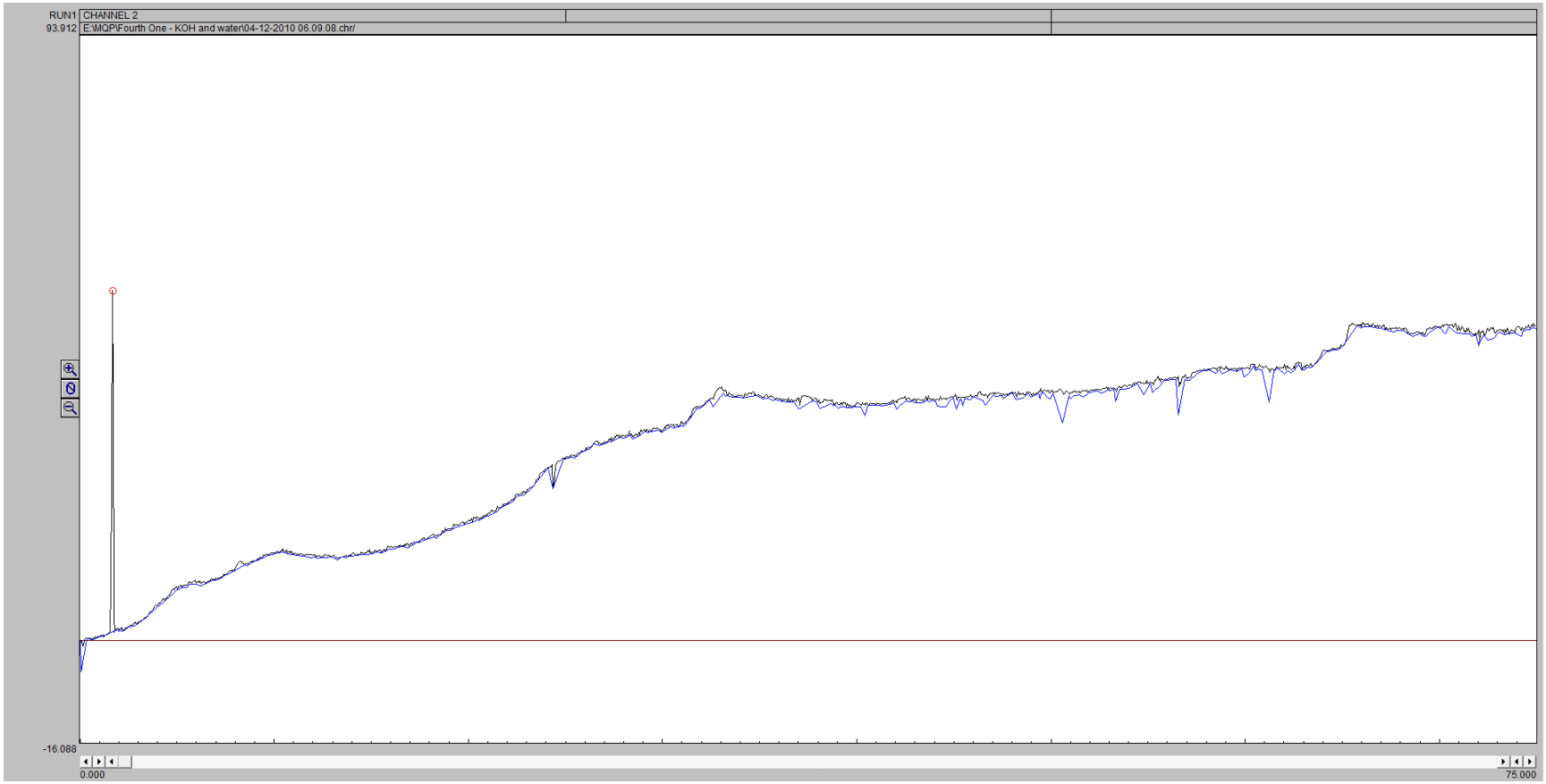

Gas Sample 385 Minutes

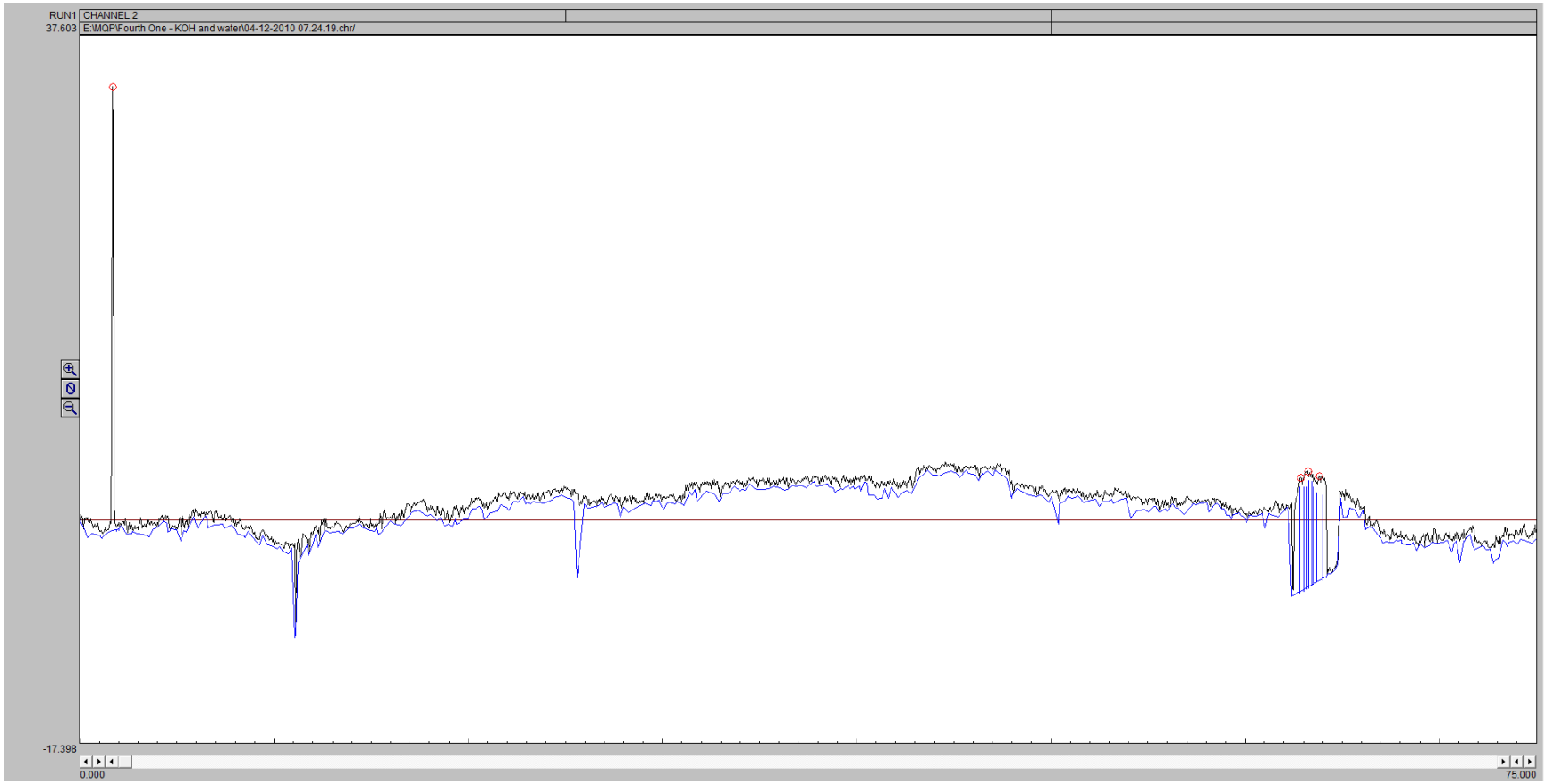

Gas Sample 460 Minutes

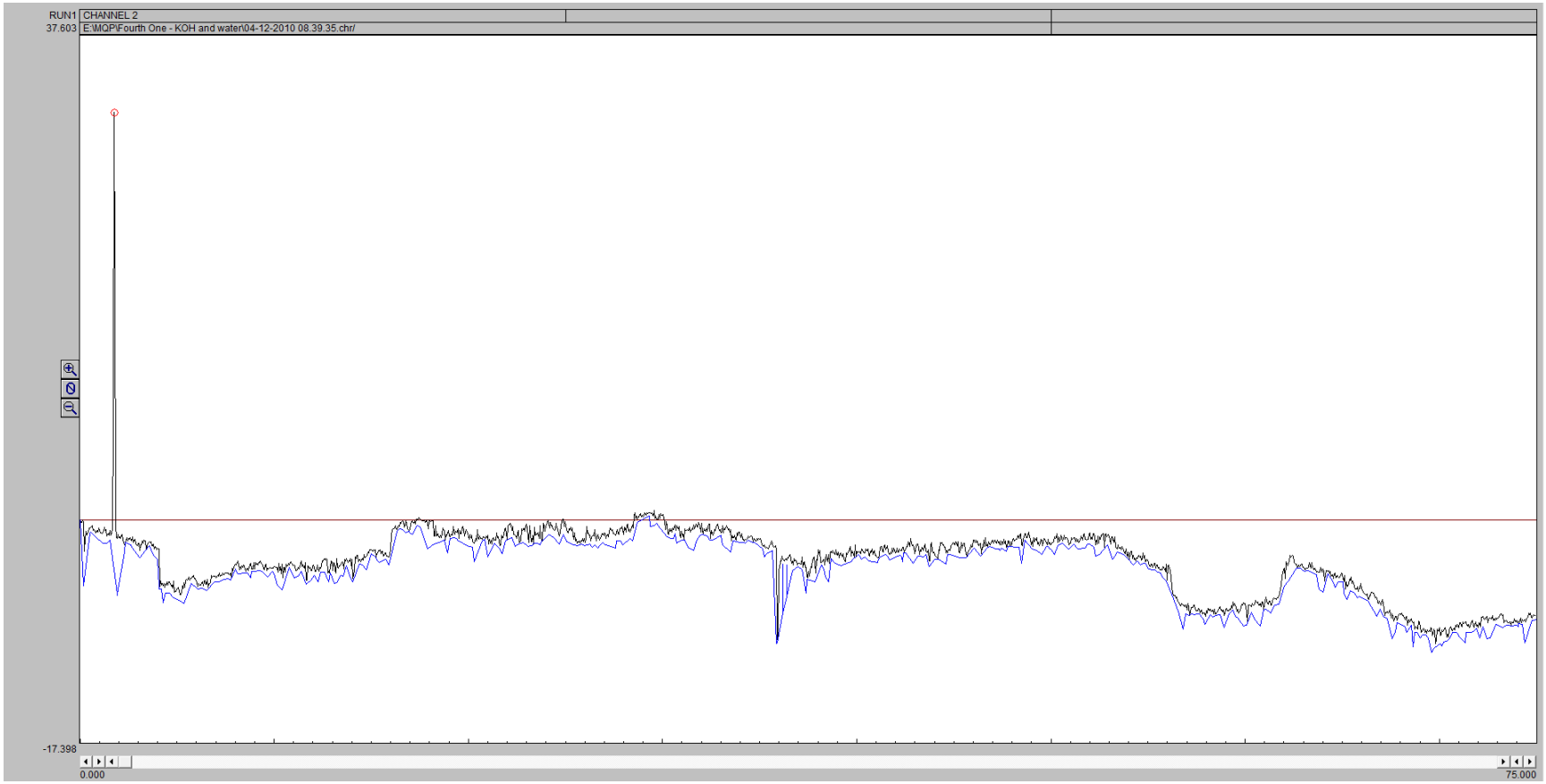

Gas Sample 535 Minutes

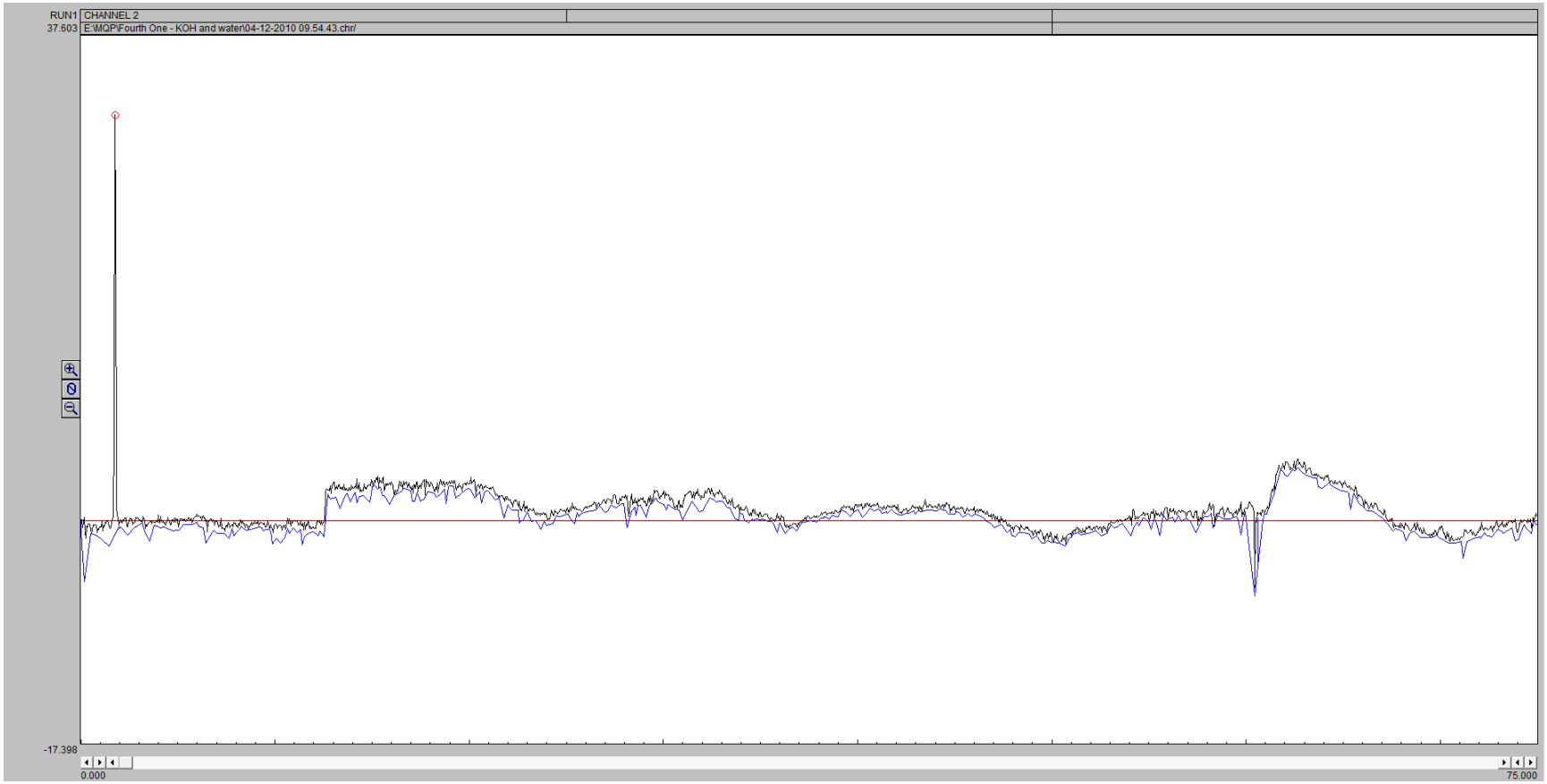

GC Liquids Data

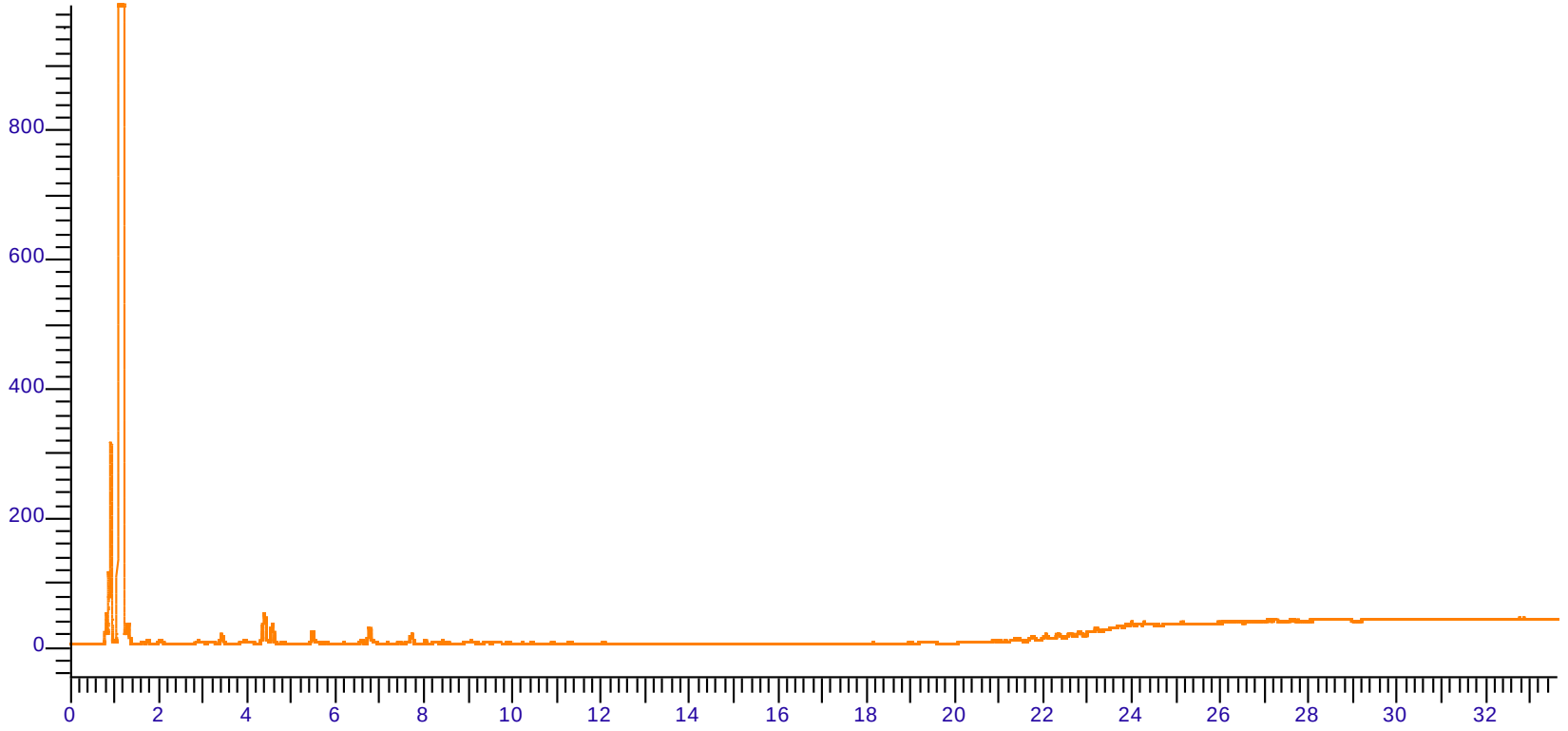

NMR Liquids Data

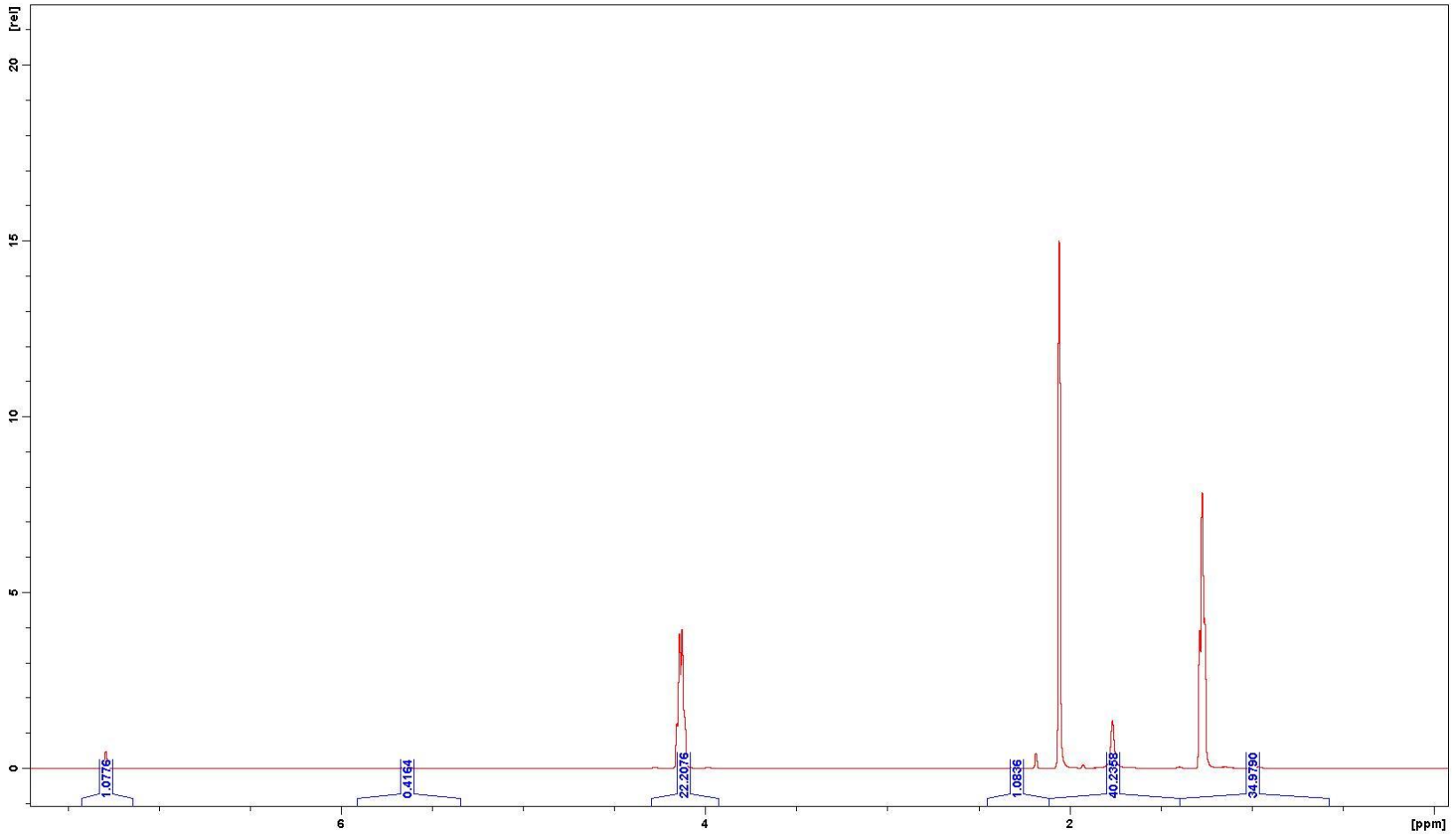

G9

Gas Concentrations over Time

	Mole %			
Time Stamp	H_2	CO	CH_4	CO_2
10	0.62	0	0	99.38
85	5.26	0	0	94.74
160	3.44	0	0	96.57
235	1.42	0	0	98.58

Gas Sample 10 Minutes

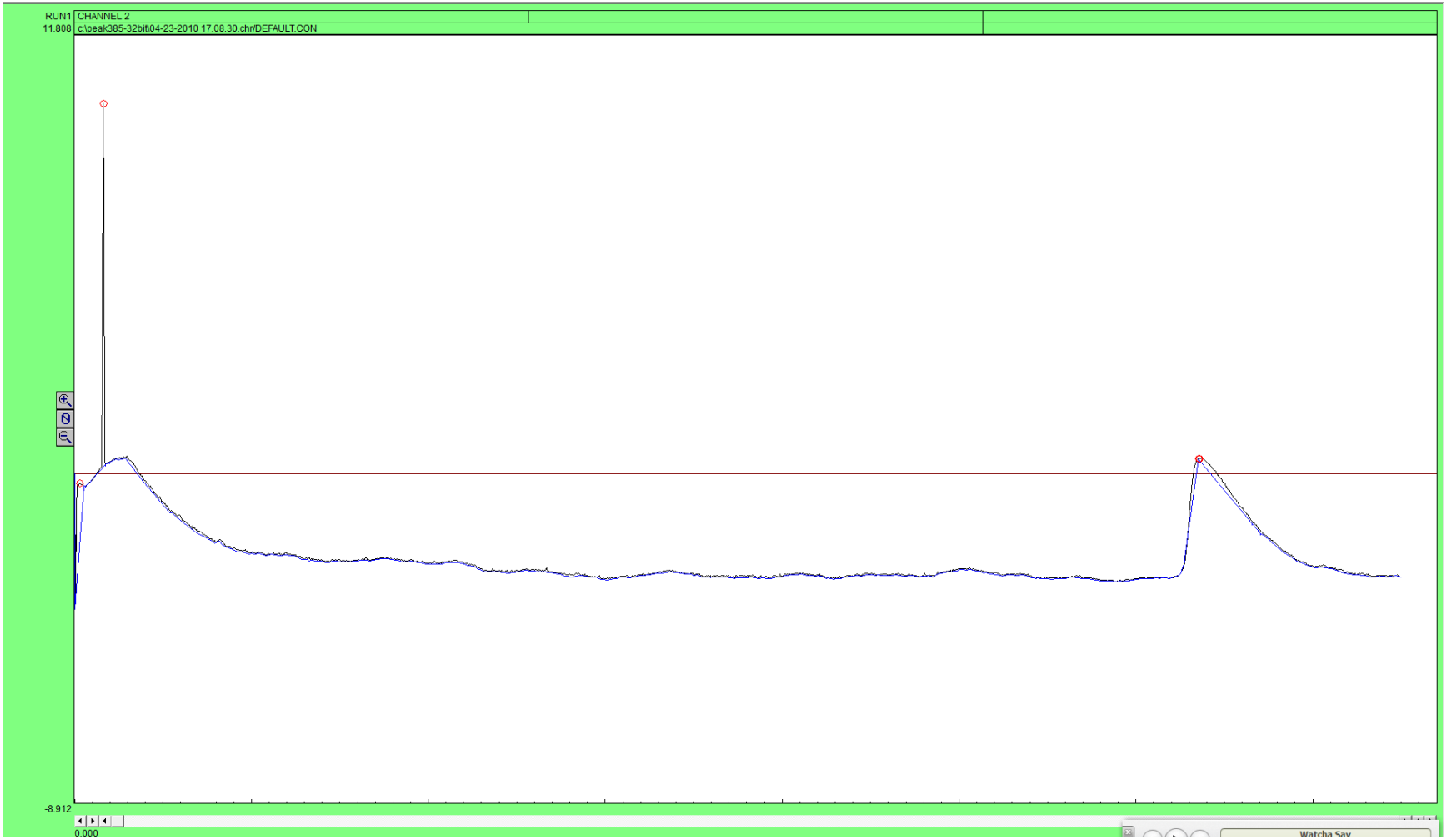

Gas Sample 85 Minutes

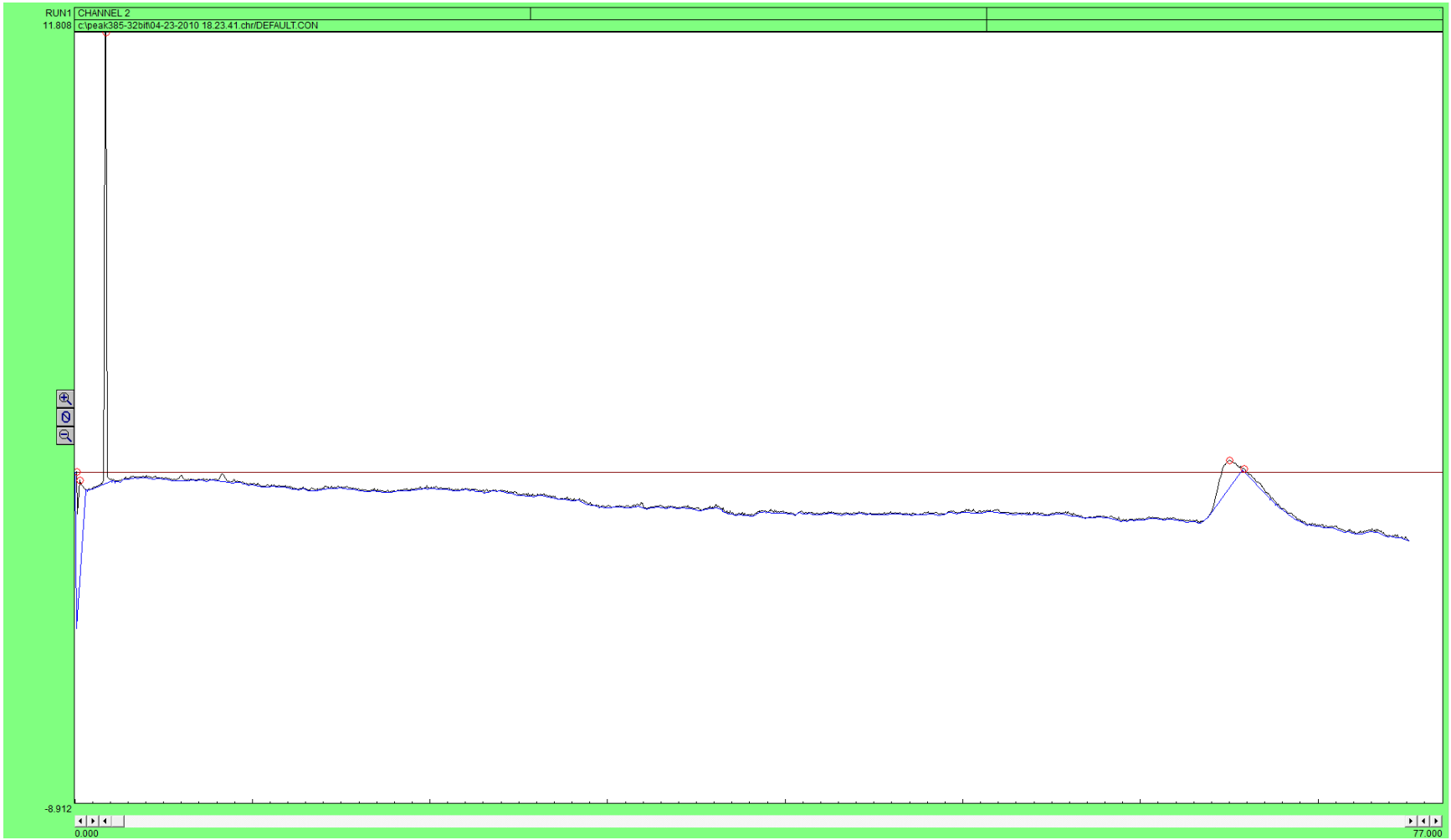

Gas Sample 160 Minutes

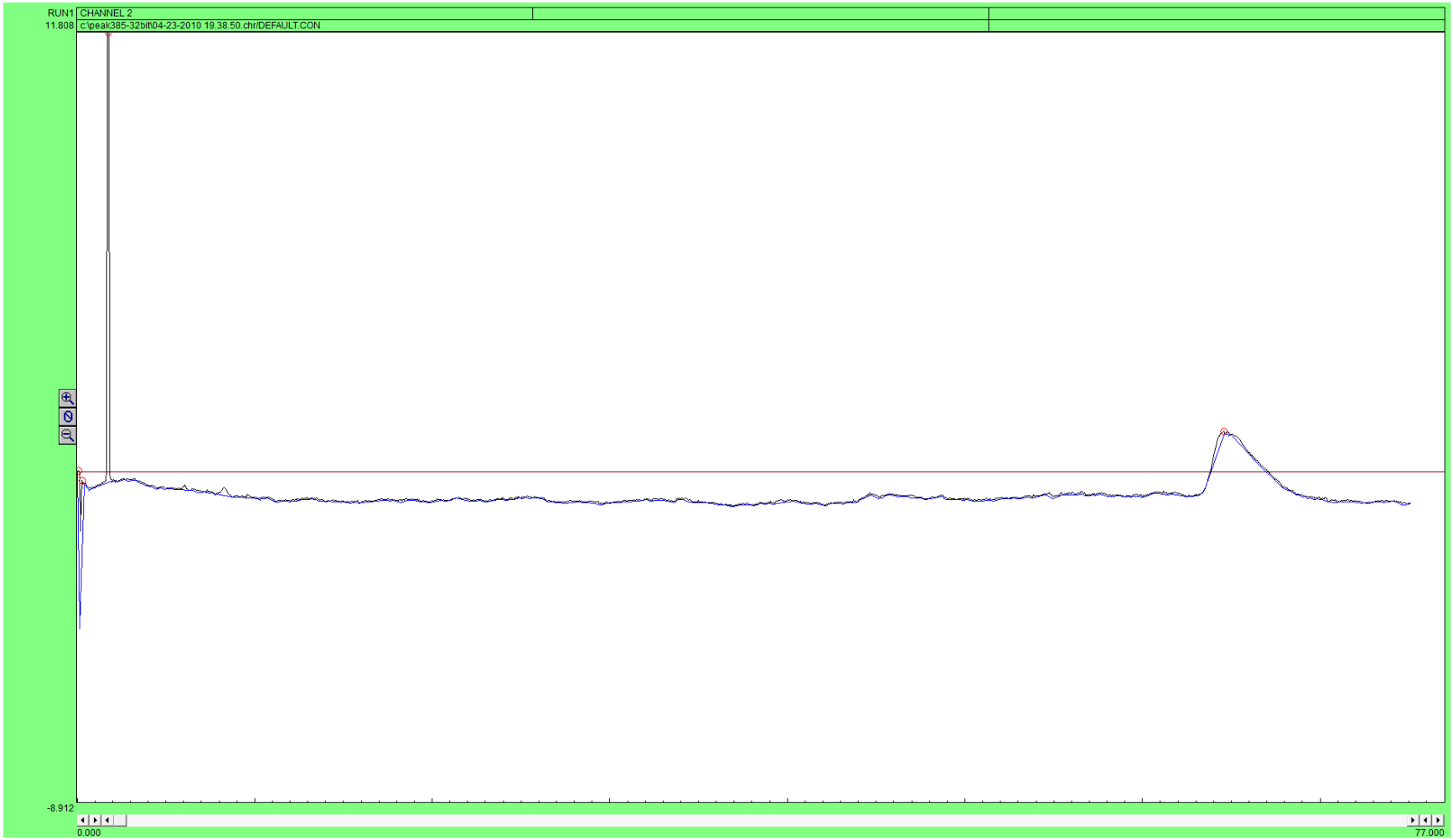

Gas Sample 235 Minutes

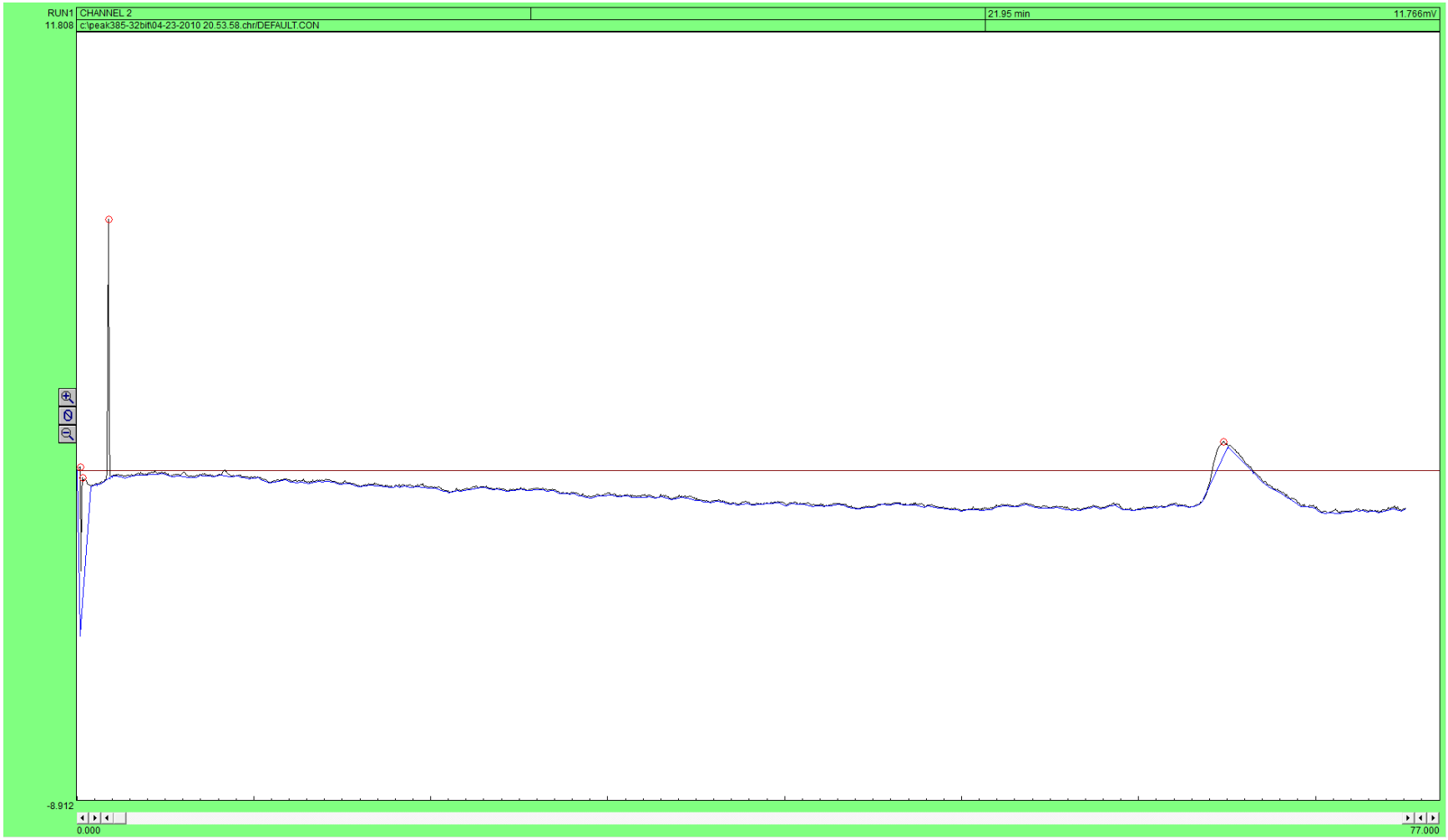

Gas Sample 310 Minutes

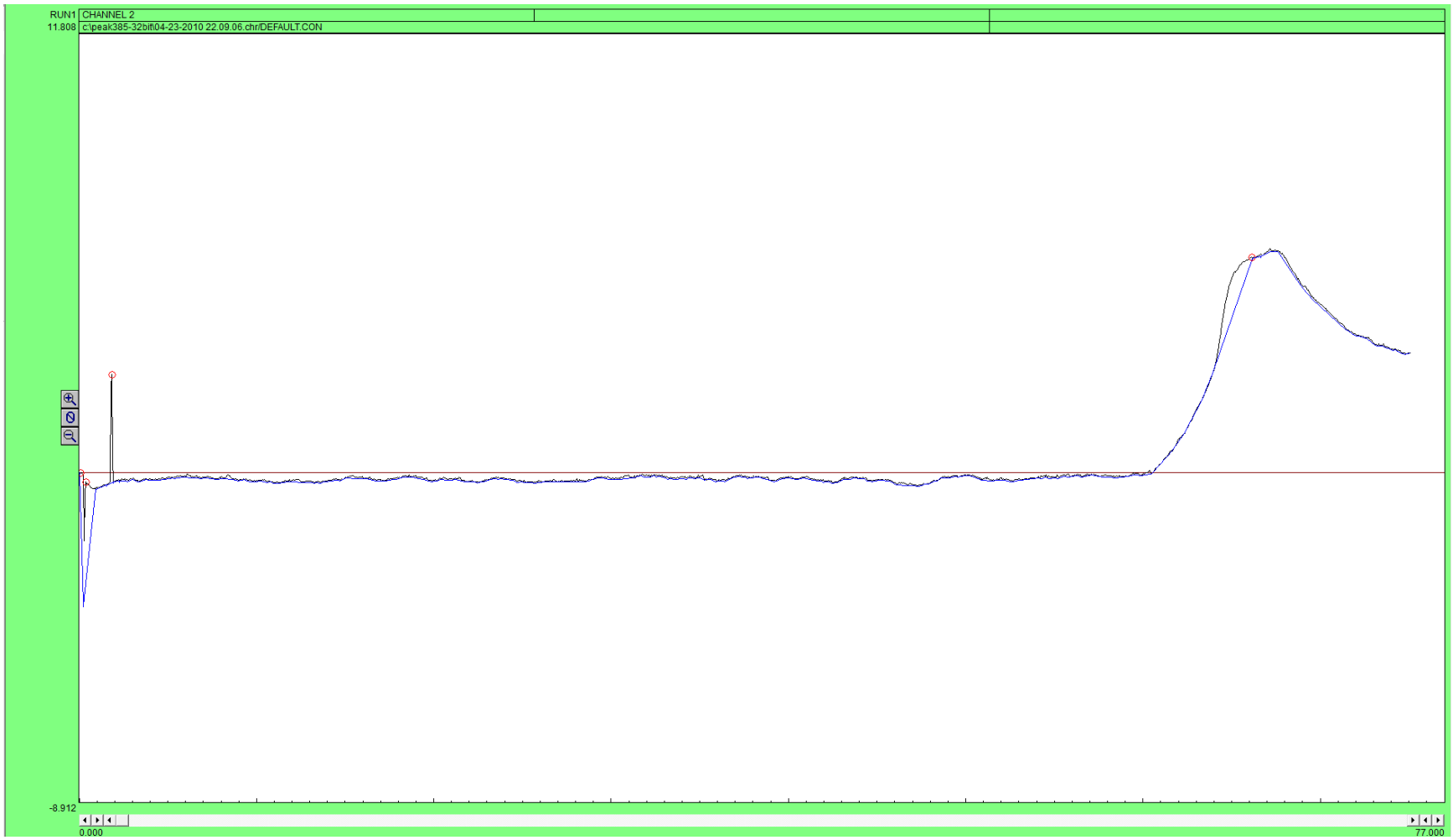

Gas Sample 385 Minutes

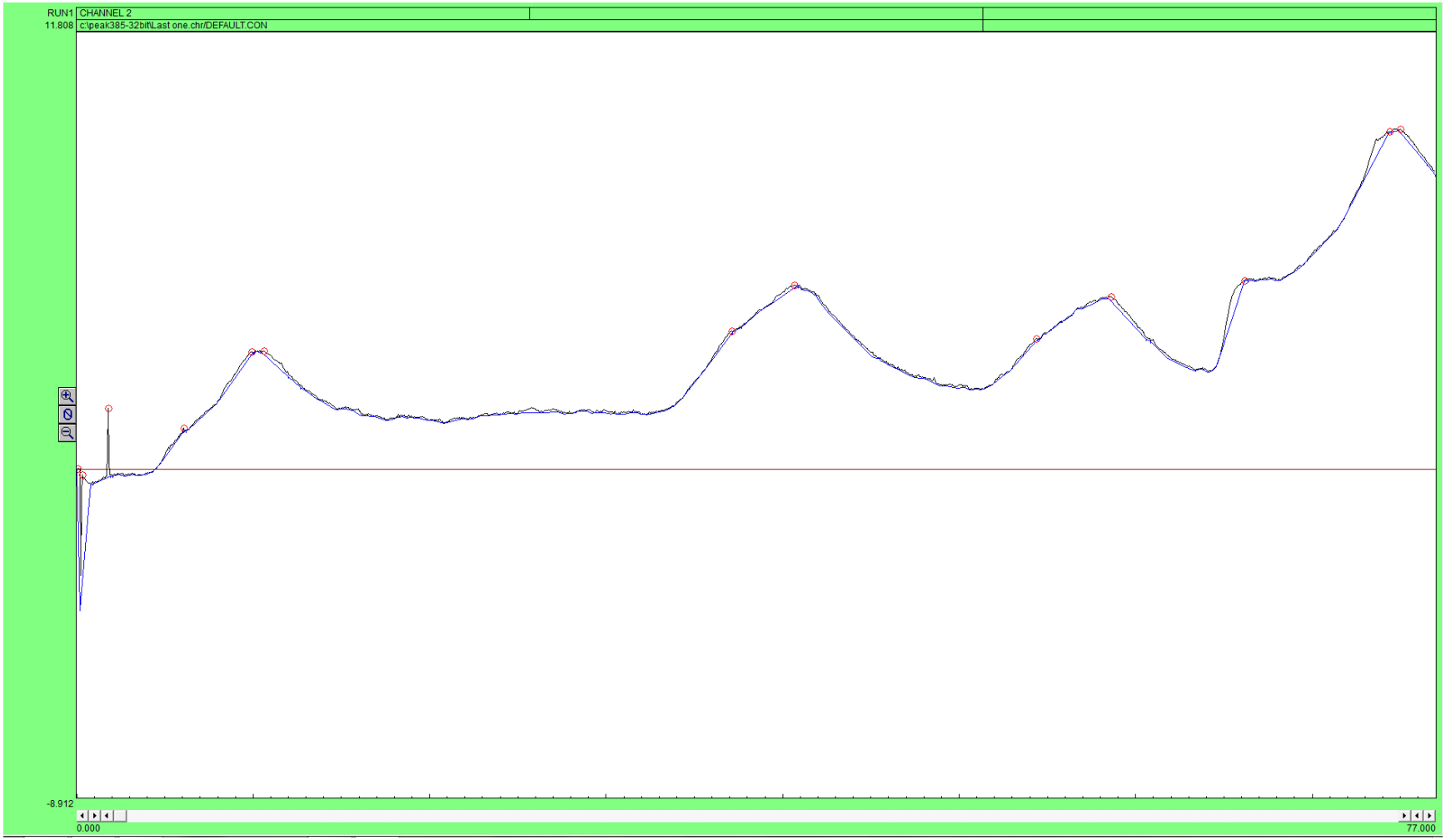

GC Liquids Data

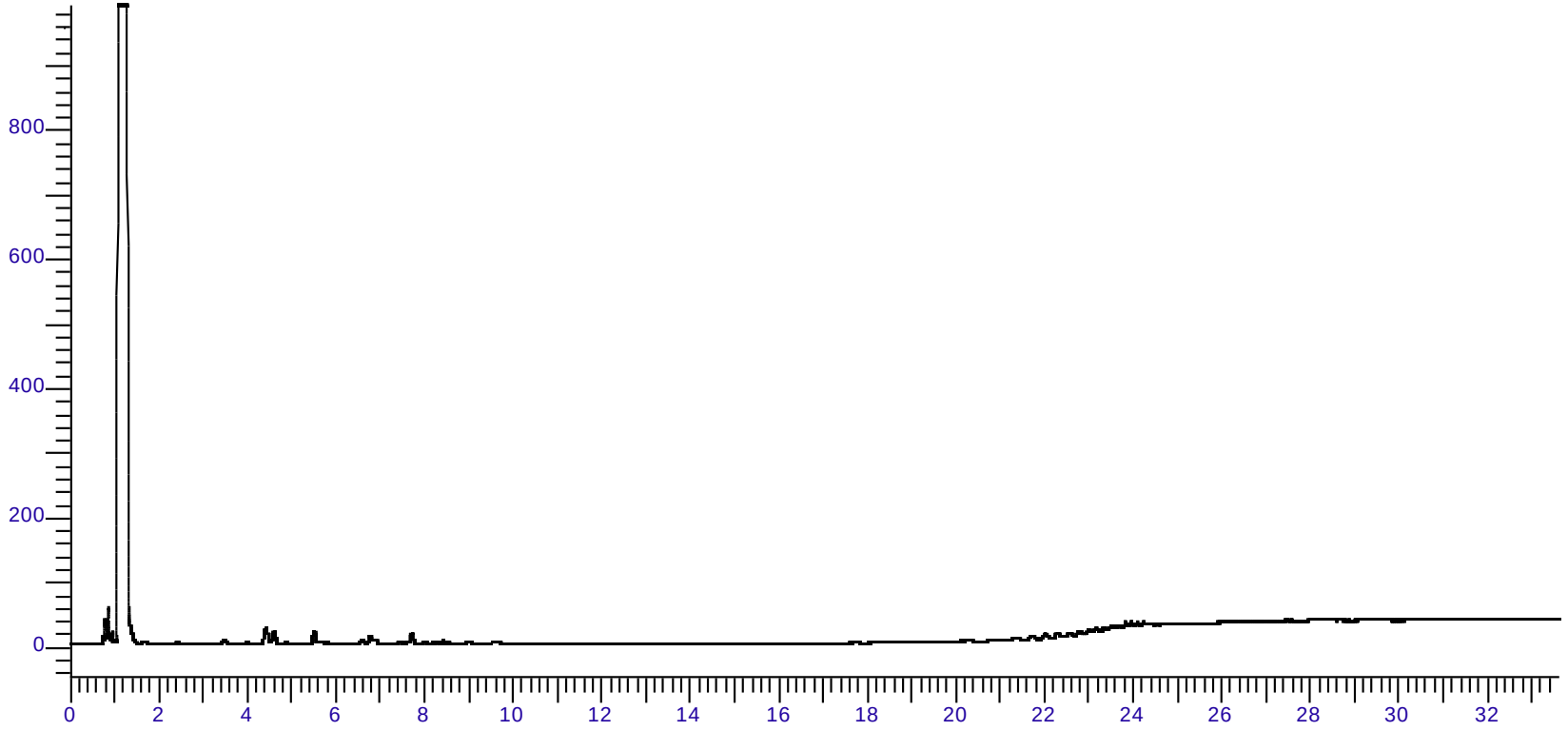

Appendix D Raw Data for Bench Top Hydrolysis / Transesterification

BT1 Vegetable Oil Hydrolysis

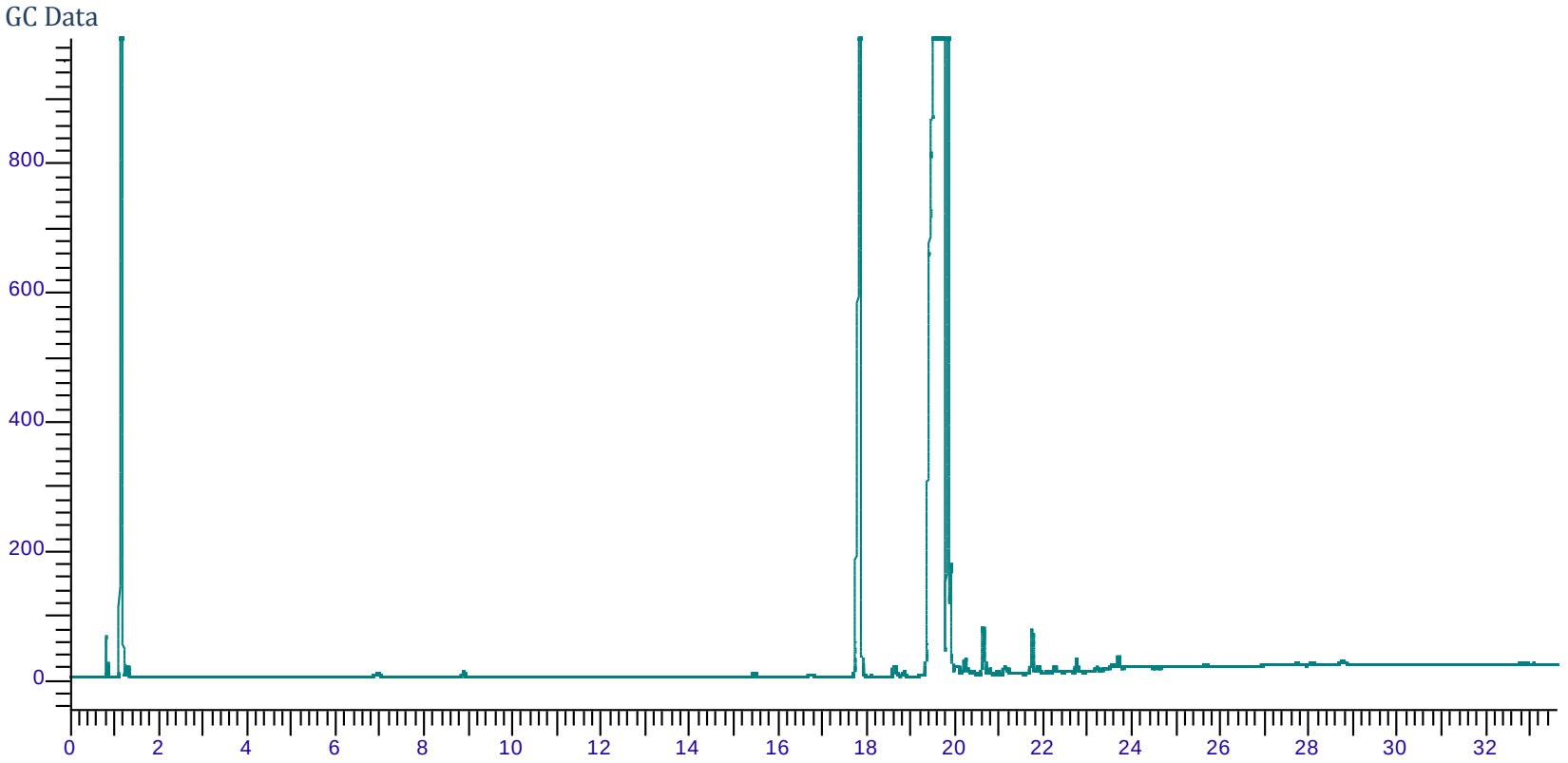

NMR Data

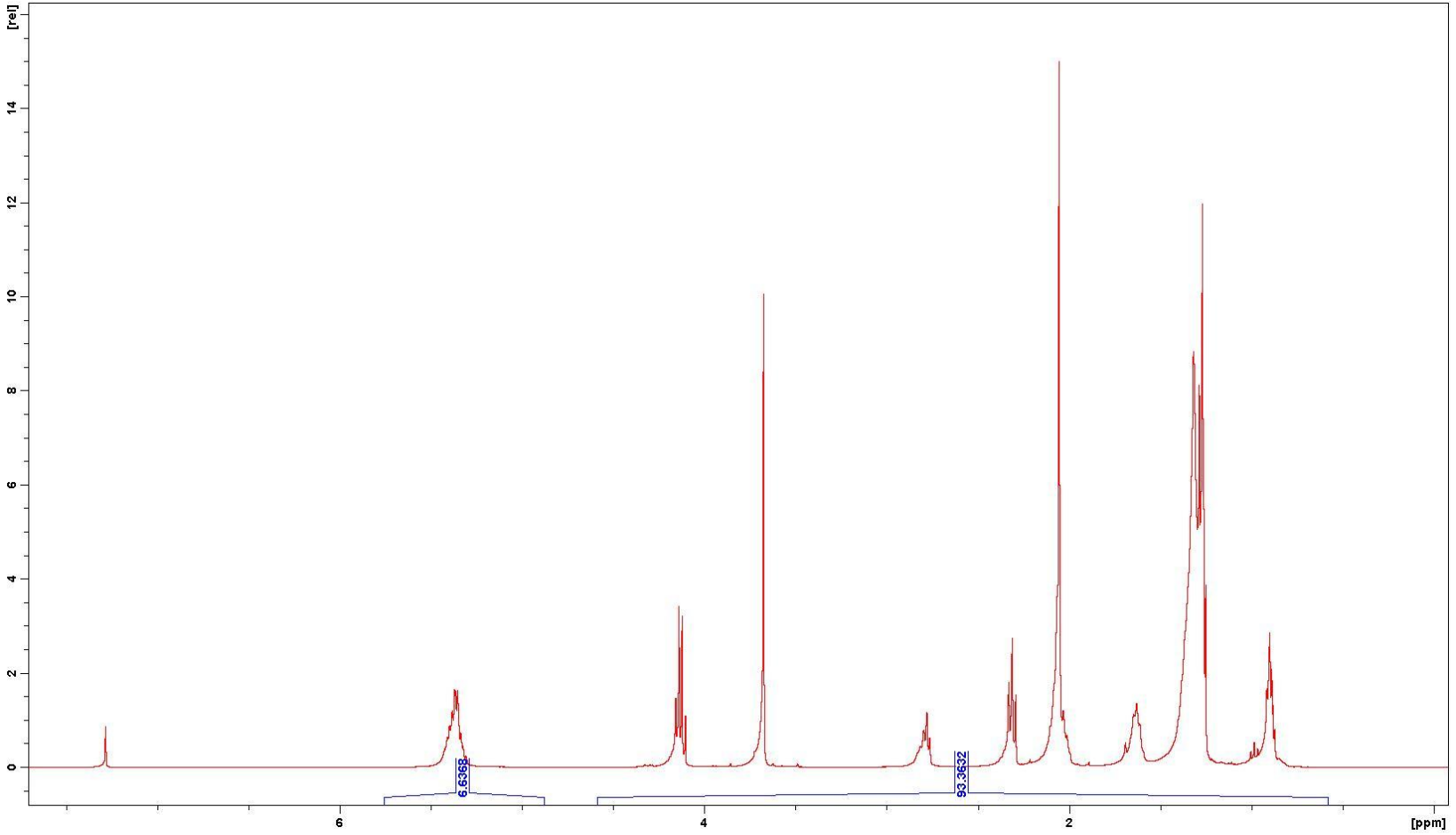

BT2 Vegetable Oil Transesterification

GC Data

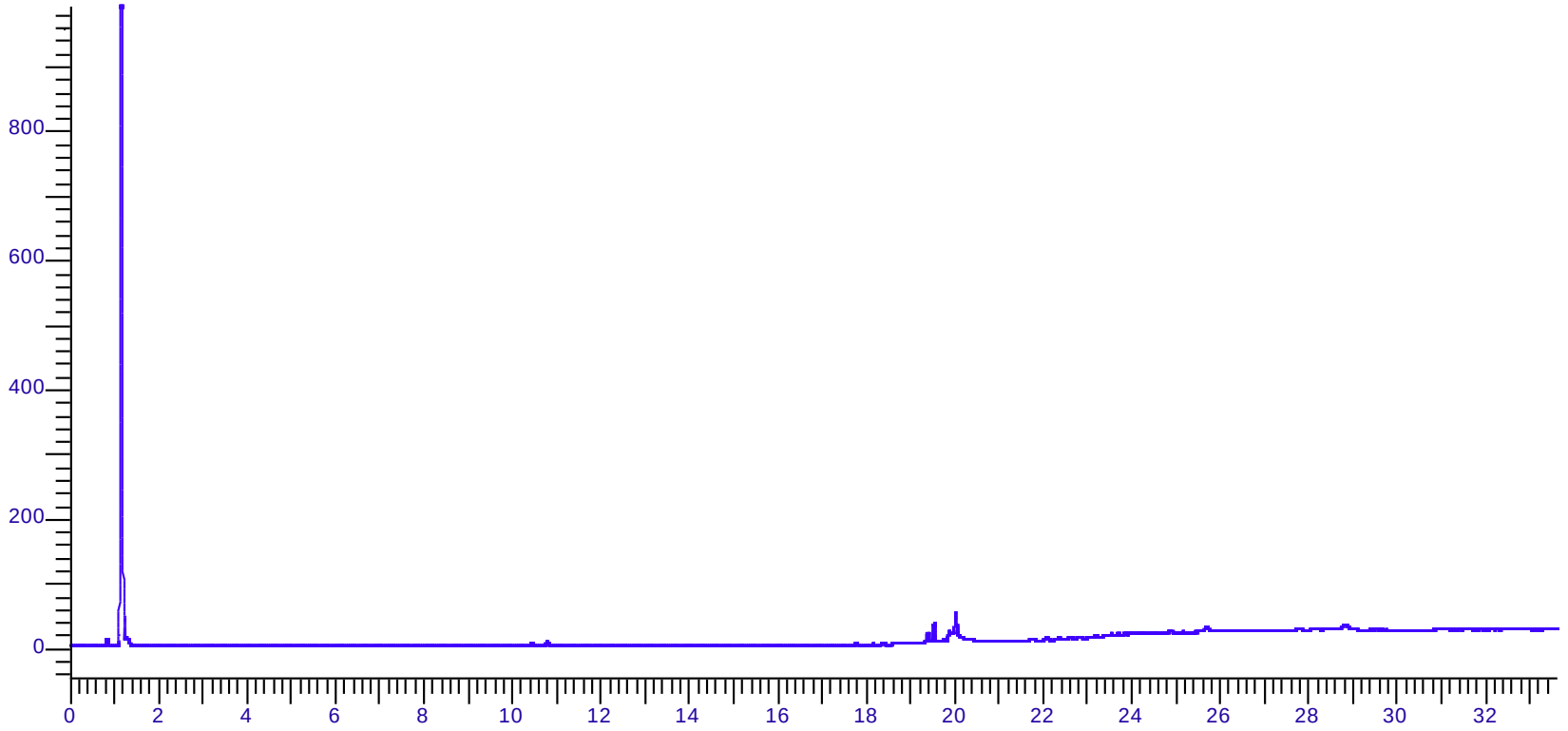

NMR Data

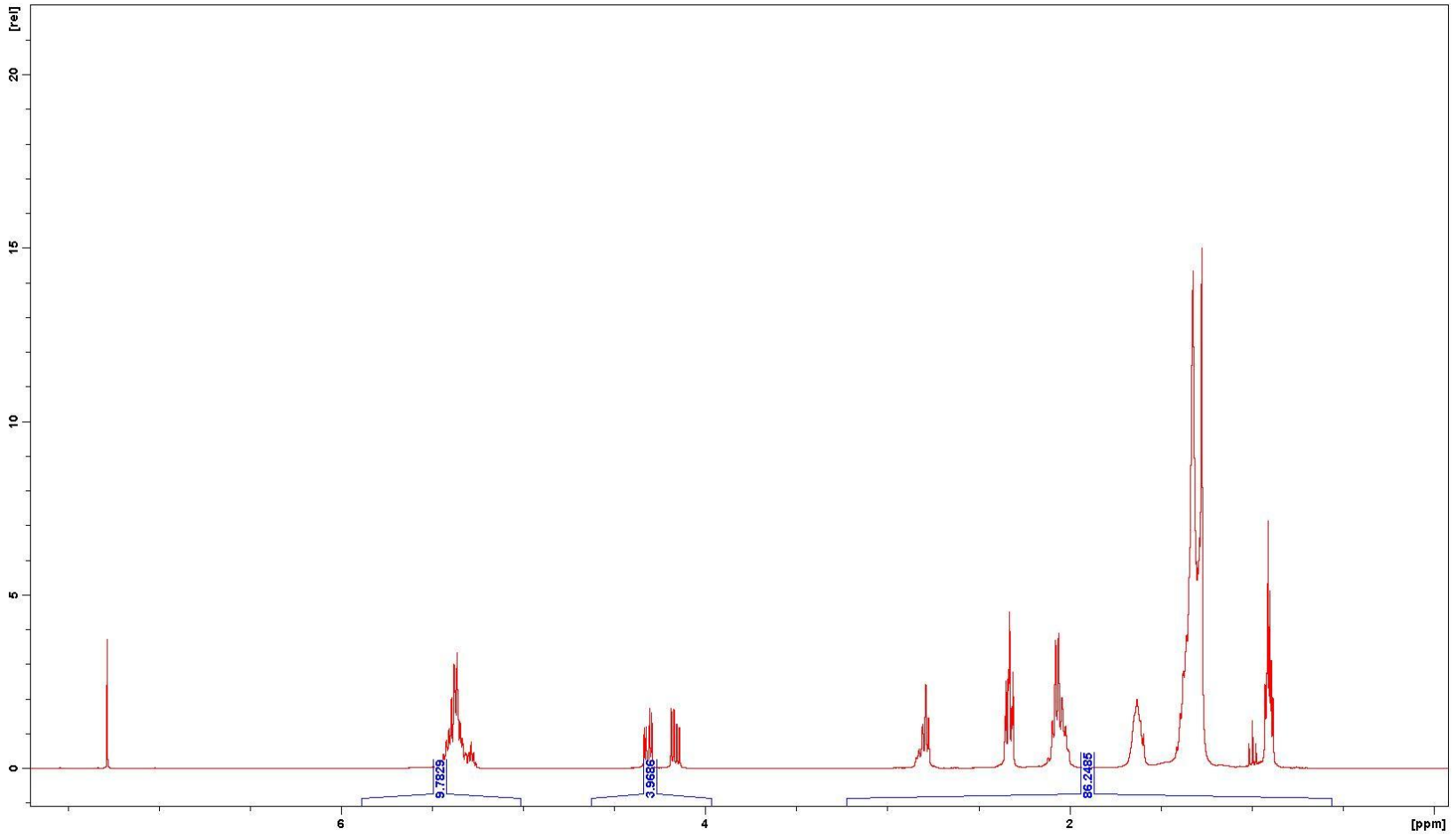

BT3 Tributyrin Hydrolysis

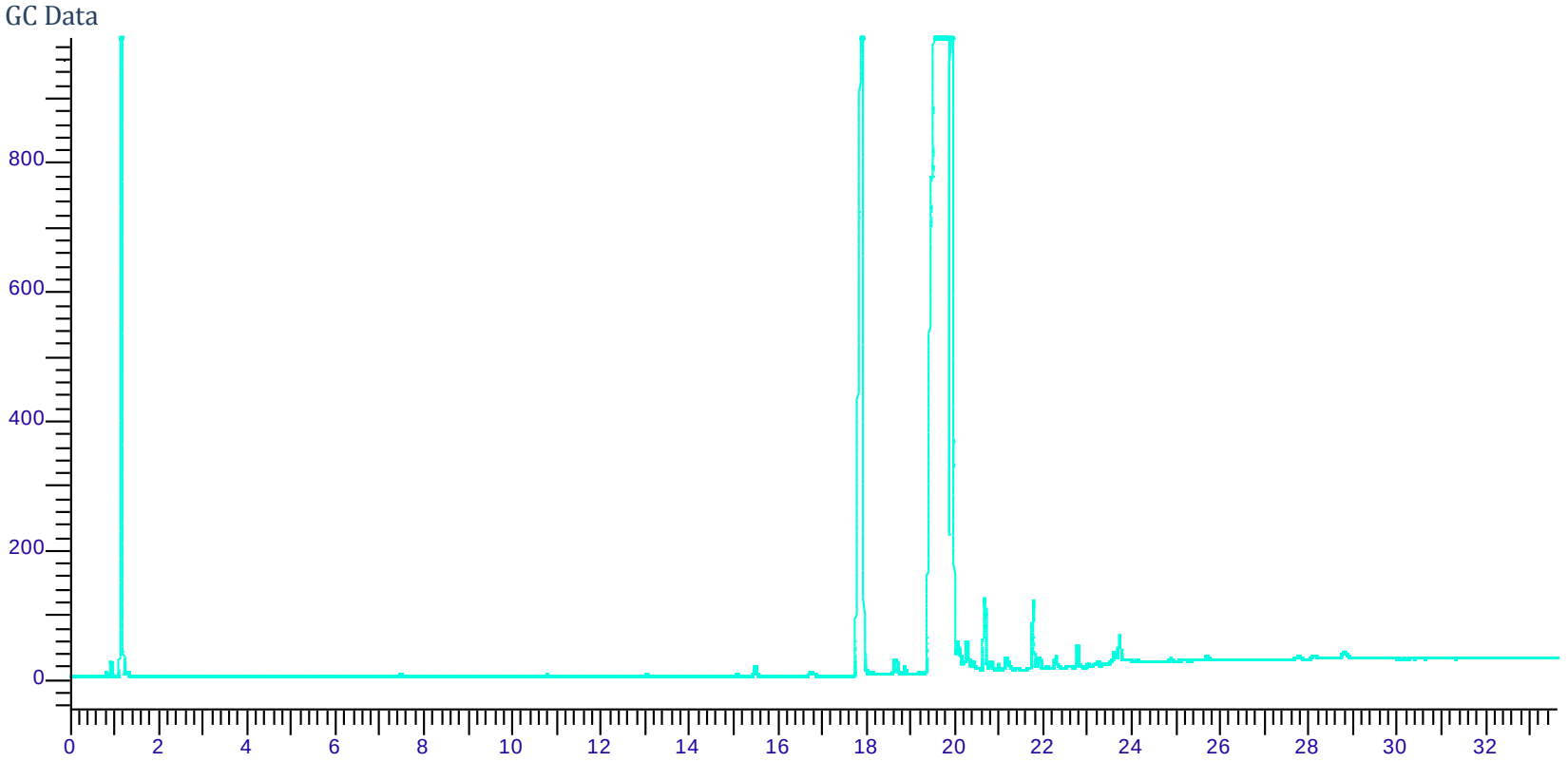

NMR Data

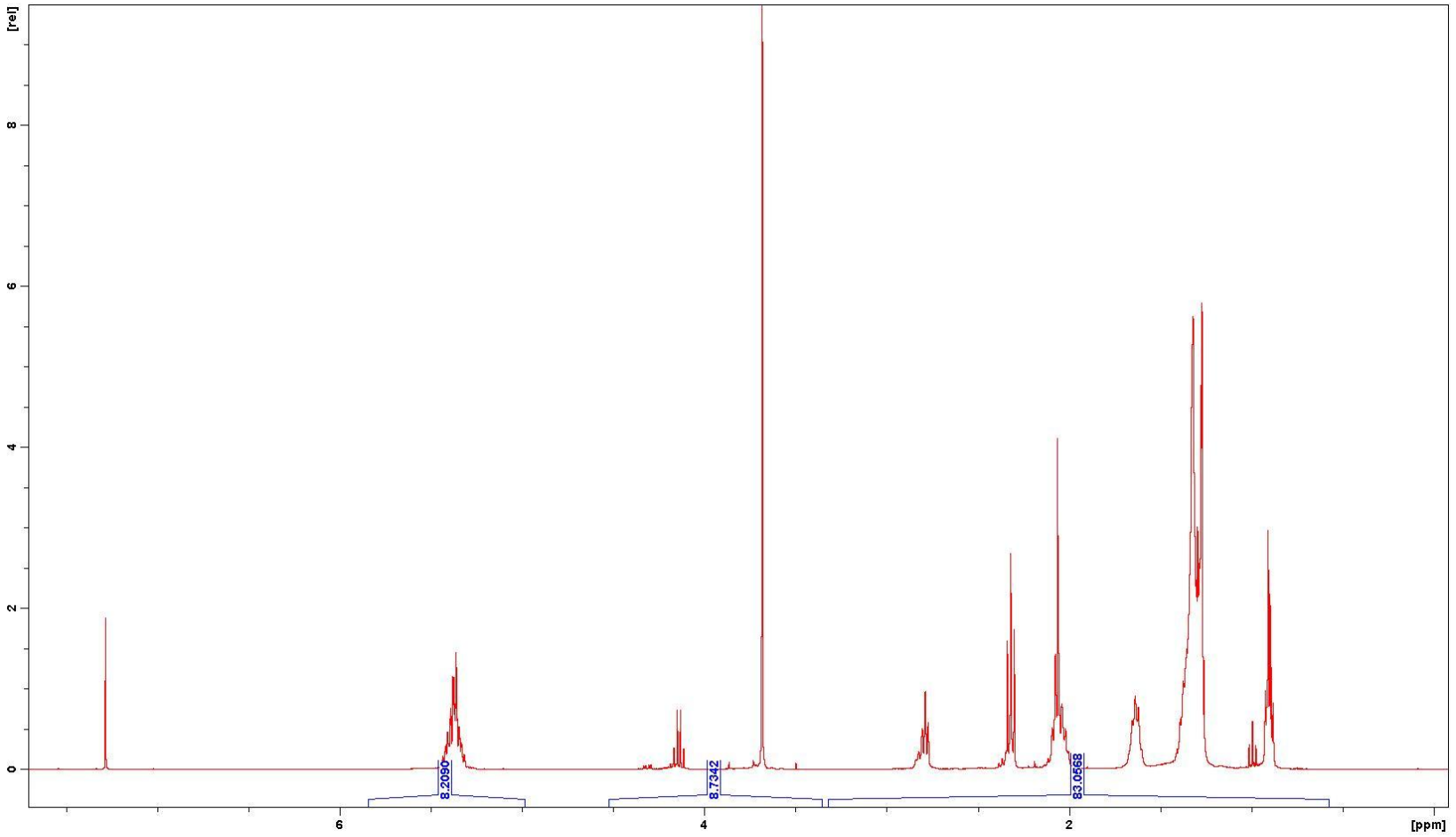

BT4 Tributyrin Transesterification

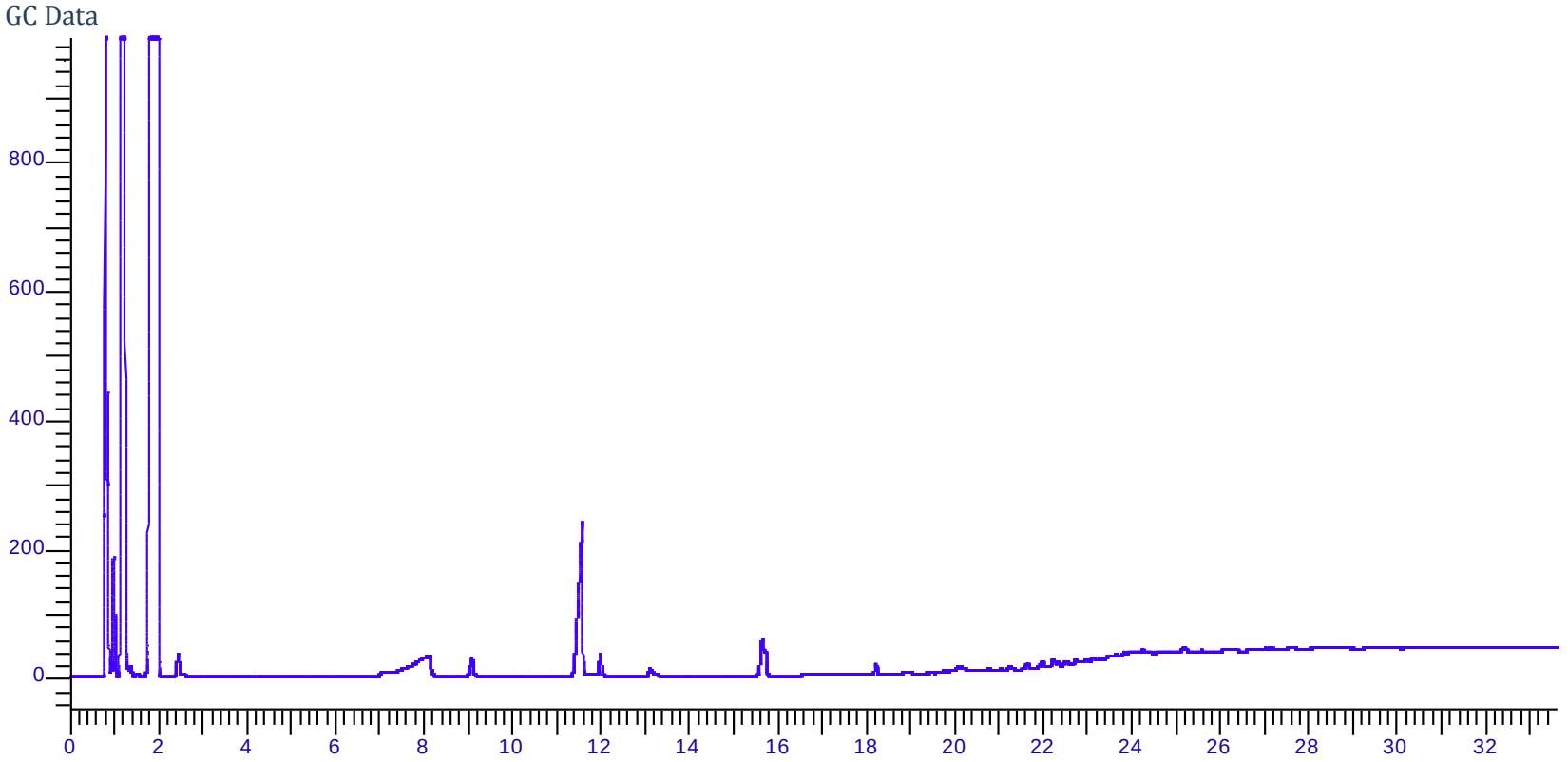

NMR Data

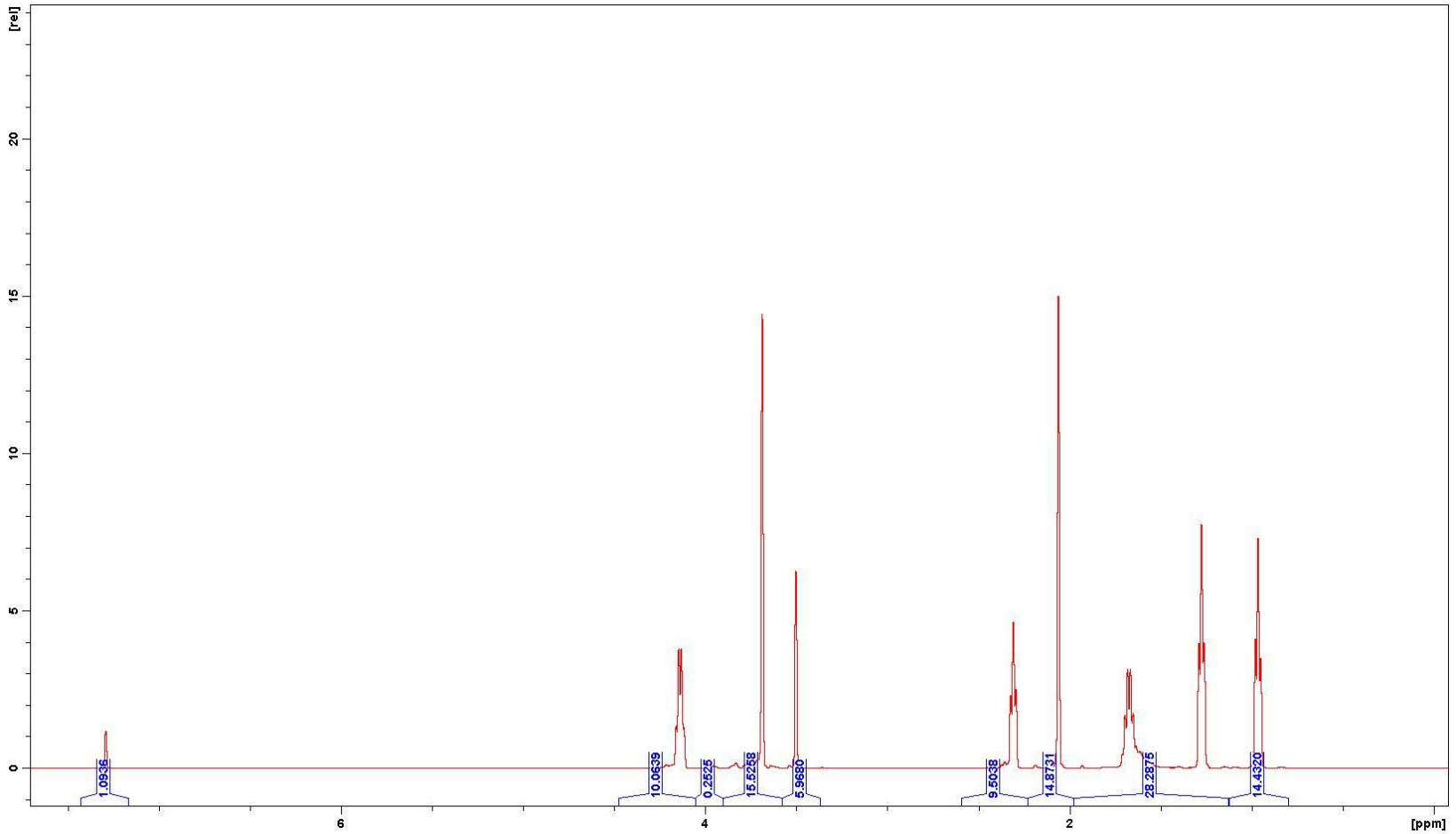
[rel]
20
15
10
5
0
1.0936
10.0639
0.2525
15.5258
5.9680
9.5038
14.8731
28.2875
14.4320
6
4
2
[ppm]

Appendix E Raw Data for Liquid Analysis – Hydrolysis / Transesterification

HT1 Vegetable Oil Hydrolysis

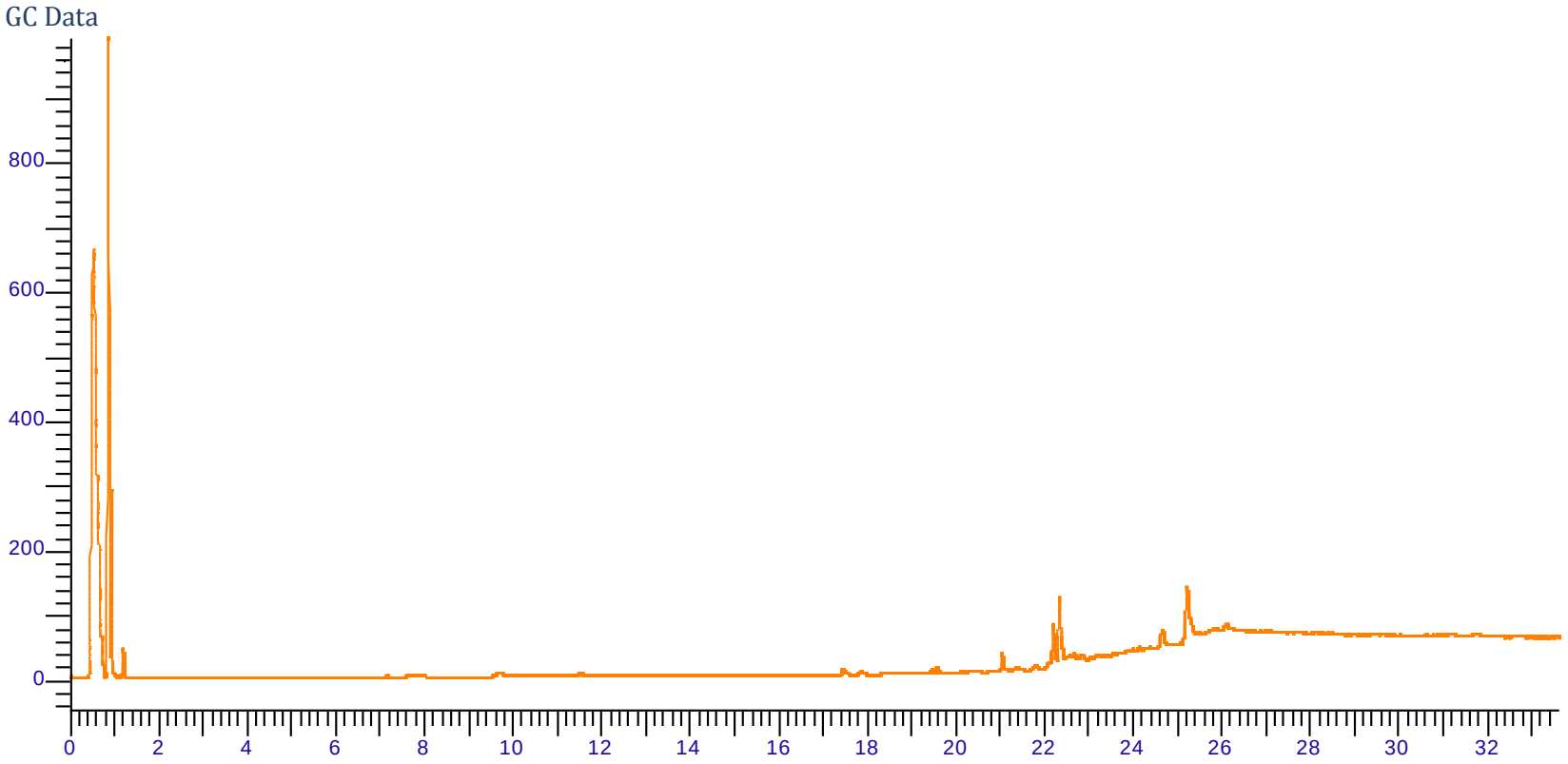

NMR Data

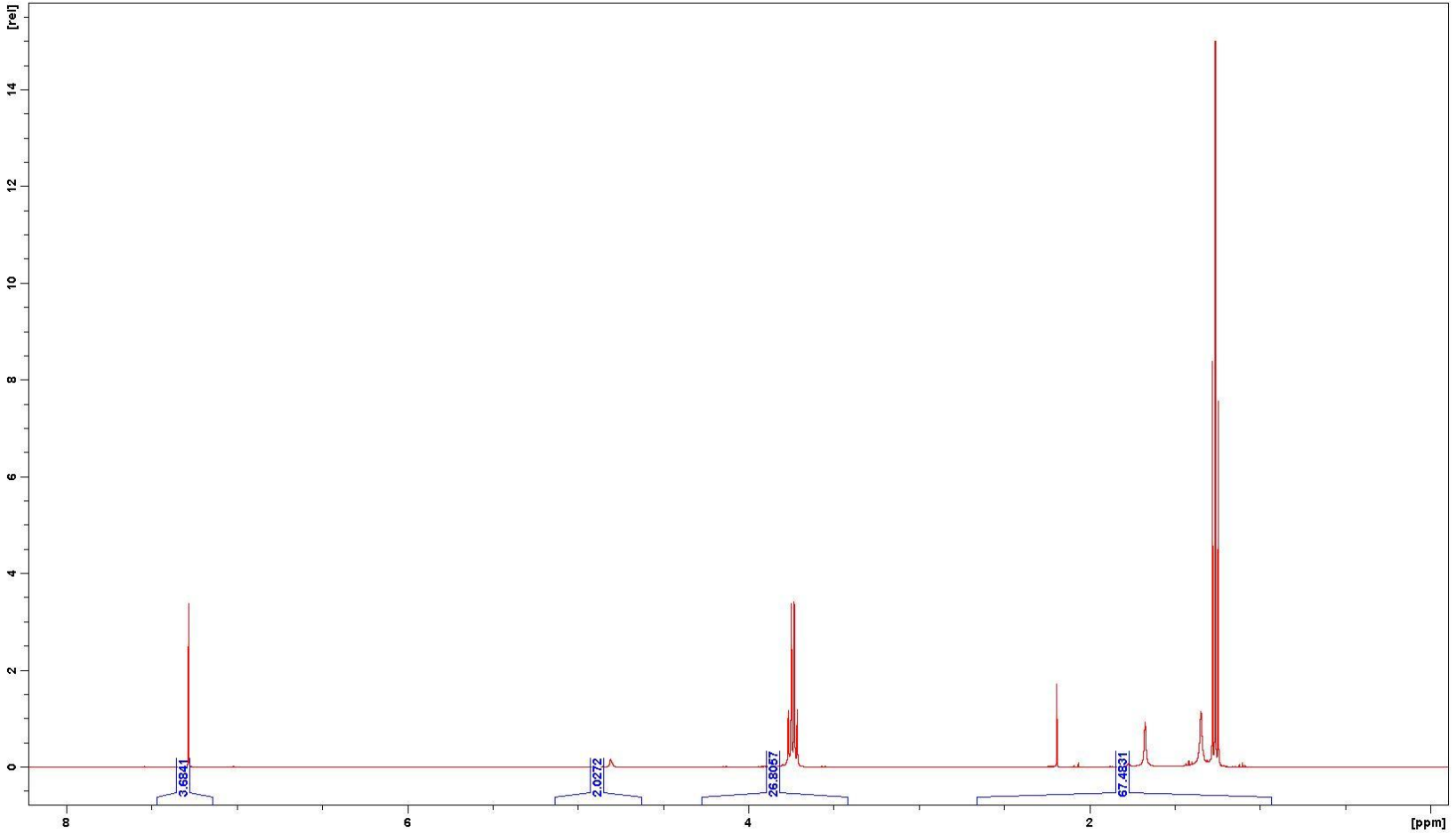

HT2 Vegetable Oil Hydrolysis

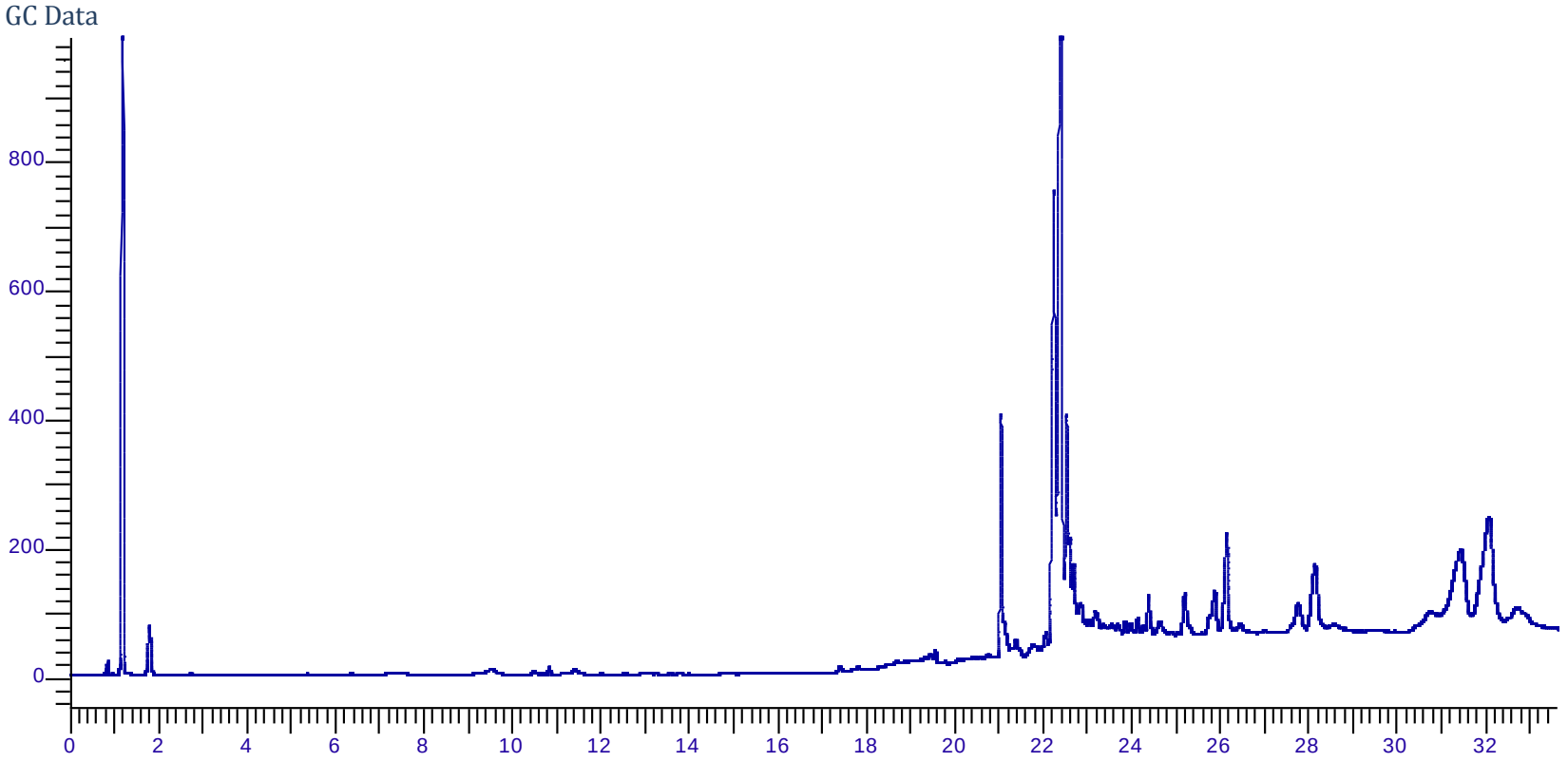

NMR Data

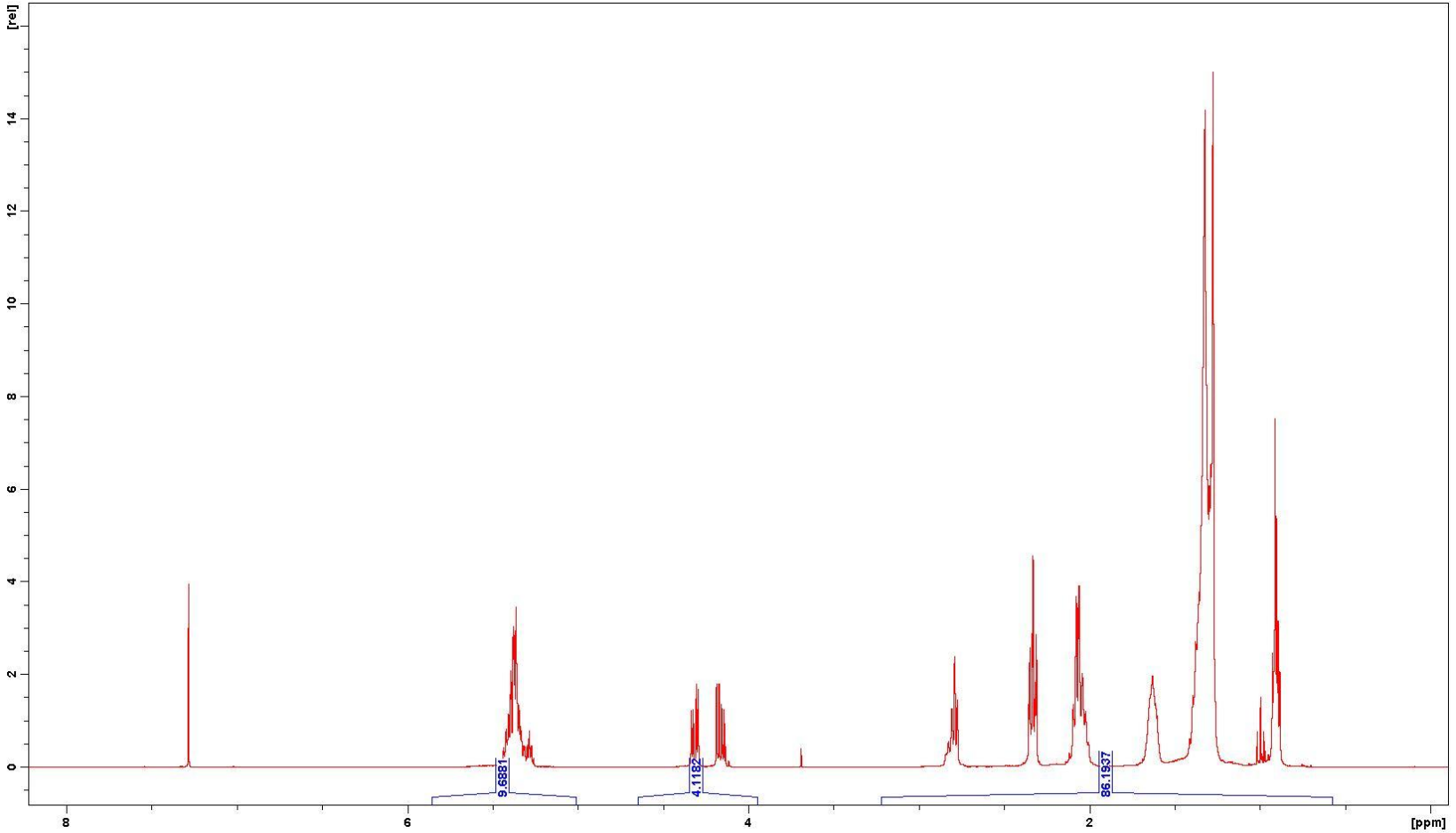

HT3 Vegetable Oil Hydrolysis

GC Data

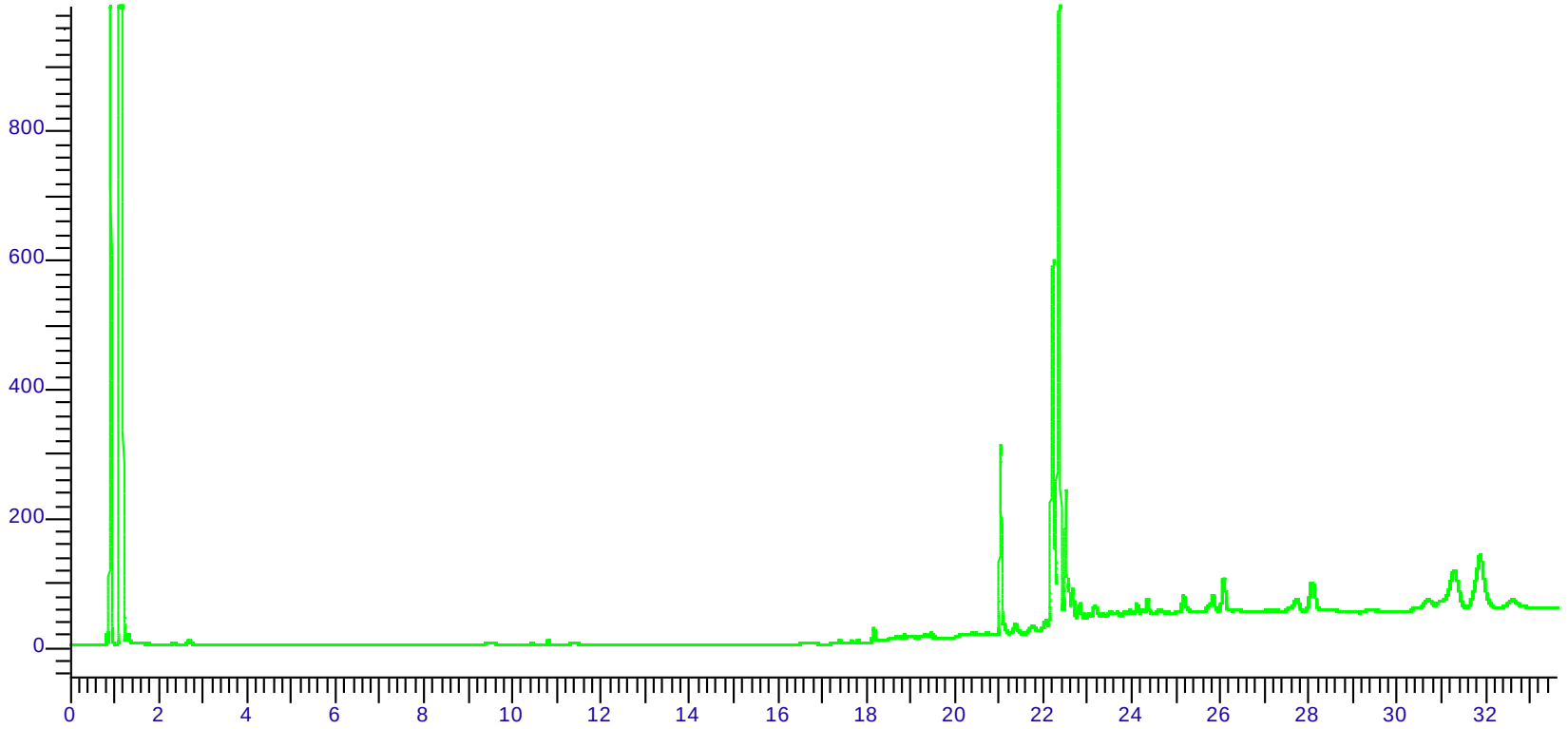

NMR Data

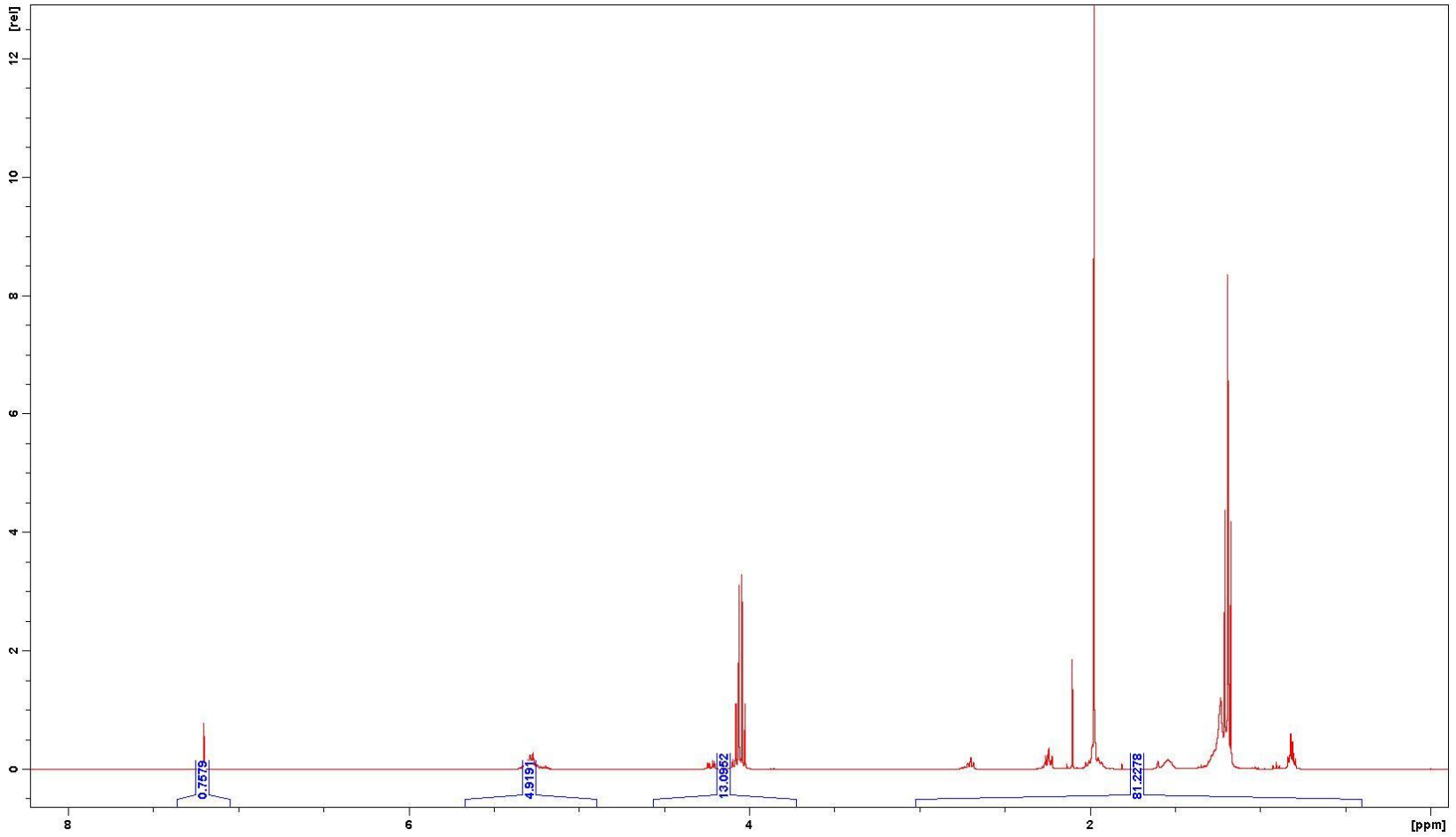

HT4 Vegetable Oil Hydrolysis

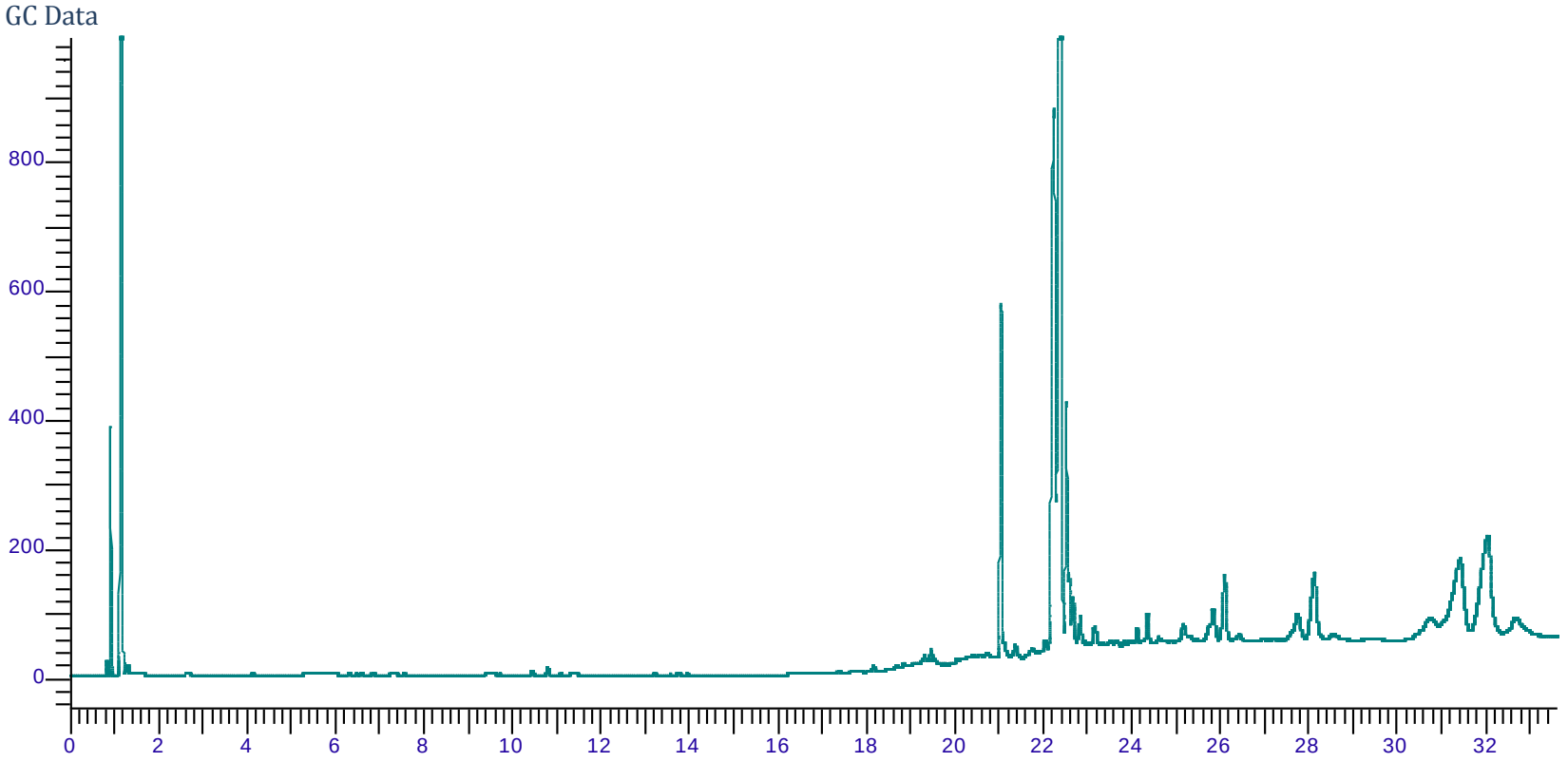

NMR Data

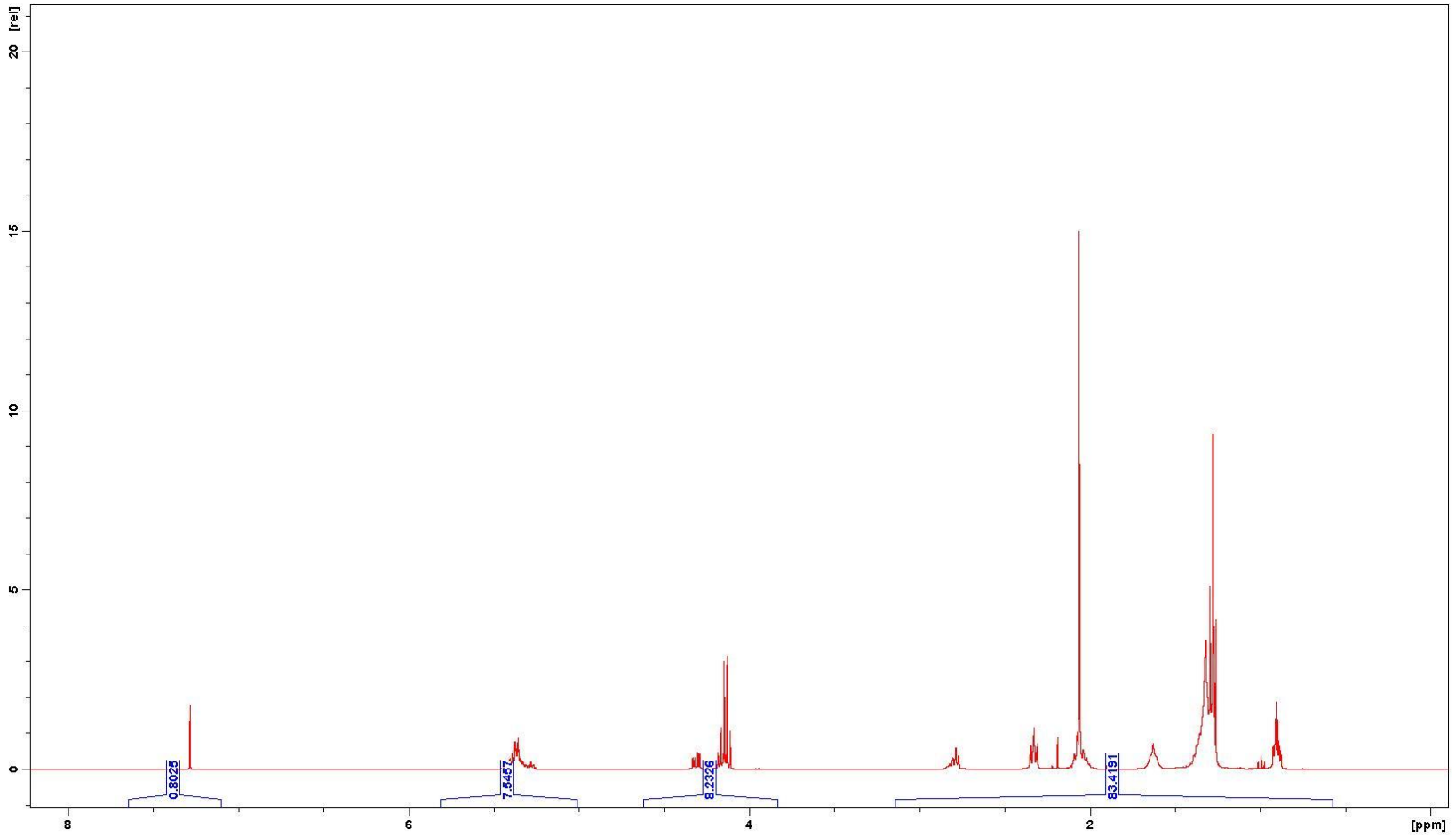

HT5 Tributyrin Hydrolysis

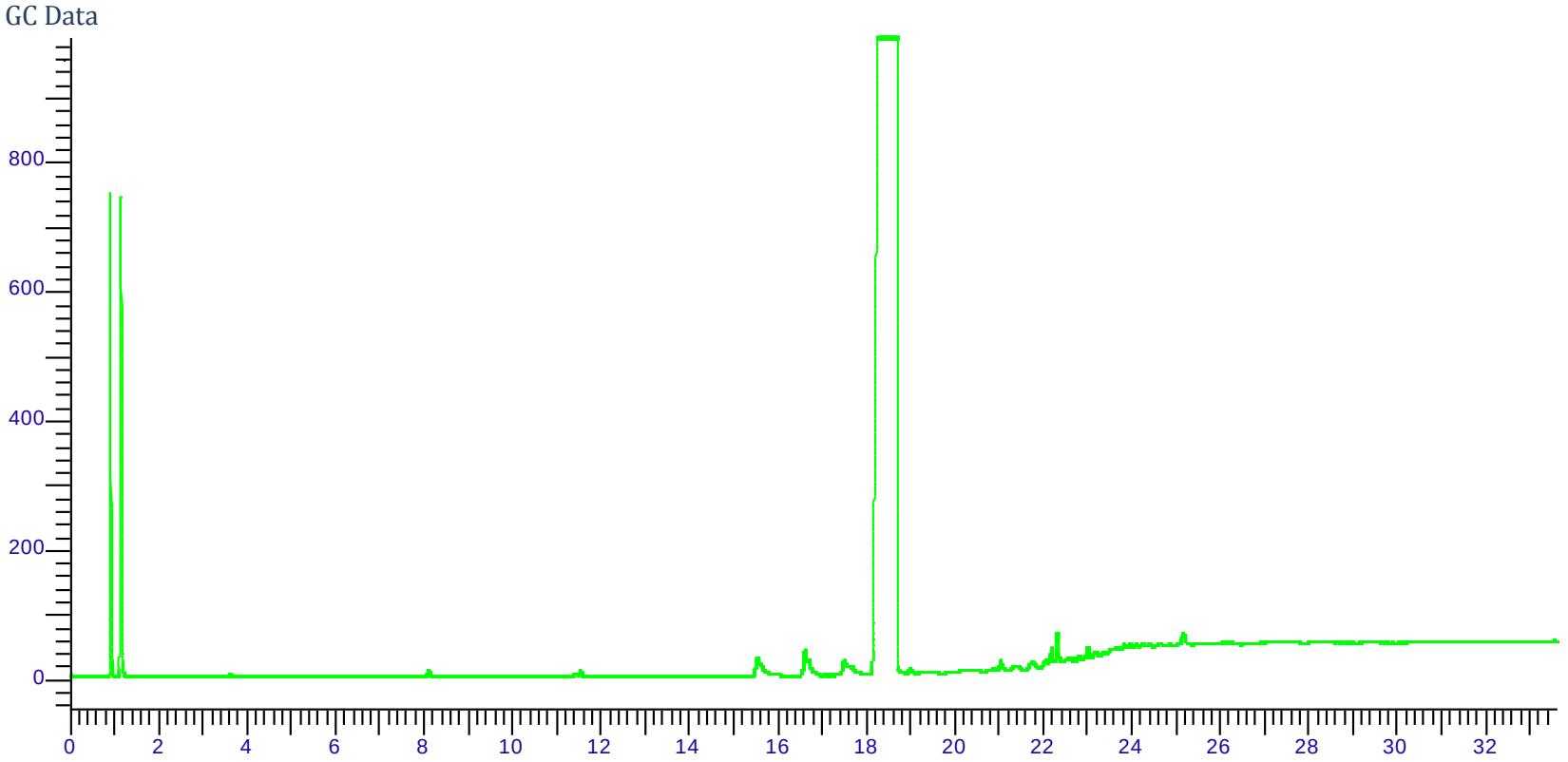

NMR Data

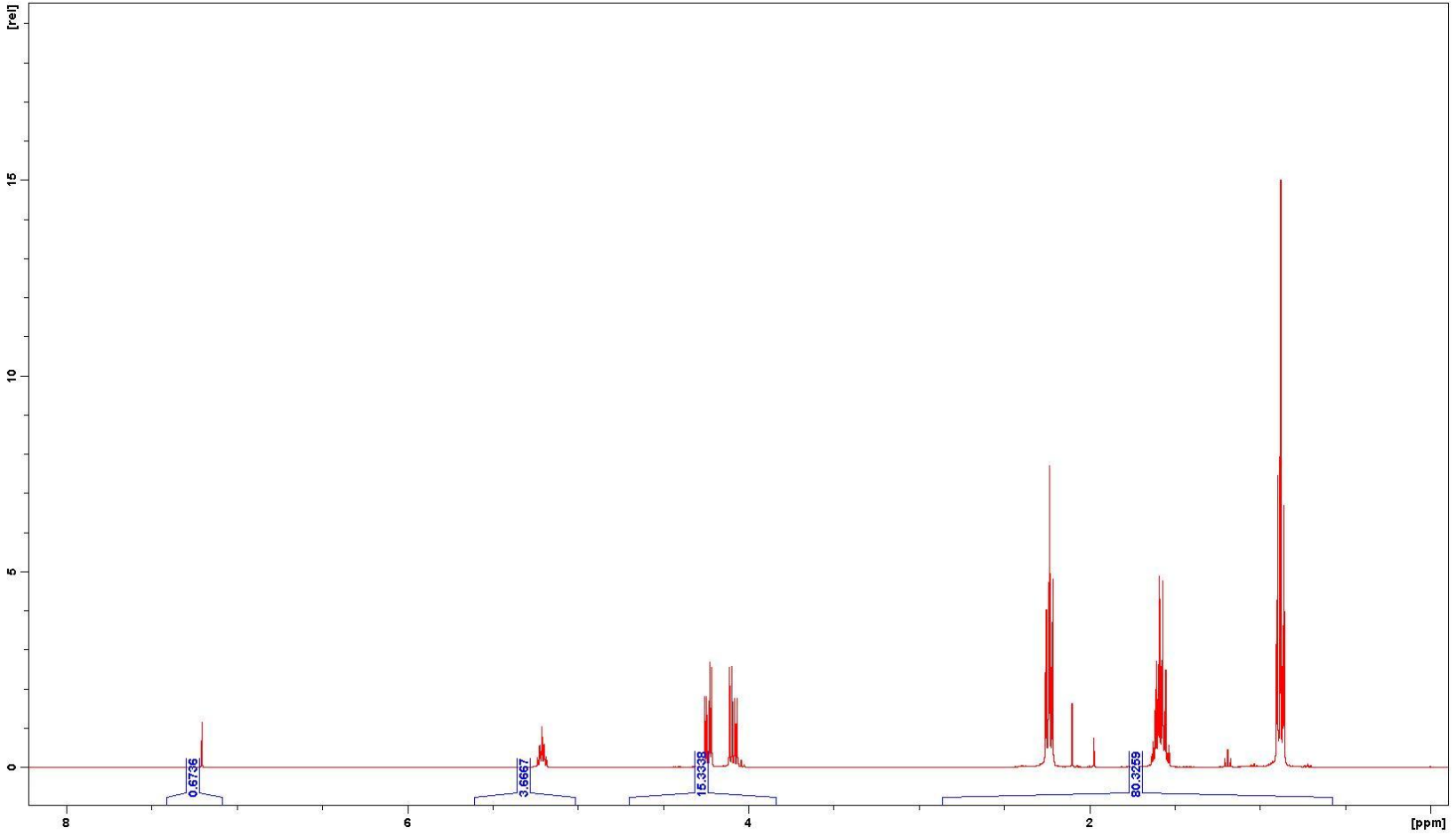

HT6 Tributyrin Hydrolysis

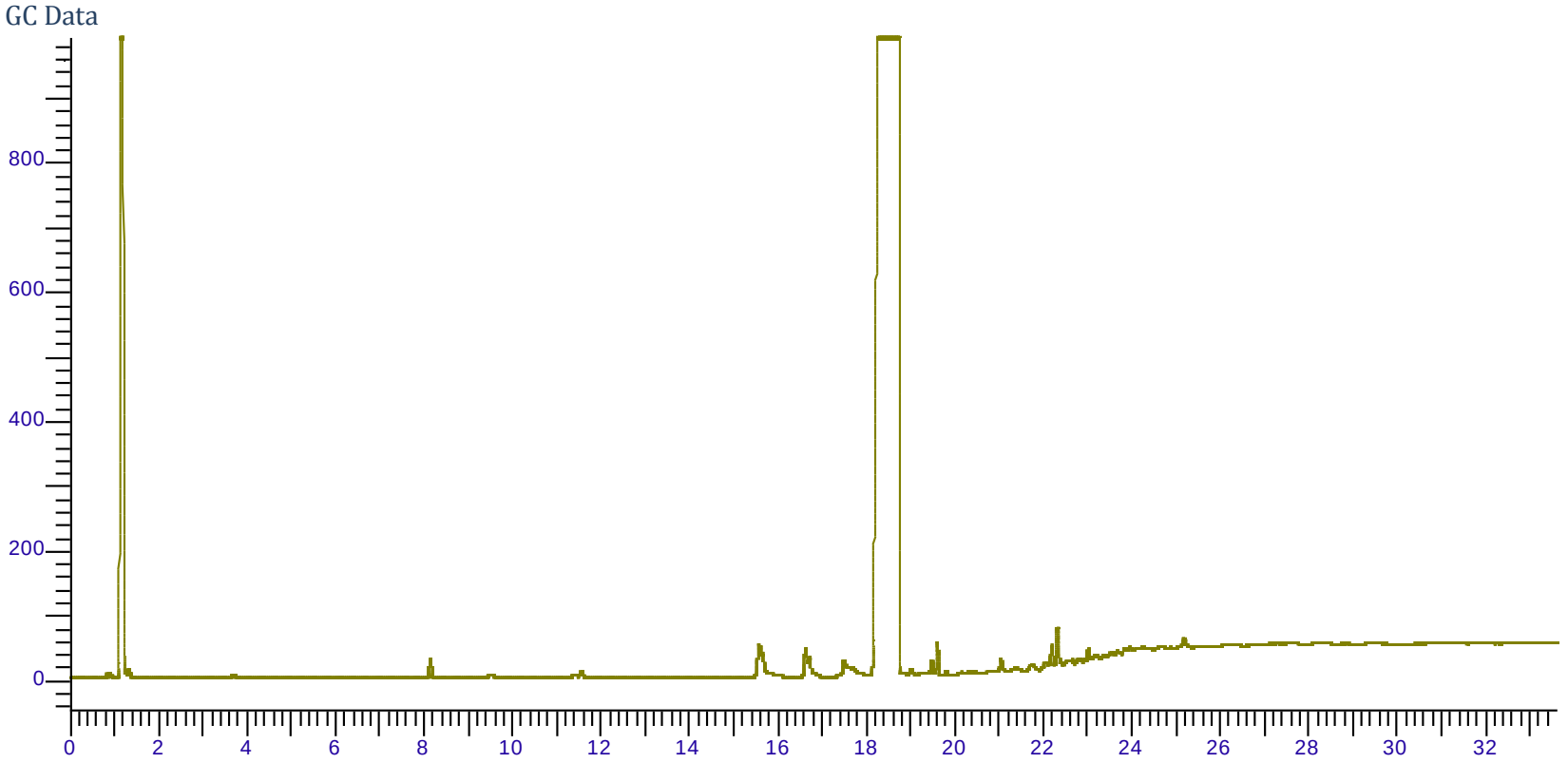

NMR Data

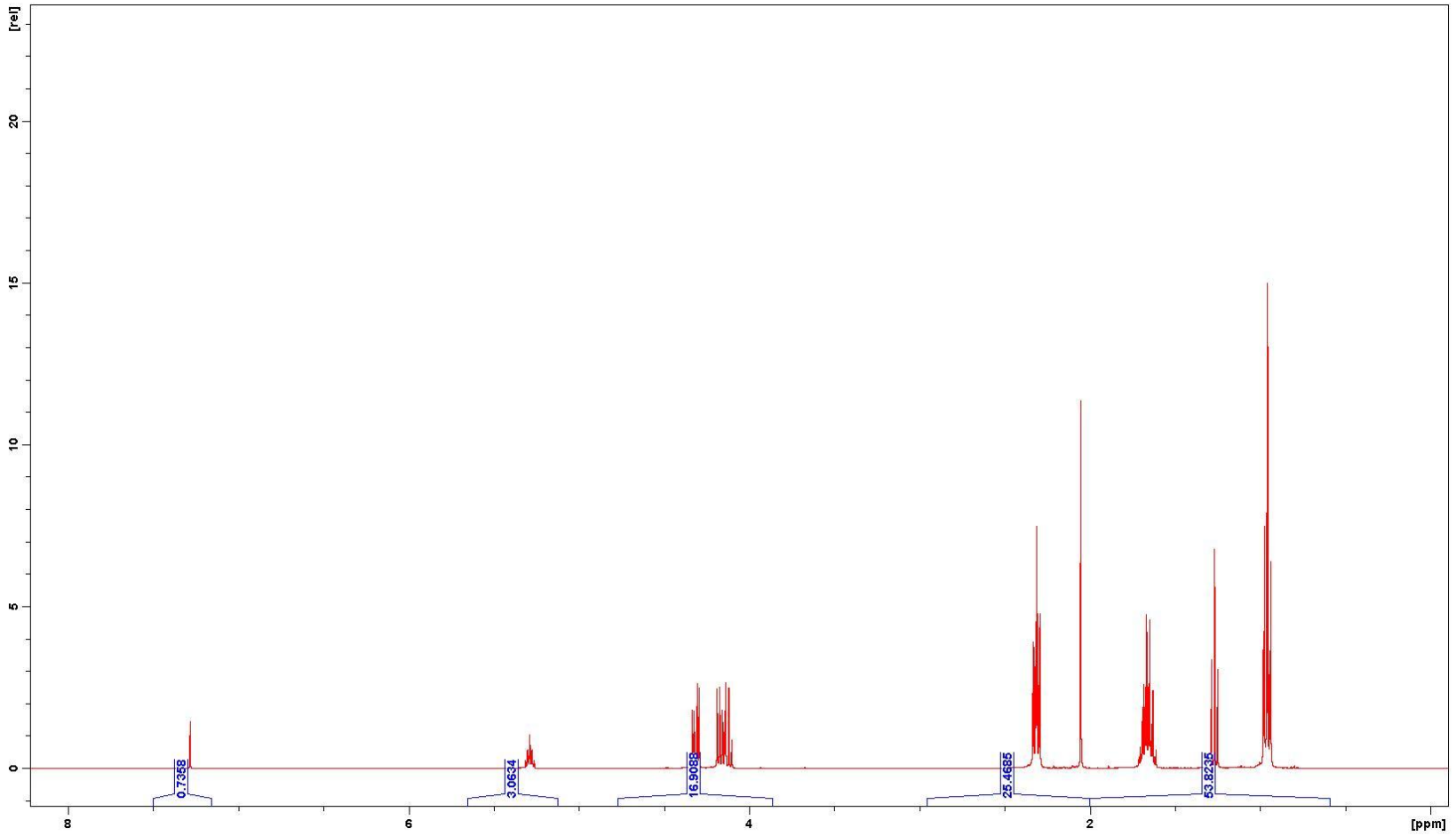

HT7 Tributyrin Hydrolysis

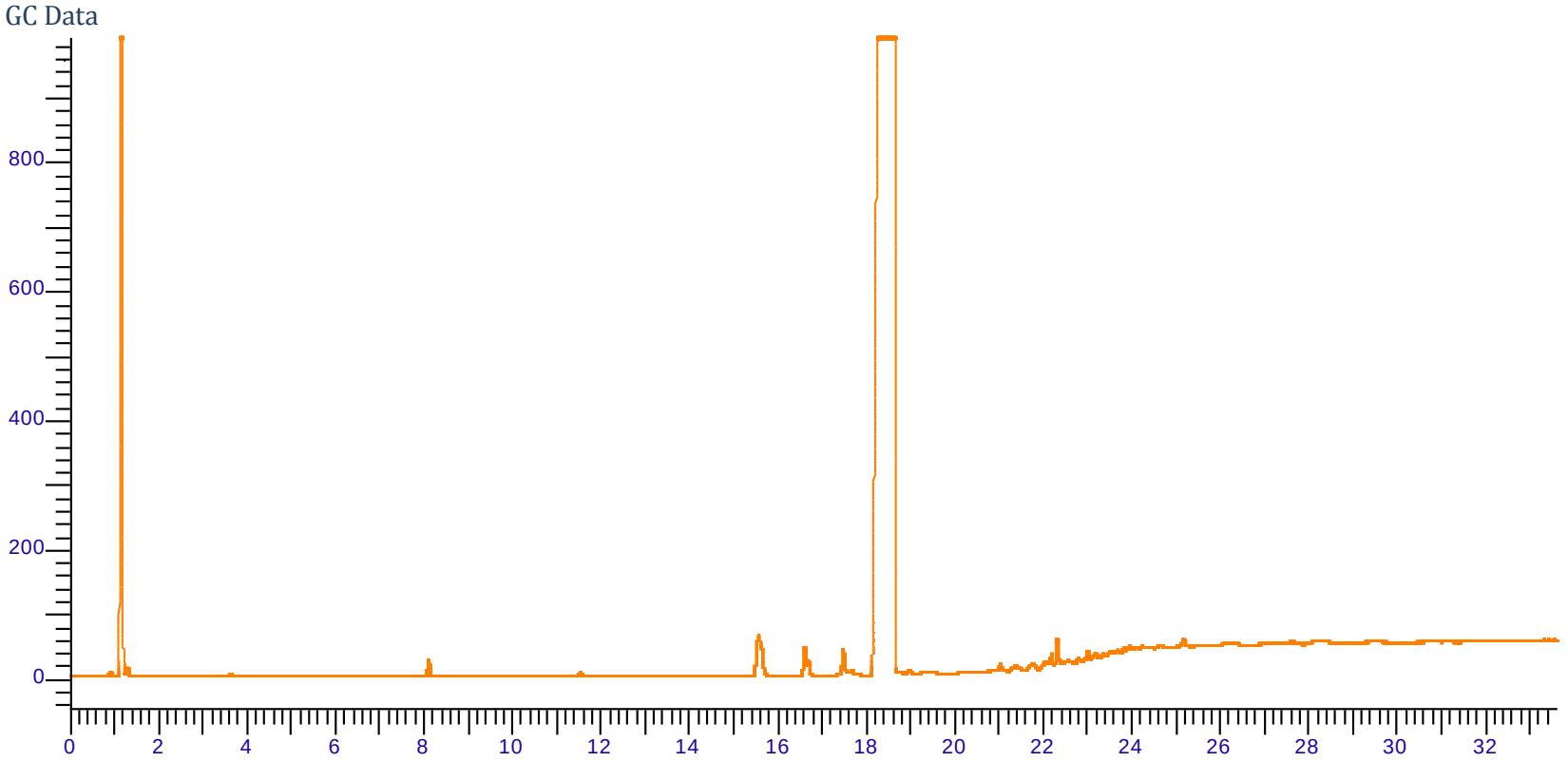

NMR Data

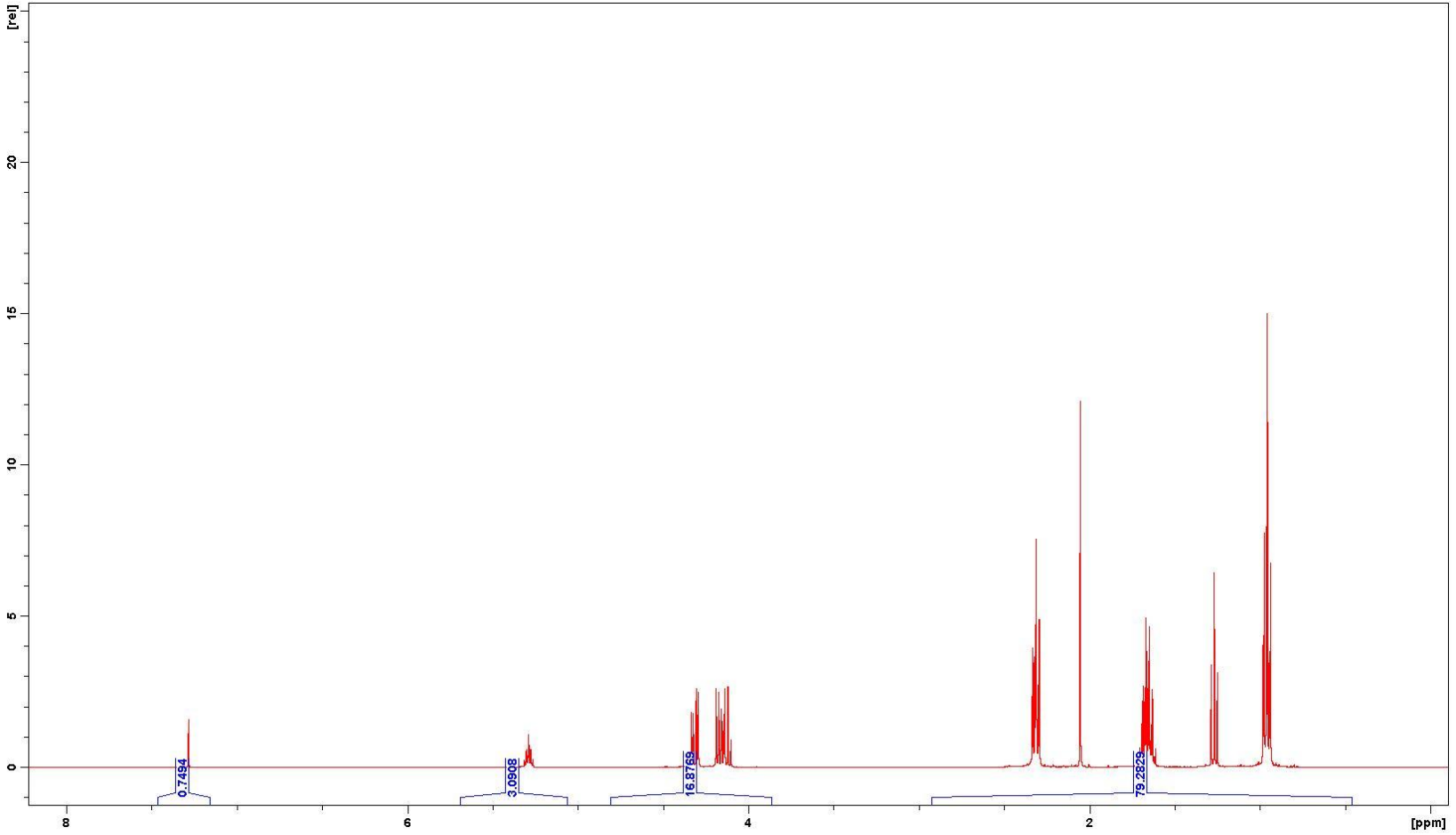

HT8 Tributyrin Hydrolysis

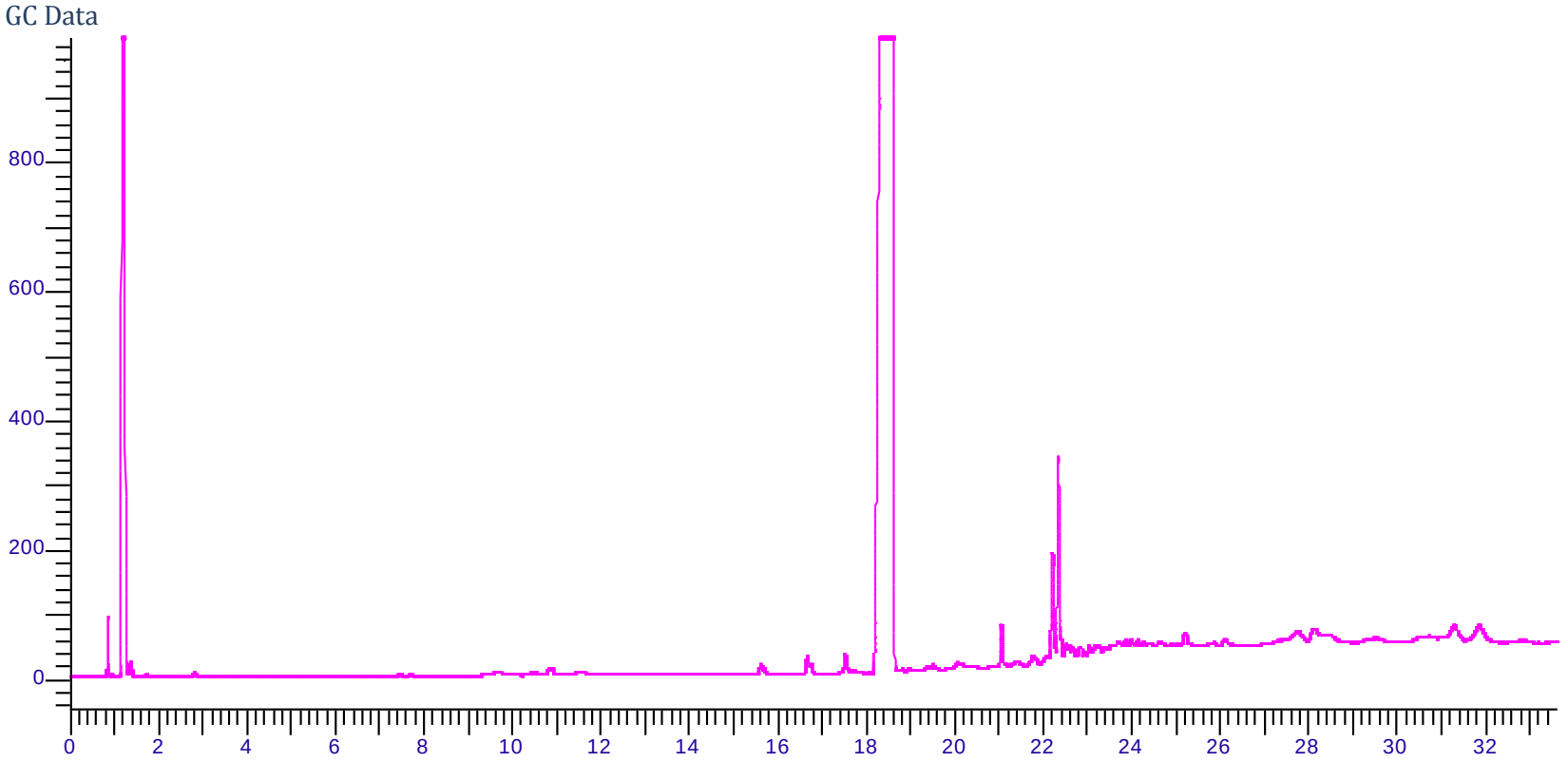

NMR Data

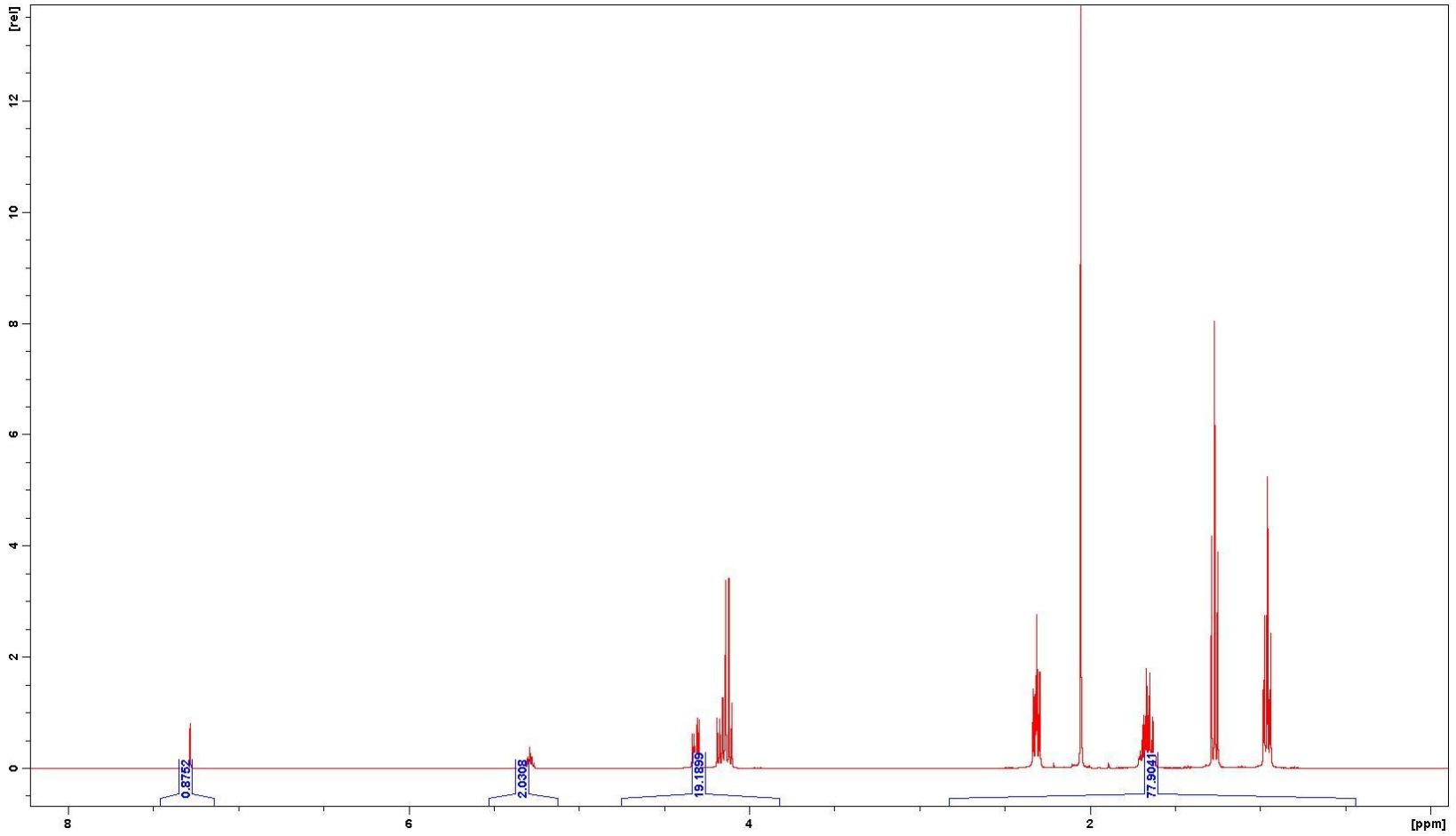

HT9 Tributyrin Hydrolysis

GC data

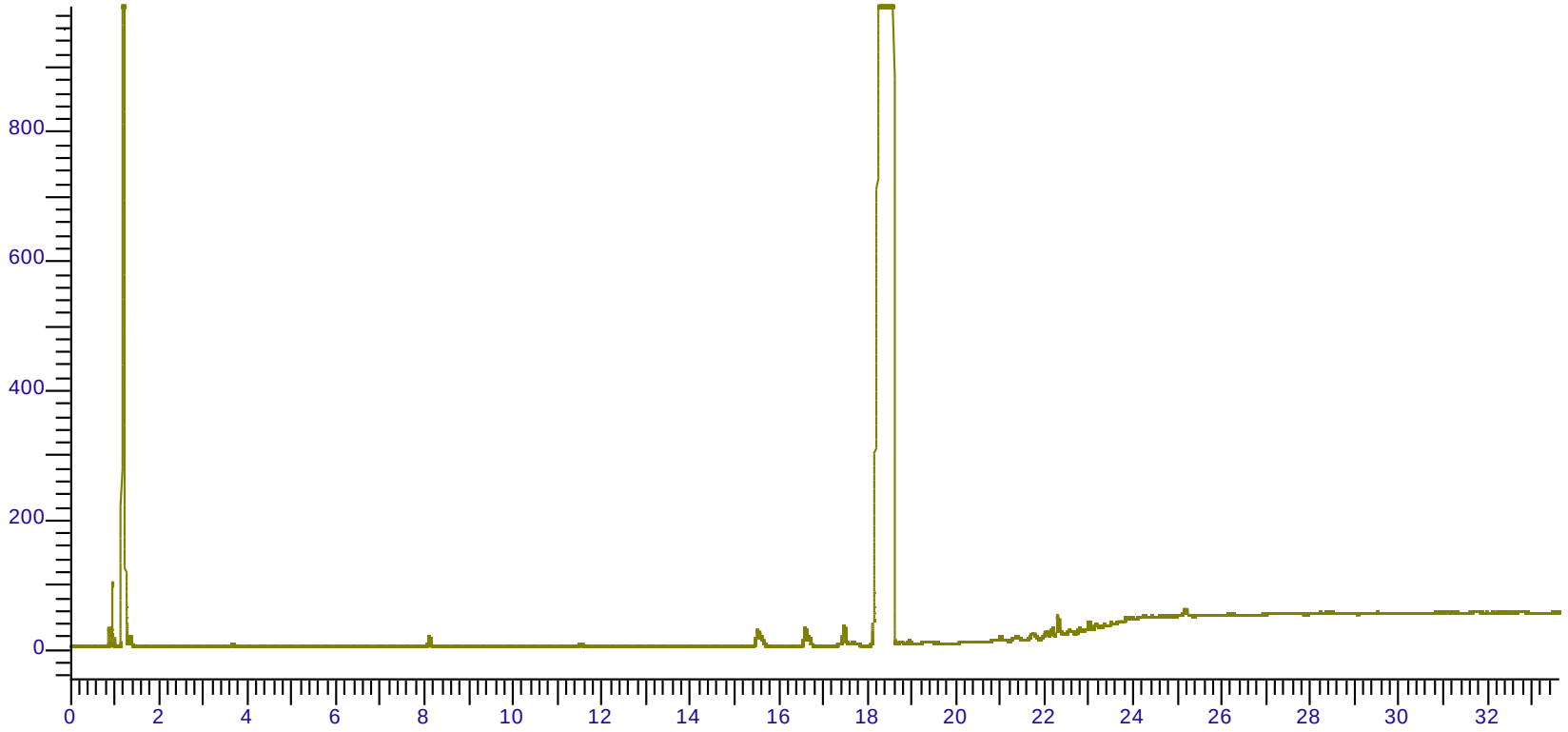

NMR Data

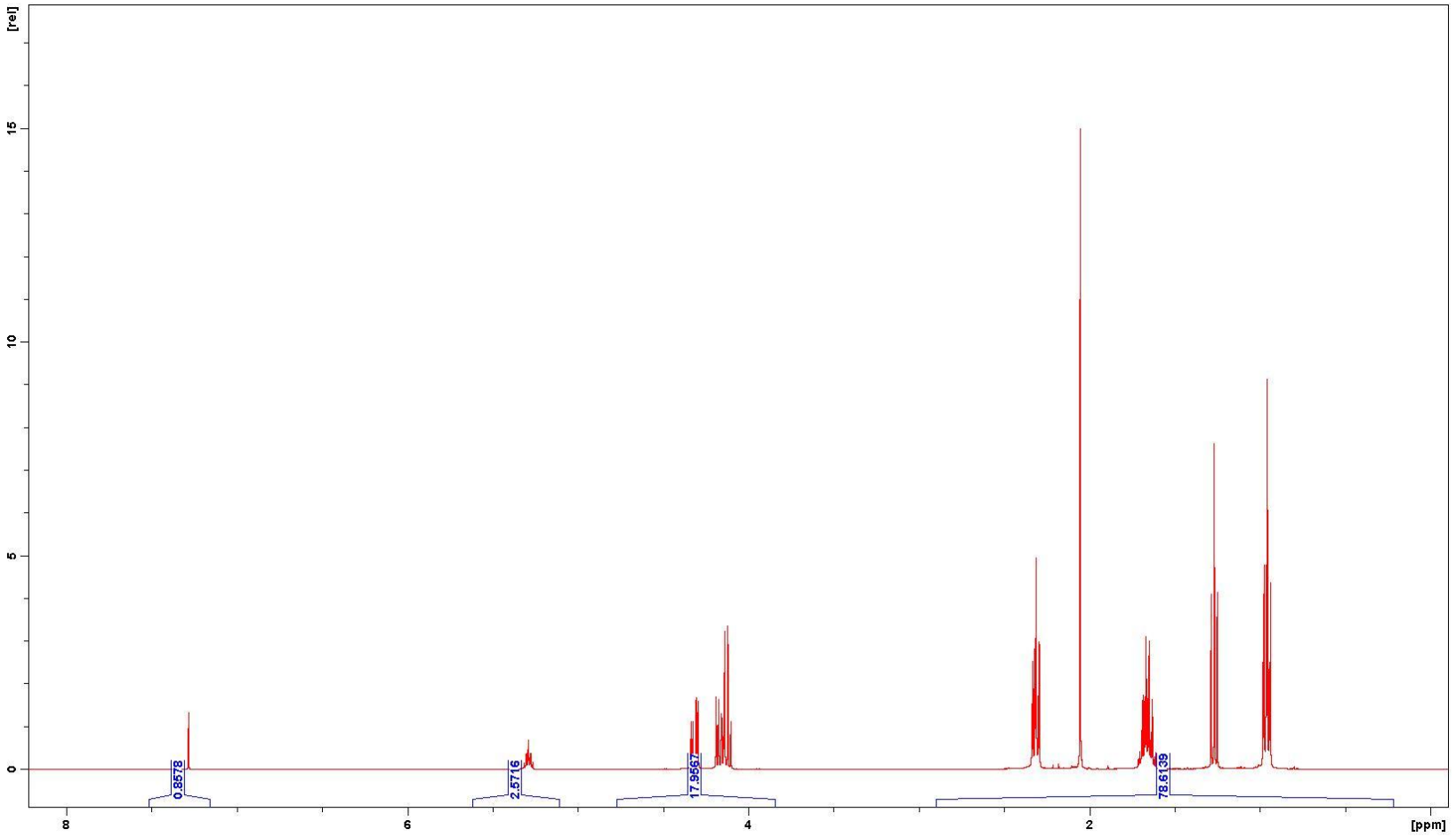

HT10 Tributyrin Hydrolysis

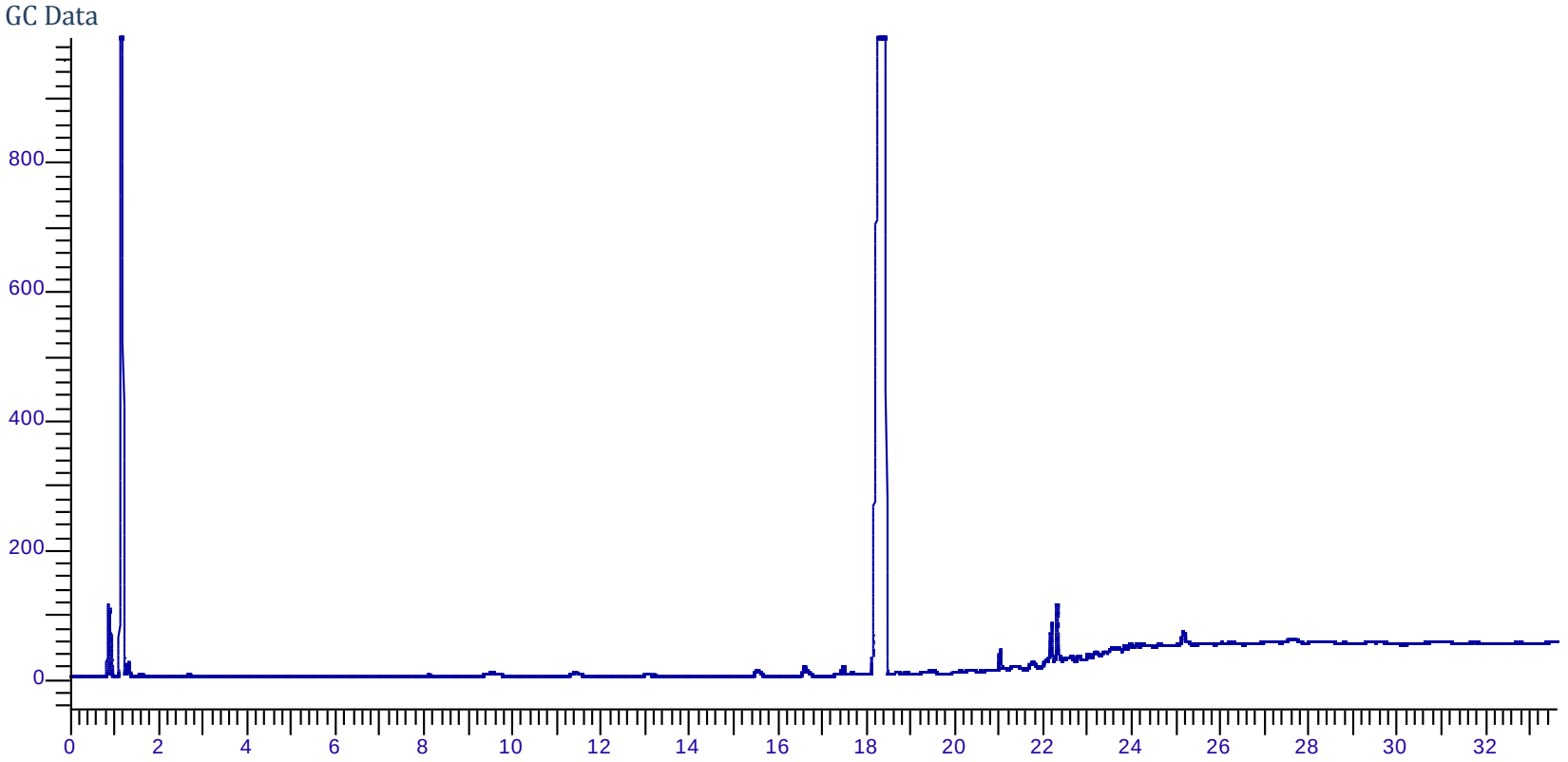

NMR Data

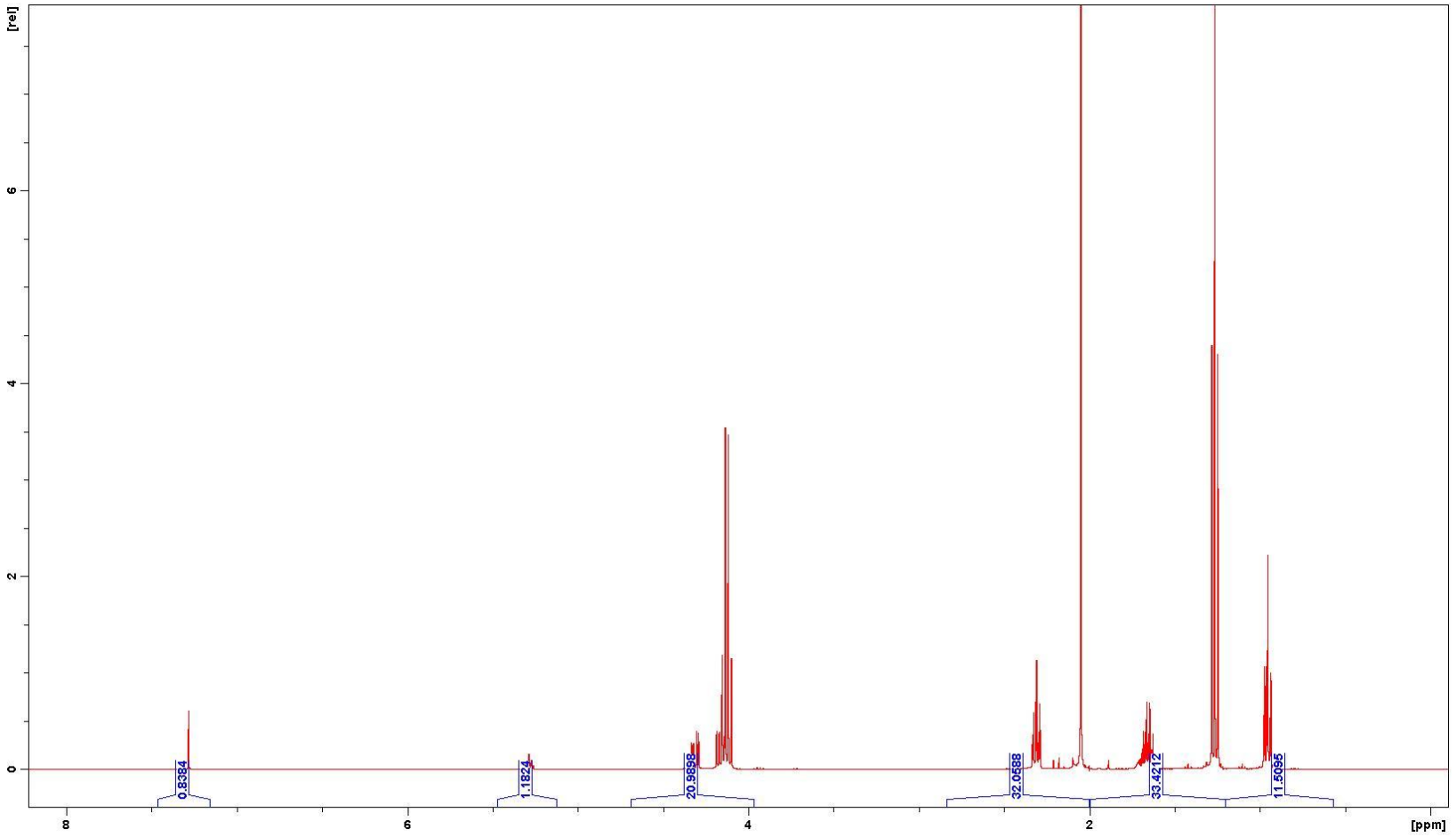

HT11 Tributyrin Hydrolysis

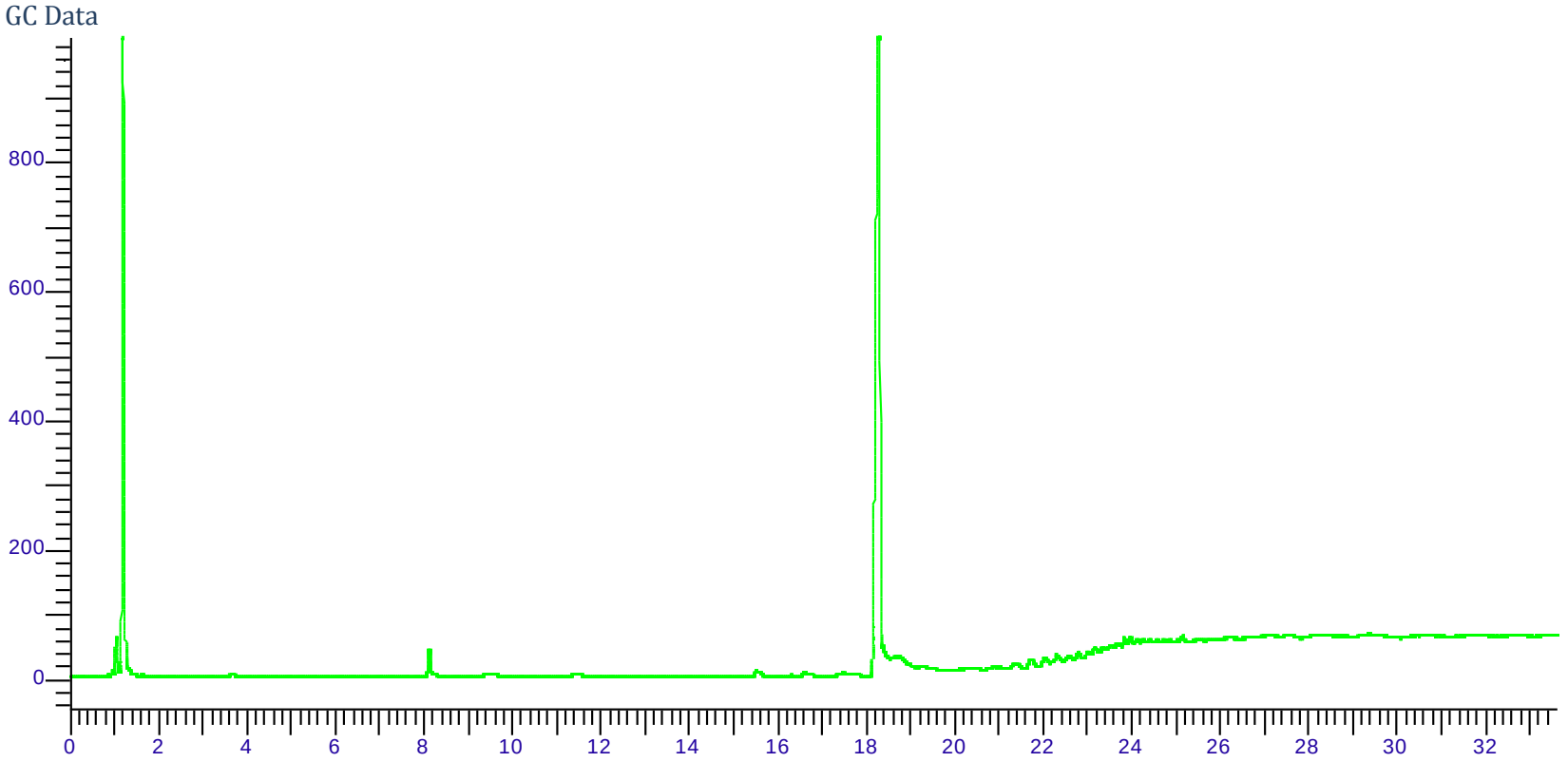

NMR Data

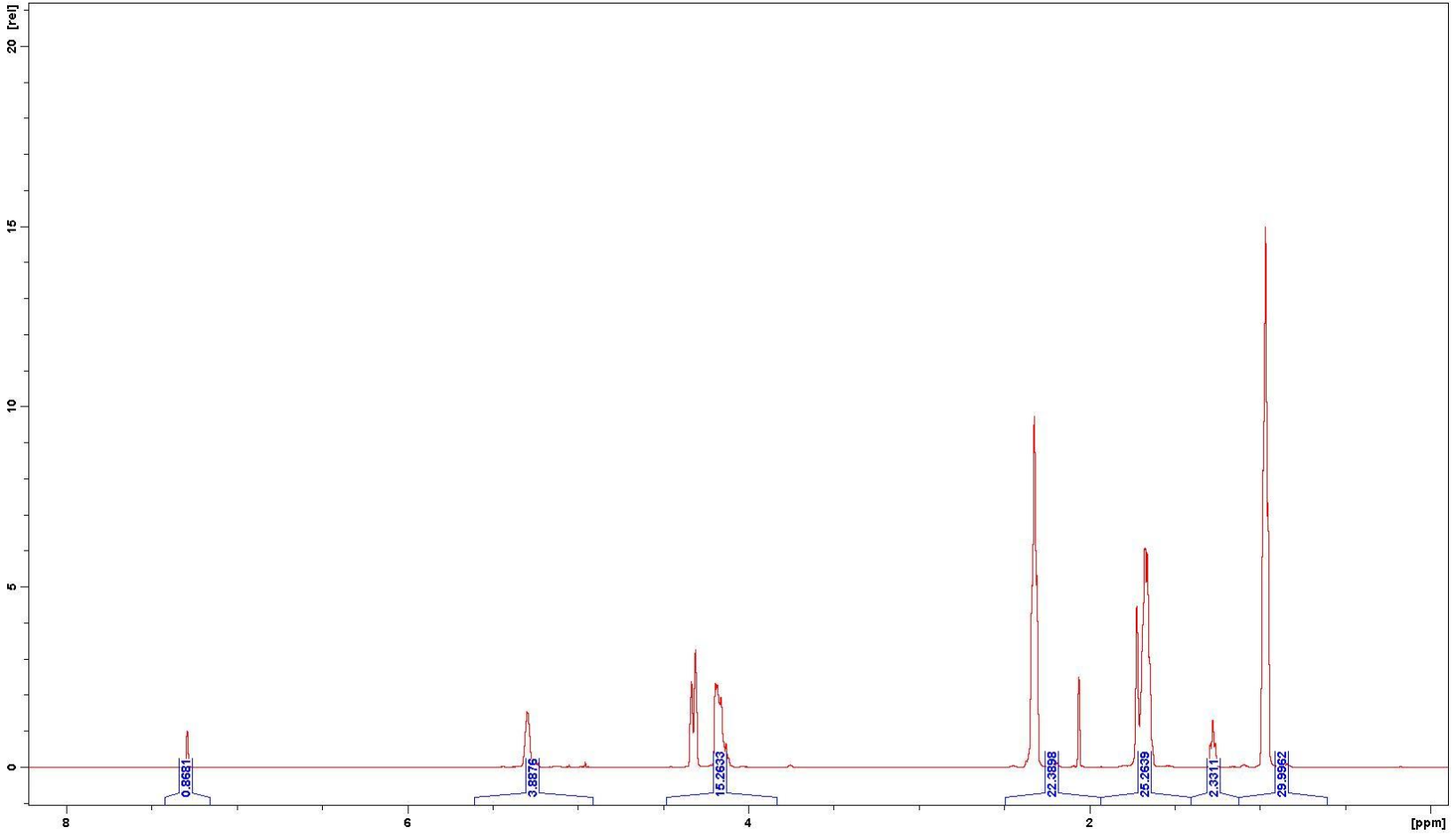
20 [rel]
15
10
5
0
0.8681
3.8876
15.2633
22.3898
25.2639
2.3311
29.9962
8
6
4
2
[ppm]

HT12 Tributyrin Hydrolysis

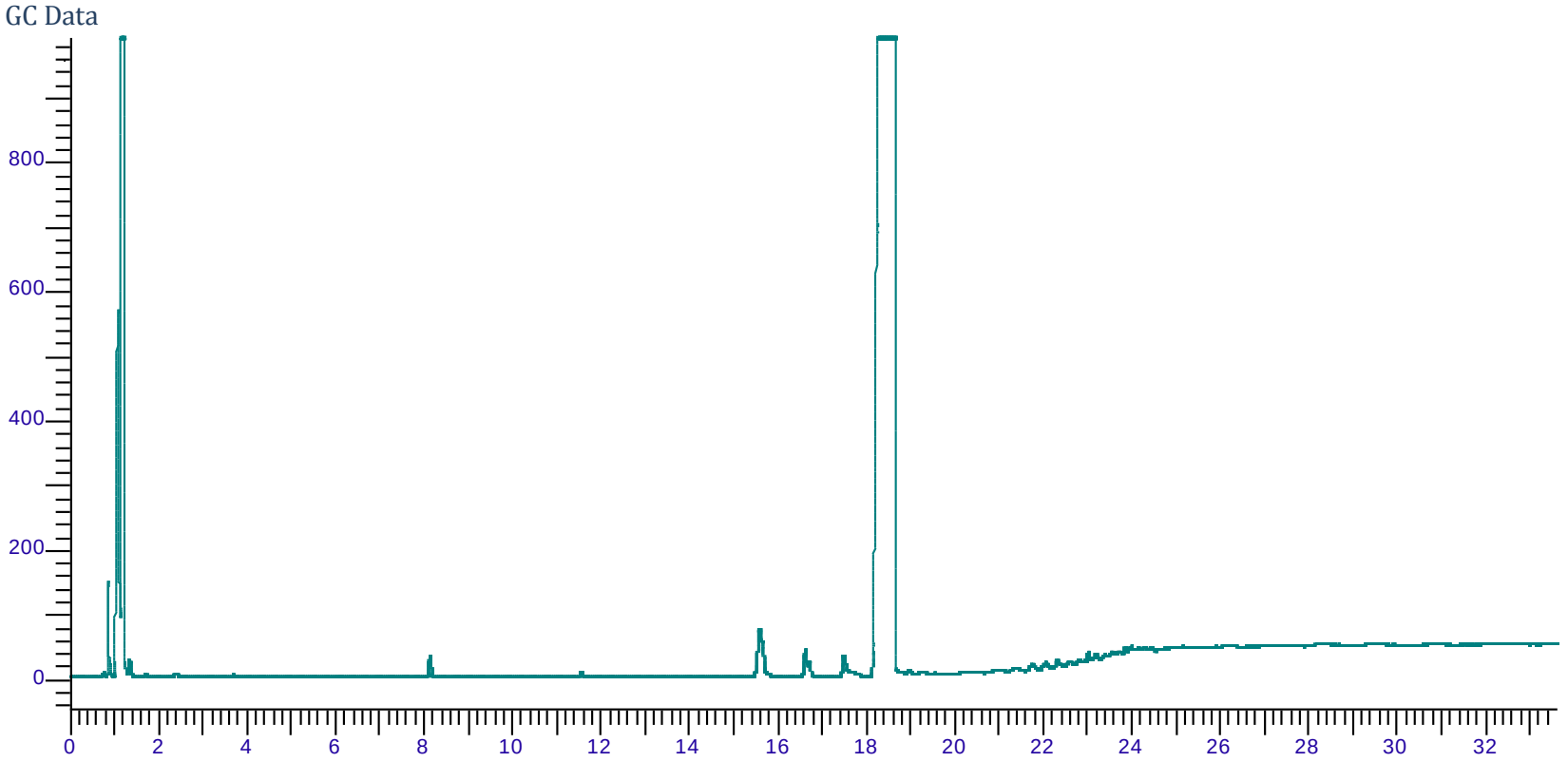

NMR Data

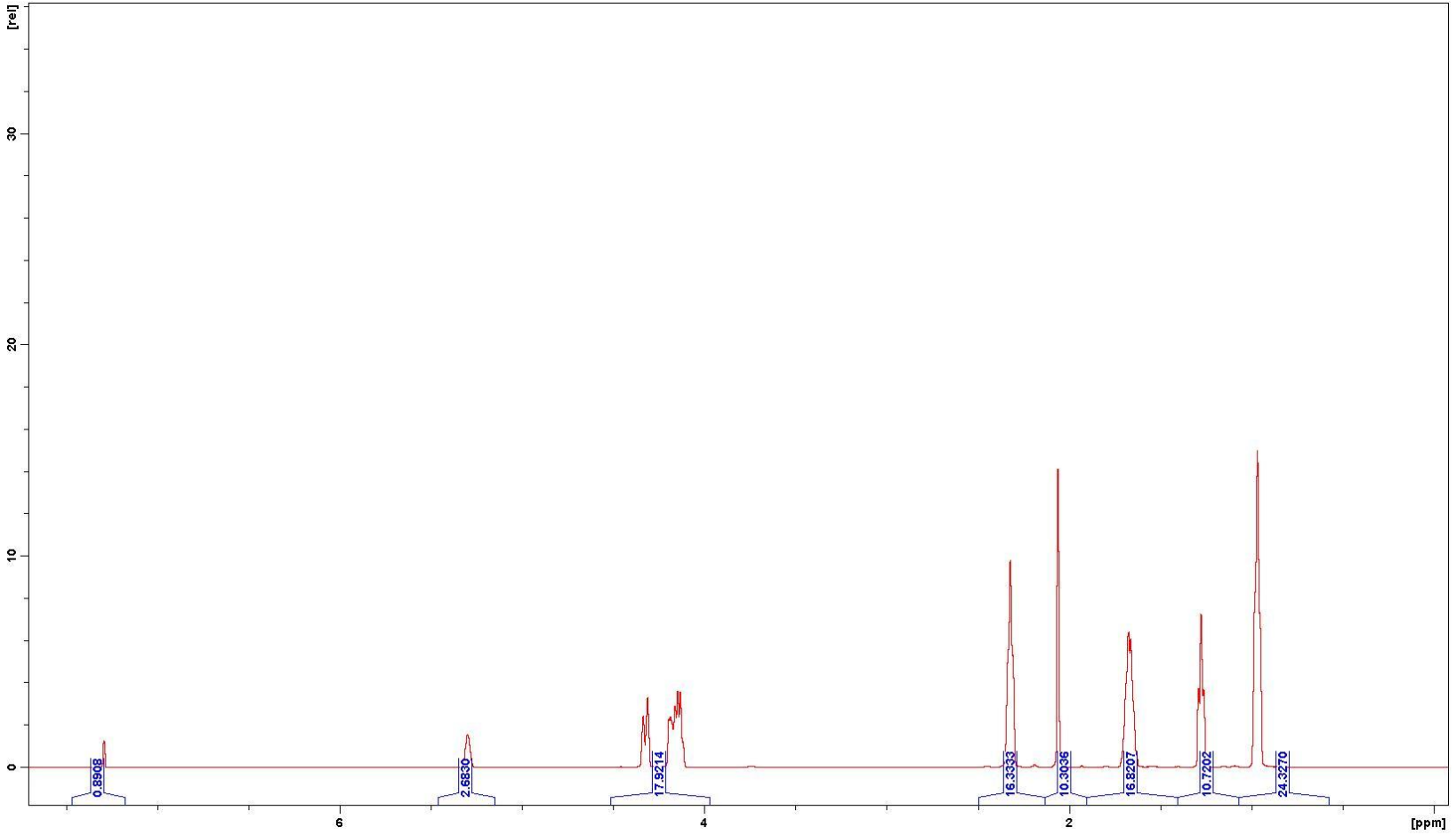
[rel]
30
20
10
0
0.8908
2.6830
17.9214
16.3333
10.3036
16.8207
10.7202
24.3270
6
4
2
[ppm]

HT13 Tributyrin Hydrolysis

GC Data

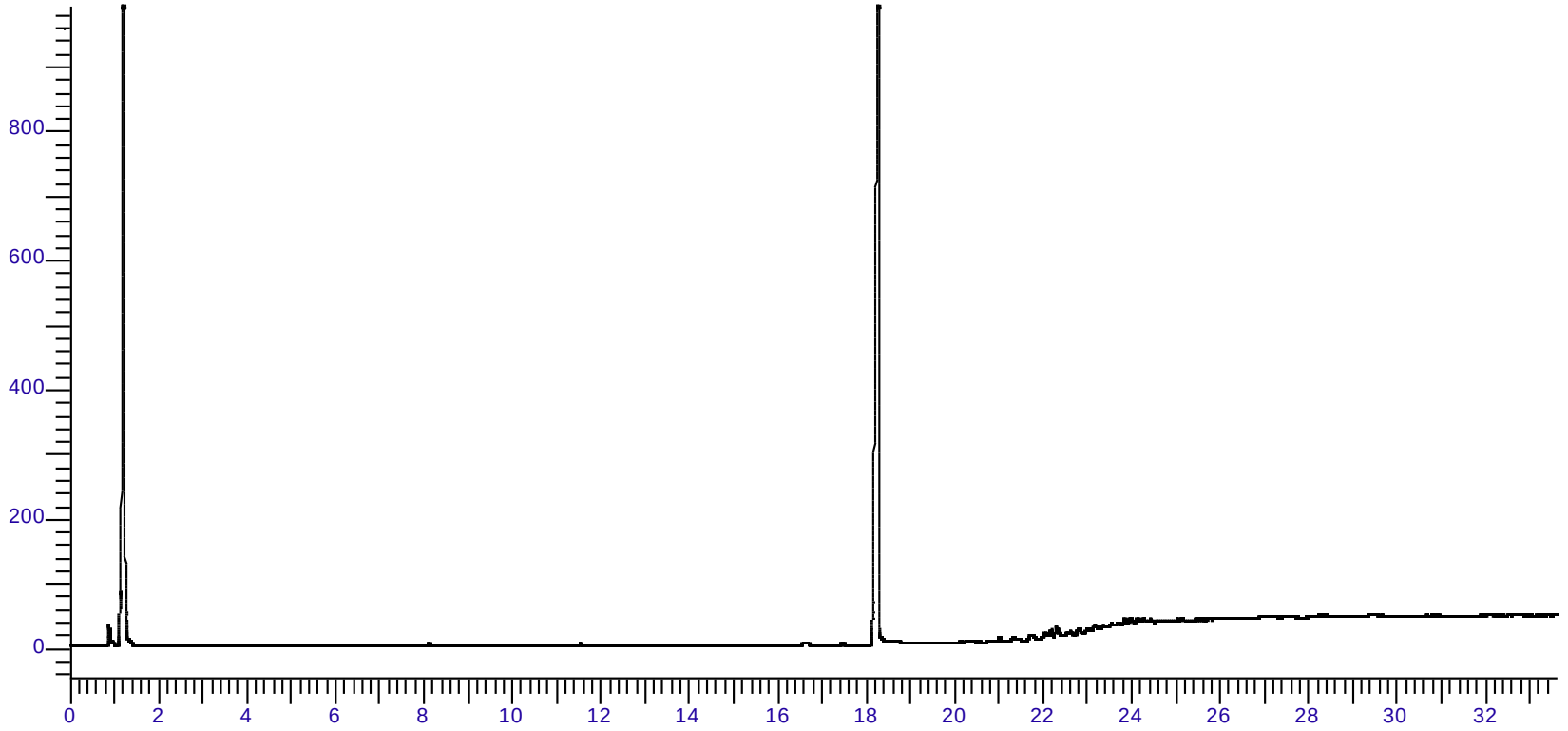

NMR Data

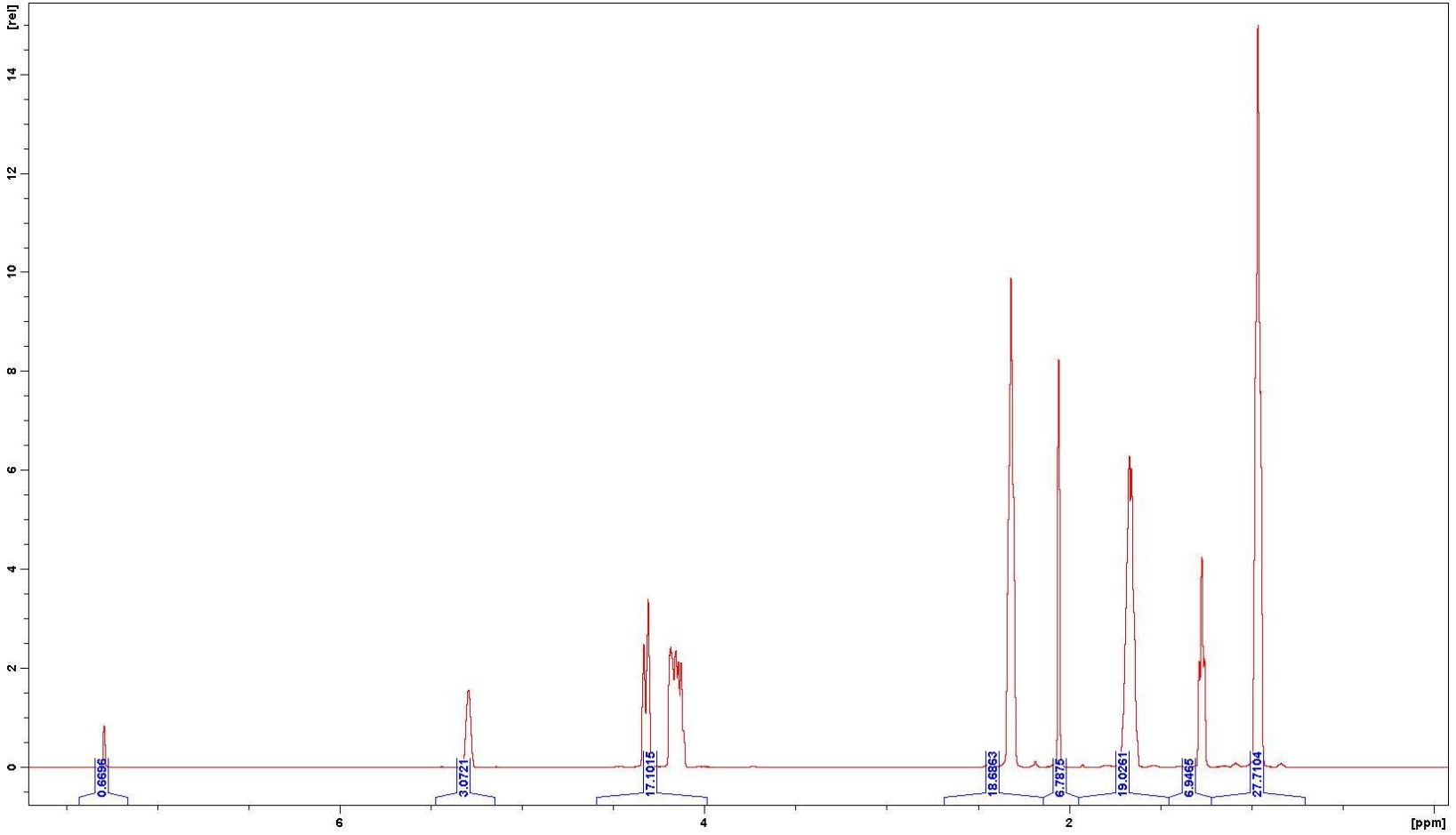
[rel]
14
12
10
8
6
4
2
0
0.6696
3.0721
17.1015
18.6863
6.7875
19.0261
6.9465
27.7104
6
4
2
[ppm]

HT14 Tributyrin Transesterification

GC Data

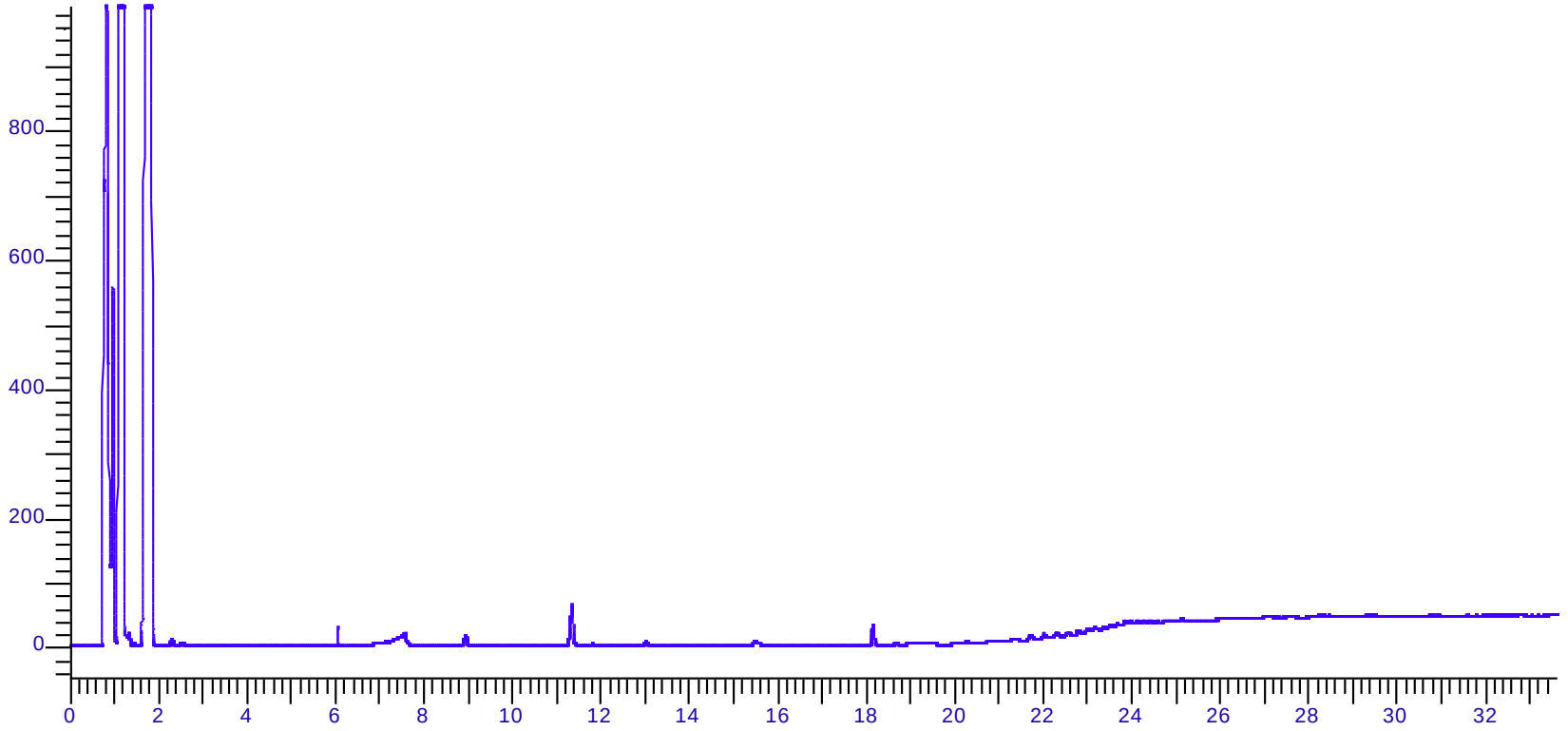

NMR Data

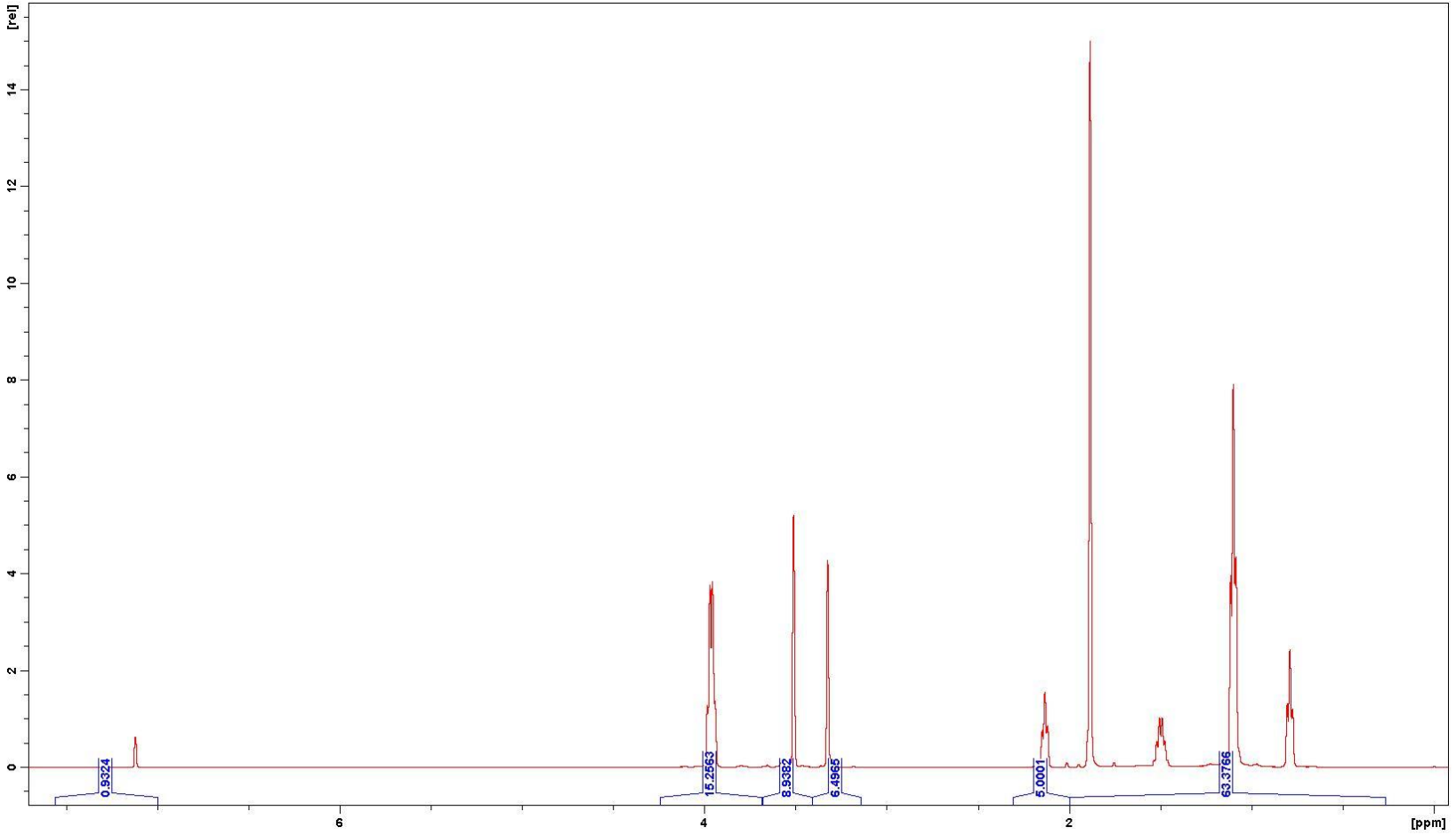
[rel]
14
12
10
8
6
4
2
0
0.9324
15.2563
8.9382
6.4965
5.0001
63.3766
6
4
2
[ppm]

HT15 Tributyrin Transesterification

GC Data

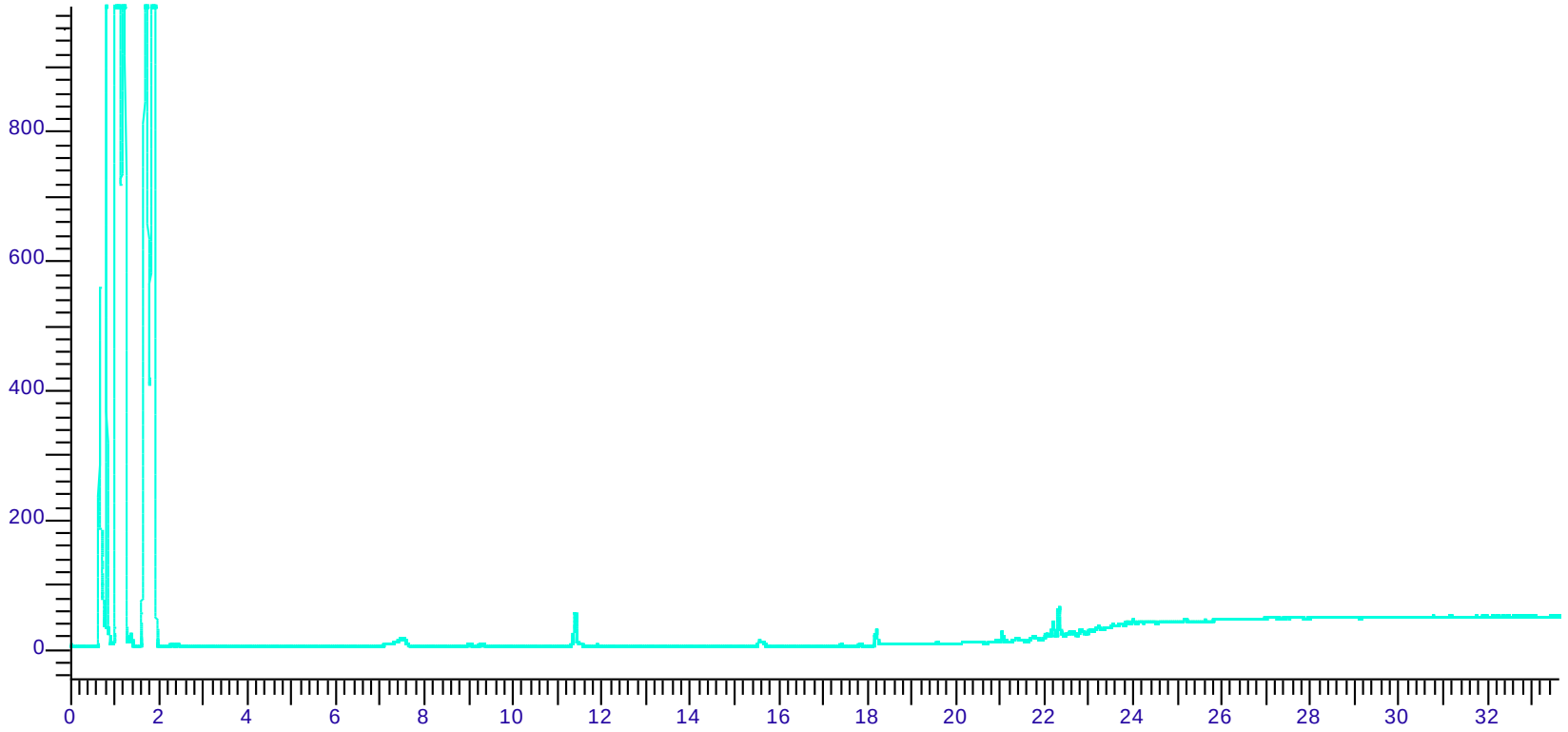

NMR Data

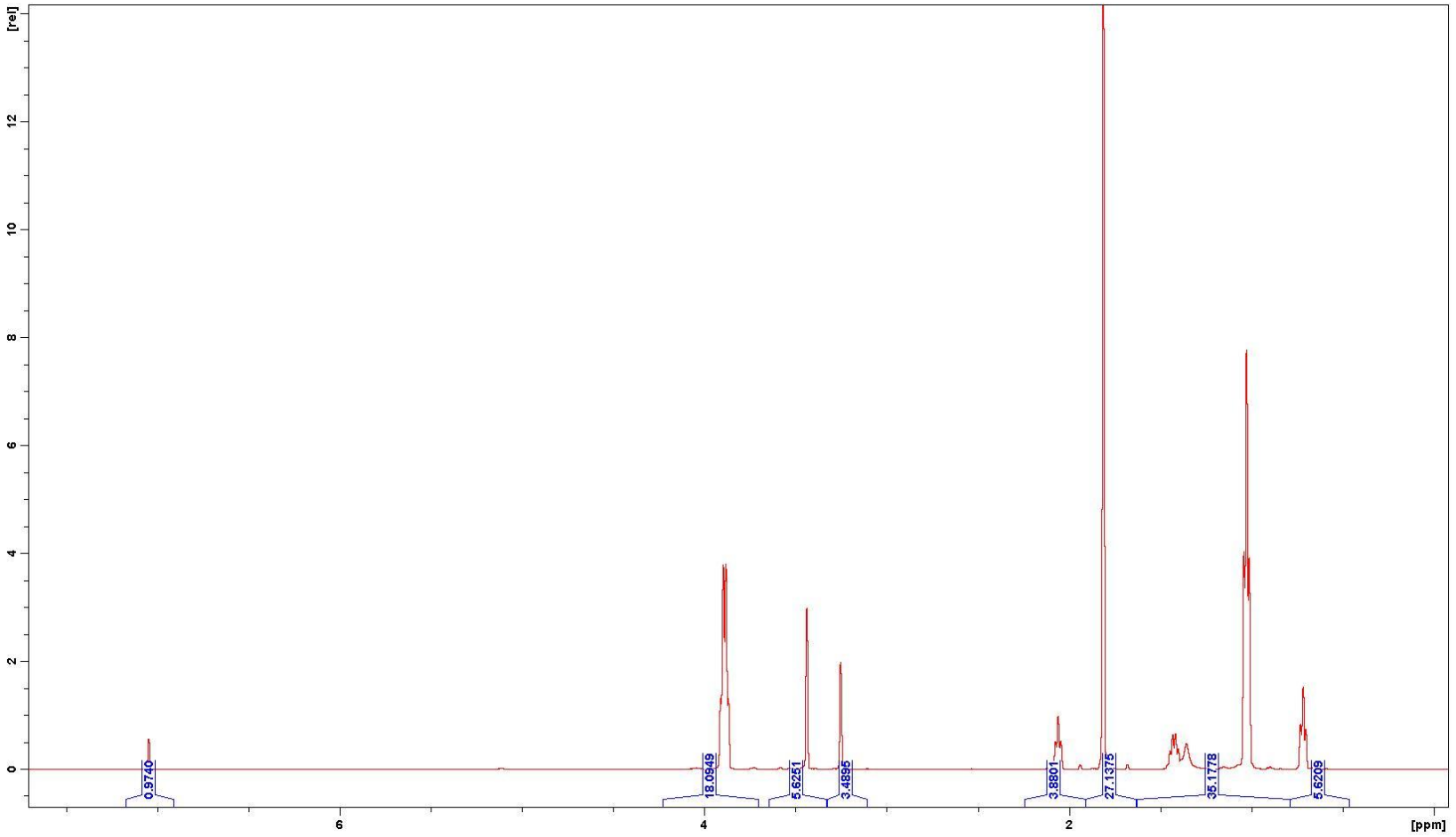
[rel]
12
10
8
6
4
2
0
0.9740
18.0949
5.6251
3.4895
3.8801
27.1375
35.1778
5.6209
6
4
2
[ppm]

HT16 Tributyrin Transesterification

GC Data

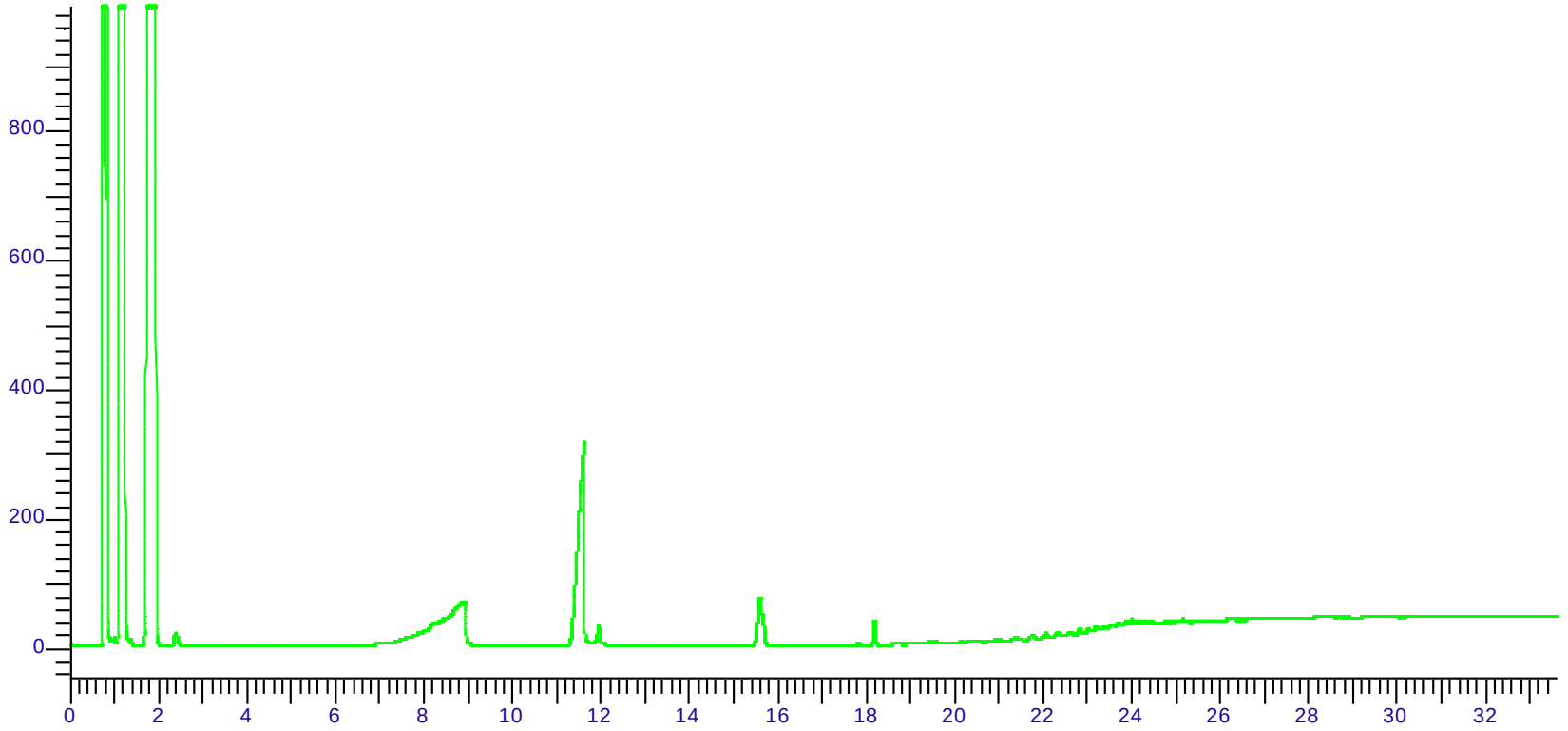

NMR Data

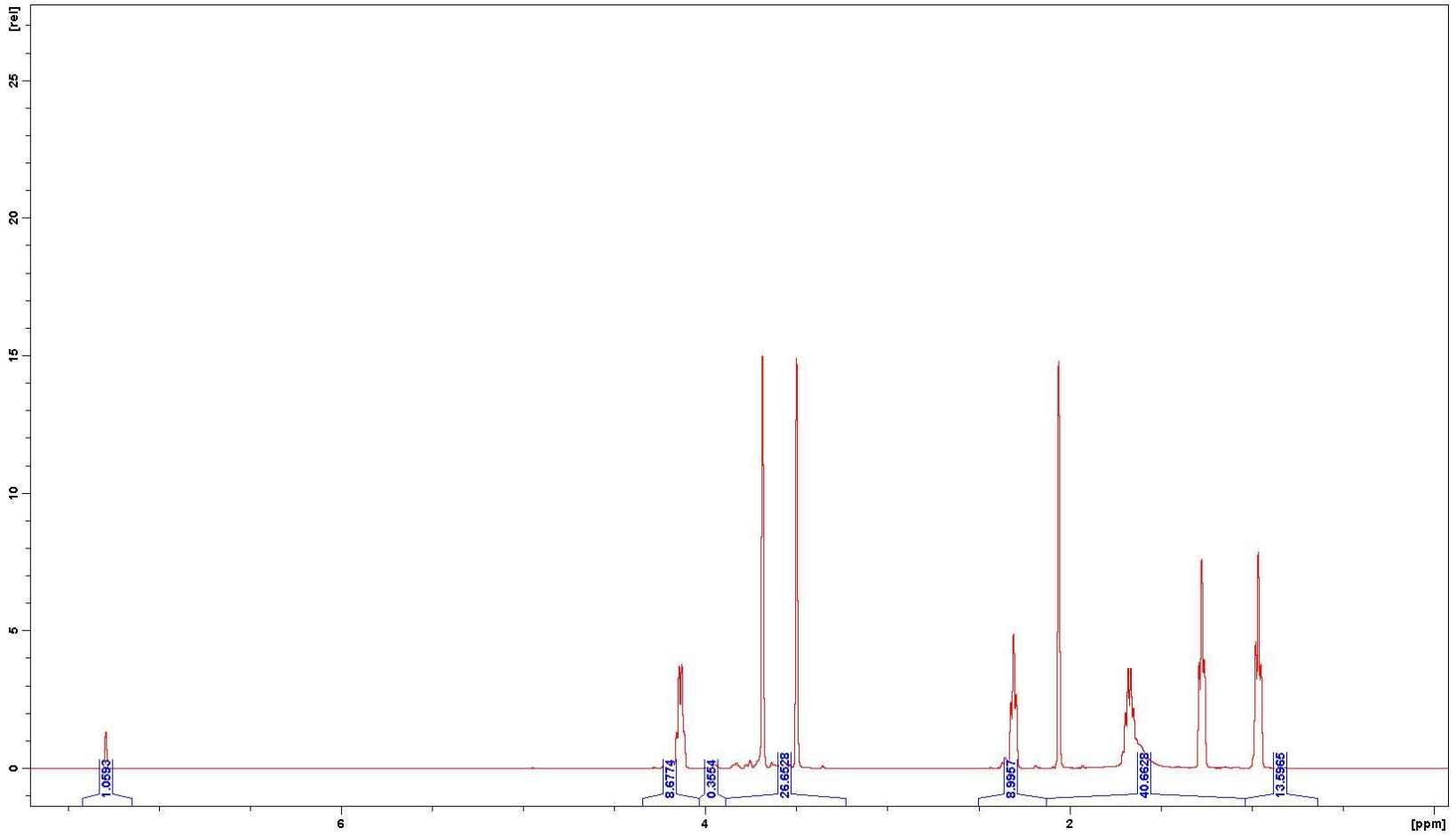
[rel]
25
20
15
10
5
0
1.0593
8.6774
0.3554
26.6528
8.9957
40.6628
13.5965
6
4
2
[ppm]

Appendix F Enzymatic Biocatalysis GC and NMR Data

B1 Overnight Digestion – Gasification Trial

GC Data – Gas collected from reactor

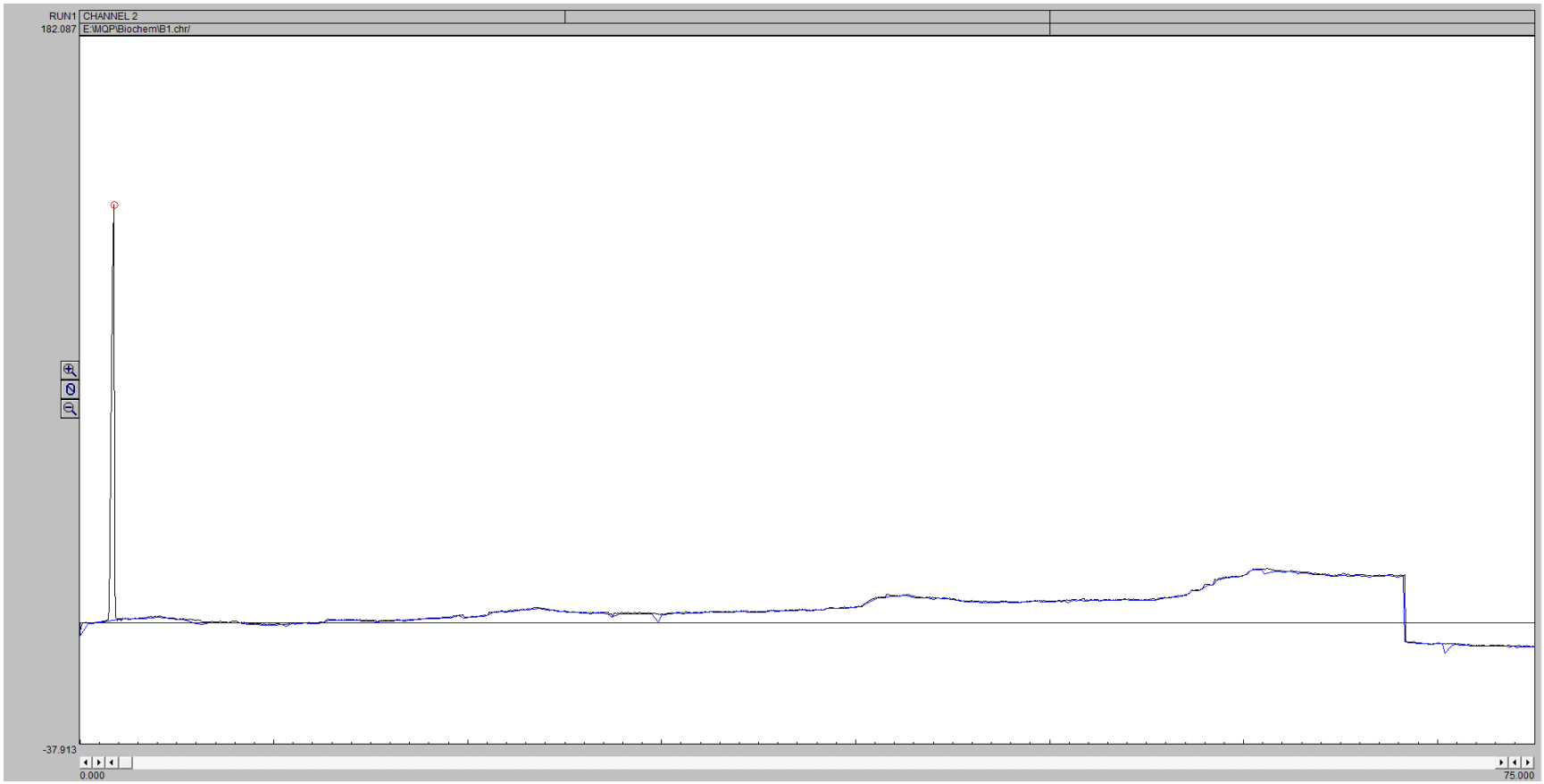

GC Data – Liquids collected from cold trap

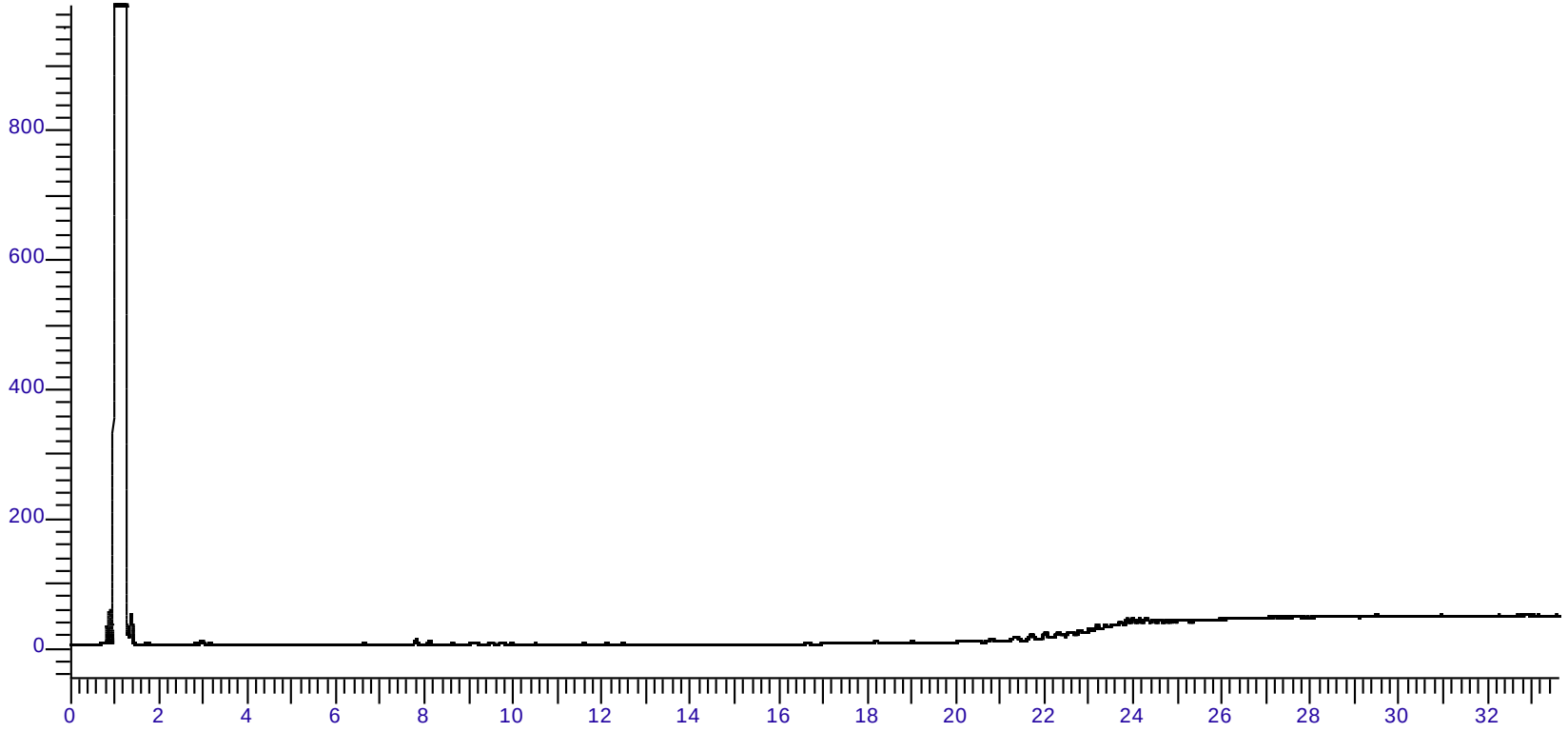

NMR Data

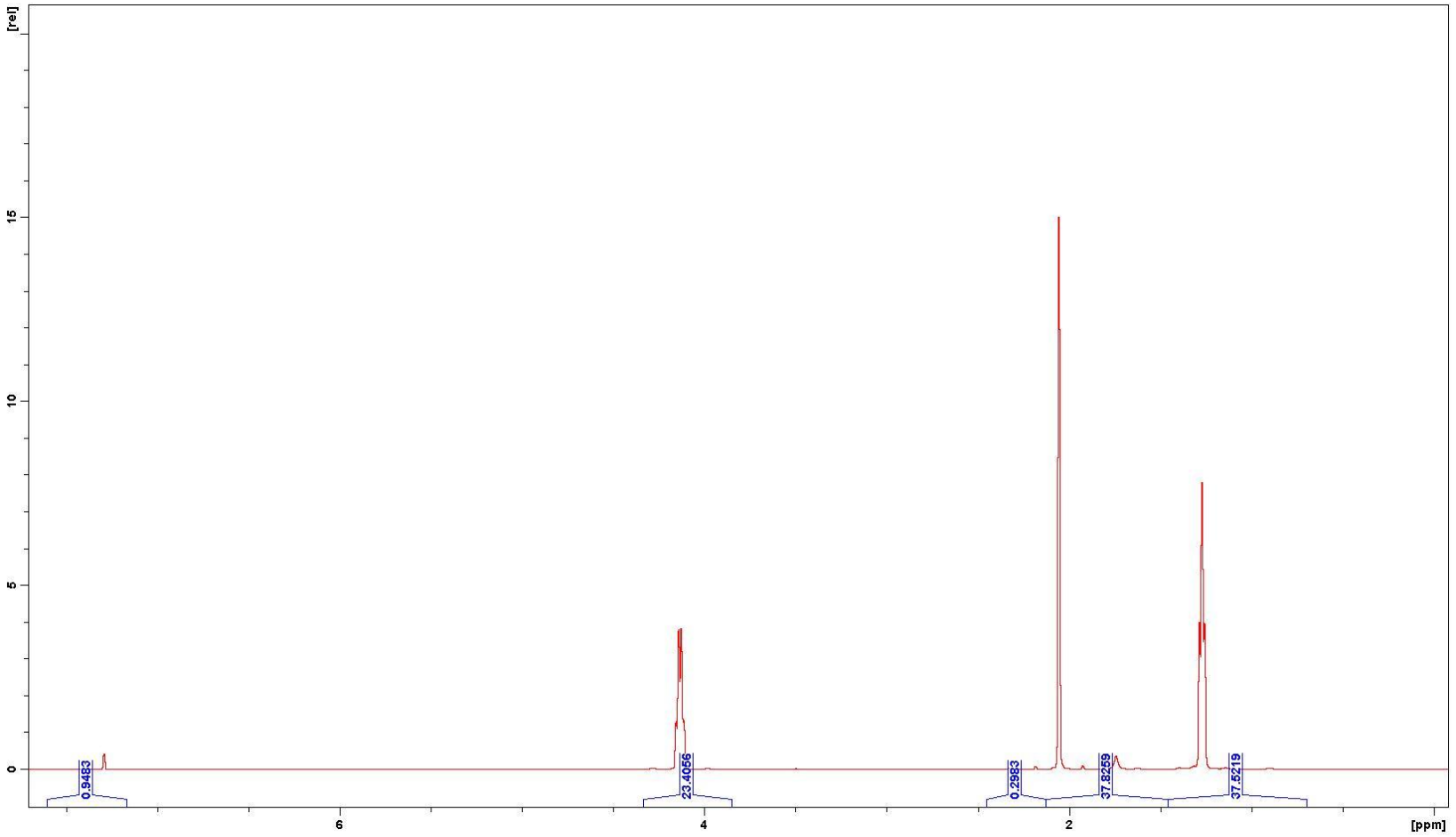

B2 Overnight Digestion – Transesterification

GC Data – Liquids collected from reactor

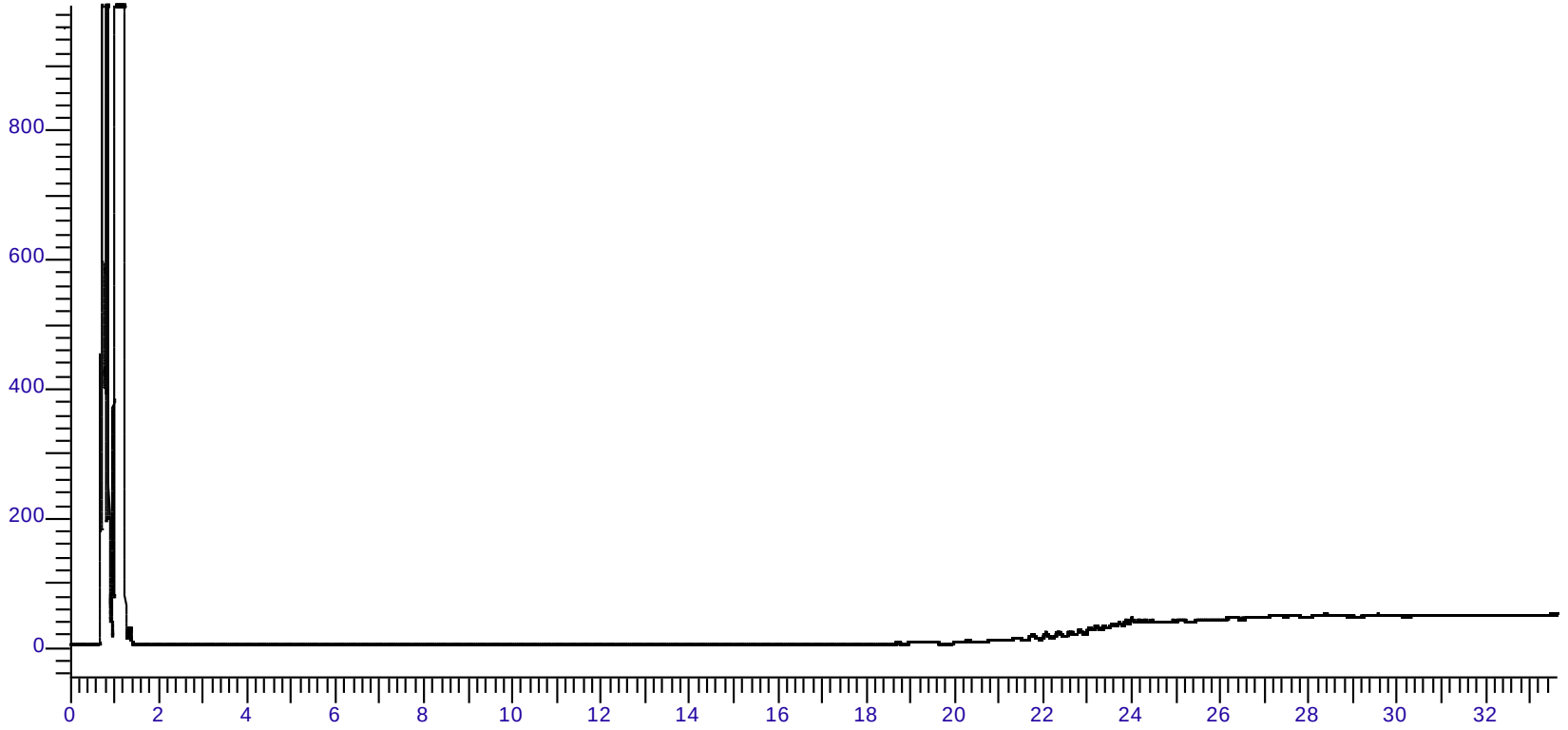

NMR Data

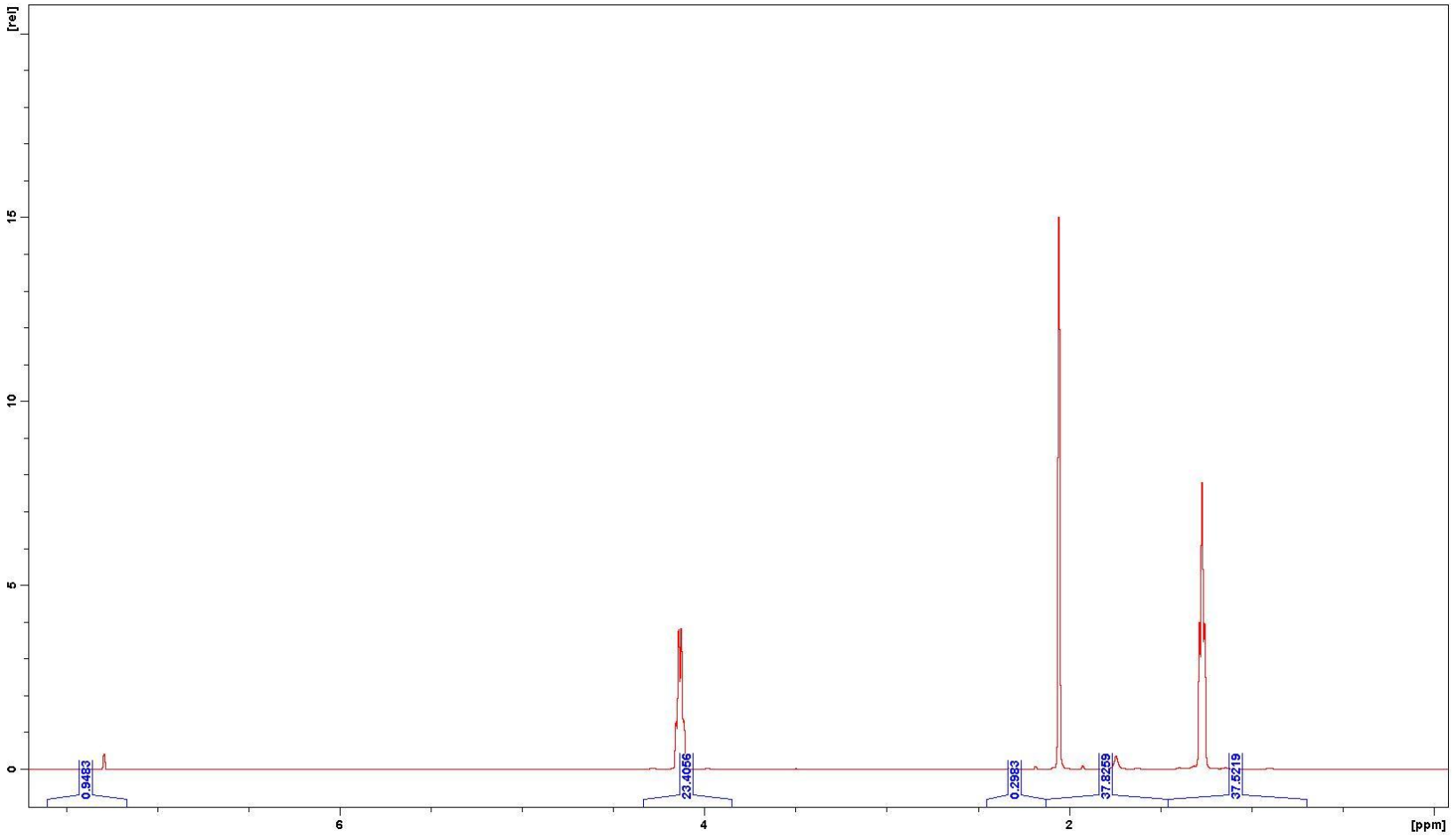

B3 Three Hour Digestion – Gasification

GC Data – Gas collected from reactor

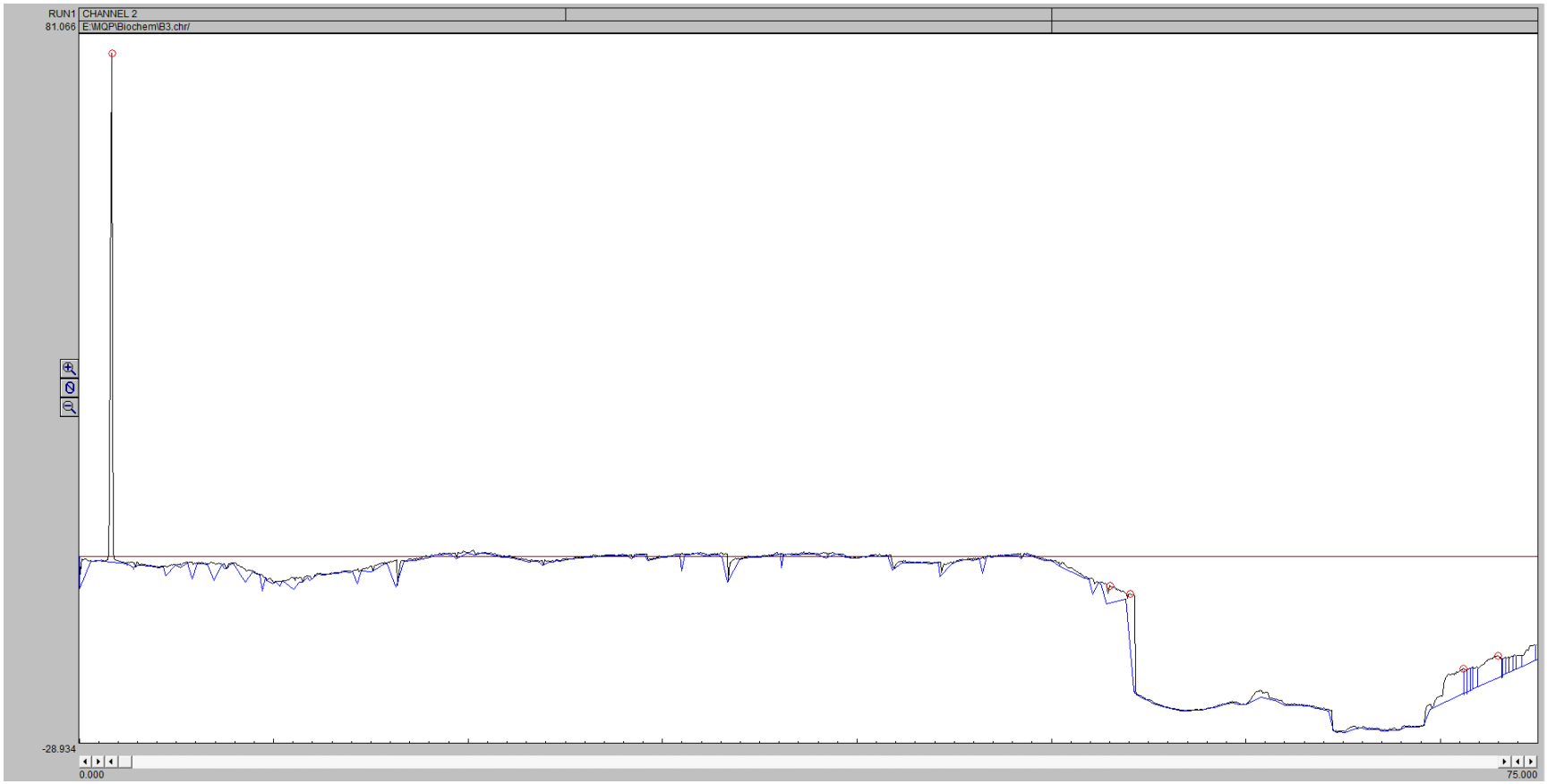

GC Data – Liquids collected from cold trap

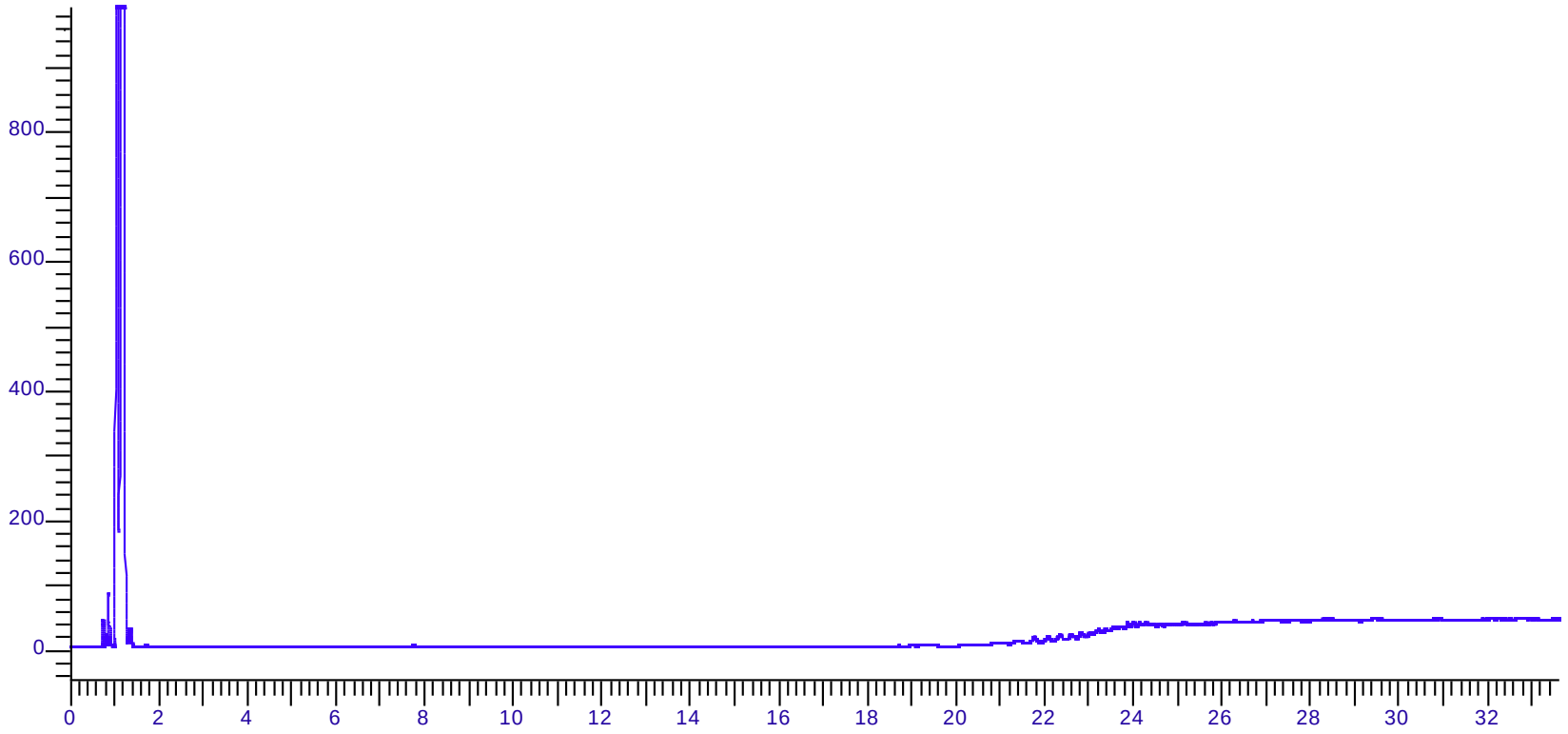

NMR Data

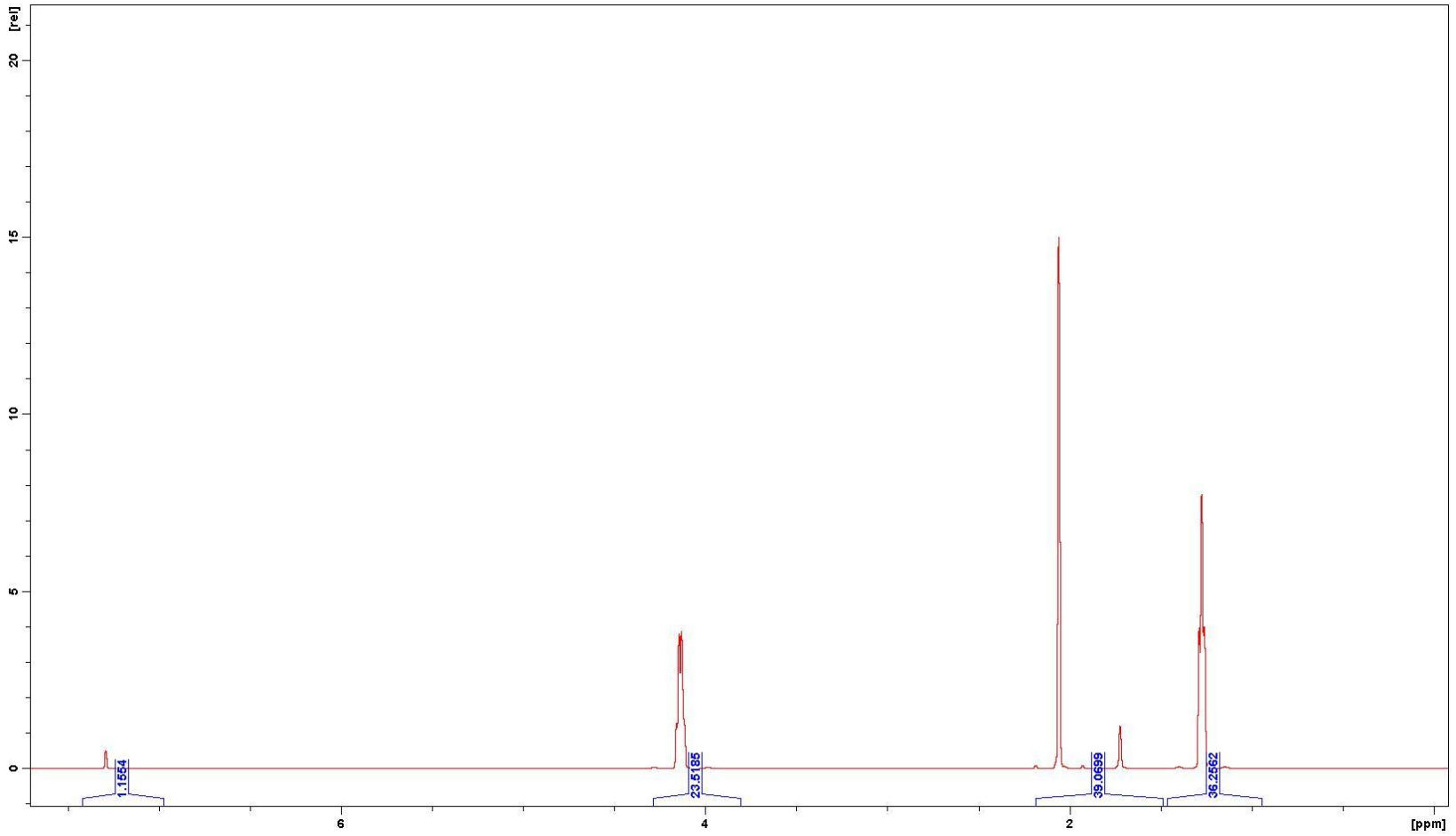

B4 Three Hour Digestion – Transesterification

GC Data – Liquids collected from reactor

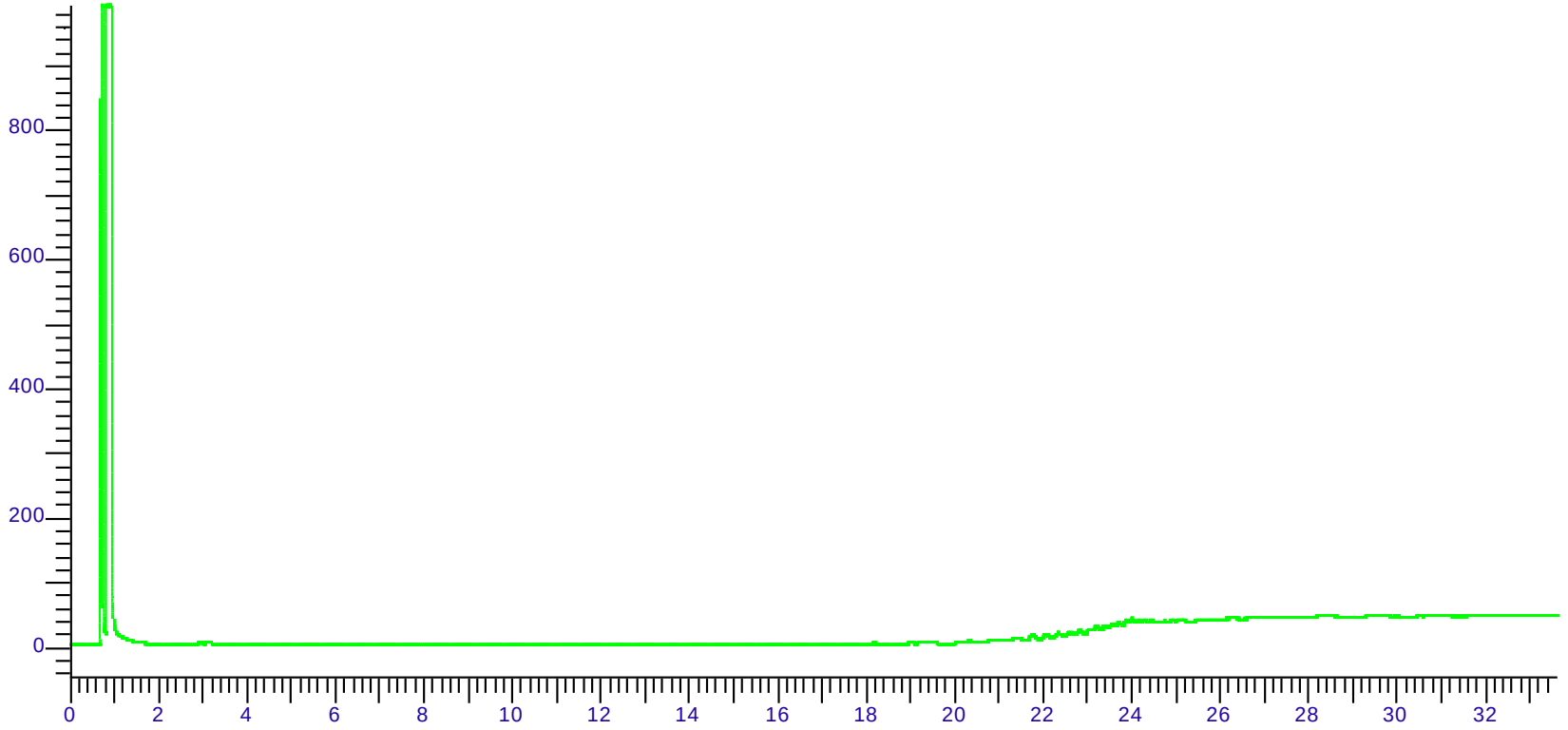

NMR Data

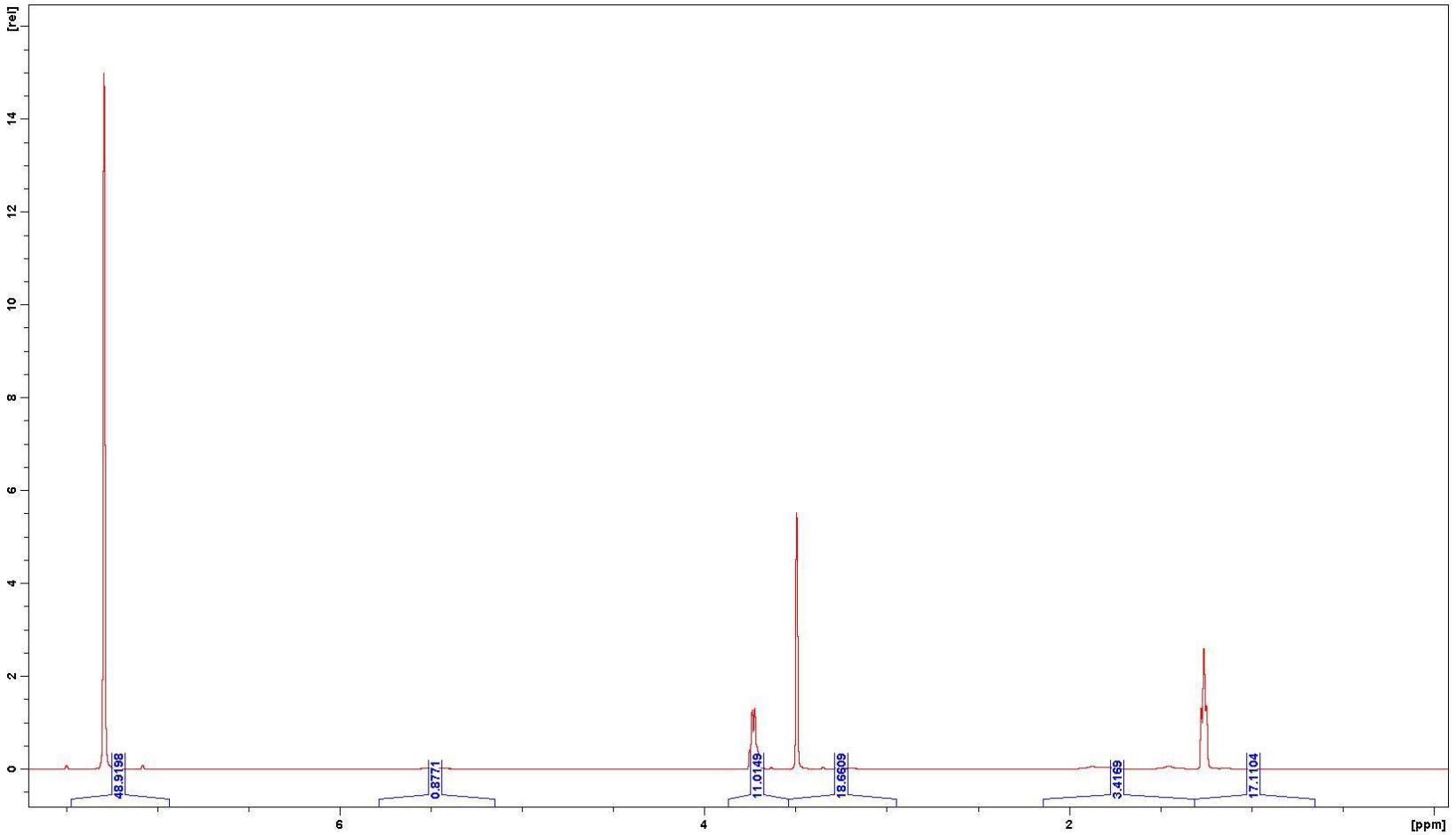
[rel]
14
12
10
8
6
4
2
0
48.9198
0.8771
11.0149
18.6609
3.4169
17.1104
6
4
2
[ppm]

B5 No Proteinase K in Buffer – Gasification

GC Data – Gas collected from reactor

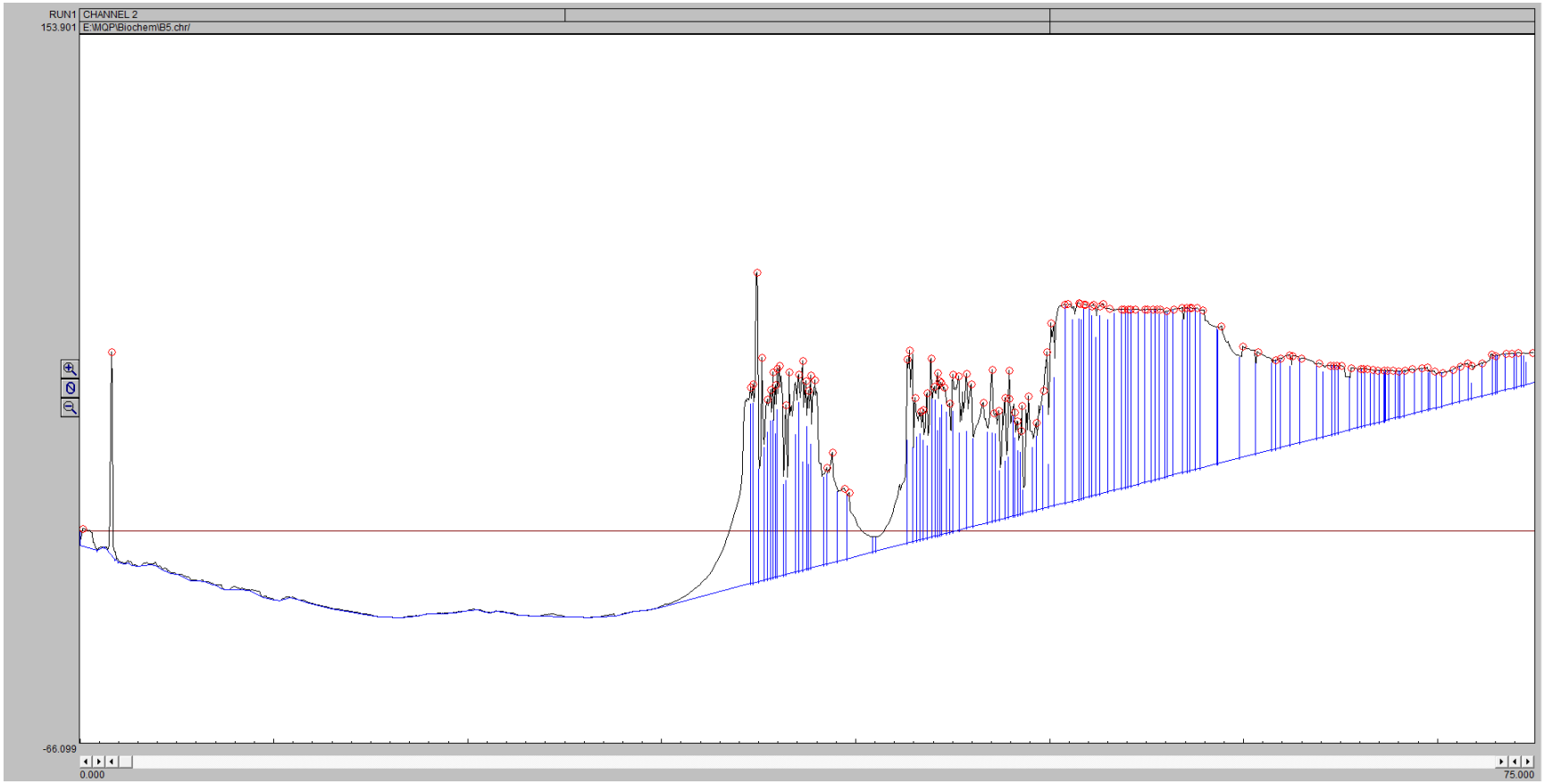

GC Data – Liquids collected from cold trap

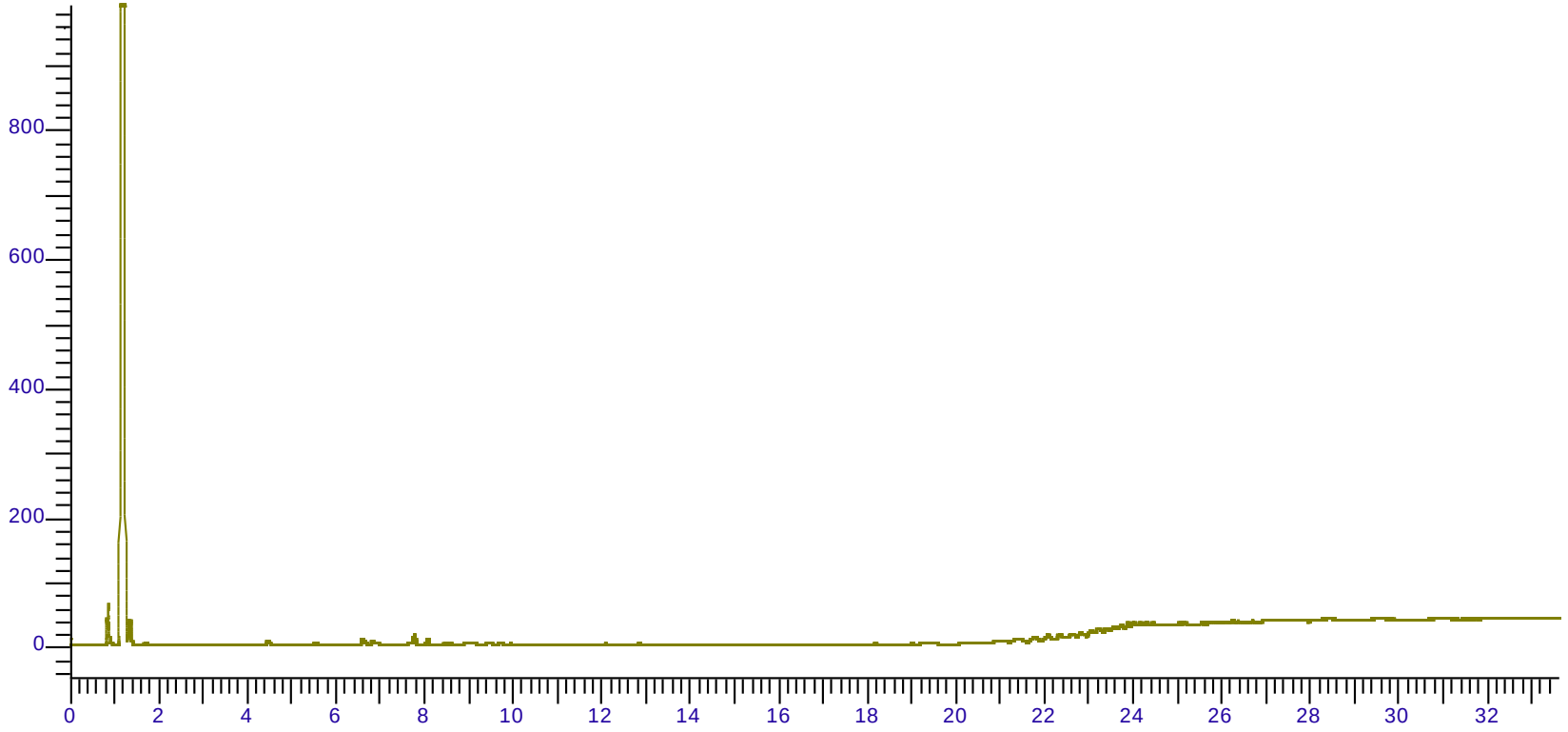

NMR Data

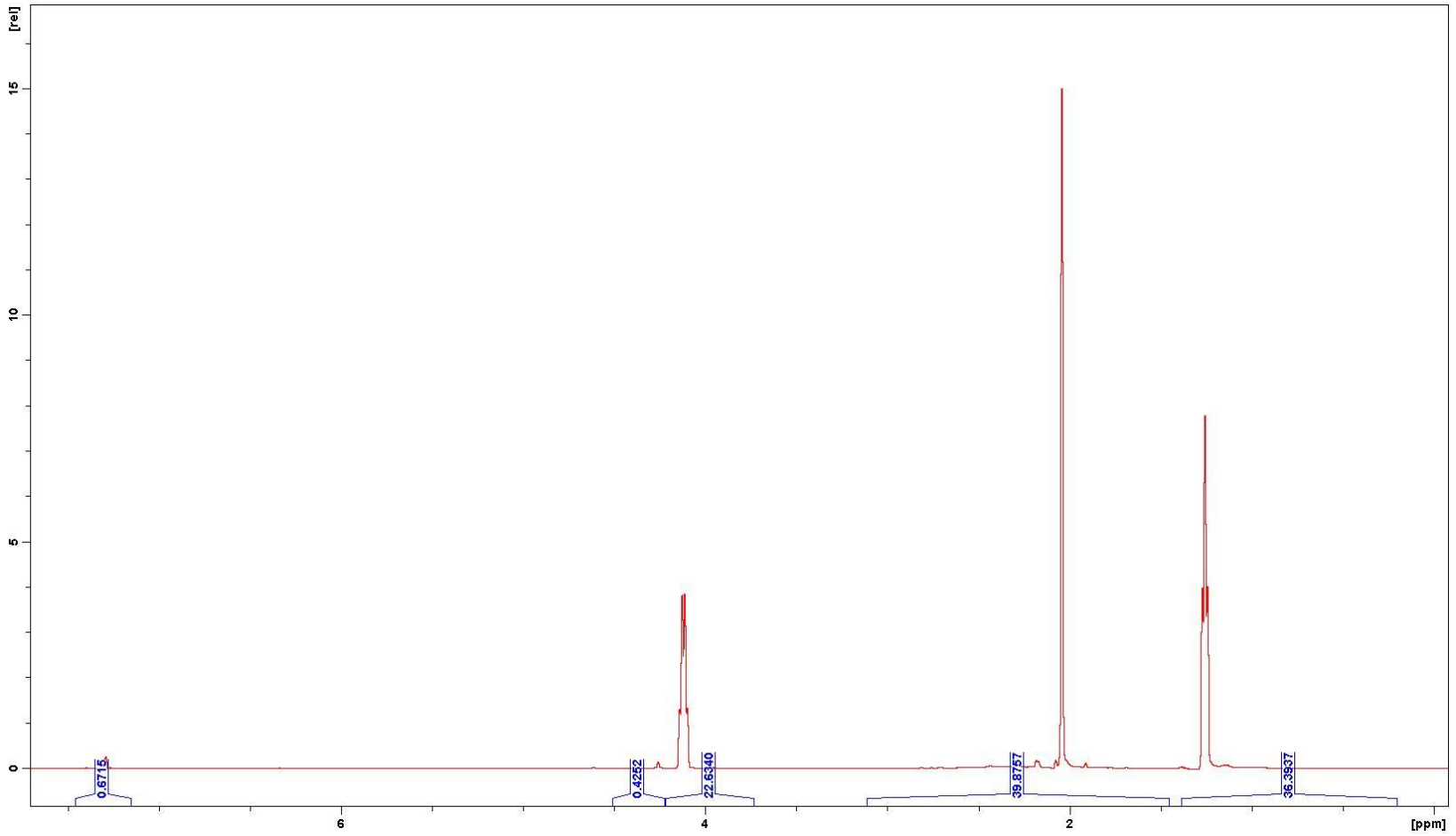

B6 No Proteinase K in Buffer – Transesterification

GC Data – Liquids collected from reactor

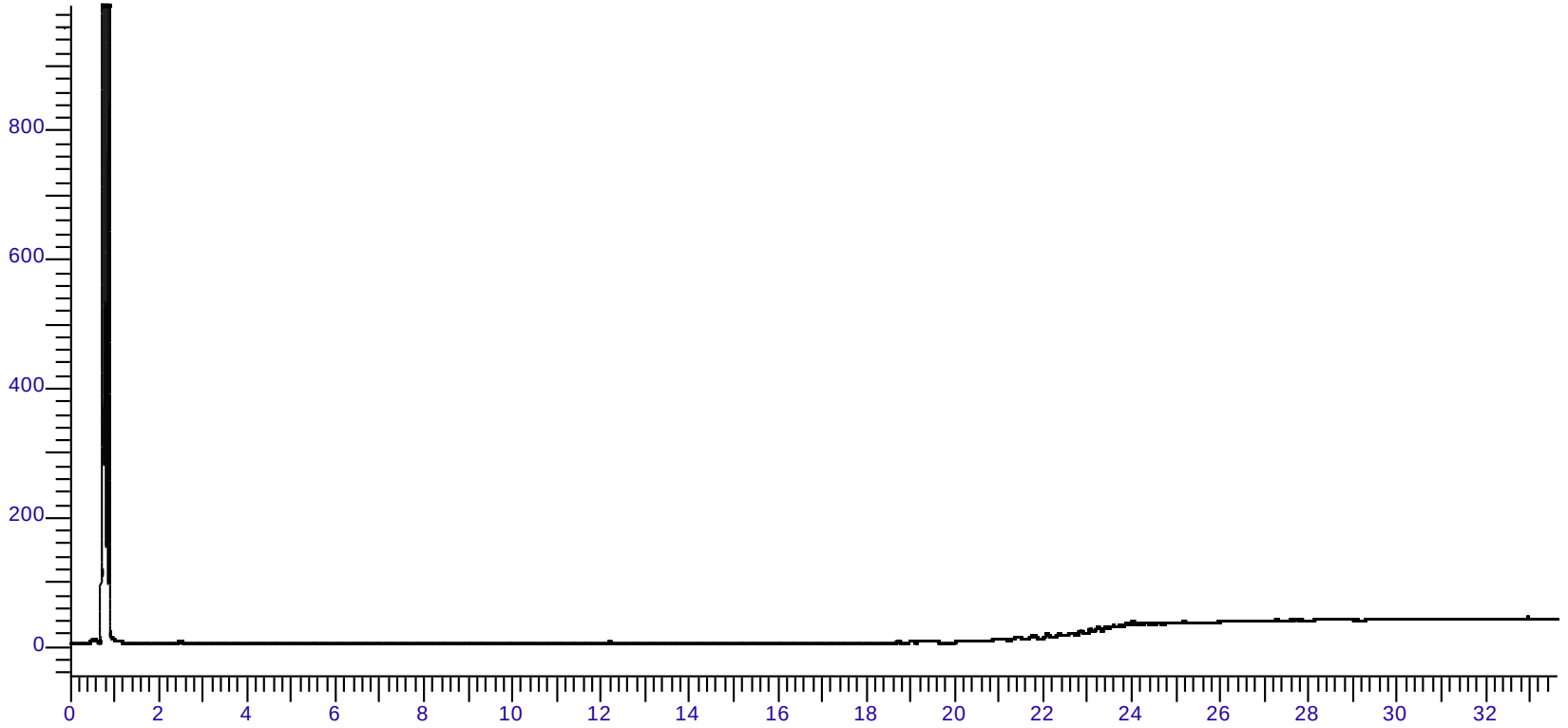

NMR Data

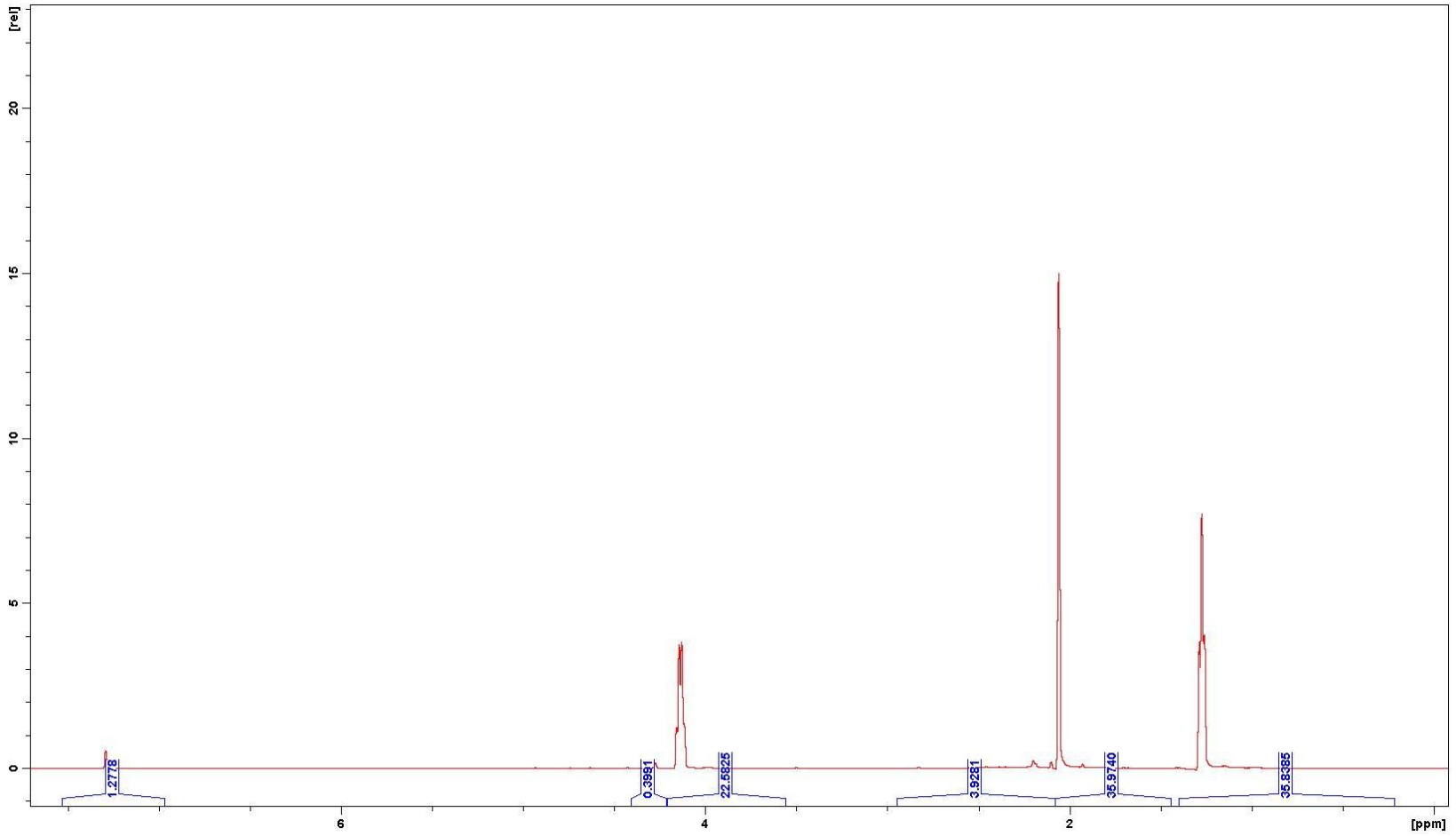
[rel]
20
15
10
5
0
1.2778
0.3991
22.5825
3.9281
35.9740
35.8385
6
4
2
[ppm]

B7 Control Lima Bean Transesterification

No liquids collected to analyze

B8 Control Lima Bean Gasification with Liquid in Reactor to Start and with Sparger

GC Data – Gas collected from reactor

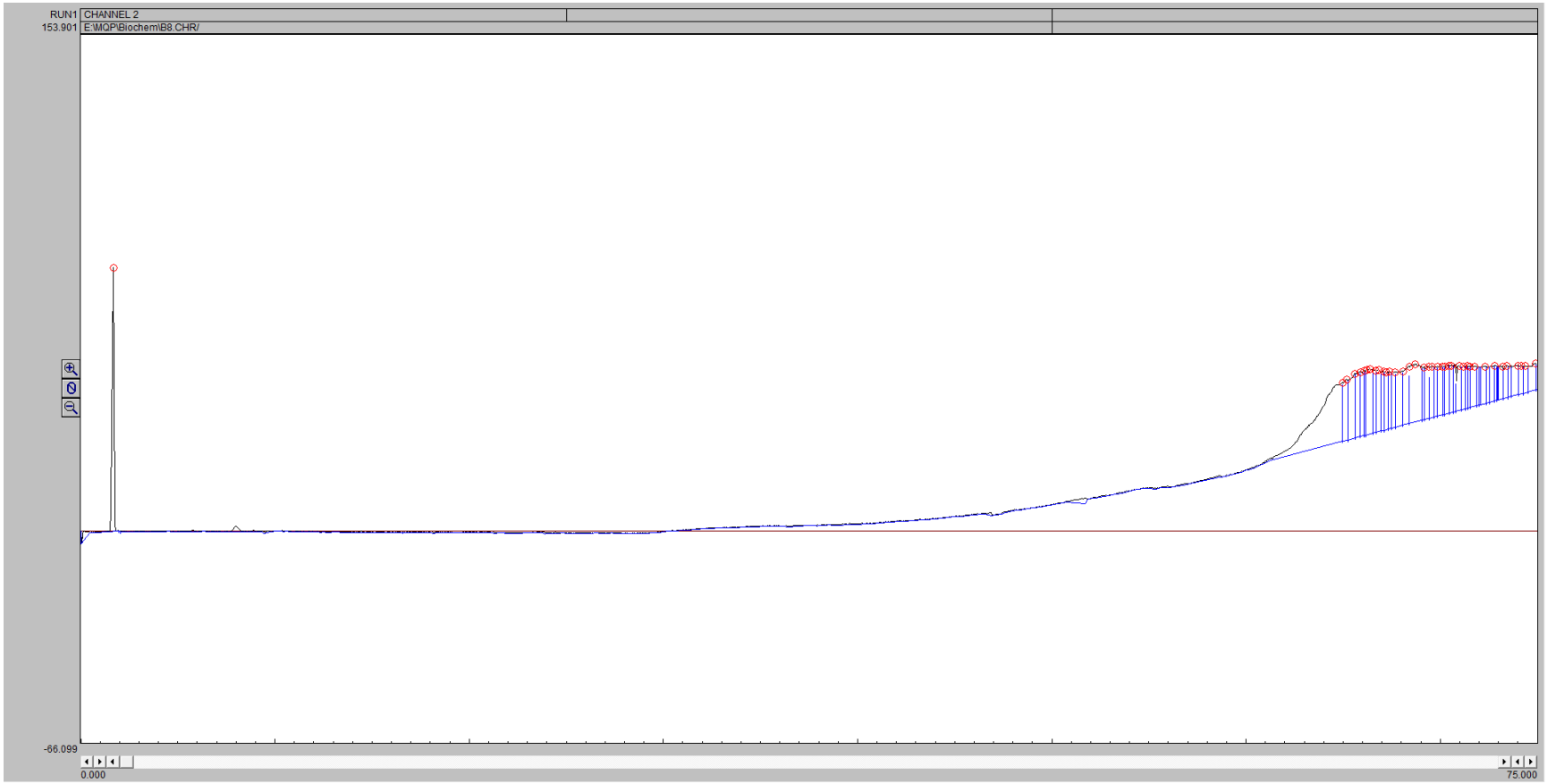

GC Data – Liquids collected from cold trap

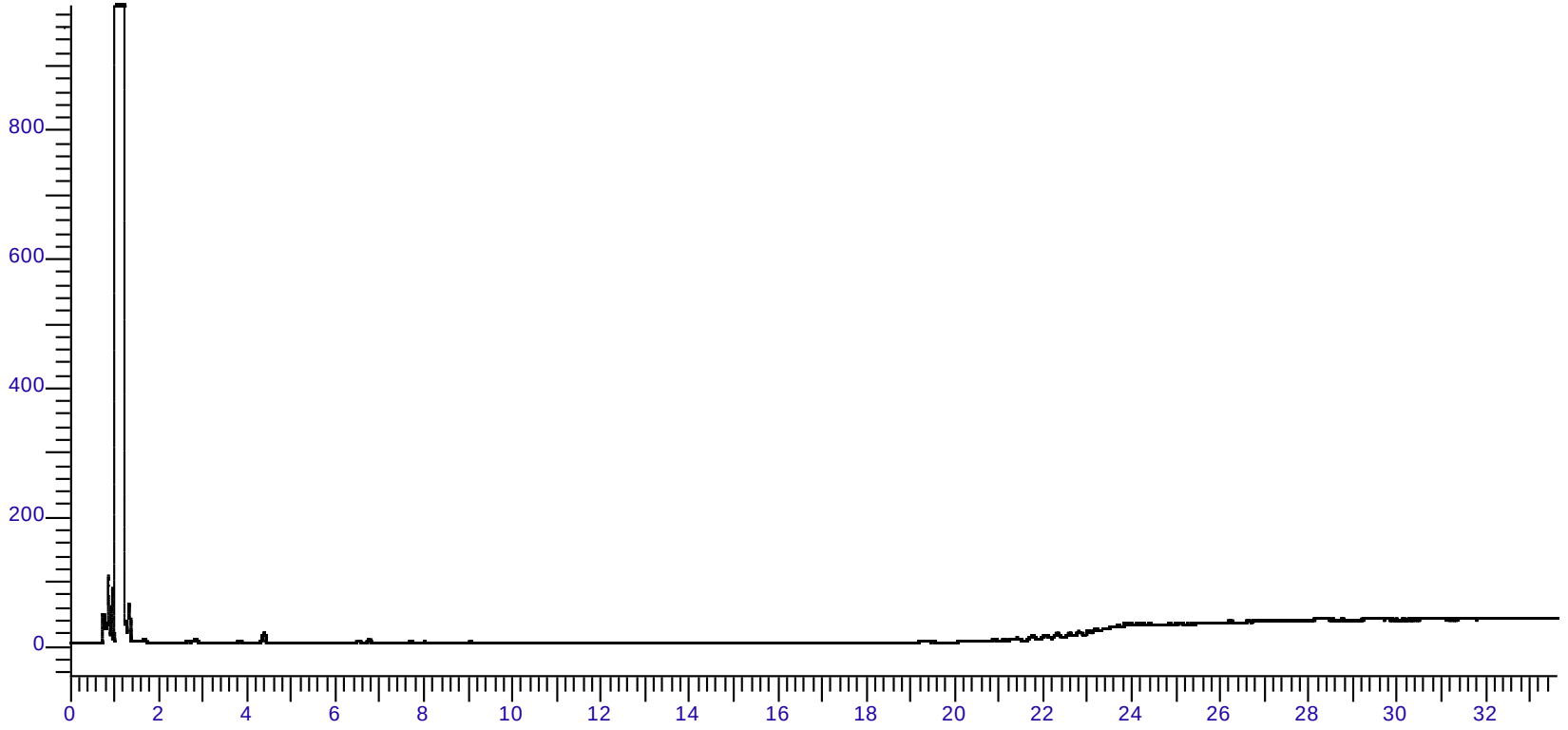

NMR Data

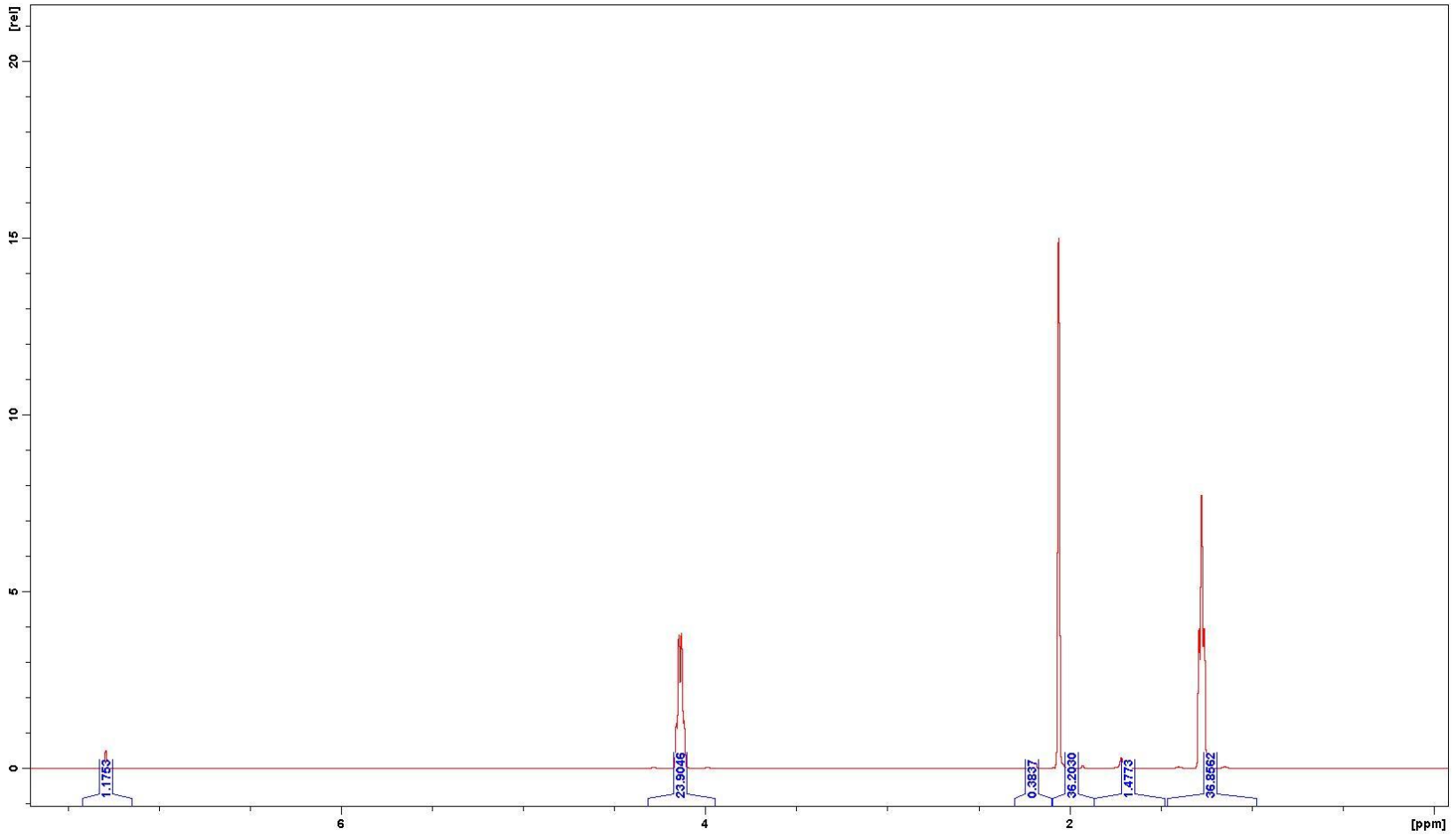
[rel]
20
15
10
5
0
1.1753
23.9046
0.3837
36.2030
1.4773
36.8562
6
4
2
[ppm]

B9 Control Lima Bean Gasification with Only a Sparger

GC Data – Gas collected from reactor

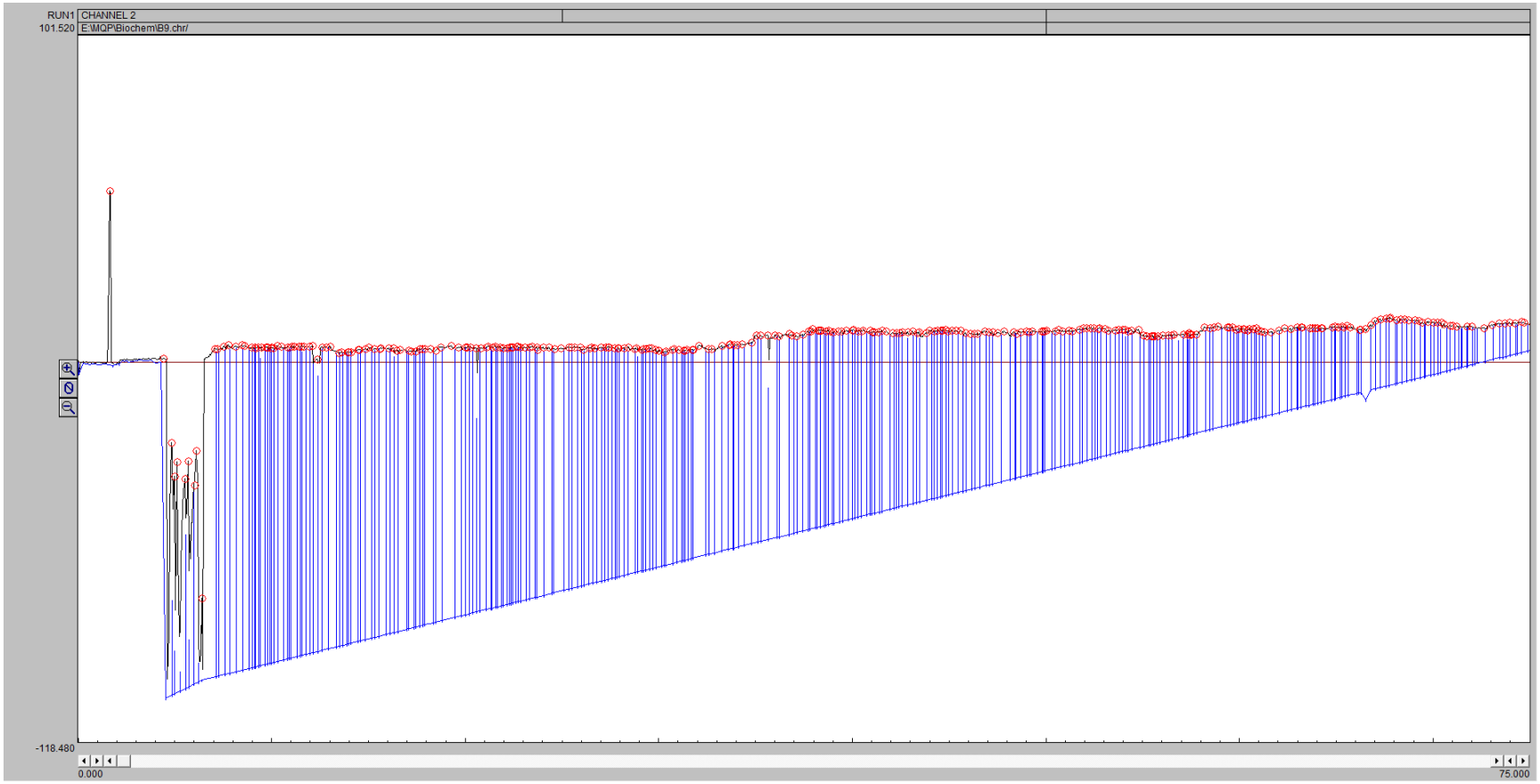

GC Data – Liquids collected from cold trap

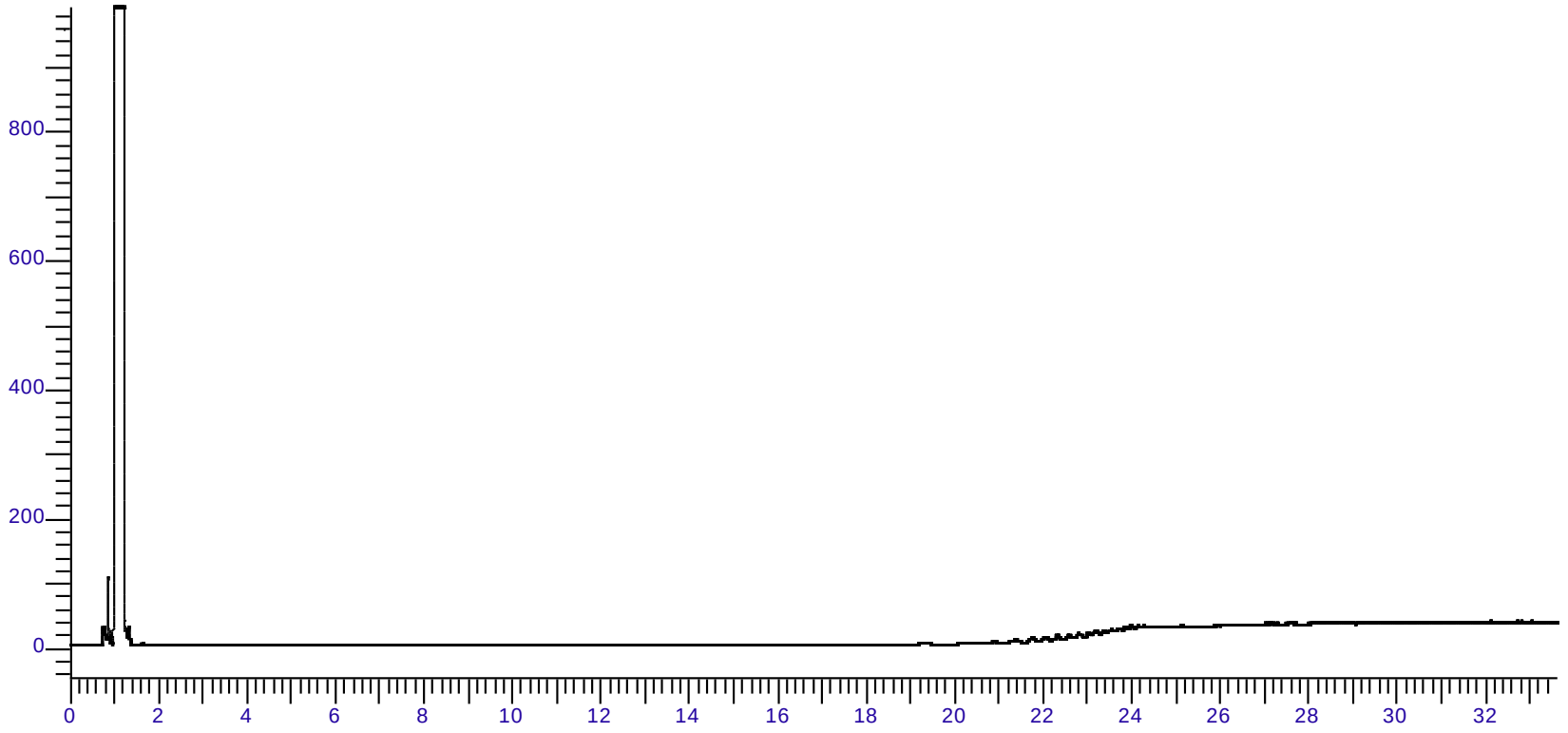

NMR Data

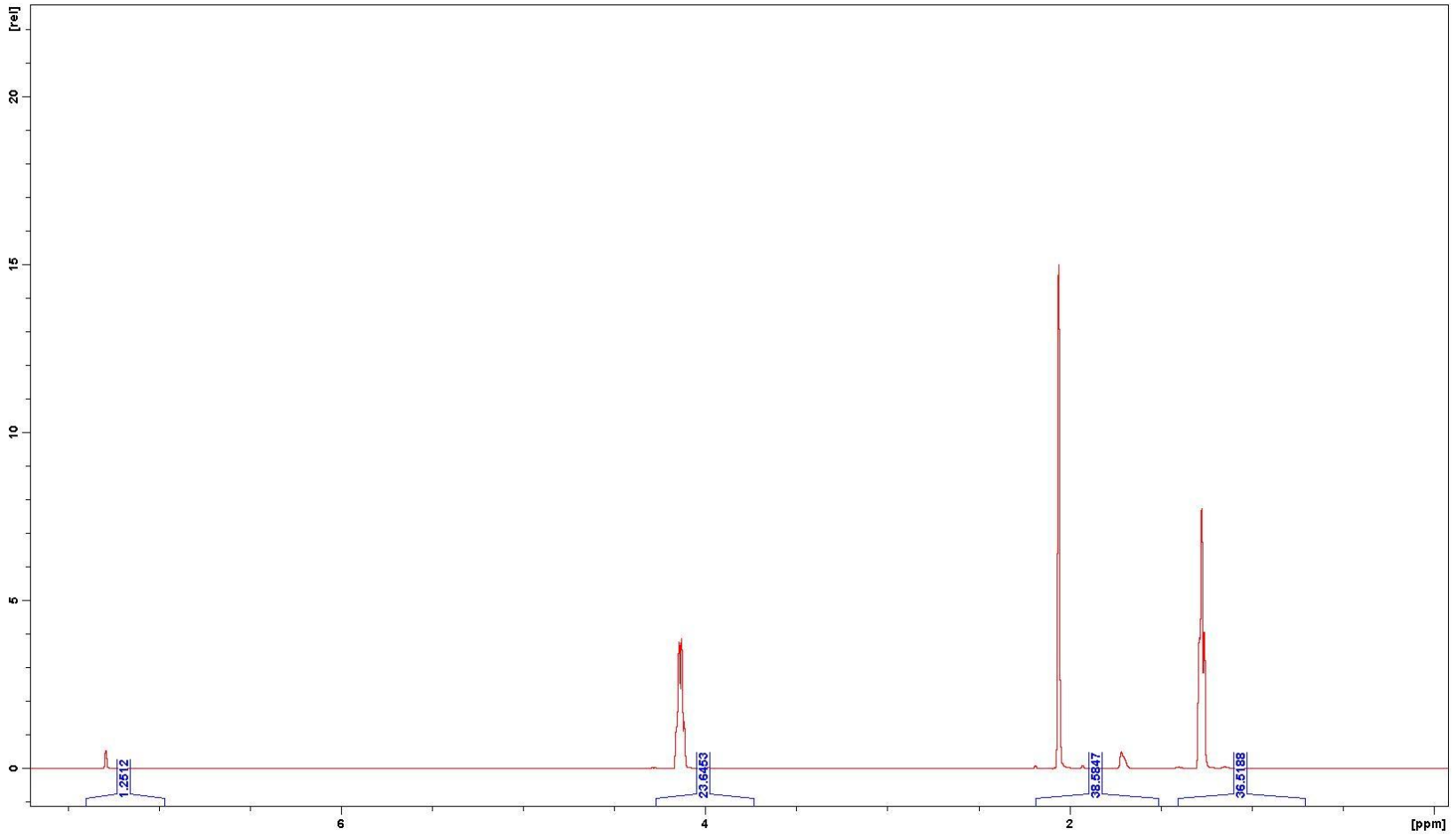

Appendix G GC and NMR Analysis of Control Samples

Butyric Acid

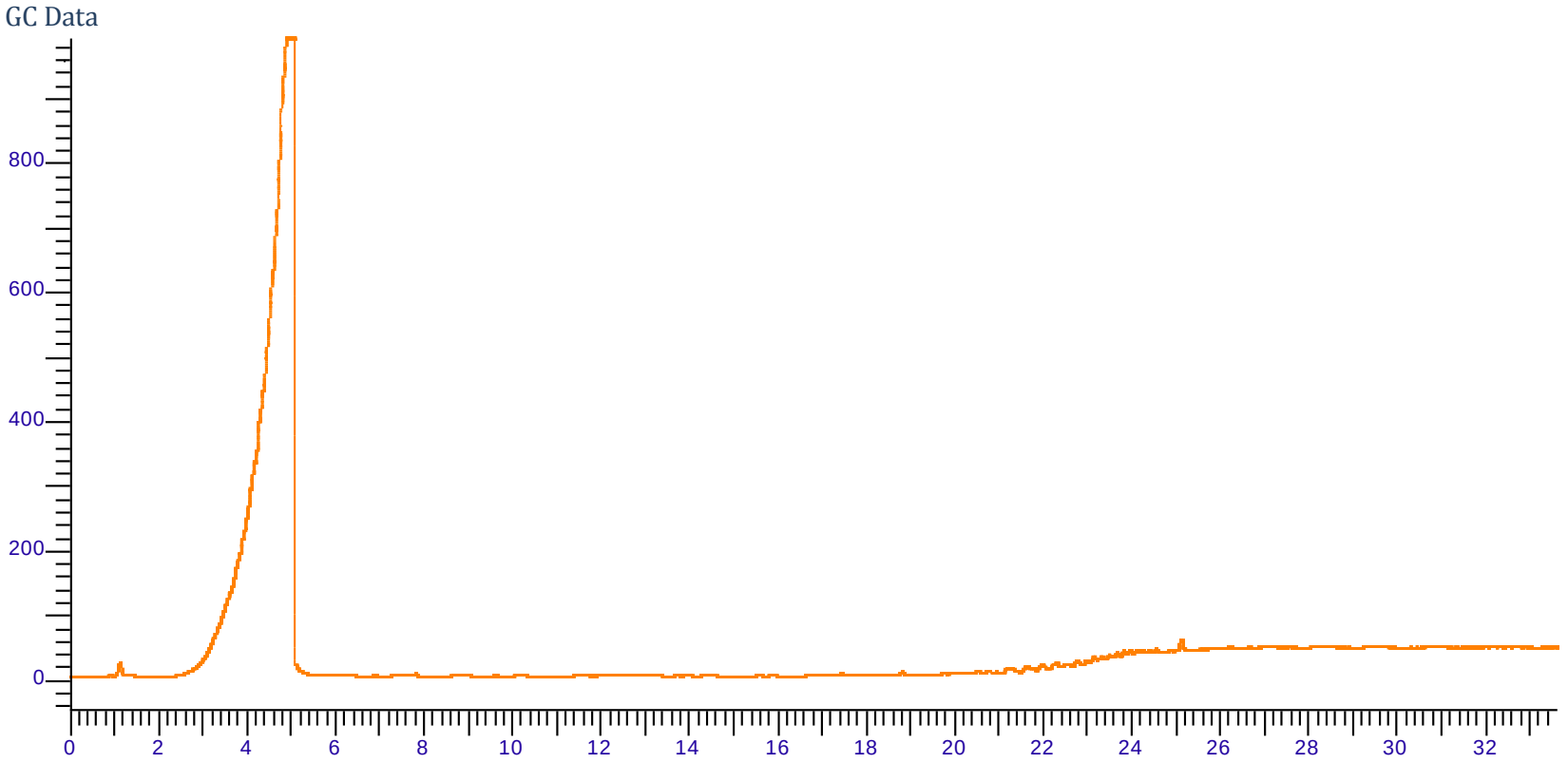

NMR Data

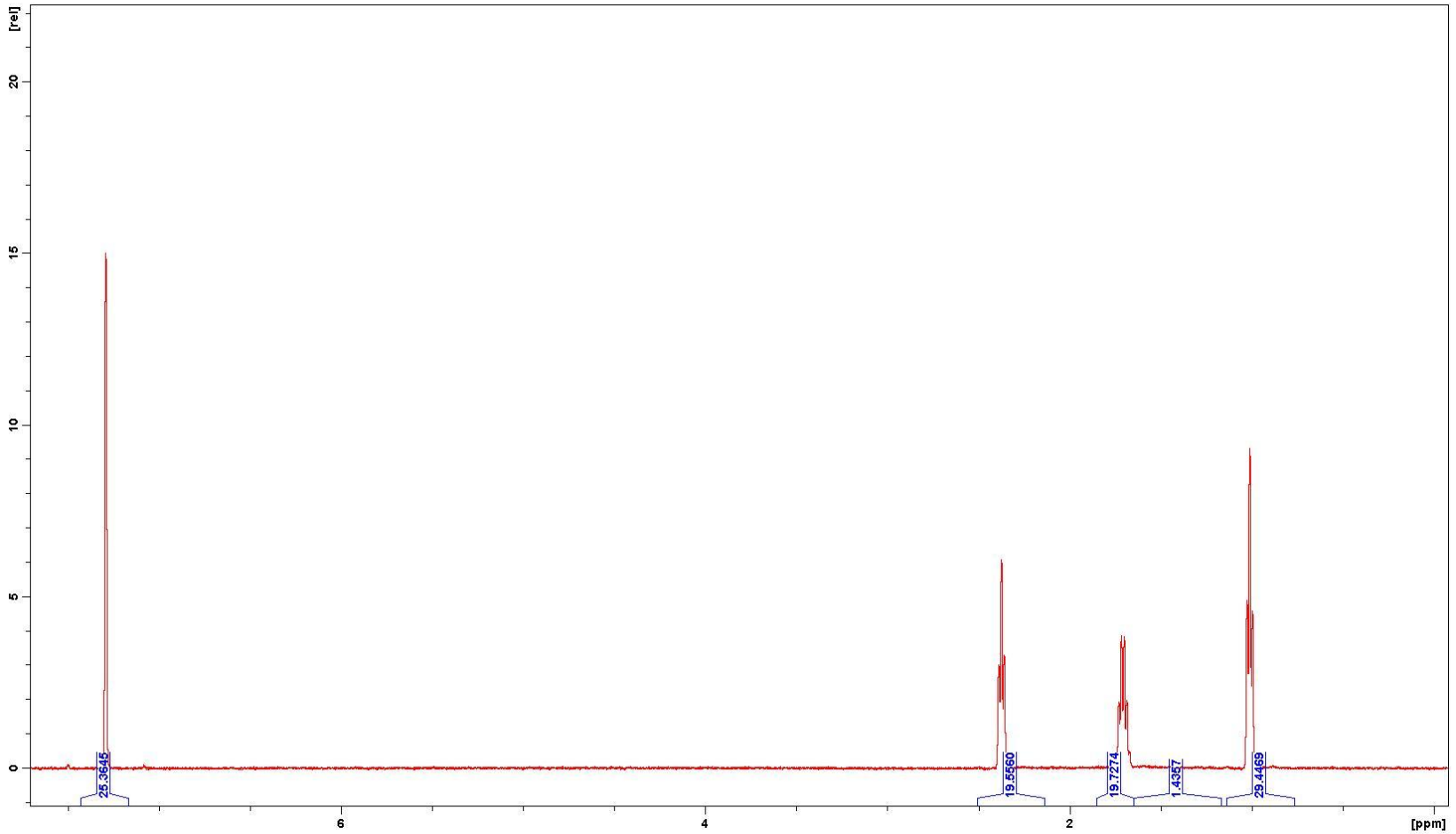

Ethyl Acetate

GC Data

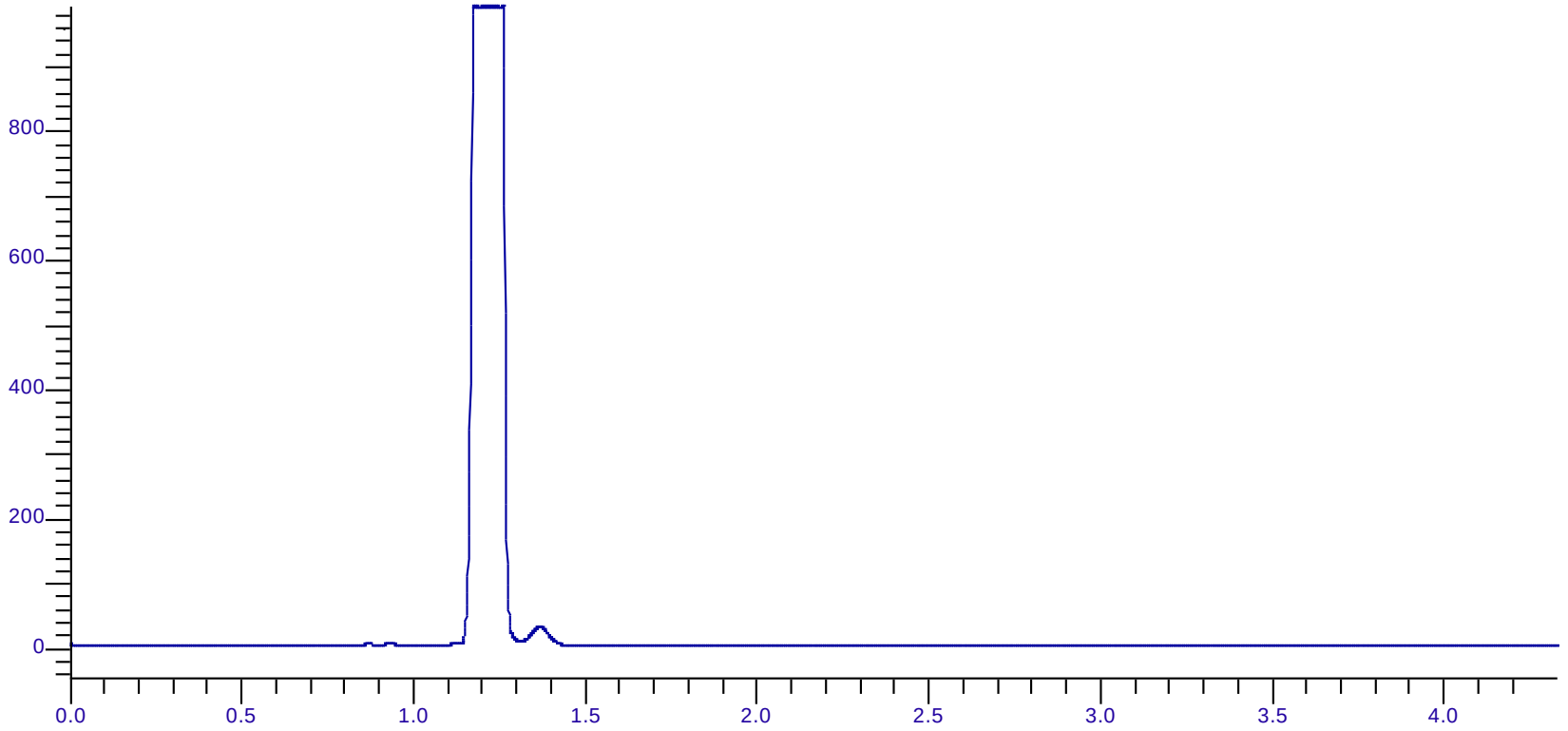

NMR Data

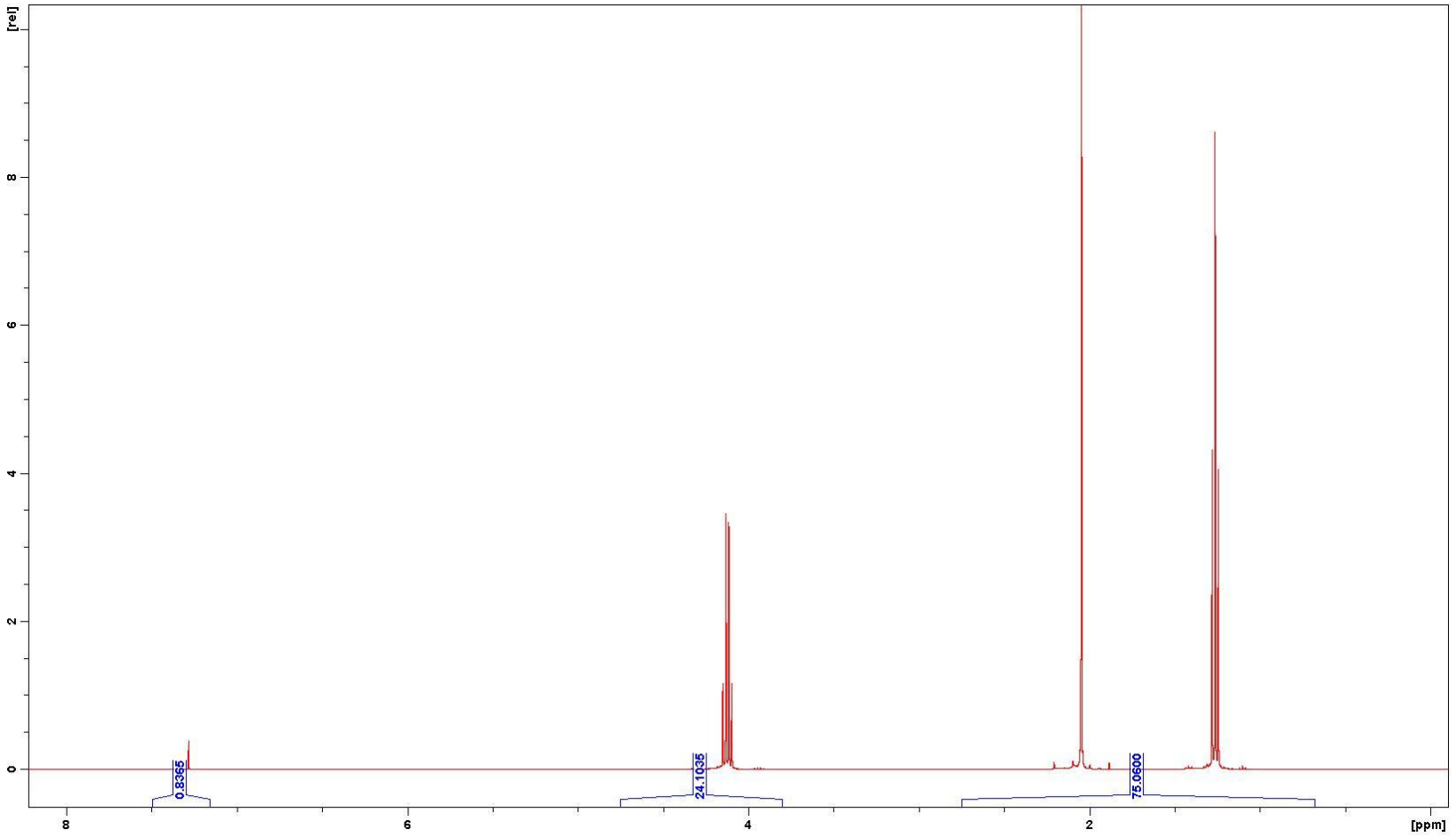

Glycerol

GC Data

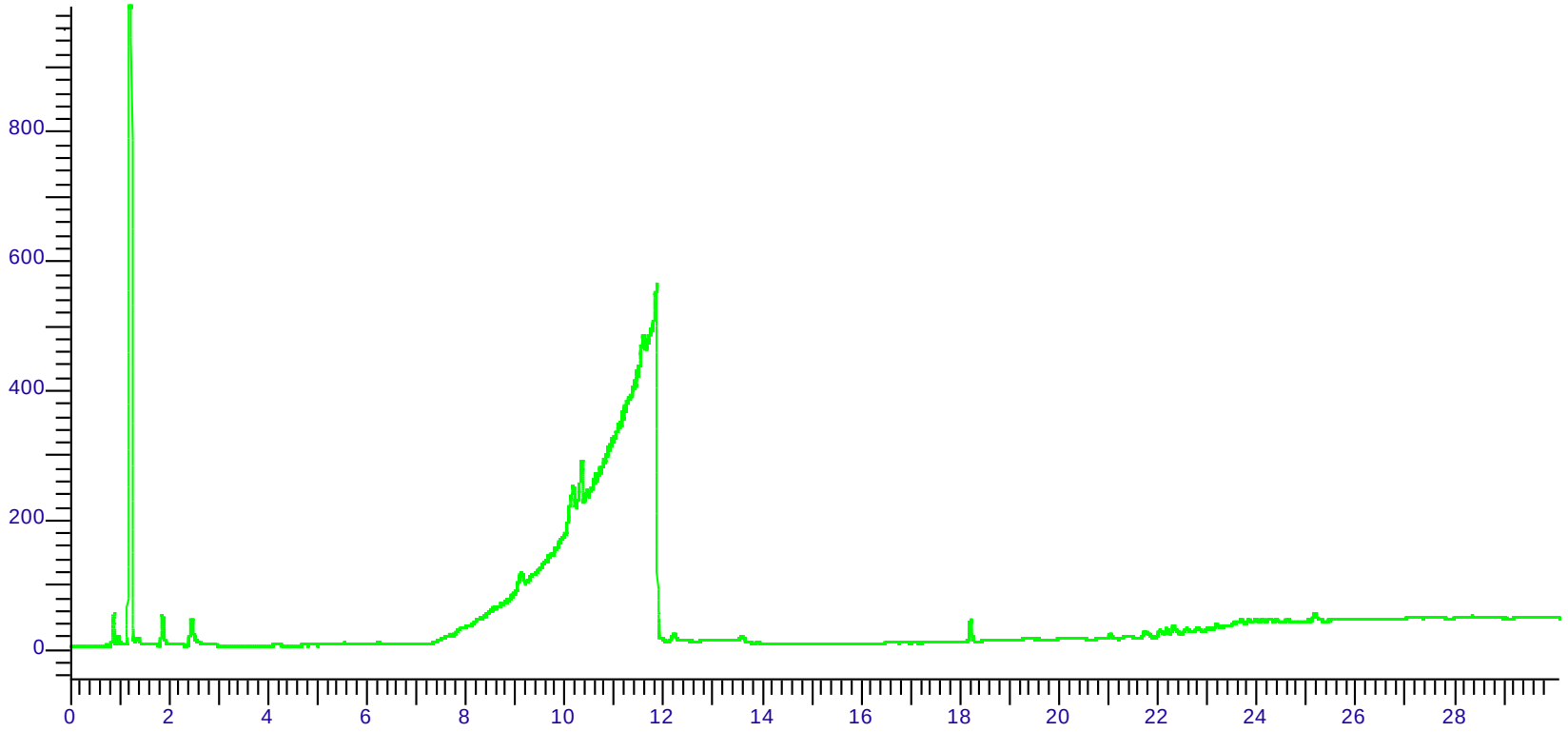

NMR Data

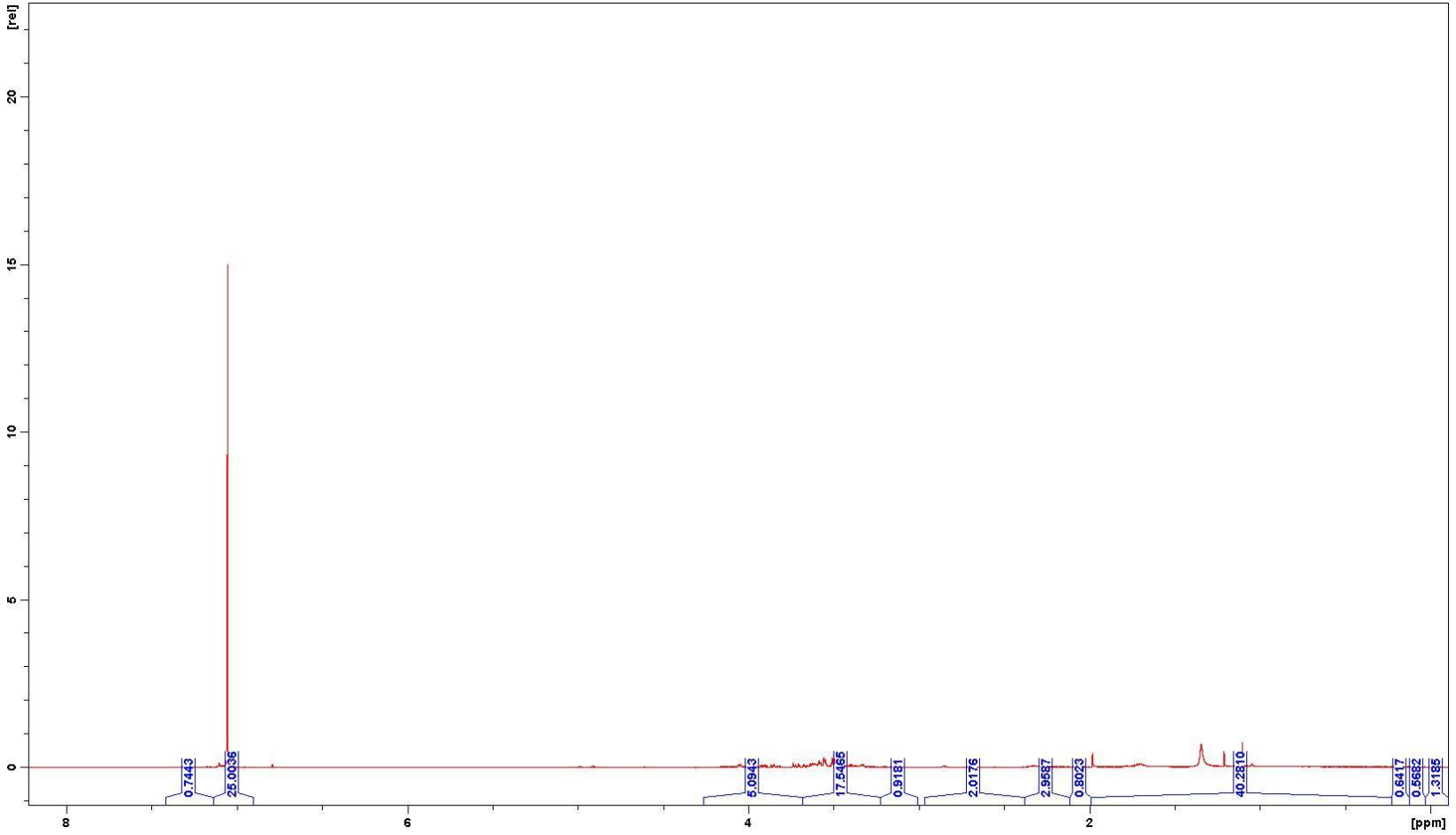
[rel]
20
15
10
5
0
0.7443
25.0036
5.0943
17.5465
0.9181
2.0176
2.9587
0.8023
40.2810
0.6417
0.5682
1.3185
8
6
4
2
[ppm]

Methanol

GC Data

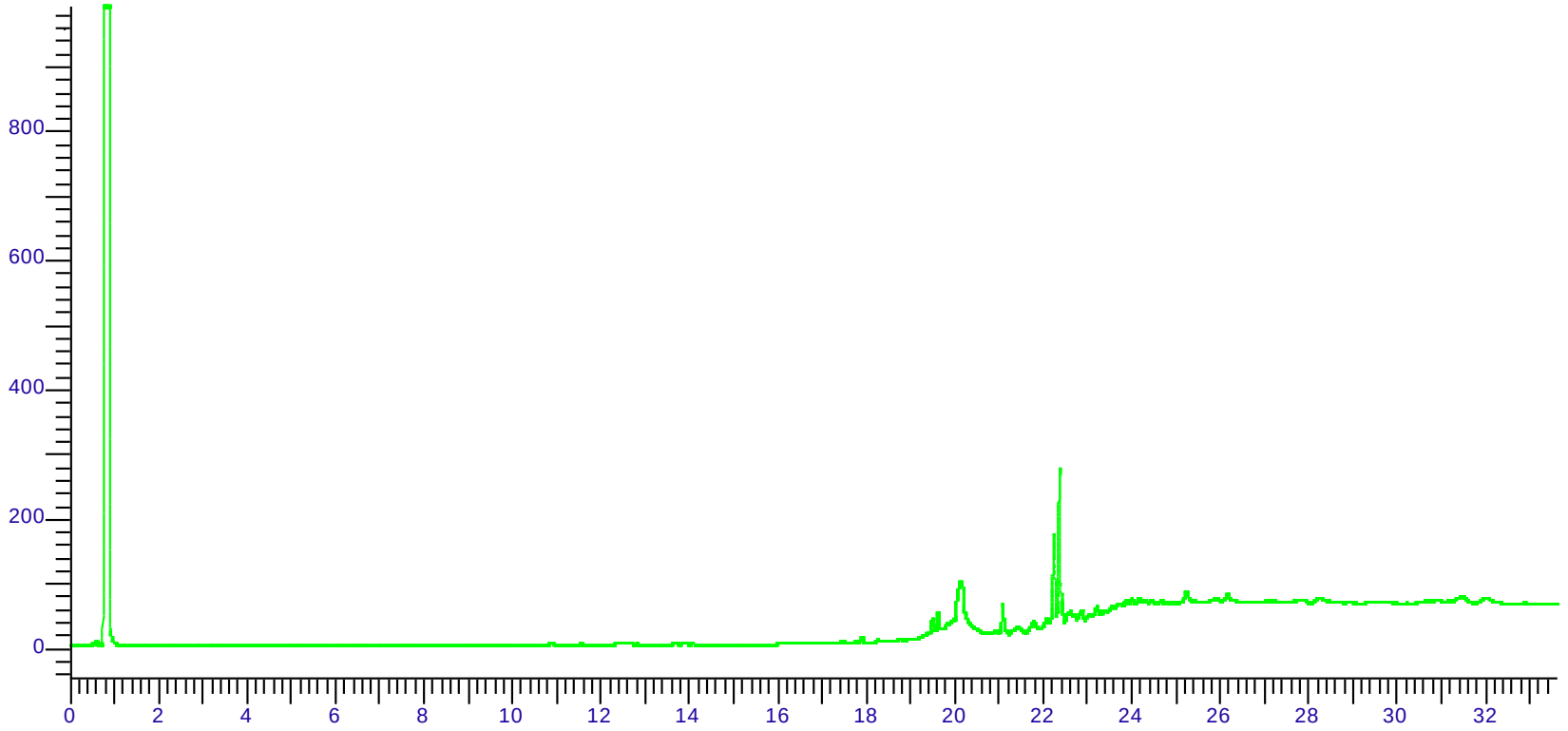

NMR Data

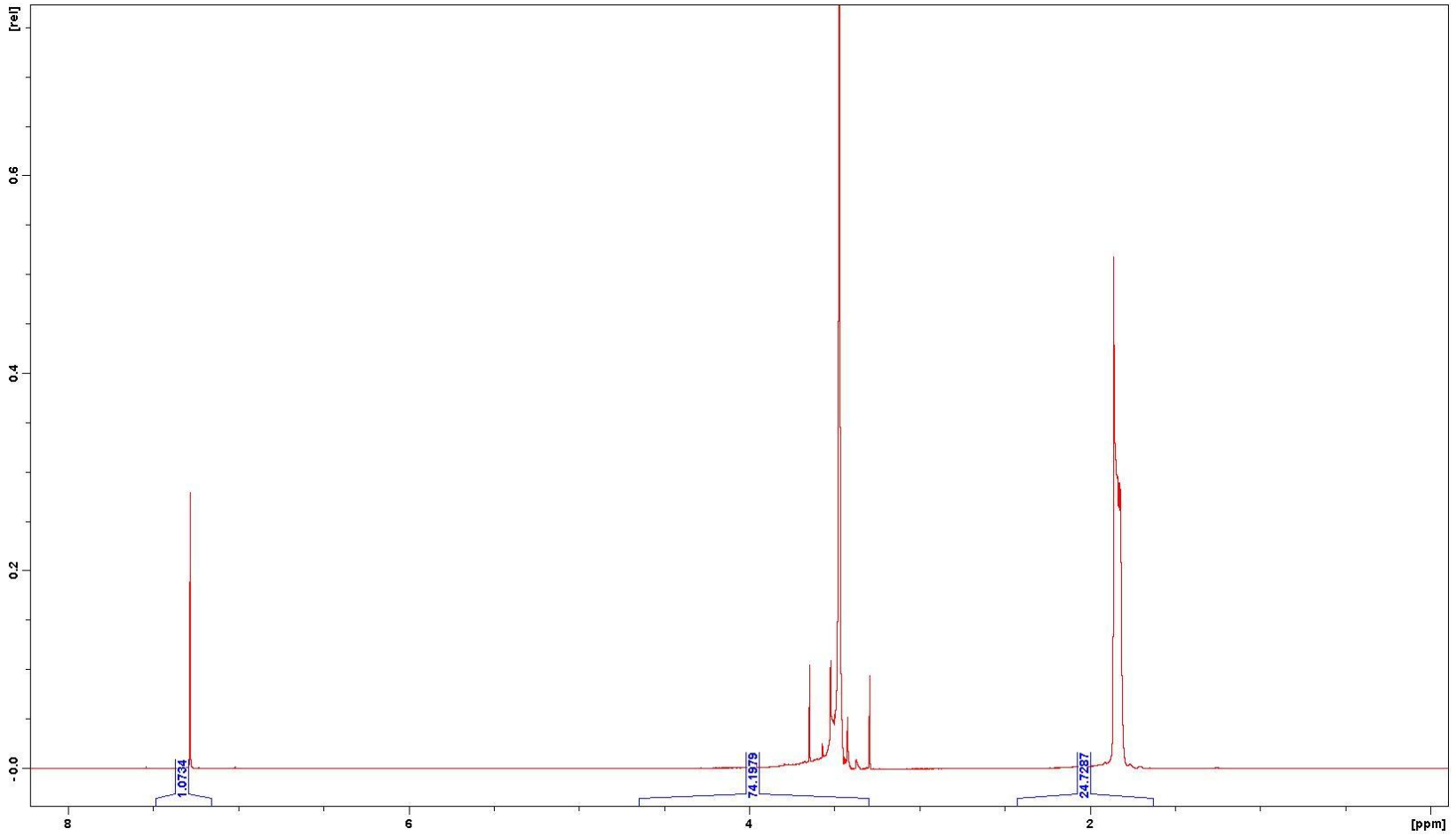

Methyl Butyrate

GC Data

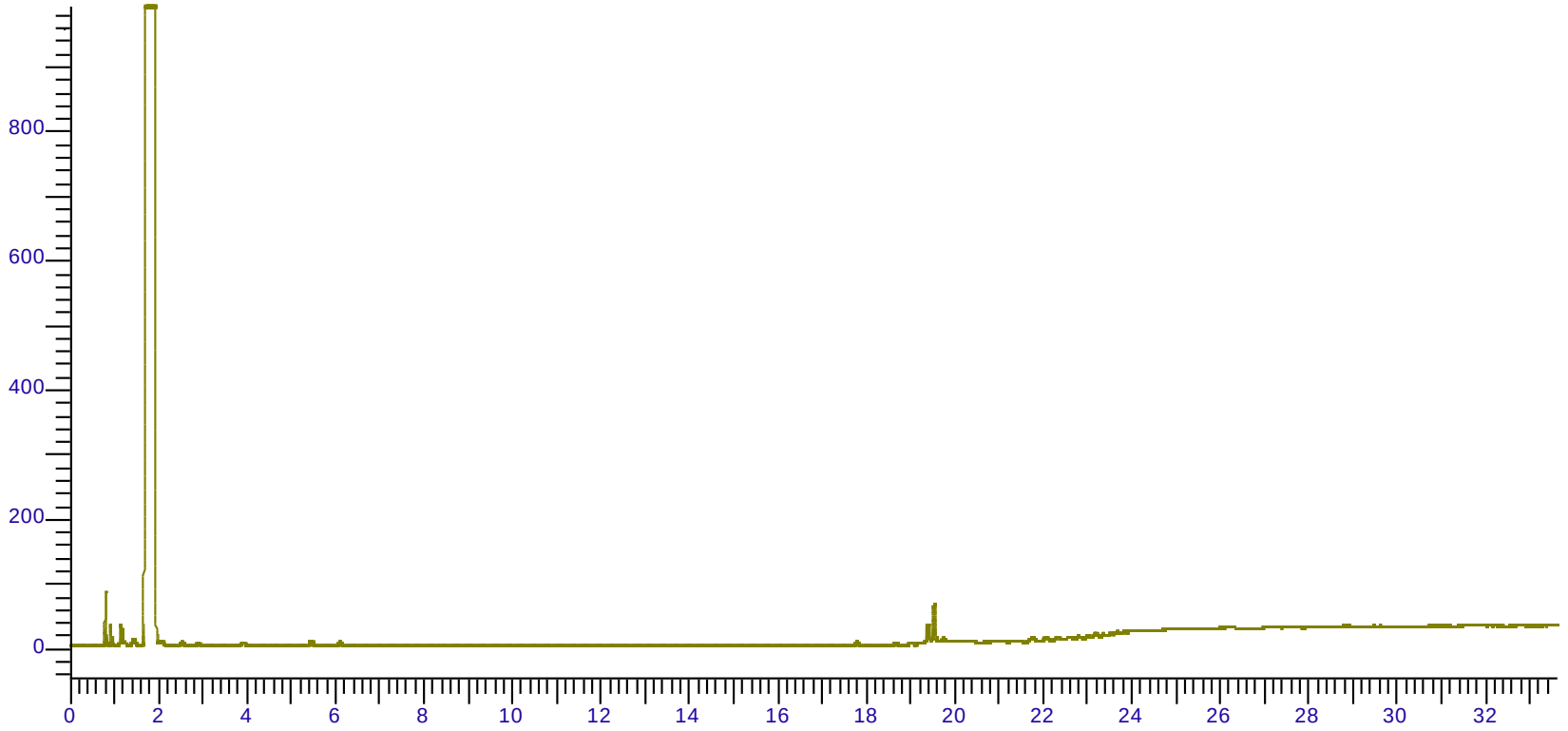

NMR Data

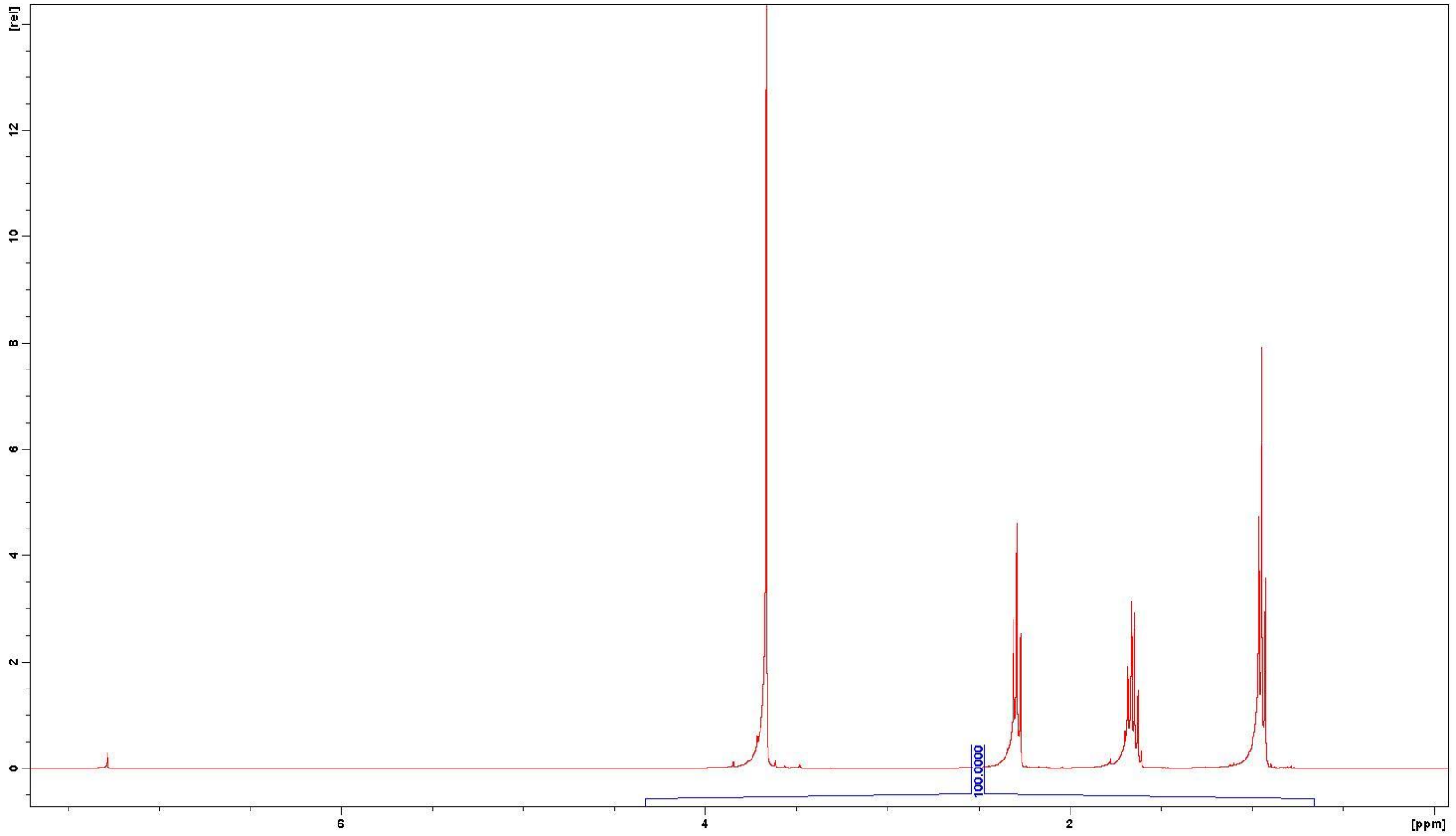

Tributyrin

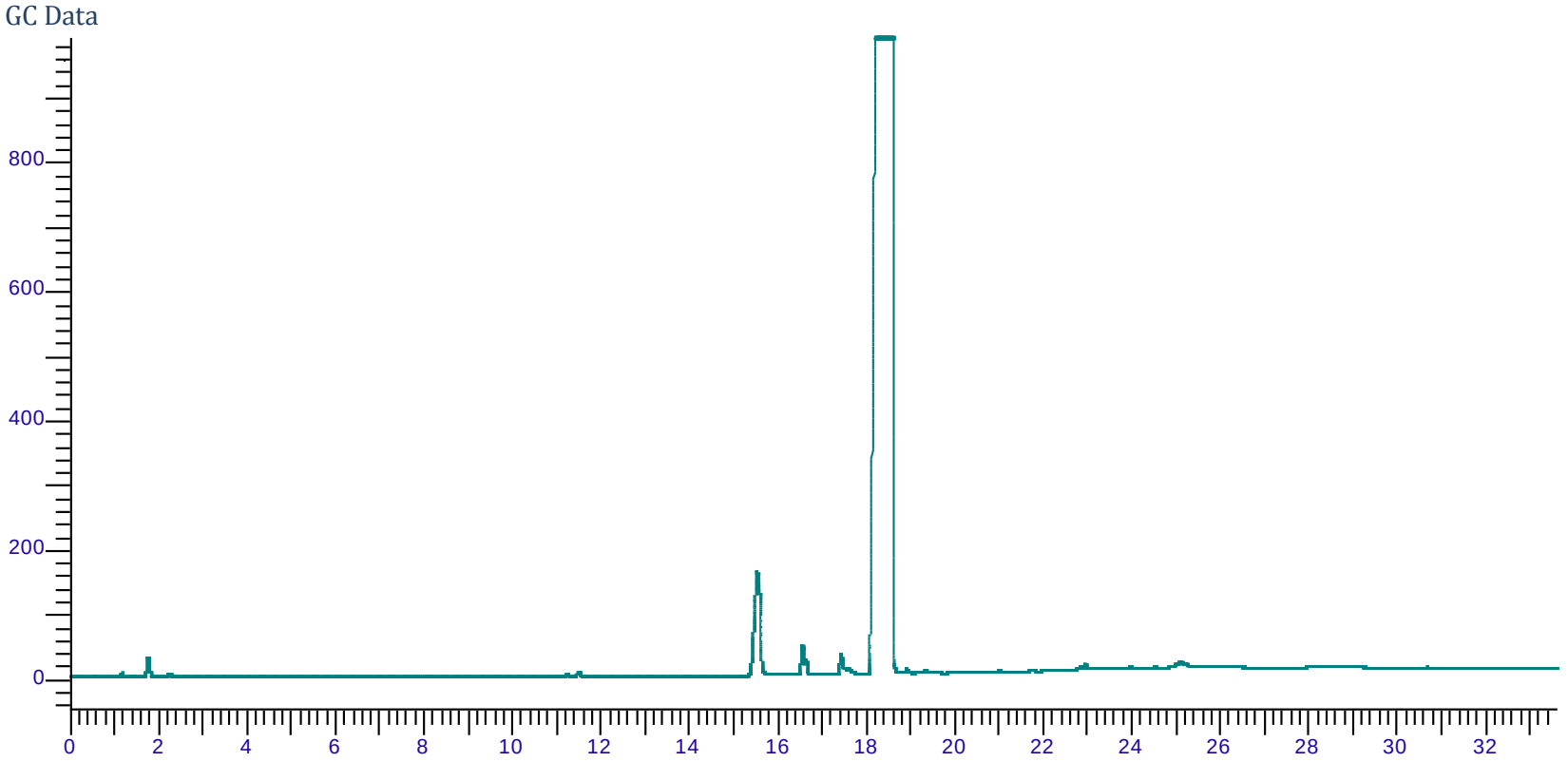

NMR Data

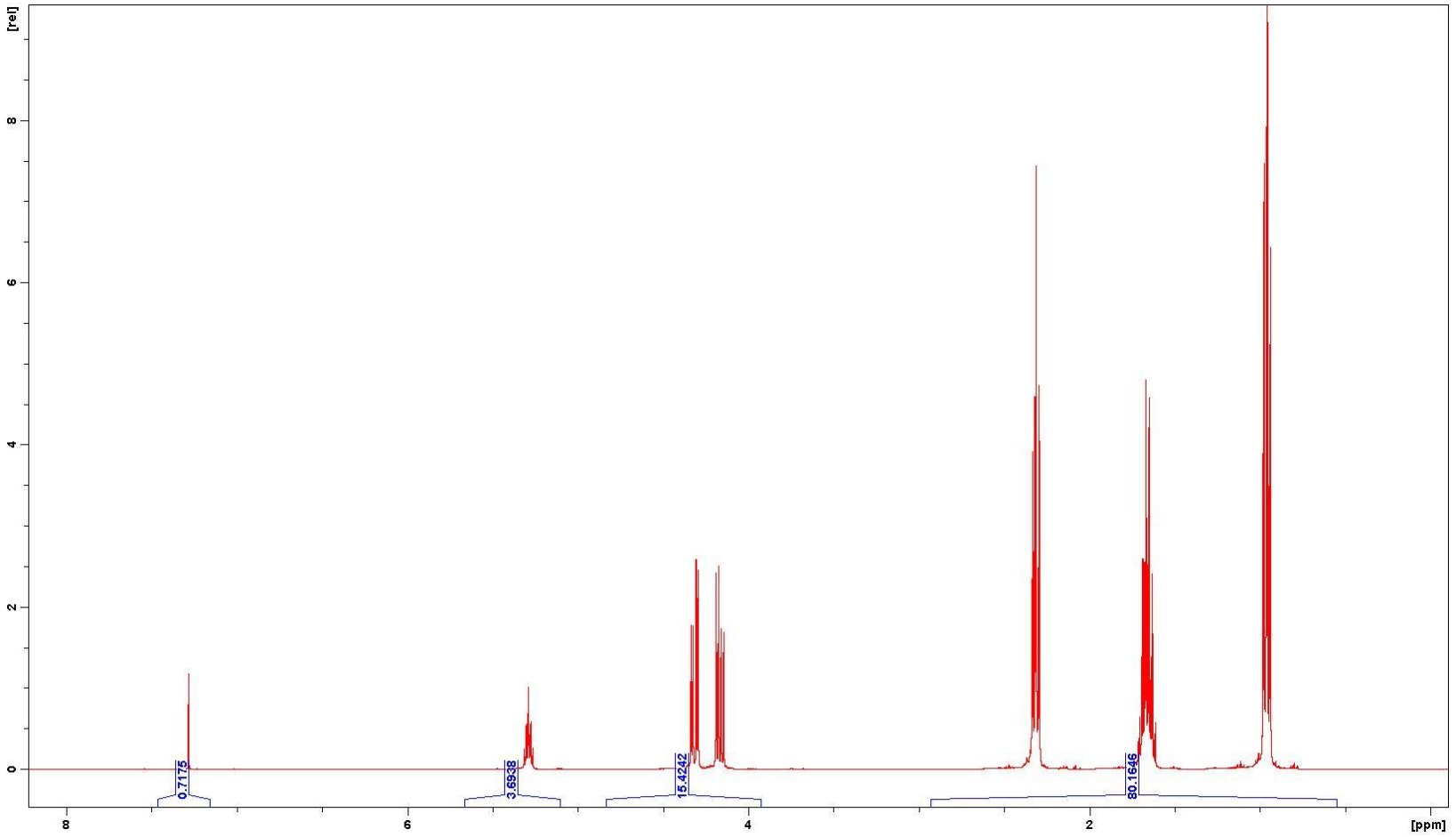

Vegetable Oil

GC Data

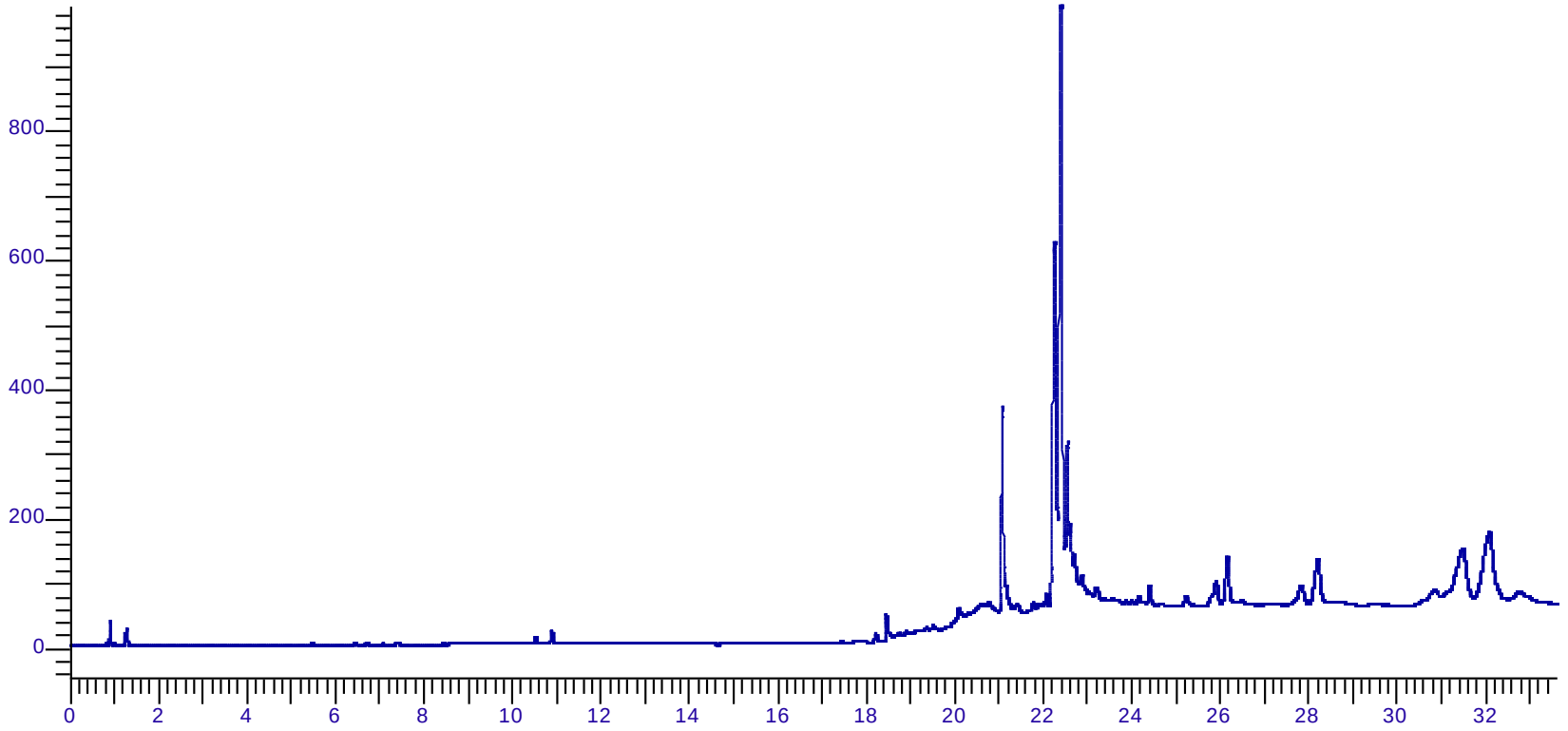

NMR Data

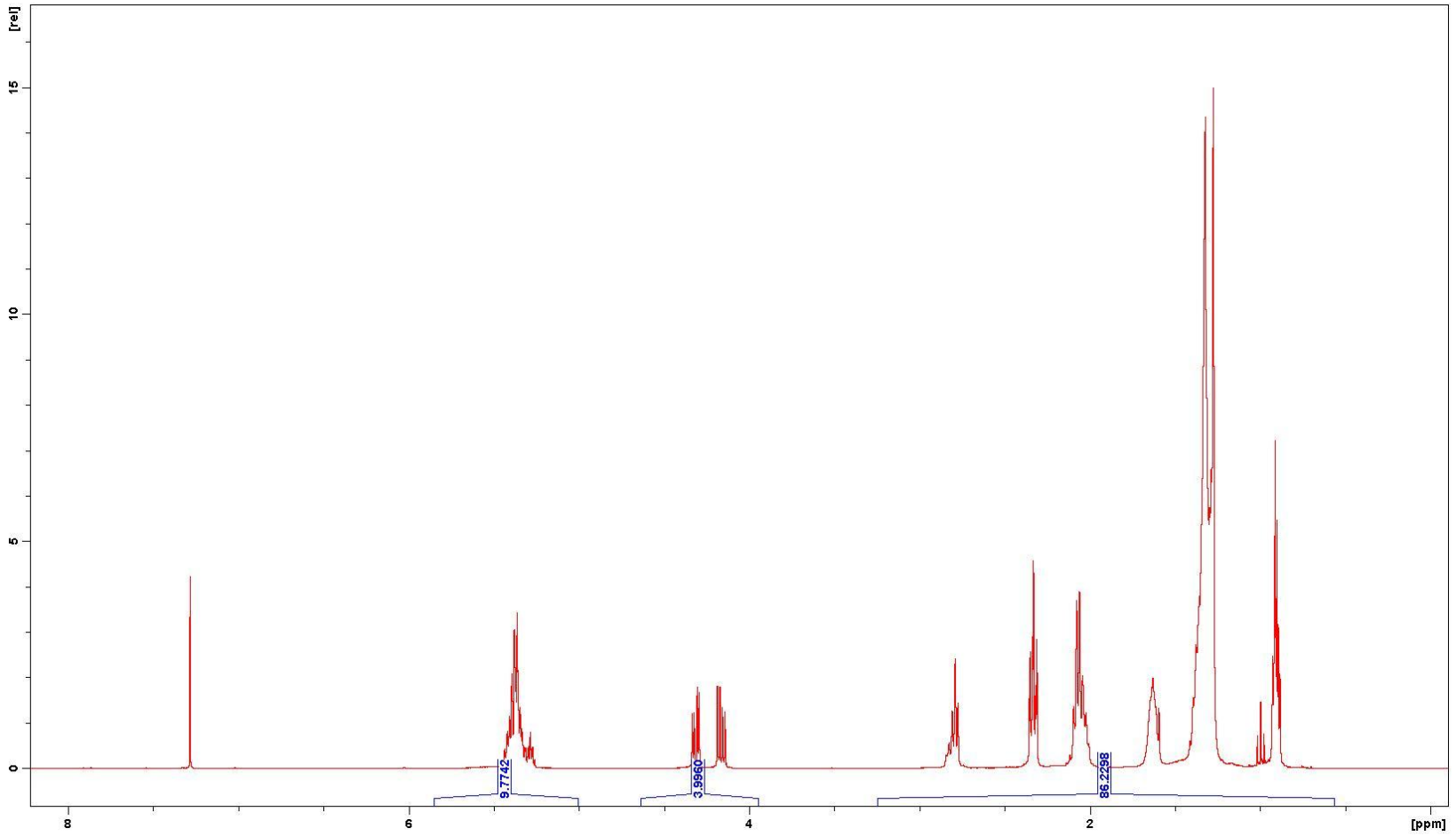

CO_2

Column 1

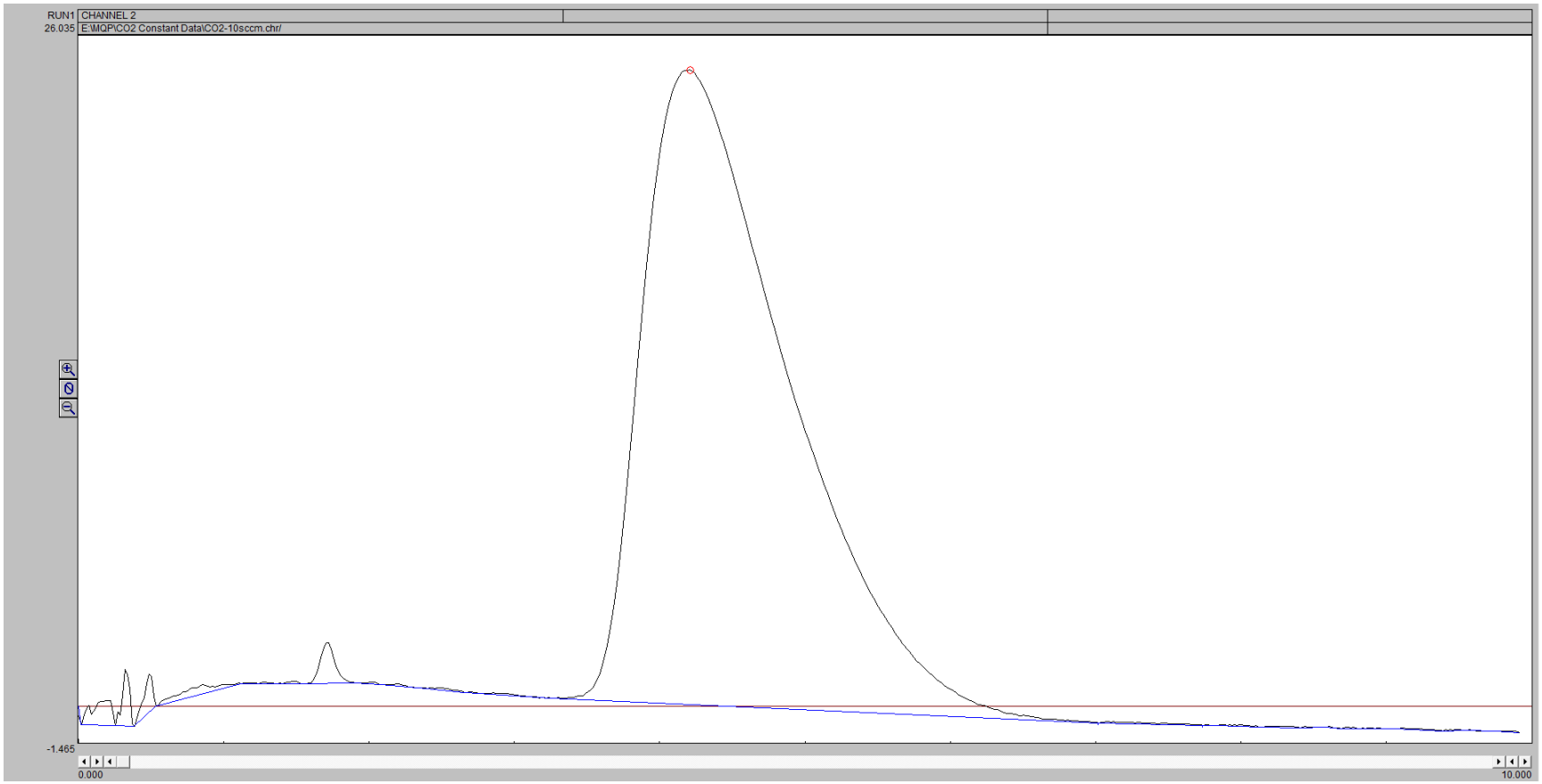
RUN1 CHANNEL 2
26.035 E:\MQP\CO2 Constant Data\CO2-10sccm.chr/
-1.465
0.000
10.000

Column 2

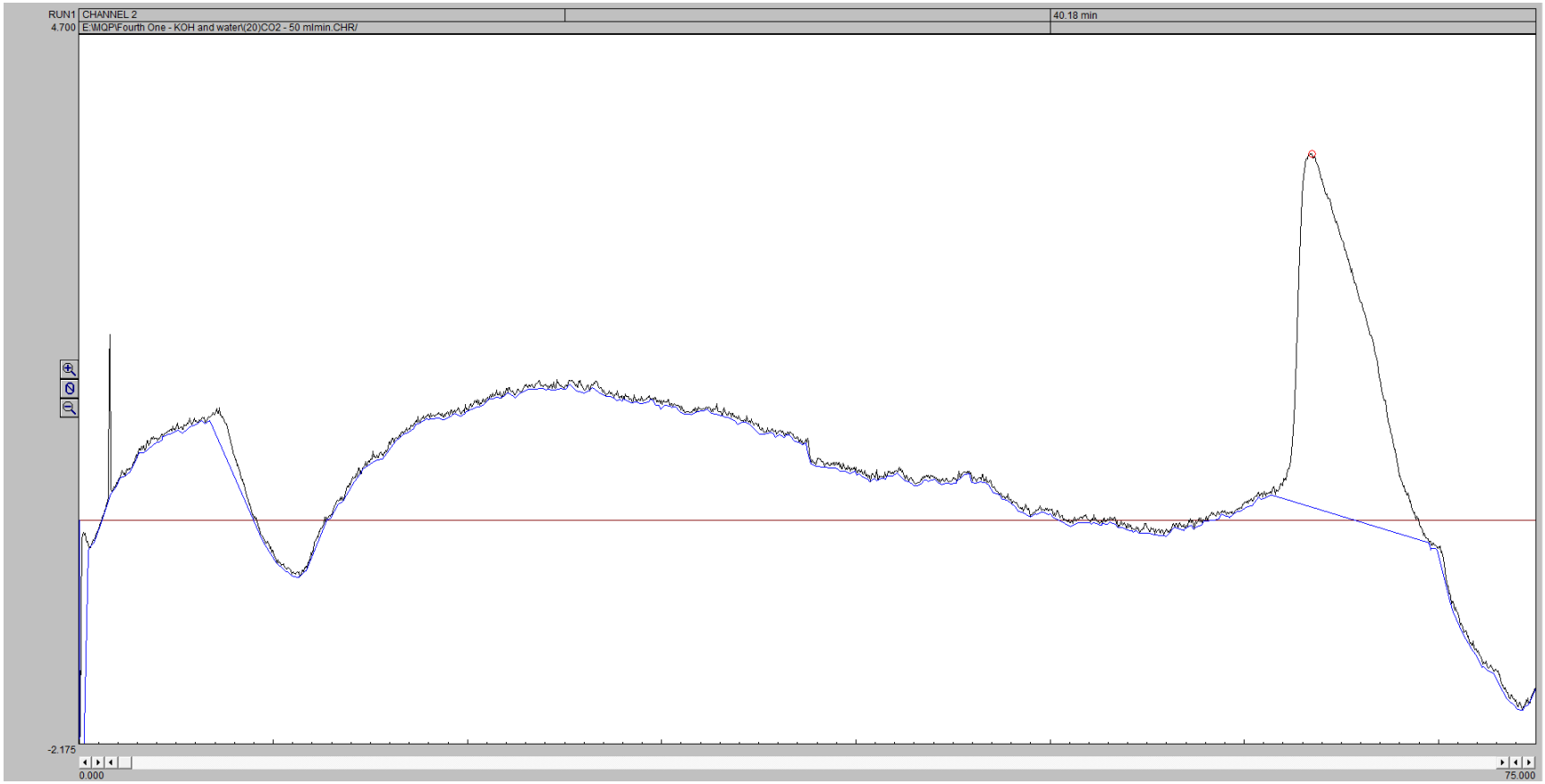
RUN1
CHANNEL 2
40.18 min
4.700
E:\MQP\Fourth One - KOH and water\(20)CO2 - 50 mlmin.CHR/
-2.175
0.000
75.000

CH_4

Column 1

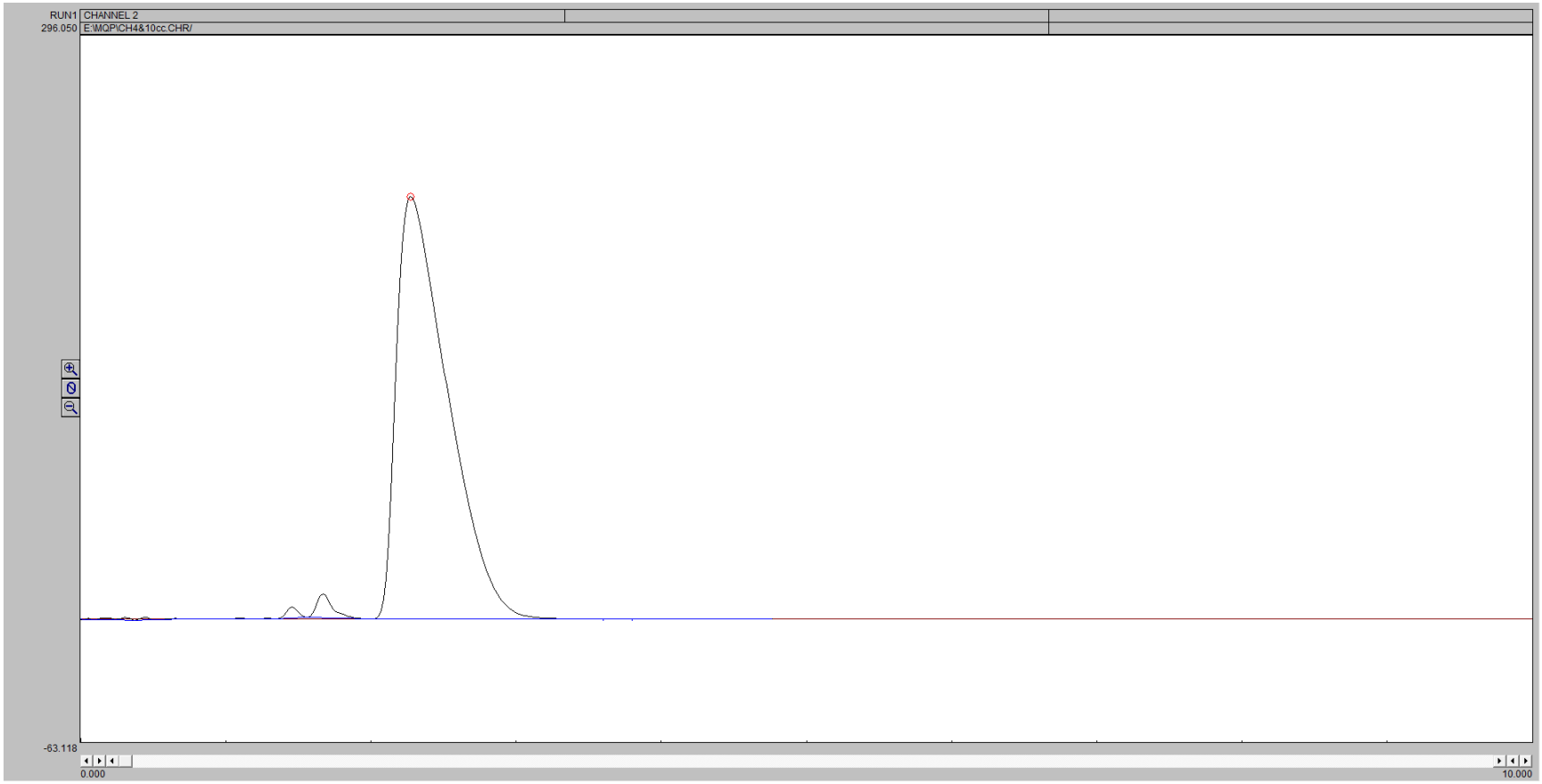

Column 2

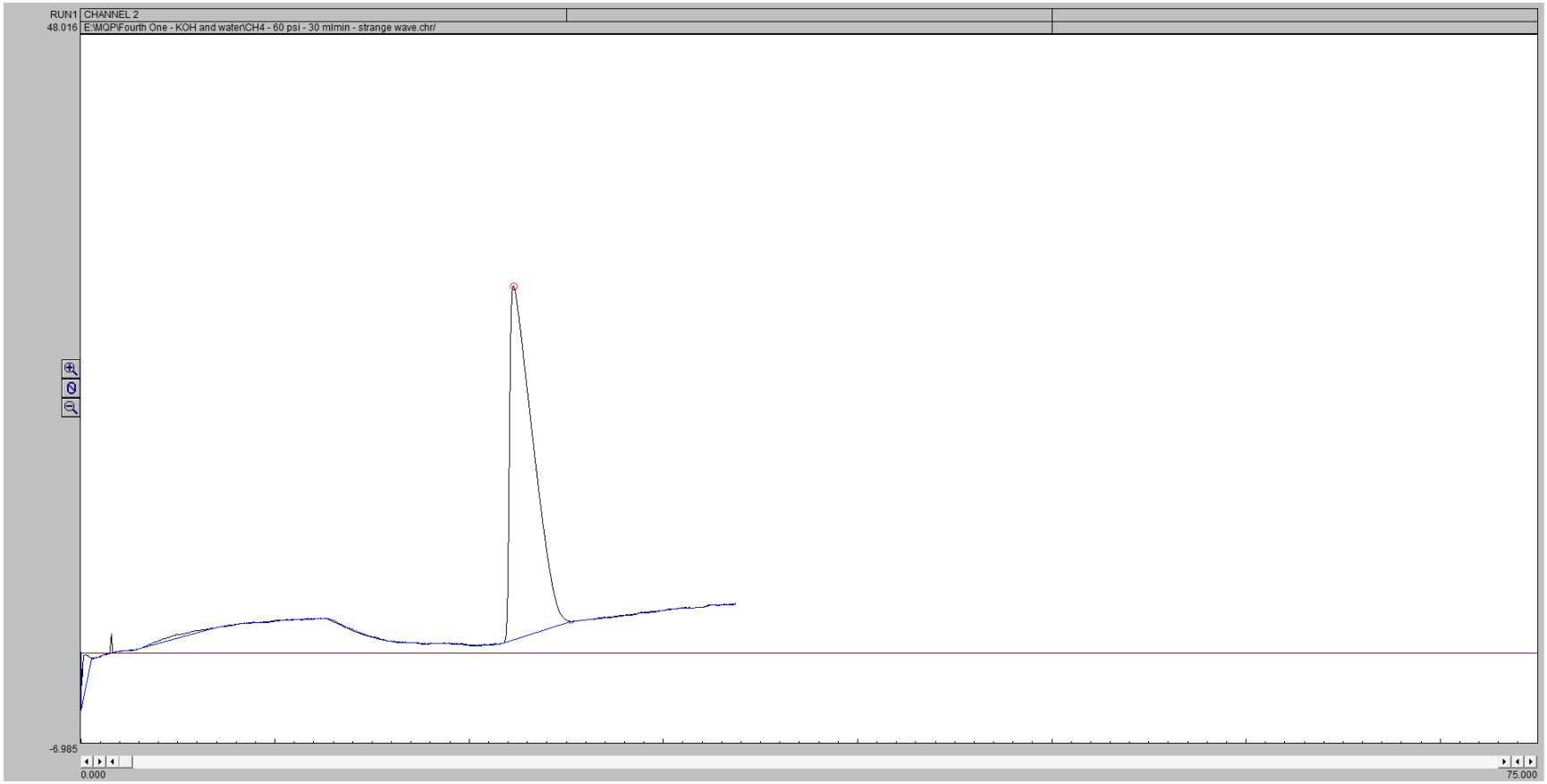
RUN1
CHANNEL 2
48.016
E:\MQP\Fourth One - KOH and water\CH4 - 60 psi - 30 ml\min - strange wave.chr/
-6.985
0.000
75.000

H_2

Column 1

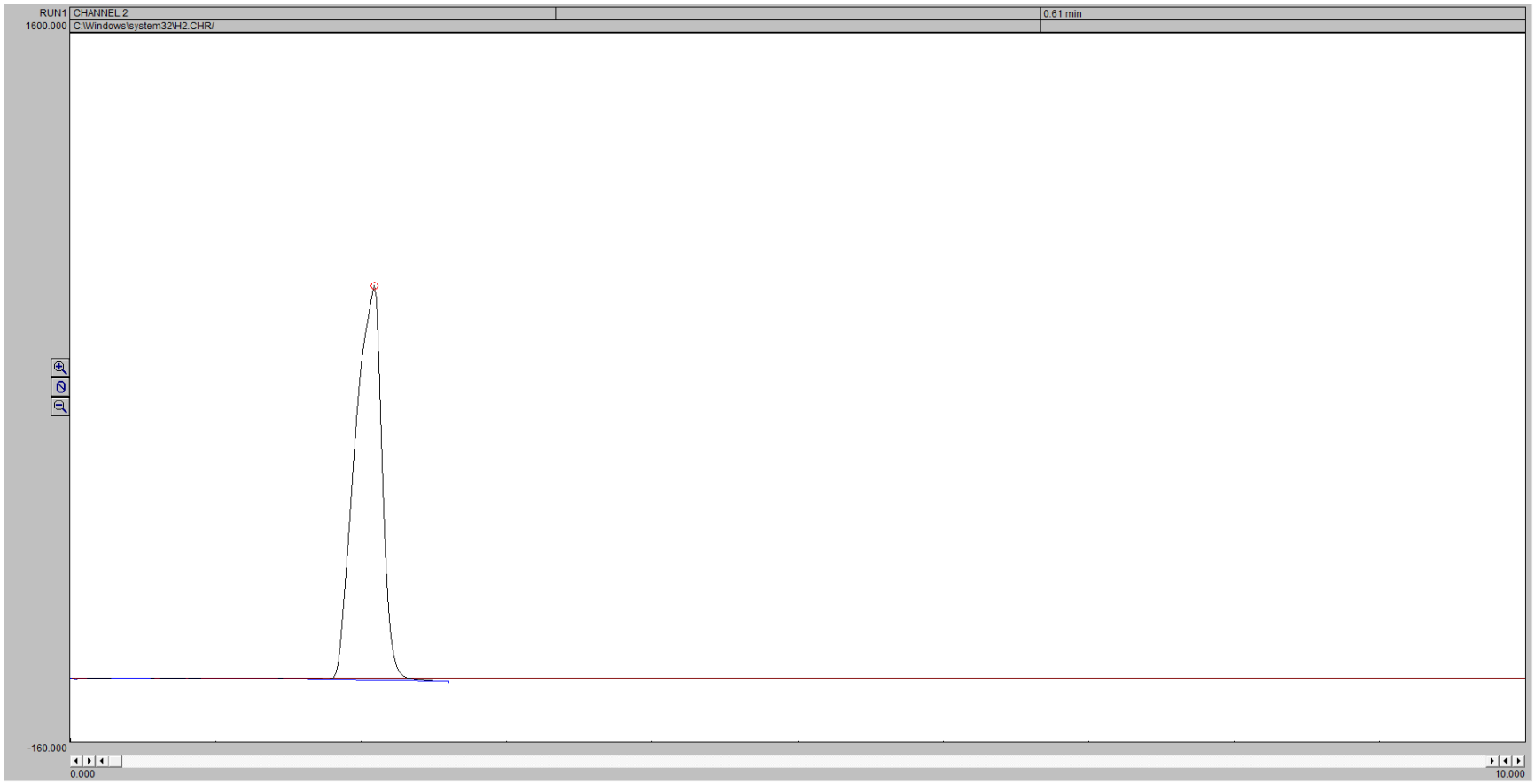
RUN1
CHANNEL 2
0.61 min
1600.000
C:\Windows\system32\H2.CHR/
-160.000
0.000
10.000

Column 2

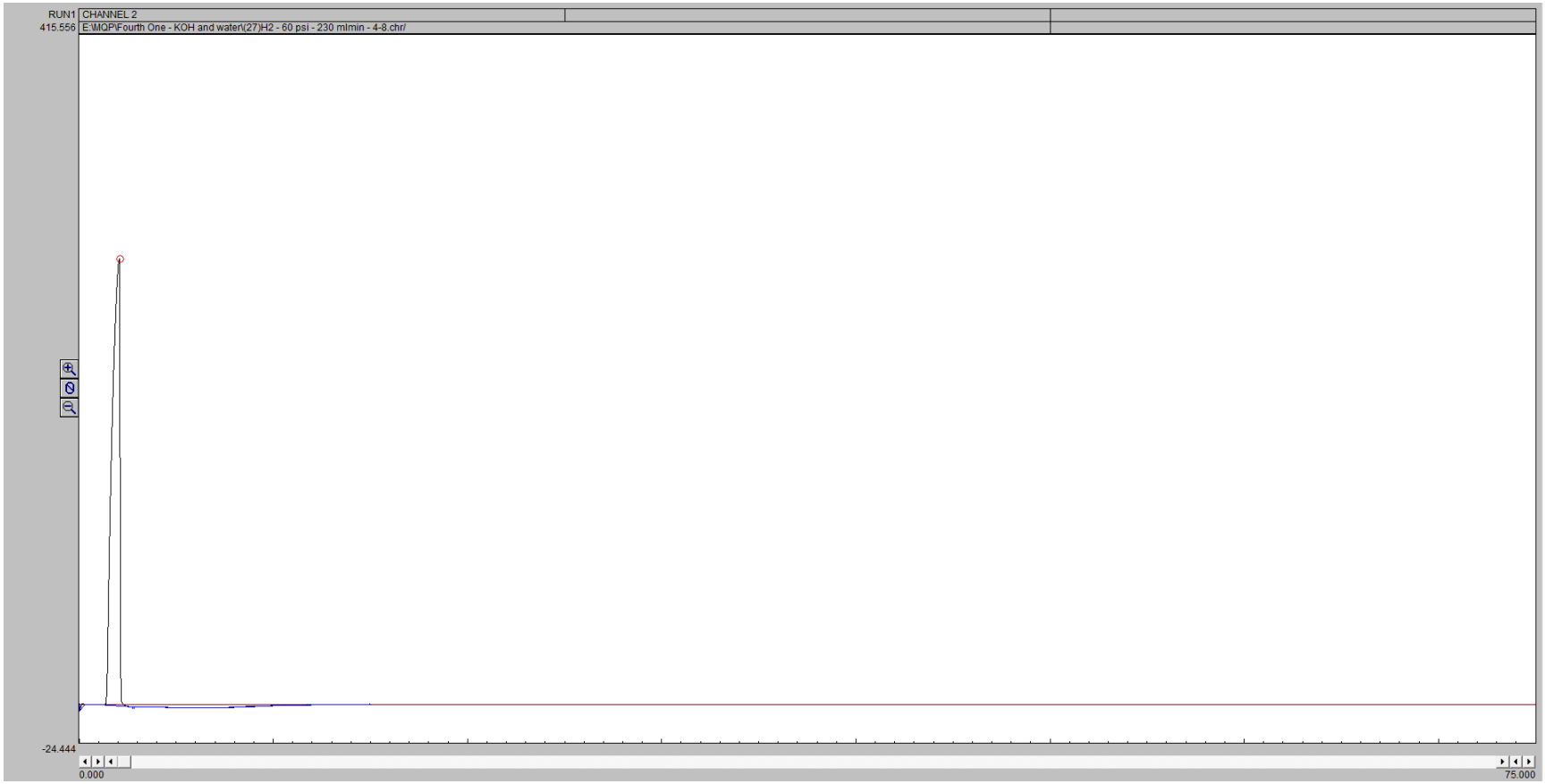
RUN1
CHANNEL 2
415.556
E:\MQP\Fourth One - KOH and water\(27)H2 - 60 psi - 230 mlmin - 4-8.chr/
-24.444
0.000
75.000

CO

Column 1

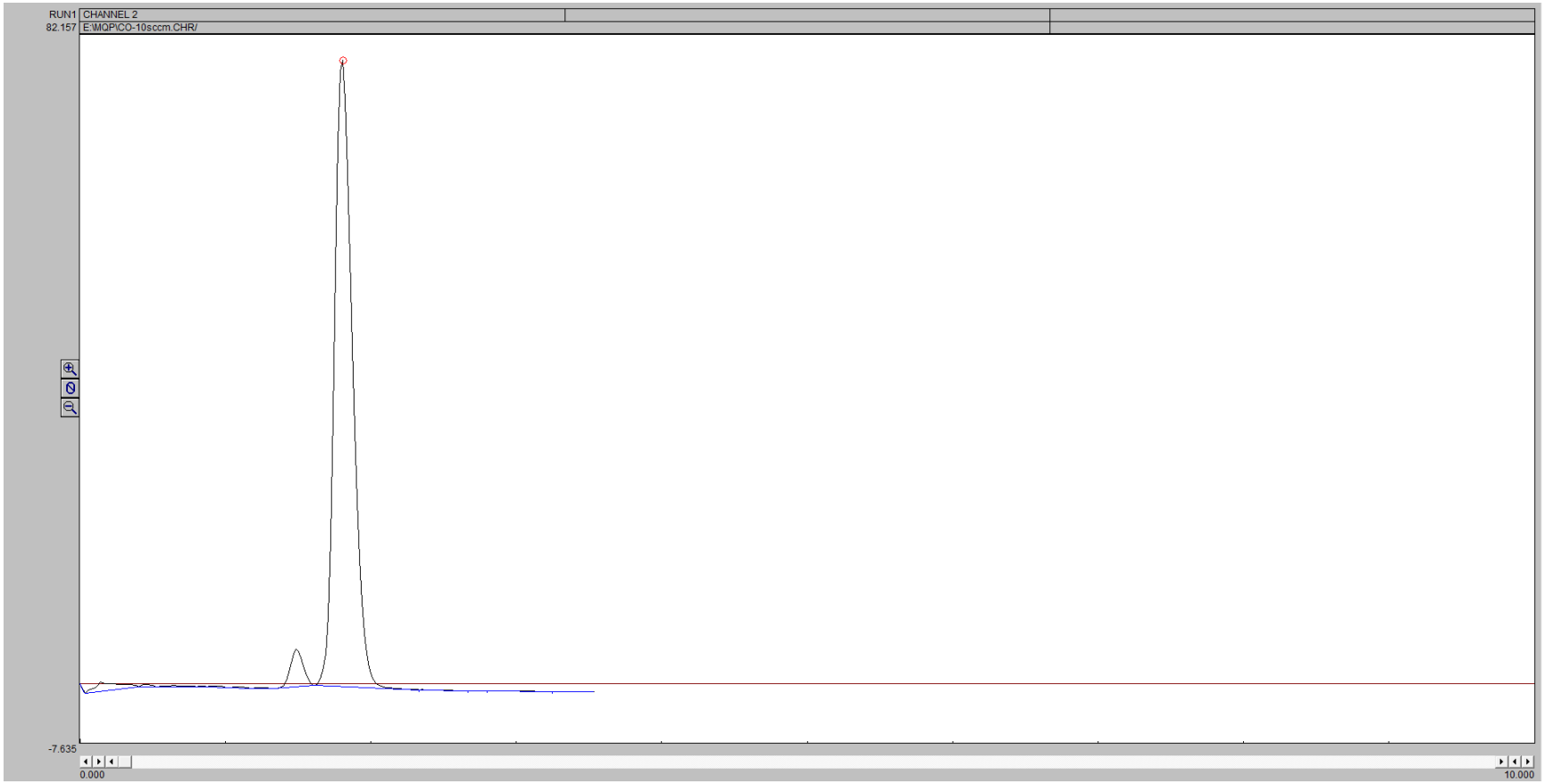

Column 2

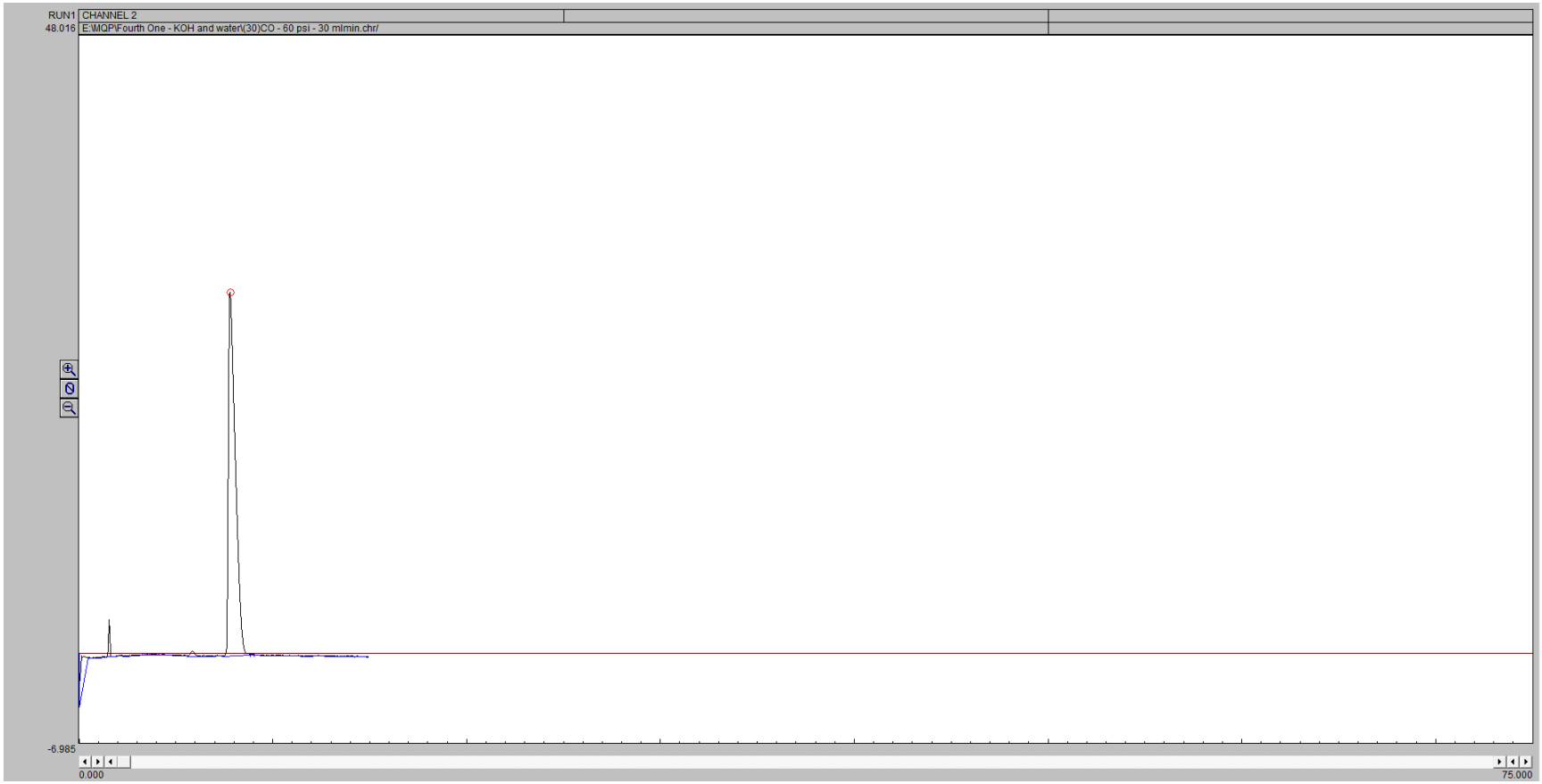
RUN1 CHANNEL 2
48.016
E:\MQP\Fourth One - KOH and water\(30)CO - 60 psi - 30 ml\min.chr/
-6.985
0.000
75.000

Appendix H Reactor Pressure Calculations

Total Pressure Increase Due to Reaction

Transesterification saw a majority of our batch trials. The overall reaction for the transesterification of tributyrin is:

$$C_{15}H_{26}O_6 + 3\,CH_4O \rightarrow 3\,C_5H_{10}O_2 + C_3H_5(OH)_3 \quad (7)$$

With the boiling point of glycerin and methyl butyrate being well below 500 degrees Celsius it was assumed that complete conversion occurred and all products were vaporized for the sake of pressure calculations. Therefore when the reactor was input with 5.0 mL of tributyrin the following calculations were performed:

$$5.0\ mL\ Tributyrin * \frac{1.035\ g\ Tributyrin}{g\ Water} = 5.035\ g\ of\ Tributyrin \quad (8)$$

$$5.035\ g\ Tributyrin * \frac{mol\ Tributyrin}{302.36\ g\ Tributyrin} = 0.01665\ mol\ of\ Tributyrin \quad (9)$$

Therefore, for every mol of tributyrin placed into the reactor 4 moles of products would be vaporized in the reactor theoretically. Next, the ideal gas law was applied to the product liquids.

$$P = \frac{nRT}{V} \quad (10)$$

$$P = \frac{(4*0.01665\ mol)(0.0821\frac{L*atm}{mol*K})(773.15\ K)}{\pi*0.01905^2 m^2*0.4318\ m*\frac{1000L}{1m^3}} = 8.59\ atm \quad (11)$$

Total Pressure Due to Vaporization of Reactants

However, some of these reactions used water as a reactant as well. Therefore, pressure calculations for 5 and 10 milliliters of water were completed at the temperature of 500 degrees Celsius.

5 mL of Water

$$5.0\ mL\ Water * \frac{1.00\ g\ water}{mL\ Water} = 5.00\ g\ of\ Water \quad (12)$$

$$5.00\ g\ Water * \frac{mol\ Tributyrin}{18.0\ g\ Tributyrin} = 0.2777\ mol\ of\ Water \quad (13)$$

$$P = \frac{(0.2777\ mol)\left(0.0821\frac{L*atm}{mol*K}\right)(773.15\ K)}{\pi*0.01905^2 m^2*0.4318\ m*\frac{1000L}{1m^3}} = 35.81\ atm \quad (14)$$

10 mL of Water

$$10.0\ mL\ Water * \frac{1.00\ g\ water}{mL\ Water} = 10.00\ g\ of\ Water \quad (15)$$

$$10.00\ g\ Water * \frac{mol\ Tributyrin}{18.0\ g\ Tributyrin} = 0.5554\ mol\ of\ Water \quad (16)$$

$$P = \frac{(0.5554\ mol)(0.0821\frac{L*atm}{mol*K})(773.15\ K)}{\pi*0.01905^2 m^2*0.4318\ m*\frac{1000\ L}{1m^3}} = 71.61\ atm \quad (17)$$

Therefore, the maximum pressure we would expect to see would be with 10 mL of water and 5 mL of tributyrin products. When these pressures are summed, a total pressure of 80.2 atm is achieved. The maximum pressure allowed by the reactor at this temperature is 136 atm so the maximum theoretical pressure of 80.2 is well below this to ensure the reactor is operated well within the range of safety.